Electrospun three dimensional scaffolds for bone tissue regeneration

by

Elena Irina Paşcu, MEng, BSc

Thesis presented to Dublin City University in fulfilment of the requirements for the degree of

Doctor of Philosophy

Supervisors:
Dr. Joseph Stokes
Dr. Garrett McGuinness

School of Mechanical and Manufacturing Engineering
Dublin City University
Ireland
2013

DECLARATION

I hereby certify that this material, which I now submit for assessment on the programme of study leading to the award of Doctor of Philosophy is entirely my own work, that I have exercised reasonable care to ensure that the work is original, and does not to the best of my knowledge breach any law of copyright, and has not been taken from the work of others save and to the extent that such work has been cited and acknowledged within the text of my work.

Signed: _____

   (Elena Irina Paşcu)

ID No.: 57127930   **Date:** _____

TO

My parents, for all that I am today

ACKNOWLEDGEMENTS

PUBLICATIONS AND PRESENTATIONS

Publications

1. **<u>Elena I. Pașcu</u>**, Joseph Stokes, Garrett B. McGuinness, *Electrospun Composites of PHB/PHV, Silk Fibroin and nano-Hydroxyapatite for Bone Tissue Engineering* (Journal of Materials Science & Engineering C-Materials for Biological Applications, in press)

Presentations

1. **<u>E. Irina Pașcu</u>,** Garrett B. McGuinness, Joseph Stokes*, Bioactive and Biodegradable three-dimensional Fibrous Scaffolds for Orthopaedic Applications*, Conference Proceedings of the 3rd TERMIS World Congress, Vienna, Austria (2012) (poster)

2. **<u>E. Irina Pașcu</u>,** Garrett B. McGuinness, Joseph Stokes*, Manufacturing and Characterization of Bioactive Electrospun Nanocomposites*, Conference Proceedings of The 18th Annual Conference of Bioengineering …in Ireland, Belfast, Northern Ireland (2012) (oral presentation)

3. **<u>E. Irina Pașcu</u>,** Garrett B. McGuinness, Joseph Stokes*, Manufacturing and characterization of Biodegradable Electrospinning Tri-phasic Nanocomposites*, Conference Proceedings of the 24th European Conference on Biomaterials (ESB), Dublin, Ireland (2012) (poster)

4. **<u>E. Irina Pașcu</u>,** Garrett B. McGuinness, Joseph Stokes*, Manufacturing and Characterization of Bioactive Electrospun Nanocomposites*, Sir Bernand Crossland Symposium, Dublin City University, Dublin, Ireland (2012), (poster)

5. **E. Irina Paşcu,** Garrett B. McGuinness, Joseph Stokes*, Polymer/Bioceramic Composite Electrospinning for Orthopaedic Applications*, Conference Proceedings of The 17th Annual Conference on Bioengineering…in Ireland, Galway, Ireland (2011) (oral presentation)

AWARDS

1. Winner of the 'Tell the world about your research" competition awarded a three-week internship with Silicon Republic, Ireland (2011)

2. Travel Award from The 18th Annual Conference of Bioengineering …in Ireland, Belfast, Northern Ireland (2012)

Table of Contents

LIST OF FIGURES

XIII

XV

XVII

XVIII

LIST OF TABLES

LIST OF ABBREVIATIONS

3D	Three Dimensional
ANOVA	Analysis of Variance
BALP	Bone-alkaline phosphatise
BBD	Box-Behnken Design
BMP-2	bone morphogenetic protein-2
BSA	Bovine serum albumin
BSE	back scattered electrons
ß-TCP	ß-tricalcium phosphate
$CaCl_2$	Calcium chloride
CCD	Central Composite Design
CHO	Chloroform
COL I	Collagen type I
D	Distance
DAPI	4'-6-Diamidino-2-phenylindole
DMSO	Dimethlysulphoxide
DNA	Deoxyribonucleic acid
DoE	Design of Experiments
DTA	Differential Thermal Analysis
ECM	Extracellular matrix
EDTA	Ethlyenediamine Tetracetic Acid
EDX	Electron dispersed xray
ELISA	enzyme-linked immunosorbent assay
ETH	Ethanol

f-actin	Filamentous actin
FBS	Fetal Bovine Serum
FITC	Fluorescein Isothiocyanate
FR	Feeding rate
FTIR	Fourier Transform Infrared spectroscopy
GAPDH	Glyceraldehyde 3-phosphate dehydrogenase
HAp	Hydroxyapatite
HCA	hydroxy carbonate apatite
HCl	Hydrochloric acid
H	Hour
HEPES	(4-(2-hydroxyethyl)-1-piperazineethanesulfonic acid)
HOB	Human osteoblast
hMSC	Human mesenchymal stem cells
HRP	horseradish peroxidise
ICC	Immunocytochemistry
KCl	Potassium chloride
$K_2HPO_4*3H_2O$	Potassium phosphate dibasis trihydrate
MA	Methanol treated and autoclaved
MCL	Medium –chain- length
MC3T3- E1	mouse pre-osteoblast cells from bone-calvaria
M	Methanol treated
Min	Minutes
mm	Milimeter
NaCl	Sodium chloride

NAM	Non methanol treated/ non autoclaved
Na_2SO_4	Sodium sulphate
nHAp	Nano hydroxyapatite
OSPN	Osteopontin
PBS	Dulbecco's Phosphate buffer solution
PCL	Polycaprolactone
PEO	Polyethyl oxide
PHAs	Poly(hydroxyalkanoate)s
PHB	Polyhydroxybutyrate
PHB/PHV	polyhydroxybutyrate (98%)/ polyhydroxyvalerate (2%)
PHV	Polyhydroxyvalerate
PLGA	Poly lactic glycolic acid
PLA	Polylactic acid
PLLA	poly-L-lactic acid
qRT-PCR	Quantitative Real Time Polymerase Chain Reaction
RNA	Ribonucleic acid
RSM	Response Surface Methodology
SBF	Simulated body fluid
SCL	Short -chain-length
SEM	Scanning electron microscope
SF	Silk fibroin
STA	Simultaneous Thermal Analysis
T	Temperature
t	Time

TCPS	Tissue Culture Polystyrene
TE	Tissue engineering
TGA	Thermal gravimetric analysis
μm	Micrometer
UTS	Ultimate tensile strength
V	Voltage
XRD	X-Ray Diffractometer

ABSTRACT

Electrospun three dimensional scaffolds for bone tissue regeneration
Elena Irina Paşcu, MEng, BSc

Bone is a complex and highly specialized form of connective tissue which acts as the main supporting organ of the body. It is hard and dynamic by its nature, with a unique combination of organic and inorganic elements embedded in a fibrous extracellular matrix (ECM), onto which cells attach, proliferate and differentiate. When bone repair mechanisms fail, due to infection or defect magnitude, bone formation can be stimulated with the use of autologous bone grafts or donor allografts. However, autografts are associated with limitations such as donor site morbidity and limited availability, while allografts have the potential to cause an immune response and also carry the risk of pathogen transfer. Bone tissue engineering has emerged as an alternative to these approaches by attempting to mimic the architecture of the bone tissue while providing appropriate cues for cellular attachment, growth and proliferation, as well as the mechanical strength necessary to maintain their structural integrity during remodelling.

The present study aims to create three dimensional fibrous scaffolds containing nano-hydroxyapatite (nHAp) embedded in a matrix of functional biomacromolecules, polyhydroxybutyrate/hydroxyvalerate (PHB/PHV) and *Bombyx mori* silk fibroin (SF) with the use of the simple and versatile technique of electrospinning. This approach will offer an attractive route to mimicking the natural bone tissue architecture through electrospinng of the ceramic phase within the polymeric one. The created functional fibrous substrates could be used for *in vitro* or *in vivo* tissue regeneration. For these reasons they are intended to support cell attachment, proliferation and differentiation, while the role of nHAp would be to induce cells to secrete ECM for mineralization to

form bone. After choosing the materials, screening tests were conducted to determine a suitable composite solution and its electrospinning parameters, followed by a Design of Experiments analysis in order to explore and understand the relationship between process factors: feed rate, voltage, collection distance and solution composition.

Physico-chemical and *in vitro* biological tests were performed on produced constructs in order to study the suitability of the proposed material combination for such an application. Simultaneous electrospinning of composites of 2% valerate fraction PHB/PHV , nano hydroxyapatite (nHAp), and *Bombyx mori* silk fibroin (SF) has been achieved for nHAp and SF solution concentrations of 2 (w/vol) % each and 5 (w/vol) % each and three dimensional fibrous scaffolds were constructed. Further findings of this work supported the hypothesis that the proposed composite scaffolds have appropiate fibrous morphology of the ECM showing continuous fibres deposition and no bead defect formation. Furthermore the structures support apatite formation on their surface, thus being bioactive while exhibiting a low degradation rate that is adequate for bone regeneration. The 2% composite constructs (2% nHAp and 2% SF content) possess appropriate compressive properties for bone tissue regeneration while the Young's modulus varies with the ceramic/ proteic content. Additionally when placed in culture the 3D structures enhance the osteoblast phenotype with cells travelling in the depth of the construct after only 3 days after seeding. All these resultssuggest that these scaffolds are appropriate cell carriers for osseous tissue engineering, offering an alternative in the biomaterials area of study

CHAPTER 1   INTRODUCTION

When Gloria Causen, a middle school teacher from Mendham, N.J., was told by her doctor that she had a rare, cancerous tumour in her left leg, she was presented with two options: have the leg amputated below the knee or have a bone transplant that would save her leg. Like many patients faced with similar situations one of her first questions was: 'Where will you get the bone?' [1].

1.1 Bone defects

Bone defects can be caused by injury, disease, or surgical interventions. Defects up to about 1/3 of an inch in a large bone can heal by themselves in a healthy non-smoker, but bone defects larger than this, or even smaller in small bones never heal completely.

In order to facilitate more complete and faster bone healing, alternatives such as bone replacement or bone enhancement materials are needed to fill the defect. These alternatives provide mechanical and structural support, fill defect gaps and enhance bone tissue formation. They are widely used on orthopaedic surgery, plastic surgery, oral and maxillofacial surgery, and dental surgery. This makes bone the second most transplanted tissue in humans.

1.2. The need for bone regeneration

Bone is a connective tissue largely composed of an organic protein; collagen and the inorganic mineral hydroxyapatite, which combine to provide a mechanical and support role in the body. Bone is a hard but relatively lightweight tissue, able to withstand considerable pressure while being sufficiently elastic to withstand moderate torsion. Inside the hard, mineralized tissue is a matrix in which bone cells can proliferate and adhere.

Bone is known as a dynamic, highly vascularised tissue with a unique capacity to heal and remodel without leaving a scar [2]. These properties, together with its capacity to rapidly mobilize mineral stores on metabolic demand, define bone as a smart material. Its main role is to provide structural support for the body. Furthermore the skeleton also serves as a mineral reservoir, supports muscular contraction resulting in motion, withstands load bearing and protects internal organs [2, 3].

Bone loss and failure from injuries or diseases remain frequent and serious health problems despite great advances in medical technologies and life sciences. Currently, bone grafting procedures are used to promote the healing of fracture non-union and the repairing of other bone defects. The traditional biological methods of bone-defect management include autografting and allografting cancellous bone, applying vascular grafts of the fibula and iliac crest, and using other bone transport techniques [4]. Although major progress has been achieved in the field of regenerative

medicine over the years, current therapies still have several limitations. Autologous grafts mean putting the patient through additional surgery and therefore the supply of self-donated tissue is, obviously, limited. Donor grafts pose risks of disease, graft rejection and other long-term complications. Furthermore, the new bone volume maintenance can be problematic due to unpredictable bone resorption. In large defects, the grafts can be resorbed by the body before osteogenesis is complete leaving no template for the new bone formation which may lead to further bone defects [4]. Vascularized grafts require a major microsurgical operative procedure requiring sophisticated infrastructure. Distraction osteogenesis techniques are often laborious and lengthy processes that are reserved for the most motivated patients. Another method of bone defect repair is via bone cement fillers. Bone cements are prepared in the operating room and therefore can be susceptible to infection.

The efforts to address these clinical problems and limitations have led to the development of new biomaterials and alternatives therapies, among which the bone tissue engineering approach appears to be of great promise. Bone tissue engineering may provide alternative solutions. Bone tissue engineering can be classified into two main areas: *in vivo* and *in vitro*. The *in vitro* approach requires a specifically designed environment for regeneration, while an *in vivo* approach tries to achieve natural regeneration of bone by stimulating the natural healing process and using the body's microenvironment [5]. Neotissues are constructed using biodegradable three-dimensional porous scaffolds which act as a templates mimicking the extracellular matrix (ECM) of the body, followed by *in vitro* culture and *in vivo* implantation to the desired sites. The scaffold may be used with or without seeded cells prior to implantation. Bone tissue regeneration is dependent on the in - growth of the

surrounding tissue in a process called tissue induction, or more precisely osteoinduction [6].

Bone regeneration requires four components: a morphogenetic signal, responsive host cells that will respond to the signal, a suitable carrier of this signal that can deliver it to the specific sites then serve as scaffolding for growth of the responsive cells, and a viable, well vascularised host bed. For bone tissue engineering, major issues include:

- the use of appropriate matrix materials for scaffolds

- control of porosity and pore characteristics

- mechanical properties

- bioactivity.

1.3 Polyhydroxybutyrate/polyhydroxyvalerate (PHB/PHV) 3D porous scaffolds

The microenvironment in which cells reside *in vivo* exhibits a multitude of signals which play an essential role in a diverse set of cellular processes [7]. Many of these cues are offered by the extracellular matrix (ECM), which plays the role of the cellular scaffold and is the primary extracellular component of tissues [8].

Since most primary organ cells, are known to be anchorage-dependent and require specific environments for growth, the success of tissue engineering depends of the development of suitable scaffolds for *in vitro* tissue culture and *in vivo* neotissue formation [5].

Biologically active scaffolds are highly porous materials based on simple analogues of the extracellular matrix (ECM) that can induce tissue regeneration and are the strategic choice in several pathological situation that are currently treated with organ transplantation.

The challenge of orthopaedic tissue engineering is to develop a suitable scaffold that will present sufficient porosity and mechanical strength to allow cell adhesion, migration, growth and proliferation thus adequate integration with the surrounding tissue [9]. One of the most important factors when tailoring the artificial graft for the specific tissue is the chosen material. Several factors such as mechanical properties, degradation rate and cell proliferation, and adhesion on the material must be considered when selecting one for specific atissue or organ scaffold [10].

Polyhydroxybutyrate/ polyhydroxyvalerate (PHB/PHV) is a natural polymer, from the class of poly(hydroxyalkanoate)s (PHAs). It has attracted attention as a potential biomaterial for tissue regeneration because of its non-cytotoxicity, biocompatibility, biodegradability and thermoprocesability. It was demonstrated to produce a consistent favourable bone tissue adaptation response with no evidence of an undesirable chronic inflammatory response after implantation periods up to 12 months while particulate hydroxyapatite (HAp) incorporated into PHA forms a bioactive and biodegradable composite for applications in hard tissue replacement and regeneration

5

[11, 12]. In addition, PHA/HAp composites have similar mechanical strength in compression to that of human bone, thus it is an interesting biomaterial when used in fracture fixation [13]. Depending on the property requirements for different applications, PHA can be either blended, surface modified or composited with other polymers, enzymes, or even inorganic materials to further adjust their mechanical properties or biocompatibility.

1.4 Research, objectives and methodology

The natural extracellular matrix (ECM) is a complex structure that is built to meet the specific requirements of the tissue and organ. Primarily consisting of small diameter fibrils, ECM may contain other vital substances such as proteoglycans, glycosaminoglycan and various minerals [14]. The ECM in particular is able to influence the cells by both chemical cues and the physical arrangement of fibres [10]. The major solid components of human bone are collagen (type I) and a biological apatite that differs in composition from the stoichiometric hydroxyapatite [HA, $Ca_{10}(PO_4)_6(OH)_2$] by the presence of other ions, of which carbonate is the most abundant species (~ 8 wt%) [15].

Structural biocompatibility is affected by the physical morphology of a scaffold, primarily by its architecture and the dimensions of its components. The dimensions of the building components of a scaffold are important factors in regulating cell activities. Cell behaviour is known to be regulated by the physical properties of an engineered scaffold, such as the architecture and topography. Previous studies have shown that cell

6

proliferation is influenced by the architectural scale of the structure and that adhesion is affected by the topography of the material [16, 17]. Current research in tissue engineering involves trying to replicate the ECM to provide the environment for tissue regeneration. In order to mimic bone structure and composition, researchers have prepared polymer/ceramic bone analogue composites using a variety of conventional methods such as direct mineralization or chemical precipitation. The physical structure, composition and arrangement of the ECM are often tissue specific, thus an appropiate technique should be used to fabricate three-dimensional scaffolds that would mimic the fibrous structure of the natural ECM.

The electrospinning process has frequently been applied to the search of biomimetic bone tissue engineering scaffolds. Various composite fibres, such as PCL/CaCO$_3$ [18], HAp/gelatin [19], PLA/HAp [20-22], PLA and triphasic HAp/collagen/PCL [23, 24] have been explored, with the intention of achieving better cellular adhesion, mineral formation and growth suitable for bone regeneration. Even though synthetic polymers and their blends exhibit biocompatibility and good mechanical properties, novel biopolymer composites (biocomposites) based on biodegradable and bioresorbable materials have received an increasing interest over the last decades. The co-precipitation of HAp nanocrystals in soluble collagen has met with partial success in the fabrication of electrospun HAp–collagen nanocomposites similar to the nanostructure of real bone, though with weaker mechanical properties [25]. On the other hand, carbonate-substituted HAp–chitosan/silk fibroin composites prepared using a co-precipitation method exhibited better compressive strength and cellular response, mimicking the real bone [26]. Simultaneous gas-jet and electrospinning of composite solution containing hydroxyyapatite have been used to manufacture porous

7

scaffolds suitable for bone regeneration [27, 28]. Other attempts of adding hydroxyapatite to the electrospun fibres have been made, either by soaking the fibrous polymeric matrix in simulated body fluid (SBF) [29] or by co-precipitation and nucleation [30, 31]. PLGA/HAp fibrous composite scaffolds were also prepared, mainly used for drug delivery instead of bone repair [32-34].

It is known that structurally the bone is hierarchically organized from macro to micro to nano-scale, using basic building blocks such as the platelike HAp nanocrystals incorporated within biomacromolecular nanofibres [2]. Previous research work has been shown to contribute to the field of bone tissue regeneration with interesting concepts of manufacturing bone-like scaffolds and unique experimental results on their properties. However, in most of the studies mentioned above, the produced composite fibres were prepared by combining electrospinning with additional techniques, such as co-precipitation and nucleation, or gas-jet spraying resulting in structures with very limited bonelike characteristics. Furthermore combining two or more techniques in order to produce the composite fibres can be a time consuming approach. Another challenge was to develop formulations with sufficient electrospinnability while ensuring chemical and physical intactness of both the ceramic nanoparticles and polymer matrix.

The present research work tries to answer the following question :

Can 3D electrospun scaffolds composed of nHAp encapsulated in PHBV provide thick fibrous structures which meet the major requirements for bone tissue engineering scaffolds such as promoting apatite formation and supporting osteoblast attachment and proliferation, while also providing adequate resistance to mechanical compression?

Furthermore based on the previous work on PHAs/HAp composites and the concept of mimicking the extracellular matrix of the bone, the aim of this research was to combine the biocompatibilty, non-toxicity and biodegradability of the polyhydroxybutyrate/ polyhydroxyvalerate and silk fibroin with the bioactivity of nHAp in a one step process. The PHB/PHV was chosen as an alternative to other studied natural polymers, such as collagen, gelatine or chitosan from animal or crustacean sources. Advantages include its suitability for industrial scale production. Furthermore its degradation products do not cause an immune response or inflammation, do not alter the pH value of surrounding tissues, and have no adverse influences on bone formation [163]. Its degradation product β-hydroxybutyric acid is finally metabolized into CO_2 and H_2O, not resulting in physiological reaction with the organism [162]. Additionally nHAp particles are similar to the mineral component of natural bone and they show good osteoconductivity, while mimicking its inorganic chemical composition.

In this thesis, the electrospinning technique was used to construct a three-dimensional fibrous matrix using this unique combination of materials that to, the best of our knowledge, are being used together in electrospinning for bone tissue engineering applications for the first time. Silk fibroin, a biocompatible and cytocompatible biomaterial, was found to improve the electrospinning deposition while balancing the change in solution electrospinning dynamic produced by the addition of nHAp particles.

The specific aim of the study therefore was the development of PHB/PHV/ nHAp (coded P/H) fibrous composites for bone regeneration scaffolds. The influence of the polymer matrix materials, HAp particles and the fabrication conditions on the

9

physical and biological properties is considered critical to successful scaffold development.

To accomplish this design of bone graft, the following objectives are listed below:

1. To simultaneously electrospin the nano-hydroxyapatite phase and the PHB/PHV in order to obtain continuous deposition of fibres.

2. To fabricate a three-dimensional structure using the resultant material (electrospun flat membrane).

3. To investigate whether the final construct would support bone-like cells attachment, proliferation and matrix deposition, thus inducing the cells to function normally while maintaining their phenotype.

CHAPTER 2 LITERATURE REVIEW

2.1 Introduction

This literature review is structured into four main sections as shown in Figure 1. These are: (i) bone structure and function, (ii) bone repair, (iii) bone substitutes and (iv) electrospinning.
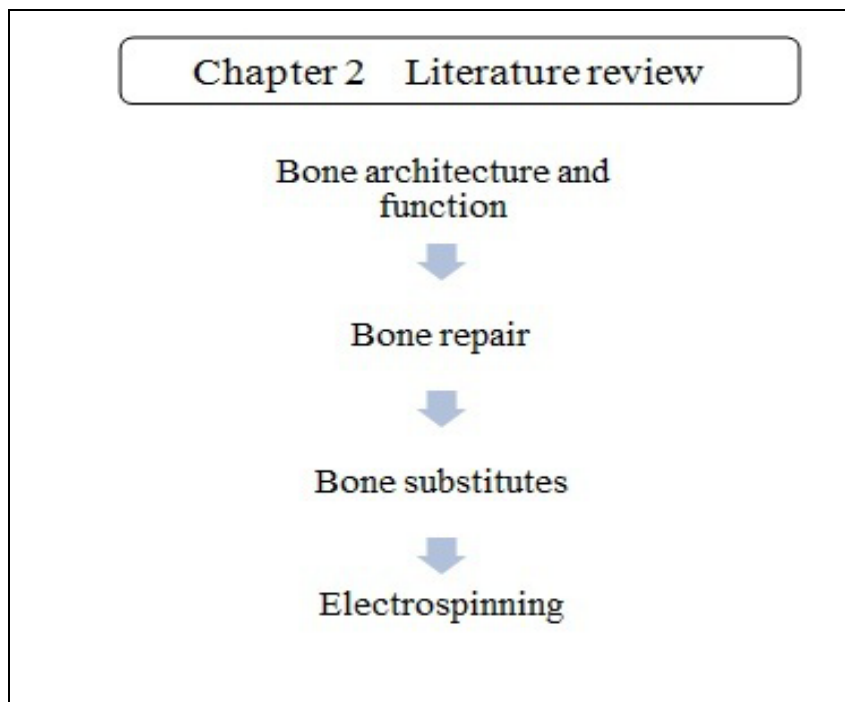
Figure 1 Structure of literature review

2.2 Bone architecture and function

An adult human has 206 bones, which account for 14 percent of the body's total weight. Bone is the major component of almost all skeletal systems in adult vertebrates. Mimicking the bone structure as much as possible is one of the common strategies of bone tissue engineering.

Bone appears to be nonliving - in fact, the word skeleton is derived from a Greek word meaning *dried up*. However, bone actually is a dynamic structure composed of both living tissues, such as bone cells, fat cells, and blood vessels, and nonliving materials, including water and minerals [35]. Bone is a unique combination of minerals and tissue that can provide excellent tensile and compressive strength. It is made up of an organic phase: tissue and cells that are responsible for ductility and maintenance, and the inorganic, mineral phase, responsible for its stiffness.The components of the bone include approximately: 60wt% mineral, 30wt% matrix and cells and 10wt% water.The matrix includes around 15wt% cells , namely osteocytes (bone cells), osteoclasts (bone resorbing cells), osteoblasts (bone building cells) and bone lining cells, known as inactive osteoblasts [35, 36]. The mineral components are mainly crystalline mineral salts and calcium, present in the form of hydroxyapatite $Ca_{10}(PO_4)_6(OH)_2$ containing many other substitutions, such as: magnesium, sodium, potassium, fluorine, chlorine, and carbonate ions. The characteristic bone cell is the osteocyte, that resides in a little chamber (lacunae), surrounded by mineralized bone matrix. This mineralized bone matrix is deposited as a non-mineralized matrix by the osteoblasts, and is calcified by the deposition of calcium salt minerals. The osteoblasts are cells that are found in new-

bone areas and border them with so-called osteoblast zones. The osteoblasts that enter the lacunae become osteocytes and those entering a resting state are called flat-bone-lining cells. In addition to the supportive role, bone has an important function in the regulation of calcium and phosphate blood level regulation. It is believed that all bone cells (osteoclast, osteoblast, and osteocytes) play a role in this process. In addition, bone harbours the bone marrow, the main place where white and red blood cells are being produced [37, 38].

Bones in human and other mammal bodies are generally classified into two types: (i) cortical bone, also known as compact bone and (ii) trabecular bone, also known as cancellous or spongy bone. A schematic of bone structure it is shown in Figure 3. Microscopically, two major forms of bone can be identified: woven and lamellar bone. The first is the immature unorganized type of bone and is present in newborns and in locations where fast bone formation takes place (growth plates-physes, fracture repair). After this type of bone is laid down, it is organized into lamellar, via remodelling.

2.2.1. Cortical bone

Cortical bone represents nearly 80% of the skeletal mass. It is also called compact bone, because it forms a protective outer shell around every other bone in the body. It is the stronger than the cancellous type. Cortical bone has a slow turnover rate and a high resistance to bending and torsion. It provides strength where bending would be undesirable as in the middle of long bones. Cortical bone is dense with a porosity

ranging between 5% and 10%. Cortical bone is found primarily in the shaft of long

bones and forms the outer shell around cancellous bone at the end of joints and the

vertebrae. The basic first level structures of cortical bone are osteons. Cortical bone

osteons are also known as Haversian systems. Each osteon is composed of a central

vascular channel surrounded by a kind of tunnel, called the Haversian canal. The canal

can contain capillaries, arterioles, venules, nerves and possibly lymphatics. Between

each osteon are interstitial lamellae (concentric layers of mineralized bone).
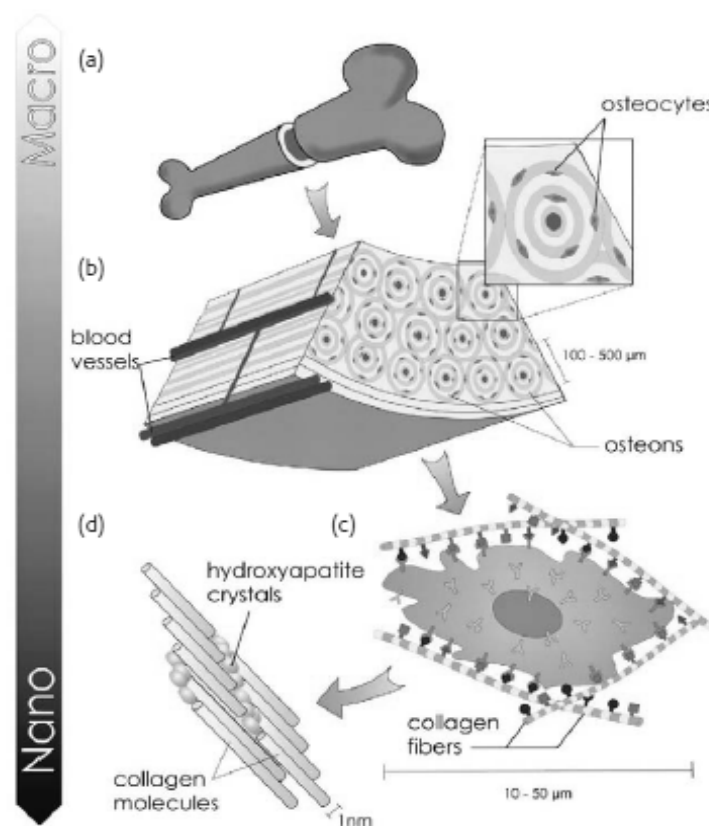
Figure 2 Hierarchical organization of bone over different length scales. Bone has a strong calcified outer compact layer (a), which comprises many cylindrical Haversian systems, or osteons (fundamental unit of the bone) (b). The resident cells are coated in a forest of cell membrane receptors that respond to specific binding sites (c) and the well-defined nanoarchitecture of the surrounding extracellular matrix (d). (Reproducedwith permission of Elsevier Limited) [38]

2.2.2 Trabecular or Cancellous Bone

Trabecular bone is much more porous with porosity ranging anywhere from 50% to 90 % [36]. It is the most dynamic part. It is active in growth, calcium homeostasis and hematopoiesis, and its supportive function is mainly in locations with a predominantly compressive type of loading, such as vertebral bodies and adjacent to articular joints (e.g. knee joint) [37]. It is believed that it can dissipate energy from cortical contact loads, due to its spongy nature. It is less dense, more compliant and has a higher turnover rate than cortical bone. It is found in the epipheseal and metaphysal regions of long bones and throughout the interior of short bones. It constitutes most of the bone tissue of the axial skeleton; bones of the skull, ribs and spine. It is formed in an intricate and structural mesh. It forms the interior scaffolding, which helps bones to maintain their shape despite compressive forces. The middle the bone contains red, yellow marrow, bone cells and other tissues. Its basic first level structure is the trabecula.

2.2.3 Bone as a nanocomposite. Physical properties

The extracellular matrix (ECM) of bone has a unique composition that enables the bone's special function as a mechanical support for the skeleton. However, bone matrix can also regulate the activities of cells that are in contact with it. The ECM constituents are known to be important regulators for cellular processes such as

chemoattraction, migration, proliferation and phenotypic expression. In each microenvironment, the ECM acts as a specialized coordinator [39].

The bone matrix is precisely composed of two phases at a nanoscale level, organic (protein) and inorganic (mineral), and this makes nanocomposites a good candidate for bone replacement. Inorganic and organic phases have several components: minerals, collagen, water, non-collagenous protein, lipids, vascular elements and cells [40]. The chemical composition and physical properties of the natural bone depend on species, age and the type of bone. The mineral phase of the bone is mainly composed of hydroxyapatite (HAp) and the bone protein is mainly composed of collagen, which acts as a structural framework in which plate-like tiny crystals of HAp are embedded to strengthen the bone.

The mechanical properties of human cortical bone from the tibia, femur, and humerus have been found to vary between subjects, although the density remains similar. In human cancellous bone, by contrast, there is no difference in the mechanical properties of the humerus, the proximal tibia, and the lumbar spine [41]. The mechanical properties of cortical bone are much higher than those of spongy bone. A number of factors influence the mechanical properties of cortical bone such as the porosity, the mineralization level and the organization of the solid matrix. Typical mechanical properties of human cortical and spongy bone properties are shown in Table 1.

The orientation of bone specimen, which can be defined as longitudinal (parallel to the predominant osteon ligaments), or transverse (through the osteon section), affects the mechanical properties. Compact bone has a compressive strength in the longitudinal

direction (parallel to the axis) twice that of the transverse direction. It exhibits also good fracture toughness, which is much higher in the transverse direction than in the longitudinal one. The mechanical properties of the trabecular bone are highly dependent on its density. It may appear that the trabeculae are arranged in a random manner, but they are organised to provide enhanced strength, similar to braces that are used to support a building [41].

Table 1 Mechanical properties of human femoral (cortical) bone tissue [42]

Mechanical properties	Test direction related to bone axis for cortical bone		Cancellous bone
	Parallel	**Normal**	**-**
Tensile Strength (MPa)	124-174	49	1.5-20
Compressive Strength (MPa)	170-193	133	2-12
Young's Modulus (GPa)	17-18.9	11.5	7-30
Fracture Toughness (MPa m$^{1/2}$)	2-12	8	2
Bending Strength (MPa)	160	-	10
Yield Tensile Strain	0.007	0.004	-
Yield Compressive Strain	0.010	0.011	-

It is believed that the strength of the bone comes from its structural hierarchy into which it is organised in a self-assembling process. The minerals are not directly bound to the collagen, but bound through non-collagenous proteins.Noncollagenous proteins compose 10 to 15% of total bone protein and make up approximately 3-5 % of the bone, which provide active sites for biomineralization and for cellular attachment. Approximately 25% of noncollagenous protein is exogenously derived, including serum albumin and α2-HS-glycoprotein, which bind to hydroxyapatite because of their acidic properties. Other exogenously derived noncollagenous proteins are growth factors and a large variety of other molecules in trace amounts that may affect bone cell activity. The degree of biomineralization is the most important one to determine the biomechanical

properties of the bone [37]. Furthermore bone strength can be affected by osteomalacia, fluoride therapy, or hypermineralization states. Bone microstructure affects bone strength also. Low bone turnover leads to accumulation of microfractures. High bone turnover, with bone resorption greater than bone formation, is the main cause of microarchitectural deterioration [43].

2.3. Bone repair

Bone healing or fracture healing is a proliferative physiological process, influenced by a variety of systemic and local factors, in which the body facilitates repair of bone fractures. The bone healing process includes three major phases of fracture healing, two of which can be further sub-divided to make a total of five phases [37]:

    a. Reactive phase

        1.1   Fracture and inflammatory phase

        1.2   Granulation tissue formation

    b. Reparative (modeling) phase

        2.1.   Callus formation

        2.2.   Lamellar bone deposition

    c. Remodelling phase

        3.1   Remodelling to original bone contour

The modelling and the remodelling phases are based on the separate actions of bone resorbing cells, called osteoclasts (multinucleated cells that form by fusion of

mononuclear precursors of haematopoetic origin), and bone forming cells, called osteoblasts (that derive from mesenchymal stem cells found in the bone marrow, periosteum and soft tissues). In the inflammatory stage, a hematoma develops within the fracture site during the first few hours and days. Inflammatory cells (macrophages, monocytes, lymphocytes and polymorphonuclear cells) and fibroblasts infiltrate the bone, under prostaglandin regulation. This results in the formation of granulated tissue, ingrowth of vascular tissue and migration of mesenchymal cells. Oxygen, needed for the healing process is provided by the exposed muscle and cancellous bone. During the repair stage, fibroblasts begin to lay down a stroma (part of the blood vessels), that supports vascular ingrowth. As vascular ingrowth progresses, a collagen matrix is produced and laid down while osteoid is secreted and mineralized, forming a soft callus around the repair site. This callus is very weak in the first 4-6 weeks and requires adequate protection in the form of bracing or internal fixation. When the callus ossifies it will form a bridge of woven bone between the fracture fragments. If proper immobilization is not used, the callus may not occur and instead a fibrous union may develop.

The last step in bone repair is the remodelling stage, in which the healing bone is restored to its original shape, structure and mechanical strength. This stage occurs over a long period of time and mechanical stress plays an important role. As the fracture site is exposed to an axial loading force, bone is generally laid down where it is needed and resorbed from where it is not needed. Adequate strength is typically achieved in 3-6 months. A schematic of fracture repair is shown in Figure 3.

Depending on the site of the bone defect, there are some differences in terms of the healing process. One example can be the case of spinal fusion versus bone repair in long bone fractures [44]. Unlike long bone fractures, bone substitutes are used in spinal

fusion procedures. Bone substitutes are incorporated by an integrated process in which old necrotic bone is slowly resorbed and simultaneously replaced with new viable bone. This process is called "creeping substitution" and this remodelling result in the replacement of necrotic bone within the substitute. The most critical period of bone repair is the first 1 to 2 weeks in which inflammation and revascularization occur. There are a variety of systemic factors that can inhibit bone healing: cigarette smoking, malnutrition, diabetes, steroid medication. Bone substitutes are also strongly influenced by local mechanical forces. The density, geometry, thickness and trabecular orientation of bone can change depending on the mechanical demands of the substitute [44].
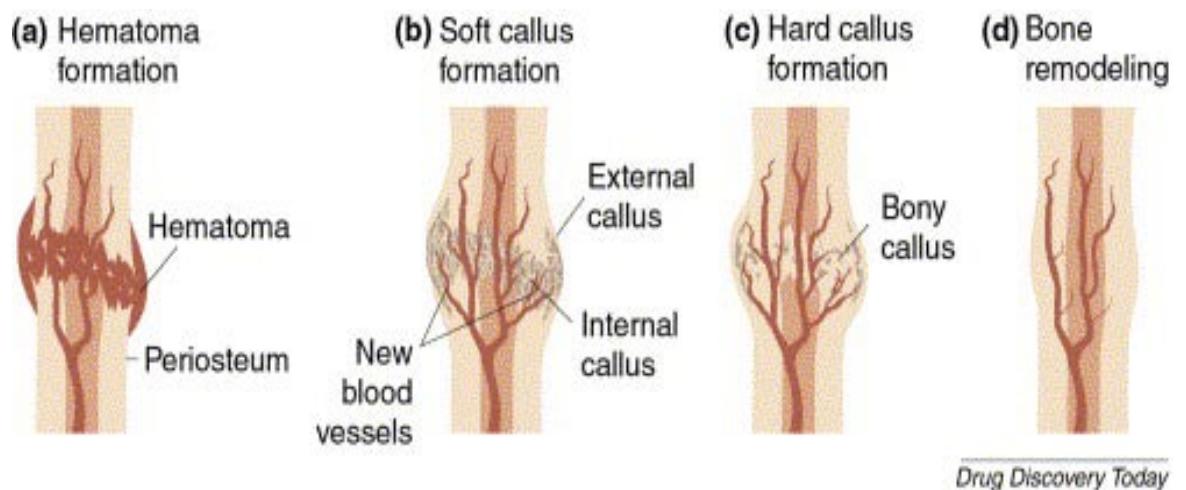
Figure 3 A schematic of bone fracture repair (Reproduced with permission of Elsevier Limited)[45]

2.4 Tissue Engineering Approach

Since its birth in mid-1980s, tissue engineering continues to evolve as an exciting and multidisciplinary field which aims to develop biological substitutes to restore, replace or regenerate defective tissues. Cells, scaffolds and growth-stimulating signals are generally known as the tissue engineering triad, the key components of engineered tissues. Scaffolds, typically made of polymeric biomaterials, provide the structural support for cell attachment and subsequent tissue development [46].

Apart from blood cells, most, if not all, other normal cells in human tissues are anchorage-dependent residing in a solid matrix called the extracellular matrix (ECM). Intuitively, the best scaffold for an engineered tissue should be the ECM of the target tissue in its native state. Nevertheless, the multiple functions, the complex composition and the dynamic nature of ECM in native tissues make it difficult to mimic exactly. Over the last two decades, four major scaffolding approaches for tissue engineering have evolved (Figure 4) [46].

1. Pre-made porous scaffolds   2. Decellularized extracellular matrix (ECM)   3. Cell sheets with secreted extracellular matrix   4. Cell encapsulated in self-assembled hydrogel

raw materials   native tissues   confluent cells   monomer solution

fabrication technologies →   decellularization →   ECM secretion →   initiation of self-assembly → ← cell mixing

porous scaffolds   porous scaffolds   cell sheet   cell encapsulated in hydrogel

cell seeding →   cell seeding →   lamination →

cell-seeded scaffolds   cell-seeded scaffolds   multiple cell sheets

Implantation   Implantation   Implantation   Injection

Defective tissues

Figure 4 Schematic diagram showing different scaffolding approaches in tissue engineering (Reproduced with permission of Springer-Verlag, Berlin-Heidelberg) [46]

One of the most commonly used and well-established scaffolding approaches is seeding therapeutic cells in pre-made porous scaffolds made of degradable biomaterials. Many types of biomaterials can be used to make porous scaffolds for tissue engineering provided that a fabrication technology compatible with the biomaterial properties is available [47-49]. In general, biomaterials used for making porous scaffolds for tissue engineering can be classified into two categories according to their sources, namely natural and synthetic biomaterials. Furthermore acellular ECM processed from allogenic or xenogenic tissues is one scaffolding approach whereby the allogenic or

xenogenic cellular antigens are removed from the tissues and specialized decellularization techniques are developed to remove cellular components. This is usually achieved by a combination of physical, chemical and enzymatic methods [50, 51]. Other scaffolding approaches are cell sheet engineering and cell encapsulation in self-assembled hydrogel matrix. The first represents an approach where cells secrete their own ECM upon confluence and are harvested without the use of enzymatic methods, while the latter is a process entrapping living cells within the confines of a semi-permeable membrane or within a homogenous solid mass [52, 53].

Over the last decade, the development of fabrication technologies for porous scaffolds has been an intensive area of research.In general these technologies can be classified into (1) processes using porogens in biomaterials, (2) solid free-form or rapid prototyping technologies and (3) techniques using woven or non-woven fibres.

In the first category solid or viscous phase materials are incorporated with porogens, which could be gases such as carbon dioxide, liquids such as water or solids such as paraffin [54], followed by porogens removal after fabrication using methods such as sublimation, evaporation and melting to leave behind a porous structure in the scaffold. In the second category, hierarchical porous structures are manufactured by sequential delivery of material and/or energy needed to bond the materials to preset points in space [55]. In the third category, woven and non-woven fibre structures can be piled together and bonded using thermal energy or adhesives to give a porous meshwork using techniques such as fibre bonding [55], or fibres can be generated by the electrospinning technique, in which a high voltage is injected to a polymer solution where the electrostatic forces are built up to overcome the surface tension of the polymer solution and therefore form a spinning fibre jet.

2.5 Bone substitutes

2.5.1 Polymeric substitutes

Polymeric materials are widely applied in the biomedical field to mimic the extracellular matrix. Polymers can serve as a matrix having various properties including biodegradation, non-toxicity and biocompatibility [56]. There are two types of biodegradable polymers namely natural polymers and synthetic polymers [57].

Recently, natural polymer-based composites have been the focus of more attention than synthetic polymer composites for bone tissue engineering applications. This is often because of the biocompatible and biodegradable behavior of natural polymers. The natural-based materials are biopolymers which include polysaccharides (starch, alginate, chitin/chitosan, hylauronic acid derivatives) or proteins (soy, collagen, fibrin gels, silk) and a variety of biofibres, such as lignocelluloses [58]. Natural polymers often possess highly organized structures and may contain an extracellular substance, called ligand, which is necessary to bind with cell receptors. Natural polymers often possess highly organized structures which can guide cells to grow at various stages of development; they may stimulate an immune response at the same time [59] and for these reasons several natural polymers have been reported for their applications in bone tissue engineering [60-62].

Collagen

Collagen is the main protein of the connective tissue in animals and the most abundant protein in mammals, making up about 25% to 35% of the whole-body protein

content. It is naturally found only in metazoa including sponges [63]. The collagen in the tissues of a vertebrate occurs in at least 10 different forms, each predominant in a specific tissue. All the forms share the triple helix structure and variations are restricted to the length of the molecule. Collagen constitutes 1% to 2% of muscle tissue, and accounts for 6% of the weight of strong, tendinous muscles. The drawbacks with using this material for tissue engineering regeneration include its relatively poor mechanical properties [64], the need for cross-linking, the risk of infectious disease being transmitted (viral infections), increase antigenicity and fast biodegradation rate. Further since collagen is a protein, it remains difficult to sterilize without alterations to its structure [65].

Chitosan

Chitosan is a cationic polysaccharide, produced by deacetylation of chitin, which is the structural element in the exoskeleton of crustaceans, like crabs or shrimps. Chitosan purified from shrimp shells is used in a granular hemostatic product, Celox. Over the past two decades, chitosan has been developed considerably in biomedical applications due to its high biocompatibility, biodegradability, porous structure, suitability for cell ingrowth, osteoconduction and intrinsic antibacterial nature [66]. Scaffolds with various pore sizes and porosities were produced by selecting the appropriate solvent and optimizing processing conditions. Despite their flexibility, chitosan scaffolds mechanical properties are inferior to those of normal bone.

Moreover, chitosan itself is not osteoconductive, although addition of ceramic materials improves its osteoconductivity and mechanical strength [67].

Silk fibroin

Silk, popularly known in the textile industry for its lustre and mechanical properties, is produced by culture silkworms and spiders. Silk-based biomaterials have demonstrated excellent biocompatibility in different materials formats for various tissue applications. Silks represent a unique family of structural proteins that are; biocompatible, degradable, mechanically superior, and non-cytotoxic, offer a wide range of properties, are amenable to aqueous or organic solvent processing and can be chemically modified to suit a wide range of biomedical applications [68]. Its unique structural assembly and its notable mechanical properties, when compared to other biopolymers-based biomaterials, make this material a promising candidate for bone tissue engineering. At the same time, silk is a thermally stable material, allowing processing over a wide range of temperatures (up to about 250°C), which makes it a good candidate for autoclave systems without loss of functional integrity [69]. Silk are fibrous proteins synthetized in specialized epithelial cells that line glands in these organisms. These properties of silk and their benefits have generated a high interest in electrospinning silk from several sources, like spider, silk worm cocoon and recombinant hybrid silk-like polymers.

Silk fibroin polymers consist of repetitive protein sequences and provide structural roles in cocoon formation, nest building, traps, web formation, safety lines and egg

protection. Silk is formed of β-sheet structures, dominated by hydrophobic domains consisting of short chain amino acids in the primary sequence. These short sequences permit tight packing of stacked sheets of hydrogen bonded anti-parallel chains of the protein. Large hydrophobic domains interspaced with smaller hydrophilic domains foster the assembly of silk and the strength and resiliency of silk fibres.

Silk from silkworms (*Bombyx mori*) and orb-weaving spiders (Nephila *clavipes*) have been explored to understand the processing mechanisms and to exploit the properties of these proteins for use as biomaterials. Functional differences among silks of different species and within a species are a result of structural differences, which emerge from differences in primary amino acid sequence. Blends of silk fibroin-PEO have been electrospun into nanoscale diameter fibres for the delivery of cell morphogens like bone morphogenetic protein-2 (BMP-2) [70]. Silk fibroin films have been cast from aqueous or organis colvents systems, and after blending with other polymers. Nanoscale silk fibroin film was produced using a layer-by-leyer technique. Due to their stability and topography hMSC adhesion and proliferation was supported [71]. Also silk fibroin film showed fibroblast attachment as high as for collagen films [72]. Since the exploration of biomaterial applications for silk, aside from sutures, is only a relative recent advance, the use of structural proteins for clinical applications needs to be investigated.

Polyhydroxybutyrate/Polyhydroxyvalerate (PHB/PHV)

Polyhydroxyalkanoates (PHAs) are emerging as a class of biodegradable polymers. These are polyesters composed of hydrocarboxylic acids, accumulated as energy/carbon

storage or reducing power material by numerous microorganisms under unfavourable growth conditions, in the presence of excess carbon sources. They are completely degradable, possessing similar properties as the synthetic polymers, which makes them suitable for use as biodegradable substitutes for polymer applications. PHAs can be classified into 2 groups: short-chain-length (SCL) PHAs, exhibiting 3-5 carbon atoms, and medium-chain-length (MCL) PHAs, consisting of 6-14 carbon atoms [73]. A recent study [74] identified in several bacteria, PHAs containing both SCL- and MCL- monomer units. These SCL-MCL-PHAs copolymers were shown to possess superior material properties compared to those containing just SCL- or MCL- monomers. Due to the variable composition of PHAs, implant made of these materials can have different physiochemical properties and degrade at a tailored rate in biological media, retaining their mechanical strength for a shorter or a longer period of time. Various *in vivo* and *in vitro* experiments have shown that polymers from PHA family are compatible with bone and cartilage tissue [75-80]. Table 2 details the properties of polyhydroxybutyrate, a member of the PHAs family.

Table 2 Properties of poly (3- hydroxybutyrate adapted from Qiang *et al* [81]

Properties	Measurements
Melting temperature (°C)	160-177
Glass transition temperature (°C)	-4 to +15
Tensile strength (MPa)	15-40
Tensile modulus (GPa)	1.1-3.5
Crystallinity (%)	55-80
Elongation at break (%)	1-6
Density(gcm$^{-3)}$	1.243
Polydispersity index	1.9-2.1
Degradation period	>52 weeks
Mode of degradation	Hydrolytic, bacterial depolymerize
Contact angle (°)	66

There are more than 100 different reported PHAs, however only a few have been studied, and no research has been conducted on the combination of SCL- MCL-PHAs has been conducted yet to use them as biomaterials for tissue engineering purposes [81, 82]. It would however be important to understand the effect of these combinations on the mechanical and structural properties of PHAs for possible future use for different tissue engineering applications.

The most common polymer from the group of PHAs is poly (3-hydroxybutyrate) (PHB). PHB is a semi-crystalline isotactic polymer, having a melting temperature in the range of 160-180°C [83] and a crystallinity ranging from 60 to 90% [84]. In addition to a bacterial synthetic route, several chemical synthetic routes have been developed for PHB synthesis. The main disadvantages of PHB use are due to its tendency to be brittle. This problem can be solved by the synthesis of copolymers of 3- hydroxybutyrate and other hydroxyalkanoates with a relatively low molecular weight and melting point [85]. Polyhydroxy valerate (PHV) is one of the copolymers used for that matter. The major advantage of the PHB/PHV copolymer over the PHB homopolymer is that the copolymer has a lower flexural modulus or level of crystallinity, which makes it

tougher and more flexible. The copolymers of PHB and PHB/PHV have similar semi-crystalline properties as PHB, however the melting temperature is lower depending on the HV content [86]. The crystallinity and mechanical properties of PHB/PHV can change with respect to the variation of the percentage ratio of the respective monomers. This type of polymers experiences surface erosion by hydrolytic cleavage of the ester bonds. Copolymers degrade by a multistage process where the greater part of the molecular weight loss occurs before the considerable mass loss [87]. Even though no correlation has been found between the degradation rate and the amount of PHV in the copolymer, PHB/PHV being less crystalline than PHB undergoes degradation at a much faster rate [86]. This could be explained by the fact that an attack by degrading enzymes is more difficult with highly crystalline polymers [88].2.5.2 Bioceramics

Bioceramics have been widely used in the biomedical engineering and bone substitution/regeneration field due to their resemblance, chemically and mechanically to the mineral phase of bone and their biocompatibility, bioactivity and osteoconductivity [89], [90]. They can also be natural (e.g. coralline hydroxyapatite (HAp)) in origin or can be synthetic, such as synthetic HAp or b-tricalcium phosphate (b-TCP) [91].

For tissue engineering use, classical ceramic production techniques are being used. Basic substitutes are prepared by chemical synthesis and used as powders. After calcinations at $900^{o}C$, the powder is sintered (heated and compacted) at around $1100^{O}C$-$1300^{O}C$. This treatment increases and consolidates the density of the powders. For biological purposes a specific porosity must be kept as to preserve the bioactive and osteocondutive properties of the implant [92]. Research has shown that by using ceramics with or without bone marrow cells, good results regarding bone regeneration

30

can be obtained [93-96]. However, these materials have some major drawbacks, such as brittleness and low mechanical stability. Furthermore, due to factors that appear *in vivo*, such as osteoclastic activity, their degradation/dissolution rates are difficult to predict. This could present a problem because if a scaffold degrades too fast it will compromise the mechanical stability of the construct, which is low by itself. At the same time as demonstrated by *Adams et al* [97], this would dramatically increase the extracellular concentrations of Ca and P, which can cause cellular death.

Hydroxyapatite

Unlike the other calcium phosphates, hydroxyapatite (HAp) ([$Ca_5 (PO_4)_3 OH$], main crystalline component of bone, does not break down under physiological conditions. HAp has a similar chemical and phase composition to the living bone, and its bioactive behaviour has proven to accelerate the integration of prostheses *in vivo* [98]. HAp has been clinically applied in many areas of dentistry and orthopaedics due to its excellent osteoconductivity and bioactivity, which are due to its similarity with the mineral portion of the hard tissue [99-101]. In fact, it is thermodynamically stable at physiological pH and actively takes part in bone bonding, forming strong chemical bonds with surrounding bone. This property has been exploited for rapid bone repair after major trauma or surgery. While its mechanical properties have been found to be unsuitable for load-bearing applications such as orthopaedics, it is used as a coating on materials such as titanium and titanium alloys, where it can contribute its 'bioactive' properties, while the metallic component supports the load applied by the body or as fillers in the composite formulation [102].

31

2.5.3. Biocomposites

The scaffolds containing polymers and ceramic materials can exhibit excellent properties such as biodegradation, biocompatibility and mechanical strength. Polymers are classified as biodegradable, versus non-degradable (permanent) depending on their *in vivo* clearance. Biodegradable polymers are polymers which are decomposed in a living body by hydrolitic or enzymatic activity [103]. Factors controlling the rate of degradation include: the crystallinity percent, the molecular weight and the hydrophobicity. Further the degradation rate varies, depending on the location in the body as the environment surrounding the polymer is different depending on its place in the body. Polymers (ionic and nonionic) with molecular mass below renal threshold barrier are usually cleared quickly from the blood and eliminated from the body via the renal system [104]. Biodegradation can be obtained by using polymers that have hydrolytically unstable linkages in the back bone. An implant prepared from biodegradable polymers can be engineered to degrade at a rate that will slowly transfer load to the healing back bone. These should possess some other requirements such as: (i) polymers and their decomposition products should be free from immunogenicity or any toxicity; (ii) degradation and absorption rates should be adequate for the formation of the novel tissue; and (iii) these products should have good processability and excellent mechanical properties to be compatible with human tissues [103].

Polymers are easily processed to form complex shapes and structures, yet they lack strong interfacial bonding of the implant to living bone tissue, thus they do not have the ability to form the active apatite layer on the implant surface (known as the bioactivity feature). At the same time they are flexible and possess low mechanical properties, which make them poor candidates to be used in surgery and in the

physiological environment on their own [105]. These are reasons to try and combine the biodegradability of the polymers with the bioactivity of the ceramics, to achieve a composite material suitable for load bearing applications, such as bone tissue engineering.

Composites are mainly being used for their improved physiological, biological and mechanical features. While a scaffold is a porous structure, providing space for cell attachment and proliferation, which enables tissue regeneration, it should also exhibit adequate mechanical properties, to properly substitute the missing bone, while the new bone is being generated. The original concept of using a bioceramic to reinforce a polymer for biomedical applications was introduced by Bonfield *et al.* in the early 1980s [106].

Hydroxyapatite provides the bone's compression strength and is one of the most extensively used bioactive ceramics to form composites with polyhydroxyalkanoates (PHAs) [81]. The research conducted by Ni and Wang [107] showed that addition of hydroxyapatite to polyhydroxybutyrate (PHB - part of PHA class of natural polymers) increased the storage modulus of the composite, by inducing the formation of apatite layer, acting as a barrier and delaying the degradation of the polymer. Hu *et al.* [108] found that the amount of hydroxyapatite had a direct influence on the rate of deterioration of the composite's properties after being immersed in simulated body fluid (SBF). At the same time, a large amount of hydroxyapatite can have a detrimental effect on the stiffness and strength of the composite, meaning there is an optimal amount of ceramic that may be added [81]. Since bone, particularly, is a natural composite made of collagen and calcium phosphate mineral, whose mineral phase accounts for 60–70% of the total dry bone weight it seems reasonable to consider biocomposites as potential artificial substitutes in bone tissue engineering, as a biomimetic approach.

2.6. Electrospinning

Electrospinning is a process of making continuous fibres with diameters ranging from nanometers to a few micrometers. Using this technique one can create fibres with different morphologies and orientation [109]. This technique offers unique capabilities in fabrics and fibres with controllable pore structure [70].

2.6.1 Electrospinning background

The technique was invented in early 1930's, but the true biomedical interest in the 1990s revived it. With smaller pores and higher surface area than regular fibres, electrospun fibres have been used in drug delivery systems, wound dressing materials, tissue scaffolds, textiles and composites. The electrospinning process is relatively simple and requires simple equipment, mainly a high voltage power supply, a solution feeder (capillary tube/syringe called spinneret) and a collector. A schematic of this equipment is shown in Figure 5.

Currently there are two standard electrospinning setups: one vertical and one horizontal. The electrospinning process can be conducted at room temperature with atmospheric conditions. Electrospun materials include polymers, glasses and ceramics. After the material is placed in the capillary tube exhibiting a needle like tip, a high voltage is applied. This charges the polymer, creating a repulsive force (a charge is induced on the surface of the solution, as result of free charges moving opposite to the

charged electrode). This repulsive force acts as a tensile force and as the voltage increases, it overcomes the surface tension of the solution and once the voltage is increased even more, a charged jet is released from the capillary tube heading towards the collector. On its way to the collector, the jet bends in a whipping motion, due to the instability of the electrical field, and it elongates into a fibre-like form. As the jet is charged it can be controlled by the electric field.
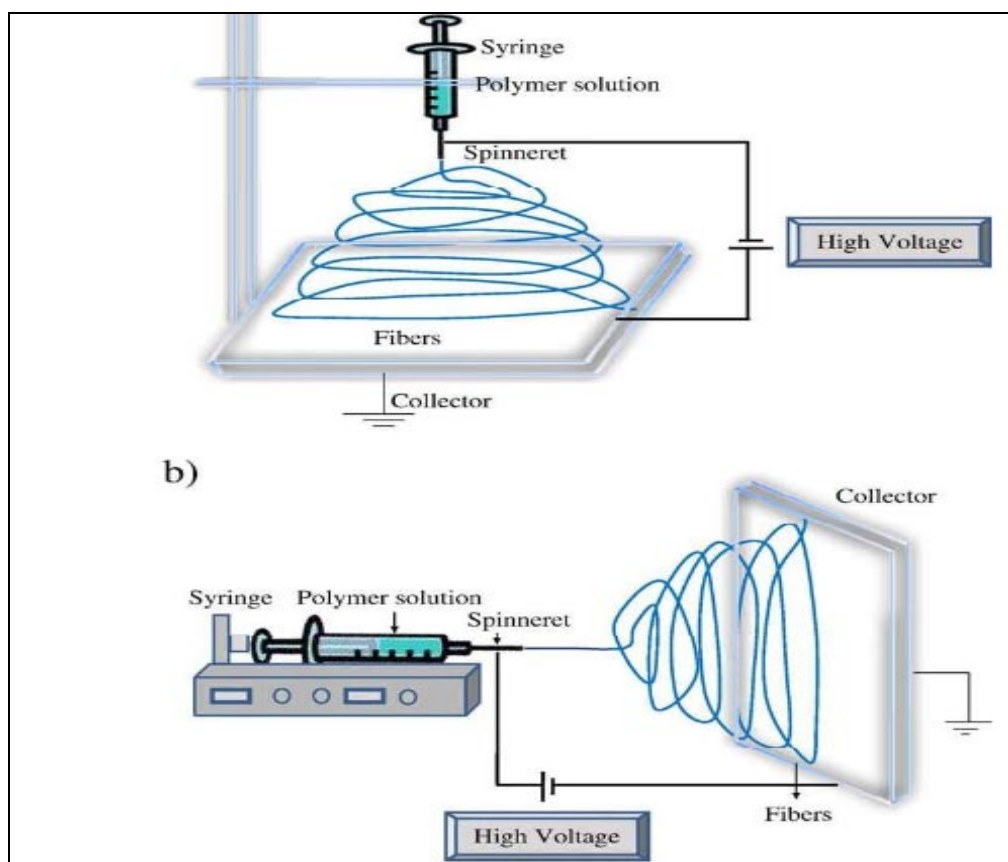
Figure 5 Schematic of electrospinning equipment: a) vertical set up b) horizontal set up (Reproduced with permission of Elsevier Limited) [110]

Research has been conducted to highlight the important factors of the electrospinning process, factors that can help control the morphology and alignment of

fibres. Control of the structure is a very important feature, especially in tissue engineering applications, because the scaffolds structures must attempt and replicate as much as possible the human body's own scaffolding architecture..

2.6.2 Electrospinning conditions

The electrospinning process is subject to the influence of several parameters, and Tan *et al.* [111] classified these into three categories: polymer solution parameters, processing parameters and ambient parameters as shown in Table 3.

Table 3 Parameters that affect the electrospinning process [111]

Polymer solution parameters	Processing parameters	Ambient parameters
Molecular weight	Applied voltage	Humidity
Viscosity	Feed rate	Type of atmosphere
Surface tension	Temperature	Pressure
Solution conductivity	Effect of collector	
	Diameter of needle	
	Distance between tip and collector	

Electrospun fibre diameter has been found [112] to depend mainly on the electrical force and the mass of the polymer. The parameters affecting electrical force and polymer mass were subsequently divided into two groups and were found that when the fibre morphology is dominated by the mass of the polymer, fibres with smaller diameters are produced if low polymer concentration, feed rate and applied voltage are being used. On the other hand, when the electrical force dominates the process, smaller diameters result if a higher voltage and solution conductivity are used.

2.6.3 Requirement of fibrous scaffolds

A scaffolding structure to support cell growth should mimic the natural extracellular matrix (ECM). Its features should match the nanofibrous scaffold to the tissue structure at the specific location. In the case of hard tissue engineering, bone is formed where stresses require its presence and resorbed where stresses do not require it.

The ECM is a complex combination of protein (collagen, fibronectin) and growth promoting proteins, that together support cell growth and adhesion [113].

Scaffolding matrix for tissue engineering applications should present:

- the correct composition of materials

- large surface area

- adequate fibre size

- open, porous structure

- high degree of interconnectivity between pores

- degradability in time

- matching mechanical properties

Currently, through engineering material properties manipulation and the variation of synthetic polymers surfaces, they can be made more conducive for cell attachment and function. At the same time, natural polymers may already present/contain signaling capabilities. On the other hand synthetic polymers provide the strength and durability to the structure, while the natural material is used to promote cell adhesion [114]. A large surface area to volume ratio can result in small diameter fibres and can be very

important parameter, giving space to a large number of cells to attach to the matrix. These cells help restore the natural tissue and its functions.

Depending on the application, pore size is an important feature of the scaffold. Pores that are too small make cell penetration impossible, thus do not promote further growth [115]. On the other hand, pores that are too large reduce the surface area. A balance must be kept between pore size and surface area requirements. *In vitro* tests for bone tissue indicated that pore size of 200-500 µm are suitable for scaffold structures [116, 117] while for liver or skin, smaller ones are required [118, 119]. At the same time a closed porous structure would not help cell penetration, which would make tissue regeneration and regrowth, impossible. A high degree of interconnectivity between pores is important for a number of reasons [115] – uniform cells distribution, cell survival, cell penetration into the structure and nutrients and waste regulation.

The scaffolding structure must mimic the ECM, as mentioned before, and provide a temporary 3D host structure for cell activity in the early stages of tissue development. Due to the matrix deposition over time by the cells the scaffold must have the ability to degrade over time, so the risk of rejecting is reduced.

One important factor when choosing the biomaterials is that of the scaffold degradation rate. Degrading too early could result in the loss of support of the cells with the natural matrix not being restored. Degrading too late may inhibit natural matrix growth and alsocell proliferation. The biodegradability feature is related to the materials being used for the production of the scaffold.

Furthermore another important factor is biocompatibility, referring to whether the material is suitable for human body use, and the cell interactions due to the chemical composition of the materials [120].

The mechanical properties are also important for the structural stability during tissue regeneration or any other load bearing requirements. Bone substitutes are also strongly influenced by local mechanical forces during the remodelling stage. The density, geometry, thickness, and trabecular orientation of bone can change depending on the mechanical demands of the substitute. In 1892, Wolff first popularized the concept of structural adaptation of bone, noting that bone placed under compressive or tensile stress is remodeled. Bone is constantly remodelled [121, 122] and this serves to regulate the structural strength of the substitute. For example, if the substitute is significantly shielded from mechanical stresses, as in the case of rigid spinal implants, excessive bone resorption can potentially occur and result in a weakening of the substitute.

2.6.4 Electrospun fibres as bone tissue scaffolds

Natural bone is a complex nano-fibril system with an intricate hierarchical structure with an orderly deposition of hydroxyapatite crystals within the polymer matrix. The crystallographic c-axis of hydroxyapatite is oriented parallel to the longitudinal axis of the polymer (collagen) fibril [123]. The alignment of electrospun fibres could be preset as to match the orientation in the natural bone. An innovative method of forming electrospun fibrous mats, with nHAp crystals could help in future approaches in bone tissue regeneration.

Even though synthetic polymers and their blends exhibit biocompatibility and good mechanical properties, novel biopolymer composites (biocomposites) based on biodegradable and bioresorbable materials have received an increasing interest over the last decades. The co-precipitation of HAp nanocrystals in soluble collagen has met with

partial success in the fabrication of electrospun HAp–collagen nanocomposites similar to the nanostructure of real bone, though with weaker mechanical properties [124]. On the other hand, carbonate-substituted HAp–chitosan/silk fibroin composites prepared using a co-precipitation method exhibited better compressive strength and cellular response, mimicking the real bone [125]. Simultaneous gas-jet and electrospinning of composite solution containing hydroxyyapatite have been used to manufacture porous scaffolds suitable for bone regeneration [28, 126]. Other attempts of adding hydroxyapatite to the electrospun fibres have been made, either by soaking the fibrous polymeric matrix in simulated body fluid (SBF) [29] or by co-precipitation and nucleation [30, 31]. PLGA/HAp fibrous composite scaffolds were also prepared, mainly used for drug delivery instead of a single repair [32-34].

2.6.5 Challenges and approaches

A major challenge for reconstructive and orthopedic surgery involves the repair of bone defects arising from tumor, trauma or bone diseases. Autogenic and allogenic bone functions better in terms of biocompatibility, but requires a second surgery to procure donor bone from the patient's own body. At the same time, a lot of work still needs to be conducted in order to mimic the natural bone [127]. However, with the development of the electrospinning process, electrospun fibrous scaffolds with large surface area-to-volume ratio, high porosity, and mechanical properties and morphology similar to the extracellular matrix (ECM) of natural tissue can be fabricated to serve as ideal bone substitutes [128, 129].

An understanding of the effect of process variables will help to control the morphology of the produced fibre structure. One big issue is the low productivity of the system which can be attributed to the low polymer ratios through the capillary. Some solutions have been proposed (multiple spinnerets, porous cylindrical tubes) but all these come with disadvantages, like interference between jets, large variation of fibre diameter. There are still shortcomings in producing highly aligned gradient structures of required thickness [130].

Also an understanding of the materials components interaction will help to control the final fibrous structure, and also predict cellular behavior in terms of bone regeneration.

This research study aims to address some of the challenges presented above and produce a three-dimensional scaffold intended for bone-tissue regeneration using a composite formulation not studied before. The main aim is to electrospin nano-hydroxyapatite within the chosen polymeric matrix, thus formulating a novel composite solution and avoiding using a two-step process for ceramic phase incorporation. Further physical and chemical analysis of the manufactured structures and continuous improvement of them is required. The final step will be the biological *in vitro* testing of the scaffolds, that aims to prove that the novel structures enhance cellular attachment, proliferation and maintain phenotype expression of bone cells, while offering a physical support over time for bone reconstruction. The three-dimensional structures produced should exhibit characteristics that would enable them to be used either as cell carrier systems for neo tissue formation *in vitro* or/and as a scaffold structure for *in vivo* tissue regeneration.

CHAPTER 3 MATERIALS AND METHODS

This chapter outlines the equipment, the materials and the experimental methods used in the current research.

3.1 Materials and equipment

Several requirements were imposed before choosing the materials. The selected materials would have to be biocompatible, biodegradable/absorbable by the body, have no toxic effects in the body, and that any degradation products could be further used by the human body (such as aminoacids). All materials used were of the highest commercially available purity. Appendix A presents the materials used in this research, while appendix B presents the list of equipments.

3.2 Methods

Figure 6 presents the experimental sequences and the associated tests.

1. Raw materials selection and characterisation

- SEM/EDX
- DTA/TGA
- FT-IR/ RAMAN

2.Screening Process (trial and error) in terms of composite composition and electrospinning parameters

- SEM/EDX
- FT-IR/RAMAN
- Contact angle measurements
- Preliminary biological testing (cell adhesion and proliferation)

3.Design of Experiments (optimal range of composites and set of parameters; two dimensional membranes fabrication)

- Contact angle
- Fibre diameter
- SEM/EDX

4. Three dimensional fibrous electrospun construct manufacturing

- Physical assessment
  - degradation behavior (pH, weight loss)
  - FT-IR/RAMAN
  - SEM.EDX
  - Mechanical testing(tensile and compression)

- Biological assessment
  - cell viability and proliferation
  - bone markers expression (osteopontin, collagen type I, bone alkaline phosphatase)

Figure 6 Schematic representation of the research work.

3.2.1. Solutions preparation

Pure polymeric solution preparation

After the physical characterization of the raw materials, solutions were prepared for further study. Firstly, pure polymer solutions (7%, 10%, and 15% PHB/PHV in chloroform) were prepared for the screening step. In order for the polymer to dissolve the solution was heated to 60ºC - 70ºC and stirred continuously for 15 minutes, until complete dissolution (15%PHB/PHV, t =15 min). Before attempting electrospinning the solution was left to cool down at room temperature (T= 21 ºC ± 1°).

Composite solution preparation

The solution used during the research process was continuously improved from an initial bi-phasic composite solution (polymer and ceramic) to a final tri-phasic composite solution (polymer + nano-ceramic + fibroin). The polymer matrix was formed by the polyhydroxybutyrate 98%- polyhydroxyvalerate 2% polymer (Good Fellow, UK), while the ceramic phase was formed by the nHAp particles (Sigma Aldrich, Ireland). As mentioned earlier to balance the change in the solution's electrospinning dynamic, silk fibroin essence (Huzhou Sunergy World Trade Co. Ltd, China).

Firstly, a pure 15% PHB/PHV solution was chosen as the most suitable for future studies, named solution P. One novel aspect of the research project was to attempt electrospinning of the ceramic phase while incorporated in the polymeric material. For this purpose a preliminary composite solution of 15%PHB/PHV – 2%

nHAp (named solution P-HAp) was formed by mixing nHAp to the 15%PHB/PHV solution for t = 5 min. After the composite solution was left to cool down (t = 30 min), the solution was used on the same day. The preliminary solution P-nHAp could not be used from one day to another, as after 24 hours the ceramic phase was not fully dispersed; rather it was visible on the bottom of the container and mixing the solution again did not disperse the nHAp phase.

In order to achieve a good dispersion of the nano-ceramic particles the solution-HAp preparation protocol was changed, as follows:

1. nHAp was added to chloroform in a glass reagent and immersed in the ultrasonic bath for t = 10 min.
2. PHB/PHV was added to the sonicated nHAp- chloroform solution.
3. The composite solution was mixed at T = 60ºC - 70ºC, using a hot plate for t= 15 min
4. The composite solution was left to cool down, t = 30min.

The following day the P-nHAp solution, prepared as described above, did not show any deposit of ceramic particles on the bottom of the container and this allowed it to be reused for several days. Further to this the P-nHAp solution was difficult to electrospin, with no continuous deposition observed. Also a change in the fluidity of the solution was observed.

In order to change the conductivity of the solution and make the fibre deposition easier and continuous, silk fibroin was added (solution P- nHAp-SF). Silk fibroin is known to be biocompatible and also as an amino acid it can be used by the human body for its metabolic processes.

The final protocol for the composite preparation is presented as follows while Table 4 highlights the solutions' formulation codes:nHAp and chloroform were sonicated for 15 minutes, in order to disperse the ceramic particles.

1. PHB/PHV was added, heated (T= 60-70ºC) and continuously mixed until complete dissolution (t = 15min). A viscous solution of desired concentration was obtained.

2. Silk fibroin (SF) was added to the P-nHAp solution and mixed for10min.

3. The tri-phasic solution (P-nHAp-SF) was left to cool down, t = 30 min.

Table 4 Naming coding to indicate the relative amount of their components mixed or dissolved in chloroform

Powder or solution	Code	Amount in the solution (wt %)
Polyhydroxybuutyrate-co-hydroxyvalerate 2% solution (15% polymer in chloroform)	P15	15
Polyhydroxybuutyrate-co-hydroxyvalerate 2%- x % hydroxyapatite solution	$P15H_X$	x= 1-30
Polyhydroxybuutyrate-co-hydroxyvalerate 2%- x% hydroxyapatite solution- y% silk fibroin	$P15H_xSF_Y$	x=1-30 y=1-30

Manufacturing of 3D constructs

Various techniques for generating 3D porous structures (hydrospinning, stacking, laser welding, sintering) were attempted using the same composite solution and the viable ones were further investigated according to the research plan.

Previous research has shown that 3D electrospun structures have been created using the hydrospinning method [211]. Using roughly the same electrospinning set-up as for a 2D sample collection (Figure 7), 3D porous constructs have been produced in our laboratory. The fibres were collected on the surface of the liquid (deionised water), where a thin layer was rapidly formed, and was kept afloat. This thin layer was picked from the surface of the liquid on a glass at certain time intervals, eventually creating a hydrospun scaffold composed of many fibrous layers. Despite their 3D structure, the scaffolds were very delicate when manipulated and were time consuming to produce. Each layer was spun for 20 minutes and each 3D construct was composed of 5-10 hydrospun layers.

Glass slide
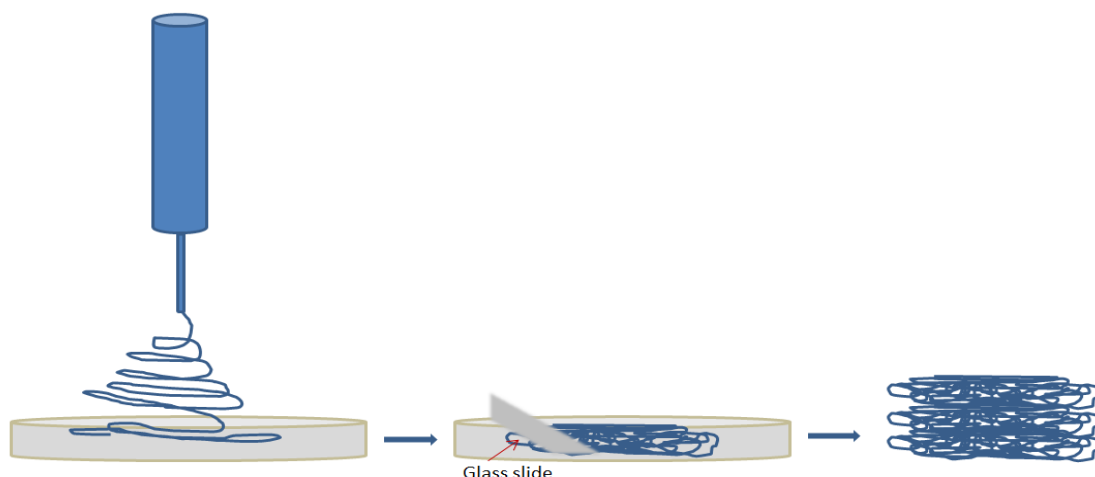
Figure 7 Hydrospinning technique schematic

Another method employed to produce prototype 3D structures used laser welding. The laser welding trials were performed by Blueacre Technology (Dundalk, Co. Louth, Ireland). The laser used to weld the sample was a Synrad CO_2 laser operating at 10.6µm wavelength. The laser power was modulated to 4W at 5kHz. The

laser spot size was approximately 300um at the 1/(e^2) point, and the laser was scanned across samples using galvanometer moving at 200mm/s, with 3 passes being made in total.

3.2.2 Surface Morphology

The surface morphology of the powders and the composites was assessed by Scanning Electron Microscope (EVO LS15 SEM/EDX from Zeiss) with image analysis and qualitative EDX capabilities. Using detectors, the microscope can detect 3 signals, such as secondary electron backscattered and characteristic x-rays.

The SEM works by scanning a high-energy beam of electrons, which interacts with the sample's atoms. These interactions produce signals which provide information about the samples' surface: topography, composition, etc. The SEM includes special detectors which interpret important signals, thus lending their name to the different SEM working modes.

The materials used in this research are non-conductive, so they need special preparation to prevent electrical charging during SEM examination. The powders/ composite were first fixed to an aluminium stub especially designed to fit into the SEM stage holes, using conductive double-sided tape. The samples were then placed into the chamber of an Edwards Pirani 501 Scancoat sputtering coater in which a gold nanometric layer (3-5nm) was deposited onto the powders for over 120 seconds. This

layer ensured the electrical conductivity of the samples, thus improving the imaging of the sample morphology. For the composite characterization the SEM back-scattered electrons signal (BSE) at an accelerated voltage of 10-20kV (samples without cells) and 5kV (samples with cells) and the EDX were used in order to study any possible chemical reaction between the polymer and the powders.3.3.3 Fibre diameter and thickness measurements The images captured by the SEM while analysing the samples morphology were used to determine the fibre diameter. The measurements were performed using the Image J image processor and the Appendix A shows the protocol that was followed. An average value of 20 measurements was used as the result.

Samples thickness was assessed using an optical microscope. Samples were mounted on glass slides for a better visualisation and 3 measurements were taken for each sample (left end, middle of the sample, right end) and the average value calculated. A set of 5 samples of each type was used for measurements.

3.3.4 Thermal Behaviour

It is important to determine the thermal characteristics of the powders and composites, specially the polymeric types, as their mechanical behaviour can depend on their thermal characteristics. The chosen polymers are natural ones and may have distinct thermal behaviour, depending on the way they were synthesized. The thermal techniques used are reviewed in this section.

Differential thermal and thermogravimetric analysis were used to thermally characterise the powders/composites used in this research. For this a DTA/TGA-

Simultaneous Thermal Analysis (STA), PL Thermal Sciences Ltd., UK was used. The analysis was carried out by linearly increasing the temperature by $20^{\circ}C$/min from $20^{\circ}C$ to $600^{\circ}C$ in a nitrogen atmosphere. The total weight of the specimen for each thermal analysis was 20 mg.

• *Differential Thermal Analysis (DTA)*

During DTA, the material to be analyzed and an inert reference material experience identical thermal cycles, and measurements are conducted to identify any temperature difference between the sample and the reference. The results are plotted against time or against temperature and this is called a 'DTA curve' or thermogram. Either exothermic or endothermic changes can be detected relative to the inert reference. Thus, a DTA curve provides data on the transformations that have occurred, such as glass transitions, crystallization, melting and sublimation. The area under a DTA peak shows the enthalpy change and is not affected by the heat capacity of the sample. Nowadays, DTA technology is incorporated into the TGA equipment, which provides both mass loss and thermal information.

• *Thermo Gravimetric Analysis (TGA)*

This test is based on the weight change of materials with temperature. Twenty milligrams of a sample areplaced inside a ceramic pan in a high precision balance. The content of the balance is placed in an electrically heated oven. Three measurements are conducted during the test: weight, temperature (using a built in thermocouple) and temperature variation. The analysis was carried out by linearly increasing the

50

temperature resulting in a weight loss curve that gives information about degradation temperature, absorbed moisture content of samples, solvent residues, etc.

3.3.5 Chemical composition

Further Fourier Transform Infrared (FTIR) spectroscopy assessed the chemical composition of the powders and the composite samples. FTIR is a chemically- specific analysis technique that can be used to identify chemical compounds and substituent groups, measuring the infrared intensity versus wavelength (wavenumber) of light. A Fourier Transform Infrared (FTIR) spectrometer obtains infrared spectra by first collecting an interferogram of a sample signal with an interferometer, which measures all the infrared frequencies simultaneously. An FTIR spectrometer acquires and digitizes an interferogram, performs the Fourier transform function, and outputs the spectrum.

The FTIR equipment used in this research was a FTIR Spectrum GX from Perkin-Elmer. A mixture of the powder to be tested (2 mg) and potassium bromide salt (200 mg) was ground in a marble mortar for 10 minutes, to avoid scattering from large crystals [131]. The ground powder was then added into a die and pressed at 12 kPa for 15 minutes to form a translucent pellet, which allows the IR beam to pass through it. Following this, the results are recorded and analysed.

A complementary technique to FT-IR is Raman spectroscopy. Raman spectroscopy provides information about molecular vibrations that can be used for sample identification and quantitation. The technique involves shining a monochromatic light source (i.e. laser) on a sample and detecting the scattered light. Raman scattering

measurements were used to determine the presence of apatite layer formed on the surface of the fibrous samples after one month in SBF. Measurements were performed using a HoribaYvon LabRAM 800 HR. The parameters used for the spectra were as follows: Excitation laser - 784.7 nm diode laser, Grating 600 g/mm, Objective 50x Fluortar, 6 accumulations at an exposure time of 4 seconds.

3.3.6 Roughness measurements

Surface roughness is a measure of the texture of the surface. It plays an important role in determing how a material interacts with its surrounding environment. Rough surfaces will wear more than smooth surfaces and have higher friction coefficients. Also having information on roughness can indicate the mechanical performances of the material, since surface irregularities may form nucleation sites for cracks and corrosion. Further the degree of roughness has also an impact on the attachment of the cells. Roughness can be measured using contact or non- contact methods. Non-contact methods include interferometry, confocal microscopy, electrical capacitance and electron microscopy.

A Surftest-402 profiler from Mitutoyo was used to determine the average surface roughness (R_a) of the samples. The profilometer was first calibrated with a surface with known roughness (1 μm), before the flat samples were placed in contact with the tip of the profilometer. The average Ra value for each deposit was calculated as the average of 10 measurements.

3.3.7. Surface hydrophilicity

A hydrophilic material is a material that can transiently bond to water through hydrogen bonding. This property makes the material dissolve more readily in water than in oil or other hydrophobic solvents. The degradation profiles of polymers are related to many factors, in which hydrophilicity plays an important role. Hydrophobicity is also linked with surface energy. Whereas surface energy describes interactions with a range of materials, surface hydrophobicity describes these interactions with water only. As water has a huge capacity for bonding, a material with high surface energy (high bonding potential) can enter into more interactions with water and consequently will be more hydrophilic. Therefore hydropobicity generally decreases as surface energy increases.

A simple method that it is used to measure the surface energy and tension is the contact angle measurement. This technique is surface sensitive, with the ability to detect properties on monolayers. If a liquid with well – known properties is used, the resulting interfacial tension can be used to identify the nature of the solid. When a droplet of liquid rests on the surface of a solid, the shape of the droplet is determined by the balance of the interfacial liquid/vapour/solid forces. When a droplet of high surface tension liquid is placed on a solid of low surface energy, the liquid surface tension will determine the droplet ability to form a spherical shape (lowest energy shape). The measurement provides information regarding the bonding energy of the solid surface and the surface tension of the droplet. Due to the fact that this method is a very simple one, yields excellent material surface analysis results when assessing wetting, adhesion and absorption.

The method used in this research was the sessile drop technique, which is shown in Figure 8, using ArtCAM 130 MI BW monochrome camera, and FTA200 contact angle analyzer software. Contact angle evolution was analyzed after 1 and 5 seconds, for samples of pure polymer and composites. For each sample 10 measurements were performed, across 10 different points on the sample surface. Before conducting the measurements the flat samples were cut and cleaned with an air pistol, in order to remove any loose particles.
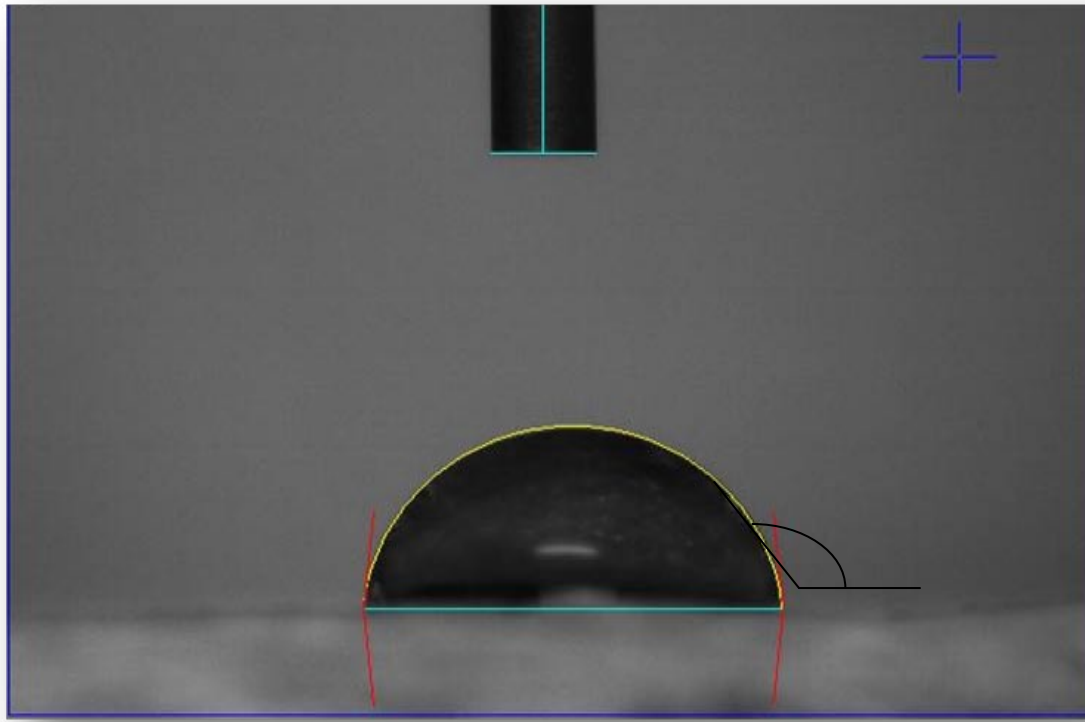
Figure 8 Contact angle measurement using sessile drop method (15%PHB/PHV)

3.3.8 In-situ degradation (pH, conductivity and weight loss measurements)

It is widely assumed that the materials used for tissue, and bone regeneration particularly should degrade over time in the body to provide new space for the extracellular matrix deposition [132]. It is desirable for the produced scaffold matrix, to degrade at a rate that will slowly transfer load to the healing tissue. The scaffold offers support to the polymer/cell/tissue construct from the cell seeding start point up to when the hard tissue transplant is remodelled by the host tissue and can assume its structural role.

Degradation measurements

The degradation process takes place in 4 steps: water sorption, reduction of mechanical properties (strength and modulus), reduction of molar mass and weight loss. There are two types of degradation: bulk erosion and surface erosion. As defined by Gopferich, "polymer degradation is defined as the chemical reaction resulting in a cleavage of main-chain bonds producing shorter oligomers, monomers, and/or other low molecular degradation products" [133]. Both *in vivo* and *in vitro* degradation occur at the same rate which shows initially no significant enzymatic contribution [134]. This is explained since the main mode of degradation for high-molecular-weight aliphatic polyesters can be hydrolytic random scission, and biodegradation is supposed to involved just low-molecular weight by-products ($M_n < 5000$) or sub-micron sized

particles that were recognized and ingested by phagocytes [135]. Degradation tests were conducted over a period of 90 days in order to investigate if the produced composite scaffolds varied the degradation rate and dynamics. In the *in vivo* results the pH changes can affect the tissue regeneration dynamic. For biological research the solution generally used for degradation tests is phosphate buffer solution (PBS). This is a solution resembling the osmolarity and ion strength of the human body, which helps maintain a constant pH. For this research deionised water was used instead of PBS, in order to follow the pH changes which indicated the degradation steps taking place. Specimens of polymeric and composite samples were cut to 1x1 cm^2 and weighed. Each was immersed in 50 ml deionised water and kept for 3 months. Every 30 days one sample was removed from the plastic jar, dried in the fume hood for 24h and weighed. Degradation was reported as % weight loss. Tests were conducted in triplicate and results were expressed in terms of mean average. The effect of degradation was also observed with SEM imaging.

Conductivity and pH change

For normal cell formation pH is a very important factor, due to the fact that cells are very sensitive to it. Cells are suited to a neutral pH level of 7.3-7.4. Even the slightest change in a pH level can cause severe consequences such as the destruction of the cell or even death of the organism. Every organism takes part in various chemical reactions that give or use up H$^+$. For this level to stay constant, a buffer comes into play to maintain the cells normal pH level. It does this by accepting or releasing H$^+$. This mechanism of maintaining a proper balance between acids and bases is called acid-base

homeostasis. Outside the range of pH which is compatible with life, proteins are denatured and digested, enzymes lose their ability to function, and the body is unable to sustain itself.

The conductivity of a solution refers to its ability to conduct an electrical current, and is the reciprocal of its electrical resistance. It is an indicator of the ionic strength of a solution and can be determined at the same time as the pH determination. Also the electrospinning technique relies on conductivity, as being one the parameters that influences fibre formation.

Conductivity and pH measurements were recorded via a Hanna HI 9813 Handheld pH, EC and TCS Meter with Probe (Hanna Instruments, Inc.) with accuracy of pH: ± 0.2 pH at ambient temperature, in order to monitor the degradation process [136].

3.3.9 Mechanical properties

Uniaxial tensile strength tests

Experience shows that polymeric materials display a wide range of mechanical behaviour, from brittle solids to rubber to plastic to strong fibres. Also it is widely known that the mechanical characteristics of a polymer alters with changes in temperature as small as a few degrees, and also if it is used to form a composite material.

For mechanical characterization purposes, flat samples (40 mm × 1mm) were manufactured, tensile strength and elastic modulus of the porous fibrous polymeric and composites samples were determined, using a Zwick/Roell Z500 N universal testing machine equipped with a 20N load cell (Zwick GmbH, Ulm, Germany). The results were plotted with Test Xpert II (Zwick GmbH, Ulm, Germany). Samples were tested up to failure. For each composition 6 samples were tested and results were expressed in terms of mean average and standard deviation.

Compressive tests

For mechanical evaluation under compression, sets of 6 electrospun fibrous cubes were tested for each composite type using a Zwick/Roell Z500 N universal testing machine equipped with a 5kN load cell (Zwick GmbH, Ulm, Germany). Electrospun flat membranes collected over a period of 20 min were folded and cubes of 1cm x 1cm were cut. Constructs thickness varied from 0.3mm for the P0 to 0.4 mm for P2 and P5 composites. The cubes were compressed at a rate of 2mm min^{-1} until 80% strain was reached. Results are expressed in terms of the secant modulus for a stress of 0.4 MPa.

3.3.10 Porosity, pore size and fibre diameter

Interconnecting macroporosity and appropriate microporosity play a fundamental role for optimum biological performance, such as scaffold-cell interaction. Appropiate

pore size and porosity are necessary for cells to interact and develop (spread, migrate), as well as for proper exchange of nutrients and metabolic products between the scaffold and the surrounding environment [137].

The porosity (ε) of the scaffolds was measured at room temperature, using the liquid intrusion method. The electrospun scaffolds were weighed and subsequently immersed in ethanol on a mechanical shaker to allow the liquid to penetrate into the scaffold voids. The surface of the samples was then blotted dry and weighed once more to determine the mass of ethanol present within the scaffold. Measurements were made on five samples of each type of scaffold. Knowing the density of the ethanol and that of each composite the porosity was calculated using [138]:

$$\Phi = V_{ETH} / (V_{ETH} + V_{composite}) \qquad \text{(Eqn. 1)}$$

V_{ETH} is the volume of intruded ethanol and was calculated as the ratio between the observed mass change after intrusion and its density (ρ_{ETH}). $V_{composite}$ is the volume of the composite fibres and was calculated as the ratio between the dry scaffold mass before intrusion and the dry scaffolds density ($\rho_{composite}$).

3.3.11 Bioactivity Test in Simulated Body Fluid (SBF)

Simulated Body Fluid (SBF) it is an acellular solution that has inorganic ion concentrations similar to those of human extracellular fluid. It is often used to

reproduce the formation of apatite on bioactive materials *in vitro*. It was first developed by Kokubo and his colleagues and is since known as SBF or Kokubo solution [139].

SBF has demonstrated its effectiveness via the surface modification of various materials [139]. Initially it was applied as a test to bio-ceramics which were part of bone implants. There are ceramics that bond to the bone through a bone-like apatite layer which forms on ceramics or modified polymers surfaces. Currently the formation of the apatite-layer is not fully understood. It is known that the biomaterial surface must express OH groups, in order to attract the positive ions from the solution and create nucleation sites. On the surface of organic polymer the apatite layer formation takes place in a two-step biomimetic process [140].

Square samples of $10mm^2$ and 50g were cut from the prepared composite membranes, with at least 4 for each HA concentration. The SBF was prepared in the laboratory following Kokubo's recipe [136]. Table 5 shows the concentrations of body plasma and SBF [141].

The samples were immersed in SBF, within plastic containers kept in a water bath (Clifton, Nickel Electro LTD, UK) at 37°C, for 4 weeks. Every week a sample for each HAp concentration was taken out, dried and analyzed using SEM/EDX and FTIR.

Table 5 Ion concentrations (mM) of SBF and human blood plasma [141]

Ion	Simulate Body Fluid (mM)	Blood plasma (mM)
Na^+	142.0	142.0
K^+	5.0	5.0
Mg^{2+}	1.5	1.5
Ca^{2+}	2.5	2.5
Cl^-	148.8	103.0
HCO_3^-	4.2	27.0
HPO_4^{2-}	1.0	1.0
SO_4^{2-}	0.5	0.5

3.3.12 Design of Experiments (DOE)

In order for a scaffold to best fit the application it is design for, it should exhibit adequate properties, resembling as much as possible the ones of the native tissue. Studies on electrospun scaffold with orthopaedic application mainly followed the classical experiment model, varying one electropinning parameter at a time in order to gain a greater understanding of the process [142, 143]. High quality scaffolds require a better understanding of the scientific phenomena involved in their production and this brings the need for more sophisticated and powerful statistical experimental methods.

The Handbook of Statistical Methods defines Design of Experiments (DOE) as follows: "DOE is a systematic, rigorous approach to engineering problem-solving that applies principles and techniques at the data collection stage to ensure the generation of valid, defensible, and supportable engineering conclusions. In addition, all of this is carried out under the constraint of a minimal expenditure of runs, time, and money" [144].

Statistically designed experiments were used to carry out the optimisation stage; using the software Design Expert 8.0 by Stat-Ease Inc. This method is advantageous from an economic perspective as a large amount of information can be obtained from a minimal number of experiments. In the DoE technique, the parameters that affect the experiment are termed "factors" or "variables". The different possibilities for a factor are called "levels". Levels can be either qualitative or quantitative. The measured output from the experiment is termed "the response". Once the experiment has been run, the effect of each factor can be evaluated by contrasting the average response when the

factor was not changed with the average result when it was changed. Responses can then be represented as a polynomial regression equation of the following form:

$$Y = b_0 + \Sigma b_i X_j + \Sigma b_{ij} X_i X_j + \Sigma b_{ijk} X_i X_j X_k \quad \text{(Eqn. 2)}$$

where i, j and k vary from 1 to the number of variables; coefficient b_0 is the mean of the responses of all the experiment; bi coefficient represents the effect of the variable X_i and bij and b_{ijk} are the coefficients of regression which represent the effects of interactions of the variable $X_i X_j$ and $X_i X_j X_k$ respectively and b_{ijk} are the coefficients of regression which represent the effects of interactions of the variable $X_i X_j$ and $X_i X_j X_k$ respectively.

The method selected for a particular experiment depends on considerations such as the objectives of the experiment, the number of factors being investigated and the resources available. For this research work Full Factorial screening design and Response Surface Methodology designs were used.

Factorial design

A factorial experiment is an experiment in which several factors are controlled and their effects at each of two or more levels are investigate [145]. Analysis of a factorial experiment allows the users identify the main effects and also interaction effects between the factors. In a full factorial experiment all possible combinations of the levels of the factors are investigated. Two-level full factorial experiments are the most common. In this type of experiment, factors are set at a low level (coded -1) and a high level (coded +1). A two level experiment with k factors is referred to as a 2^k

experiment. For example, a 2^2 experiment is used to study two factors at two levels and would consist of 4 experiments. The design for this experiment is shown in Table 6.

Table 6 2-factor, 2-level Factorial Experiment

RUN	Factors	
	A	**B**
1	-1	-1
2	+1	-1
3	-1	+1
4	+1	+1

When carrying out experiments, factors may exist that are not of primary interest but still affect the results. Examples of such factors include specific operator methods, different batches of materials and so on. It is necessary to eliminate the effect of these factors from the overall results experiments. This can be achieved by organizing the experiment into blocks. Experiments should also be run in random order to eliminate the effects of any factors that cannot be controlled and cannot be blocked.

Centrepoints are also usually added to factorial designs. These points are the centre value between the high (+1) and low (-1) values selected for each factor and are coded 0. The purpose of centre points is to allow process stability to be determined. Generally between 3 and 6 centrepoints are added to an experiment design.

If a large number of factors are being investigated, full factorial experiments are not very efficient and thus a fractional factorial experiment can be used. Fractional factorial experiments involve fewer than the full 2^k run of experiments [145]. The aim of a fractional factorial experiment is to reduce the number of experimental runs

required by extracting the part of a full factorial experiment which enables the main factors and some first order interactions to be obtained [146]. This is achieved by confounding of the effects of some of the factors and as a result, high order interactions between factors cannot be estimated. This type of experiment can be used to obtain information on the main effects and low-order interactions and is often used for screening designs.

Screening tests

Screening designs are used in the early stages of investigations to allow more information to be obtained about a process. They are generally carried out prior to carrying out a Response Surface Methodology experiment. Screening designs usually have a small number of experimental runs. These studies can identify the factors which have the greatest effect on the process and thus allow the factors under investigation to be reduced. Information can also be obtained about the parameter space under investigation and allow the correct range to be selected for each parameter. This preliminary information can be used to develop a Response Surface Methodology experiment (final optimisation).

Response Surface Methodology (RSM)

Response surface methodology (RSM) can be used to maximize or minimize a response, reduce variation by locating a region where the process is easier to manage or to optimize a response. The two most popular Response Surface Methodology

techniques are the Box-Behnken Design (BBD) and the Central Composite Design (CCD).

The Box-Behnken design is sufficient to fit a quadratic model, which contains squared terms and products of two factors. This design consists of a fraction of the experiments required for a 3-level factorial design (3k runs). It combines 2-level factorial designs with incomplete block designs [147]. As an example, the Box – Behnken design for 3 factors involves three blocks, each with 2 factors to be varied trough 4 possible combinations of high and low. The results of experiments are graphically shown in Figure 9, which include the middle points of the edges of the cube that represent the experimental space.
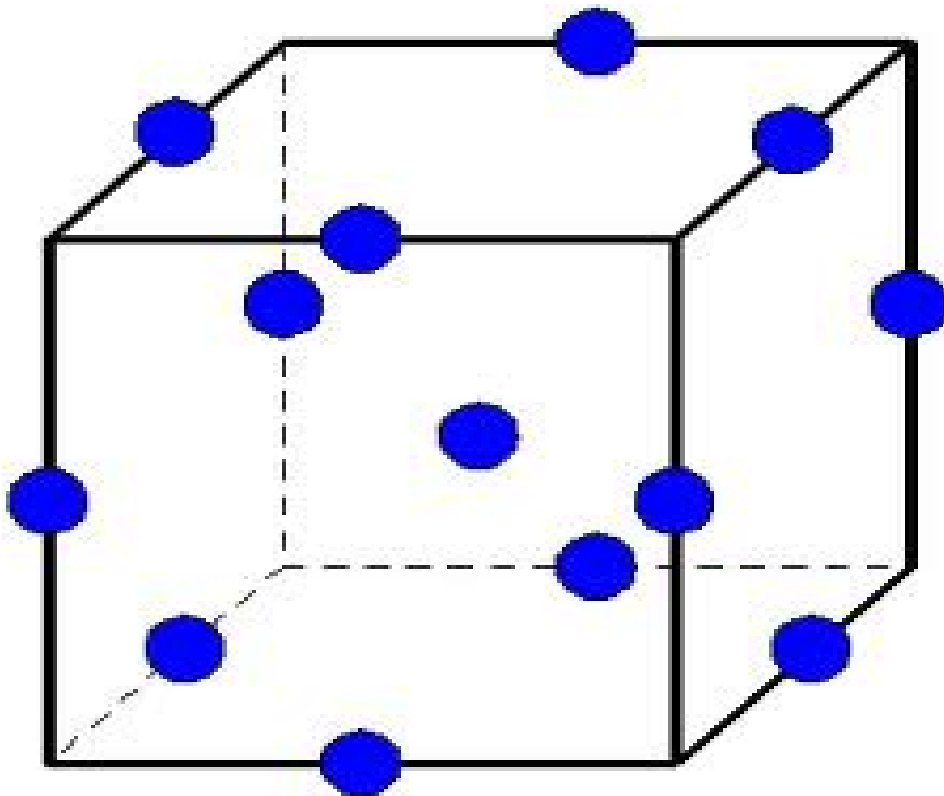
Figure 9 Graphical representation for Box Behnken design for 3 factors [147]

3.3.13 Analysis of Variance (ANOVA)

Analysis of variance was used to study the statistical models results. There are number of statistical terms which aid to evaluate the statistical significance of the models. Basically, a model is adequate if the series of hypothesis shown in Table 7 are true. It is also advisable to achieve Predicted R^2 and Adjusted R^2 values from the model as high towards 1 as possible ensuring good model fitting. The best scenario is achieved when all the three values are close to 1.

Table 7 Hypothesis for a valid model in DOE

Term	Hyphotesis
Model Prob>F	< 0.05
Lack of fit (LOF) Prob> F	>0.1
R^2	$0.6<R^2\leq1$
Predicted R^2 – Adjusted R^2	≤ 0.2
Adequate Precision	> 4

3.3.14 Biological Response of Composite Scaffolds

Qualitative preliminary biological evaluation of the preliminary obtained scaffolds

Cell culture

Human osteoblasts (HOB) (PromoCell, Germany) were used for preliminary evaluation of cell behaviour on the obtained scaffolds. The cells were cultured in PromoCell growth medium, supplemented with 10% heat inactivated foetal calf serum (FCS, PromoCell, Germany), penicillin-streptomycin 10ml/L (Sigma Aldrich, Ireland) and amphotericin 320 µl/L (Sigma Aldrich, Ireland) under standard cell culture conditions (37°C, 5% CO_2). The medium was changed every day. For the biological study cells attached to the culture flask were washed with HEPES-BSS (PromoCell, Germany), trypsinized (trypsin-EDTA; PromoCell, Germany), centrifuged at 300rpm/3min, and resuspended in the growth medium. Cells were counted with a haemocytometer and seeded on the scaffolds at a density of 50 000 viable cells per sample. Passage number 4 was used in this experiment. Cells on tested materials were incubated in standard cell culture conditions for 1 and 3 days. For the initial testing the material with the highest content of the additives was chosen (P15H5S5) and unmodified material (P15) served as a reference sample.

Cell morphology

To assess cell morphology, the Scanning Electron Microscopy (SEM) was used. At the evaluation periods (1 or 3 days), osteoblasts on the scaffolds were fixed using a solution containing 2%vol glutaraldehyde in PBS (both from Sigma Aldrich, Ireland) dehydrated in ethanol with sequential concentration, treated with hexamethyldisilazane (Fluka, Ireland) and dried in the air. Samples were then sputtered with a 3-5nm thick gold layer and observed, using Scanning Electron Microscope (Leo 440, Stereo Scan), operated at 5.0 kV.

Cell viability and spatial distribution

The cell viability and spatial distribution within the obtained scaffolds were evaluated in cells stained with LIVE/DEAD Kit (Invitrogen, USA). Briefly, on the day of experiment HOB were washed twice in PBS and stained using $2\,\mu$Mcalcein and $4\,\mu$M Ethid-1 in PBS to observe live and dead cells respectively. Images were captured by a Nikon DS-U2 camera attached to the Nikon T*i*-E epifluorescent microscope, at 10× magnification, using the associated Nikon NIS-Elements software.

Qualitative and quantitative evaluation of the three-dimensional scaffolds

Osteoblasts cells

MC3T3-E1 osteoblasts represent a suitable model for studying osteogenic development *in vitro*.The osteoblastic cell line MC3T3-E1 had been established from C57BL/6 mouse calvaria. Cells have the capacity to differentiate into osteoblasts and osteocytes and have been demonstrated to form calcified bone tissue *in vitro*. Mineral deposits were identified as hydroxyapatite.

Cell culture conditions

For determination of cell attachment, MC3T3-E1 mouse calvarian osteoblast cells were cultured under standard tissue culture conditions (37°C, 5% CO_2) in alpha-MEM medium (Gibco, USA) supplemented with 10% Fetal Bovine serum and 1% Antibiotic/ Antimycotic (Gibco, USA). All experiments were conducted with cells between passages 6-10. Each scaffold was cut into circular discs (~ 15mm diameter) and the sterilized disc specimens were placed in wells of a 24-well TCPS (Corning). The samples were sterilized by autoclaving in phosphate buffer solution at 121°C for 20 minutes, and then the cells were stored in culture medium in a CO_2 incubator for 1 hour prior to cell seeding to promote protein absorbtion. The cells were trypsinized and the cell number was quantified and then seeded onto the samples, at a concentration of

30,000 cells/ml in 2ml of medium (for SEM observation and cell proliferation) and 50,000 cells/ml in 2ml of medium (for qRT-PCR, ELISA assay and ICC techniques). The medium was changed every 3 days and the culture stopped at day 1, 3, 5, 7, 14, 21 and 28. P15 construct was used as the control scaffold, while P15H2S2 and P15H5S5 were the construct of interest.

Cell proliferation – DAPI staining

To assess cell attachment and proliferation samples were seeded with 30,000 cells/ml. At each time point samples were stained with DAPI (a DNA binding dye, to stain nuclei) and FITC- labeled Phalloidin (a fungal toxin with specific affinity for f – actin fibrils, to visualize cell cytoskeleton). Samples were fixed with 4% formalin for 15 minutes and then rinsed with PBS. Afterwards cells were permeabilized by treatment with 0.1% Triton X solution. After removal of Triton X, samples were incubated in 5% PBS-BSA solution for 1 hour at room temperature to decrease non-specific absorption of the dyes. Afterwards 1:200 dilution of FTIC-Phalloidin was applied to the samples for 40 minutes in the dark, followed 1:1000 dilution of DAPI for 15 minutes in the dark.

Cell counting data were generated from counting total number of cells (DAPI stained) in three separate fibrous constructs per time point using Image J software (Appendix B). A minimum of 5 randomly selected visual fields (at 10× magnification in a fluorescent microscope (Olympus, Japan) were counted per fibre construct. The total number of DAPI stained cells was counted at four different time points (day 3, 7, 14 and 28 of culture and differentiation) and was presented as number of cells per day of

co-culture. The results are presented as mean ± standard deviation. Data were analyzed using Student's *T*-test. *p <0.05 was considered statistically significant.

Cell morphology

Cell morphology was assessed using Scanning Electron Microscope (EVO LS15 SEM/EDX from Zeiss, Germany). After removal from the culture medium, samples were washed with PBS and immersed in 2% glutaraldehyde for 30 minutes at 4°C, followed by serial dehydration in series of ethanol solution (50%- 10 minutes, 60% - 10 minutes, 70% - 30 minutes, 80 % - 10 minutes, 90% - 10 minutes, 95% - 10 minutes, 100% - minutes, 100% - minutes). Dehydrated samples were immersed in hexamethydisilazane (HMDS) for 1 minute and dry in the air at room temperature. Samples were coated with gold for 80 seconds using an *Edwards Pirani 501 Scancoat* sputtering coater and observed under the scanning microscope.

Osteopontin (OSPN) and Collagen type I expression (COL I) - mmunnocytochemistry (ICC)

Immunocytochemistry is used to visualize the presence of a specific protein or antigen in cells. For immunocytochemistry, sample preparation involves fixing the target cells to a slide, in our case the three- dimensional scaffold. To ensure access of the antibody to its antigen, cells must be fixed and permeabilized. In an ideal situation,

71

fixation would immobilize the antigens while retaining native cellular architecture and permitting unhindered access of antibodies to all cells and subcellular compartments. To assess osteoblastic differentiation and extracellular matrix deposition the expression of two of the three chosen bone markers (osteopontin (OSPN), collagen type I (COL I) and alkaline phosphatase (ALP)) was assessed for day 1, 3, 7, 14, 21 and 28 using this technique, while ELISA was used for BALP levels quantification. Each marker was assessed on a different set of samples and P15 was used as the control sample.

Osteopontin (OSPN)

For osteopontin detection samples were stained with non-conjugated Monoclonal Anti-Osteopontin (OPN46, Sigma-Aldrich, a synthetic peptide, to bind osteopontin antigens. Samples were fixed with 4% formalin for 15 minutes and then rinsed with PBS. Afterwards cells were permeabilized by treatment with 0.1% Triton X. PBS for 10 minutes at room temperature. After removal of Triton X, cells were blocked with 5% BSA-PBS-1% Tween for 1 hour at room temperature or overnight at 4°C. Afterwards 1:100 dilution of Monoclonal Anti-Osteopontin was used for 1 hour followed by two washes with PBS-1% Tween for 5 minutes each, to wash away the non-specific binding. Afterwards a 1:200 dilution of fluorescent secondary antibody containing 1%BSA was added for 1 hour in the dark, followed by a 1:1000 DAPI dilution for 15 minutes.

Collagen type I (Col I)

Collagen type I expression was assessed using the same immunocytochemistry protocol as for osteopontin detection. A dilution of 1:100 Collagen I antibody conjugated to FITC-phalloidin (Biorbyt, a synthetic peptide to bind collagen type I antigens), followed by a 1:1000 DAPI dilution to bind the nuclei.

RNA Isolation and Quantification of gene expression (qRT- PCR)

In order to quantify the osteopontin and collagen type I markers expression pre-osteoblasts (MC3T3-E1) were seeded on the three composite type scaffolds and TCPS (Tissue culture Polystyrene) at a density of 5 x 10^4 cells/cm^2, and the total RNA was isolated using the protocol for isolation of RNA using TRIsure at day 0 (prior to seeding), 1, 3, 7, 14, 21 and 28. The cells were lysed directly on the culture dish or scaffold by adding 1ml of TRIsure per well and pippetting the cell lysate several times to ensure sufficient cell disruption. Further, samples were incubated for 5 minutes at room temperature, followed by the addition of 0.2ml of chloroform per 1ml of TRIsure used and capped tubes were shaken vigorously by hand for 15 seconds. Afterwards samples were incubated for 2-3 minutes at room temperature and centrifugated at 12,000g for 15 minutes at 2-8°C. During centrifugation samples would have separated into a pale green, phenol-chloroform phase, an interphase, and a colorless upper aqueous phase that contained RNA. The next step was RNA precipitation. This was done by transferring the aqueous phase to another tube without disturbing the

73

interphase. Further the RNA was precipitated by mixing with cold isopropyl alcohol (0.5 ml of isopropyl alcohol per 1ml TRIsure), followed by incubation for 10 minutes at room temperature and centrifugation at 12,000g for 10 minutes at 2-8°C. After removing the supernatant the pellet was washed with 75% ethanol, adding at least 1ml per TRIsure used, vortex the samples and centrifuge at 7500g at 2-8°C. After air-drying the pellet and dissolving in DEPC-treated water the samples were stored at -70°C before being analysed. Isolated RNA was quantified by measuring the absorbance at 260 nm; theoretically an absorbance of 1 corresponds to 44 μg/ml of RNA. Ratio of absorbance at 260/280 to assess for the purity measurement and Nanodrop spectrophotometer was used for the measurement of the RNA samples (Figure 10).

Finally, mRNA levels were measured by realtime qRT-PCR when cDNA was analyzed by using Rotor-Gene SYBR Green RT-PCR Kit for two bone phenotype markers (osteopontin and collagen type I) and one house keeping gene (GADPH). Reaction was carried out by using 12.5 μl of 2 X Rotor-Gene SYBR Green RT-PCR Master Mix with 10X and the necessary amount of water to complete reaction mix to 50 μl. Then the PCR reaction was carried out for 40 cycles with the following cycling conditions: Initial denaturation (94 °C): 2 min, then 40 cycles of denaturation (94 °C, 15 s), annealing (60 °C, 1 min), extension (72 °C, 1min). Primer specificity was assessed beforehand. Final results are reported by 2-ΔΔCt method.
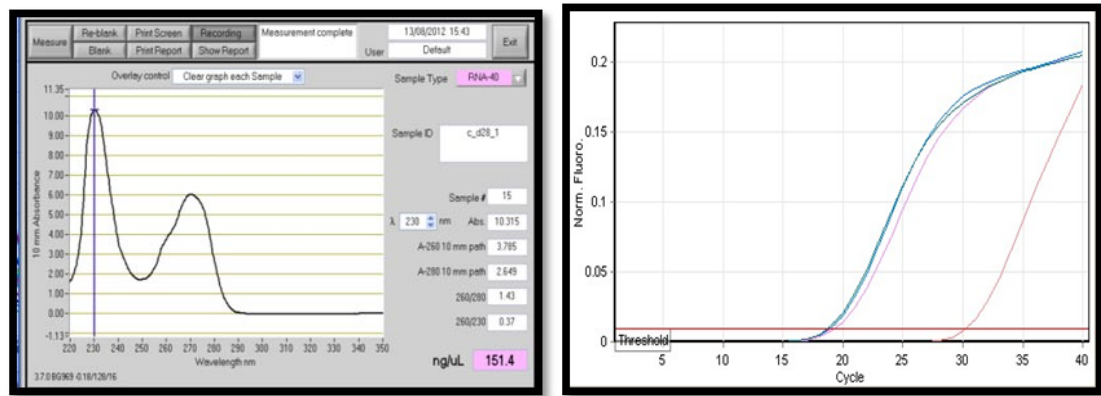
Figure 10 Representative measurement of mRNA and representative readings for Real-time RT-PCR amplification curve for COL I at day 3. Pink line (negative control). Threshold values (Ct) were determined by an algorithm available within the analysis program R 2.2

Bone Alkaline phosphatase (BALP) enzyme-linked immunosorbent assay (ELISA)

Alkaline phosphatase is an enzyme expressed by cells and is an early marker of osteoblastic differentiation. Alkaline phosphatase enzyme activity of the constructs was measured using an Alkaline Phosphatase Assay Kit from Antibodies (Germany) according to the supplier instructions. This BALP enzyme linked immunosorbent assay applies a technique called a quantitative sandwich immunoassay. The microtiter plate provided in the kit has been pre-coated with a monoclonal antibody specific for BALP. Standards or samples were then added to the microtiter plate wells and BALP if present, binded to the antibody pre-coated wells. In order to quantitatively determine the amount of BALP present in the sample, a standardized preparation of horseradish peroxidase (HRP)-conjugated polyclonal antibody, specific for BALP was added to each well to

sandwich the BALP immobilized on the plate. The microtiter plate underwent incubation, and then the wells were thoroughly washed to remove all unbound components. Next, A and B substrate solution were added to each well. The enzyme (HRP) and substrate were allowed to react over a short incubation period. Only those wells that contain BALP and enzyme-conjugated antibody have exhibited a change in colour. The enzyme-substrate reaction was terminated by the addition of a sulphuric acid solution and the colour change was measured spectrophotometrically at a wavelength of 450 nm. Samples were run in triplicate and compared against the provided standards. The results are presented as mean ± standard deviation. Data were analyzed using Student's *t*-test. $*p < 0.05$ was considered statistically significant.

CHAPTER 4 RESULTS AND DISCUSSIONS

4.1 Introduction

Orthopaedic tissue engineering applies methods from materials engineering and life sciences to create artificial constructs for regeneration of new bone [58]. The human bone, like all the other tissues and organs, is a complex biological construct and for this reason the requirements of scaffold materials for bone tissue engineering are diverse and extremely challenging. A scaffold can be used either outside of the body for cell culturing (*in vitro*), or implanted in the body (*in vivo*), offering a temporary replacement for the tissue, until the seeded cells produce the new structure. Firstly, biocompatibility of the substrate materials is imperative; the material must not elicit an unwanted inflammatory response or demonstrate immunogenicity or cytotoxicity. In addition, scaffolds may be required to provide initial mechanical strength and stiffness necessary for the mechanical function of the diseased or damaged tissue. However, scaffolds may not necessarily be required to provide complete mechanical equivalence to healthy tissue. Further as with all materials in contact with the human body, tissue scaffolds must be easily sterilizable to prevent infection [148, 149].

A further requirement for bone scaffolds in particularly is a controllable interconnected porosity in order todirect the cells to grow into the desired physical form and to support vascularization of the ingrown tissue. A typical porosity of 90% as well as a pore diameter of at least 100 μm is known to be required for cell penetration and a proper vascularization of the ingrown tissue [150-152]. Other highly desirable features

concerning scaffold processing are near-net-shape fabrication and scalability for cost-effective industrial production [58].

The development of biocompatible scaffolds for tissue regeneration has become the focus of intense research interest. One of the many approaches to combining biomaterials in the form of biopolymers and/or bioceramics (either synthetic or natural) is to seek to achieve matrices that can induce or stimulate the appropriate cell response for successful tissue regeneration [153, 153]. Any such scaffold material selected for a tissue engineering application will be subjected to *in vivo* remodelling.The remodelling process is influenced by the microenvironment of each tissue including factors such as blood supply, pH, O_2 and CO_2 concentration, mechanical stressors and the host scaffold interface leading to destructive, inductive remodelling or scarring mechanisms [154]. The degree of remodelling depends on the tissue itself (e.g. skin 4–6 weeks, bone 4–6 months), and its host anatomy and physiology.

Various fabrication technologies have been applied to process biodegradable and bioresorbable materials into 3D polymeric scaffolds of high porosity and surface area in order to mimic the three-dimensional structure of the extracellular matrix [148]. From a scaffold perspective, all techniques present advantages and disadvantages as the native tissue ECMs comprise highly specialized composite structures at the molecular level, incorporating macromolecules of differing chemistry and/or inorganic nanocrystallites, which are difficult to replicate [153] .

Electrospinning is a simple, cost effective and versatile technique. It is an interesting technique for scaffold fabrication, since the resulting fibres may have similar diameters to that of certain ECM microstructures, particularly higher-ordered collagen

78

microfibrils. Furthermore, electrospun fibres exhibit flexibility, due to their very high aspect ratio (length/diameter), which is also beneficial inallowing the seeded cells to remodel the space in their proximity. The fibre size is important in this instance as one cell may adhere to multiple micro and nanoscale fibres instead of many cells adhering to one thicker fibre [153]. The electrospinning method uses a high-voltage electric field to form solid fibres from a polymeric fluid stream delivered through a millimetre–scale nozzle. The electrospinning parameters can be varied in order to produce micro and nanofibres with complex and unique three-dimensional shapes. Polymeric and composite solutions can be transformed into fibrous structures and, depending on the specific polymer being used; a wide range of properties such as strength, weight and porosity, surface area can be achieved.

This research work aims to mimic the structure of the extracellular matrix of the bone by producing a multi–layer fibrous scaffold from a bioactive and non-toxic composite material utilising electrospinning. The layout of the work presented in Figure 7 includes several steps such as:

- ✓ choosing adequate non-toxic, biodegradable materials that show potential for this type of application;

- ✓ preliminary characterisation and composite formulation;

- ✓ characterisation of the produced fibrous structures;

Chapter 4 presents the results and discussions for each phase of the research (Figure 11). Section 4.2 includes the raw powder materials characterisation, such as morphology, chemical composition results, and thermal behaviour. Section 4.3 presents the morphological and chemical analysis, hydrophilicity and preliminary biological results of the electrospun samples produced during the trial and error screening process.

Screening tests were carried out in order to identify sets of parameters that allow continuous and uniform deposition of fibres. Further, Section 4.4 shows the Design of Experiments methodology used for the optimisation of the electrospinning parameters and the composition of the electrospinning solution. The Design of Experiments study included a more detailed investigation of the process, using as the starting point the sets of parameters from Section 4.3. Section 4.5 presents the bioactivity *in vitro* evaluation of the scaffolds, while Section 4.6 presents the biological and physical assessment results for the tri-phasic composite scaffolds
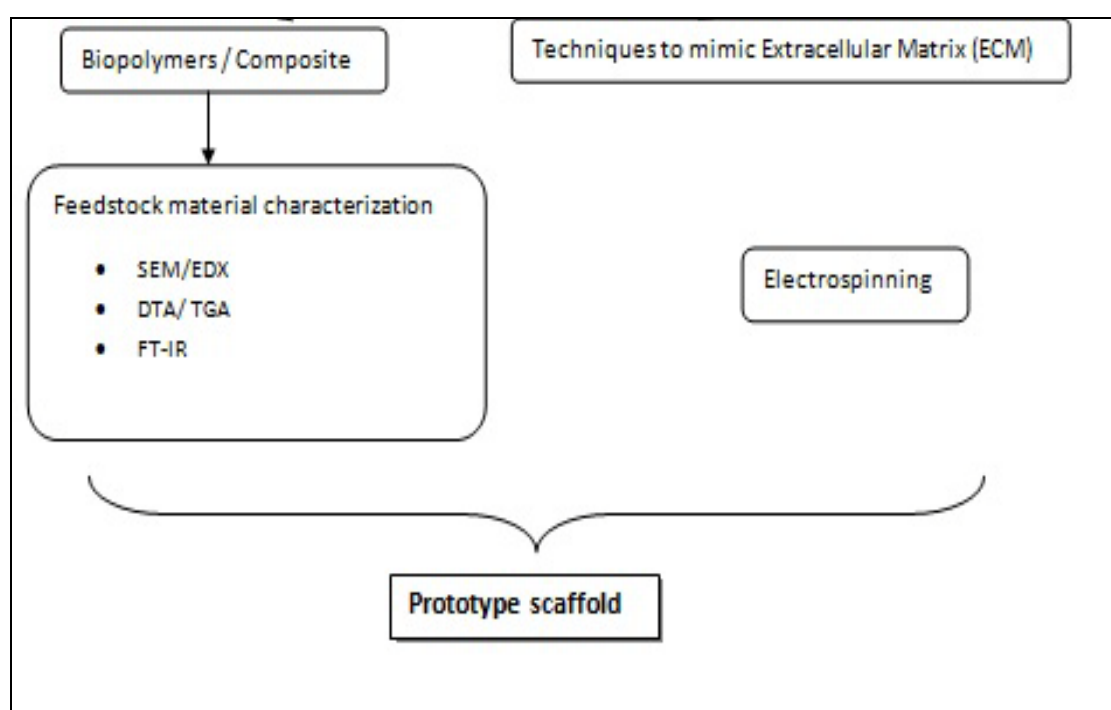
Figure 11 Schematic of Step 1 of the research plan

4.2 Powder characterisation

Polyhydroxybutyrate-co-hydroxyvalerate 2%

Since the early 1980s, various bioactive composites have been developed for hard tissue replacement [155, 156]. Due to the matrix polymers used, most of these composites were non-biodegradable. A shift in emphasis in biomaterials development in recent years has moved attention from materials that will remain completely stable in the biological environment to materials that will, in some way, alter their properties or degrade in response to the biological environment. Biodegradable materials have the advantage of allowing the new tissue, as it grows naturally, to take over their load-bearing or other functions while minimising the potential chronic problems associated with the presence of bio-stable implants [156].

Polyhydroxybutyrate (PHB) is a naturally occurring β-hydroxyacid (linear polyester). Its ability to degrade and resorb in the human body environment makes it a suitable candidate as the matrix for bioactive and biodegradable composite implants that will guide tissue growth and be replaced eventually by newly formed tissue. Its usefulness is limited by its brittleness [157]. However, the addition of polyhydroxyvalerate (PHV) to the PHB polymer chains can improve the ductility and processability of the polymer [158]. Polyhydroxybutyrate-co-hydroxyvalerate (PHB‑PHV) with varying molar ratios of HV has been the subjectof extensive, on-going research for biomedical applications [159-161]. Based on the discovery of Reusch [162] it is speculated that PHB, its oligomers and monomers are not toxic to the cells and, as Doyle *et al.* [163] demonstrated, materials based on PHB produce a consistent

favourable bone tissue adaptation response with no evidence of an undesirable chronic inflammatory response after implantation periods up to 12 months.

The powder morphology of polyhydroxybutyrate with 2% hydroxyvalerate fraction is shown in Figure 12. According to the supplier (Sigma Aldrich, Ireland) the powder contains particles of <300μm of size. The powder's thermal behaviour was studied using DTA/TGA and the results are shown in Figure 13. The polymer starts to degrade around 278ºC, when the TGA curve starts to drop down. In the literature, it was found that the thermal degradation of PHB/PHV is generally considered to be a statistical process based on a random chain scission mechanism; however, some kinetically favoured scissions occur near the ends of the macromolecules [164].
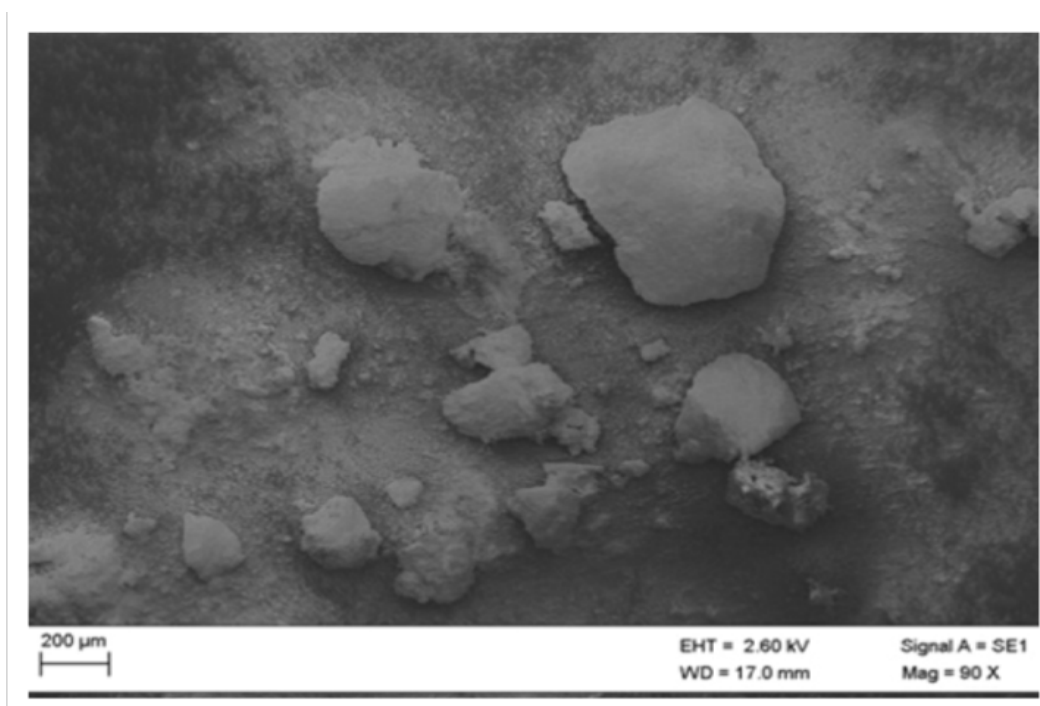
Figure 12 Polyhydroxybutyrate-co-hydroxyvalerate 2% morphology
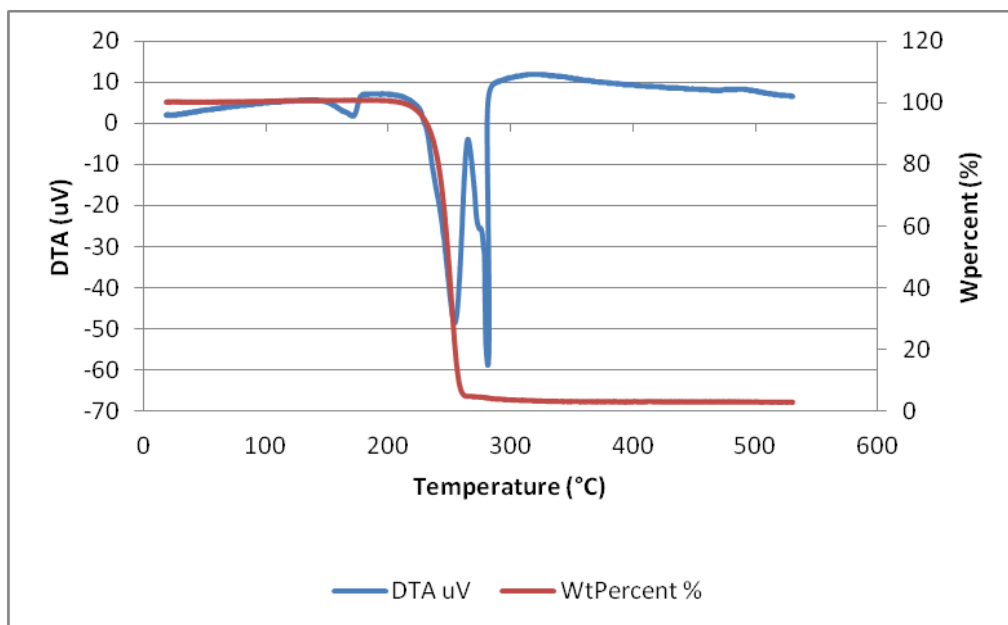
Figure 13 DTA/TGA analysis for polyhydroxybutyrate-co-hydroxyvalerate 2% powder

FT-IR chemical analysis is shown in Figure 14, while Table 8 highlights the peak assignements. Polyhydroxybutyrate-co-hydroxyvalerate 2% is a polyhydroxyalkanoate, more specifically a polyhydroxybutyrate with a 2% valerate fraction in its composition. The FT-IR characteristic bands for the polyhydroxybutyrate are: C=O stretching at 1720 cm^{-1}, -C-O-C- stretching vibration at 800-900 cm^{-1} and an antisymmetric –C-O-C- stretching band at 1060-1150 cm^{-1} [165]. The small, almost invisible, shoulder positioned at 1743 cm^{-1}, is also attributed to the same C=O stretching mode although it arises from the amorphous parts. Because the polymer used in this research contained a 2% valerate fraction, the specific bands for the pure polyhydroxybutyrate (PHB) were slightly changed, but there were still found in the polymeric powder of polyhydroxybutyrate-co-hydroxyvalerate 2%.

83
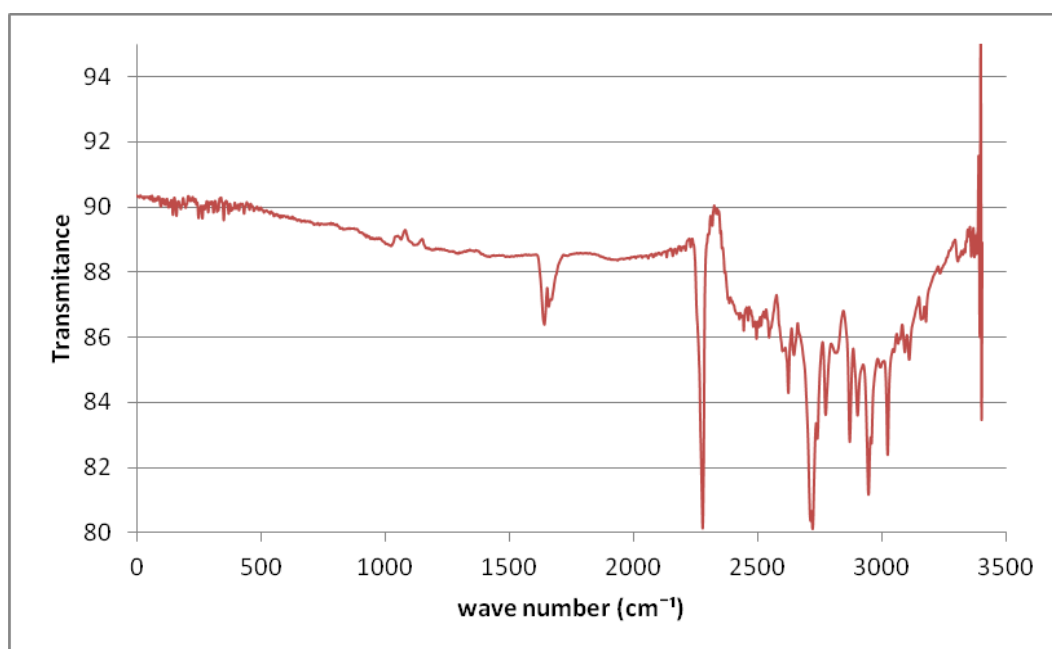
Figure 14 FTIR signal for polyhydroxybutyrate-co-hydroxyvalerate 2% powder

Table 8 Infrared bands assigned for for polyhydroxybutyrate-co-hydroxyvalerate 2% powder

Infrared frequency (cm^{-1})	Assignment
800-900cm^{-1}	C-O-C stretching vibration
1060-1150cm^{-1}	antisymetric –C-O-C- stretching
1720 cm^{-1}	C=O stretching
1743 cm^{-1}	C=O stretching (from the amorphous parts)

Nano-hydroxyapatite

Around 60 wt% of bone is made of HA $Ca_{10}(PO_4)_6(OH)_2$ and therefore it is evident why HA and related calcium phosphates (e. g. α-TCP, β-TCP) have been intensively investigated as the major component of scaffold materials for bone tissue

engineering [166]. As expected, calcium phosphates have shown excellent biocompatibility due to their close chemical and crystal resemblance to bone mineral. Although they have not shown osteoinductive ability, calcium phosphates certainly possess osteoconductive properties and may bind directly to bone under certain conditions [58]. Particulate hydroxyapatite (HAp) incorporated into PHB forms a bioactive and biodegradable composite for applications in hard tissue replacement and regeneration [11]. A common characteristic of bioactive glasses and ceramics is a time-dependent kinetic modification of the surface that occurs upon implantation. The surface forms a biologically active hydroxy carbonate apatite (HCA) layer which provides the bonding interface with tissues. The HCA phase that forms on bioactive implants is chemically and structurally equivalent to the mineral phase in bone, providing interfacial bonding [167, 168]. In addition the ceramic phase can improve the polymer brittleness and the overall composite properties.

The ceramic phase (hydroxyapatite) was supplied in powder form, with particles size <200nm. The technique of electrospinning uses a metallic nozzle to produce fibres of different diameters and the nozzle could be blocked if particles were too big or they form agglomerates larger than the nozzle diameter. Figure 15 shows the powder morphology.
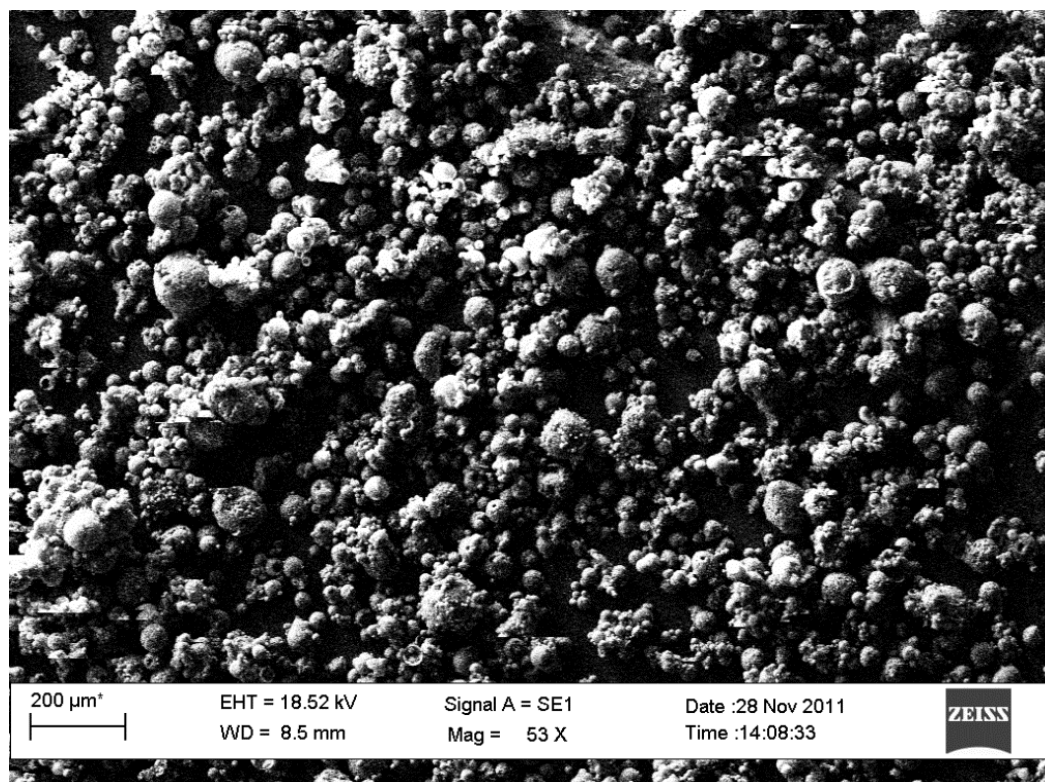
Figure 15 SEM of the nano hydroxyapatite powder as supplied

The DTA and TGA (STA: Simultaneous thermal analysis) curves for the hydroxyapatite powder are illustrated in Figure 16. The first region ranges from 90ºC to 295 ºC with a peak at about 200ºC, which corresponds to the dehydration of the precipitating complex and the loss of physically adsorbed water molecules of then HAp powder. With increasing temperature from 295 ºC to 1200 ºC two peaks have been observed that may correspond to the gradual dehydroxylation of nHAp powder [169].

Figure 17 shows the FT-IR spectra of nHAp powder. The characteristic bands (Table 9) exhibited in the sample spectra are assigned as follows: (a) two bands were observed at 3455 cm^{-1} and 622 cm^{-1} due to the stretching mode of hydrogen-bonded OH ions and liberational mode of hydrogen bonded OH- ions, respectively; (b) the band at

1040 cm^{-1} arises from υ3 PO$_4$, the bands at 603 cm^{-1} and 561 cm^{-1} arise from υ4 PO$_4$. The FT-IR analysis showed all typical absorption characteristics of hydroxyapatite. In addition, some carbonate content also was seen (CO$_3^{-2}$ peak around 1600 cm^{-1}), which is an indication of the presence of carbonate apatite. This might have originated through the absorption of carbon dioxide from the atmosphere [170].
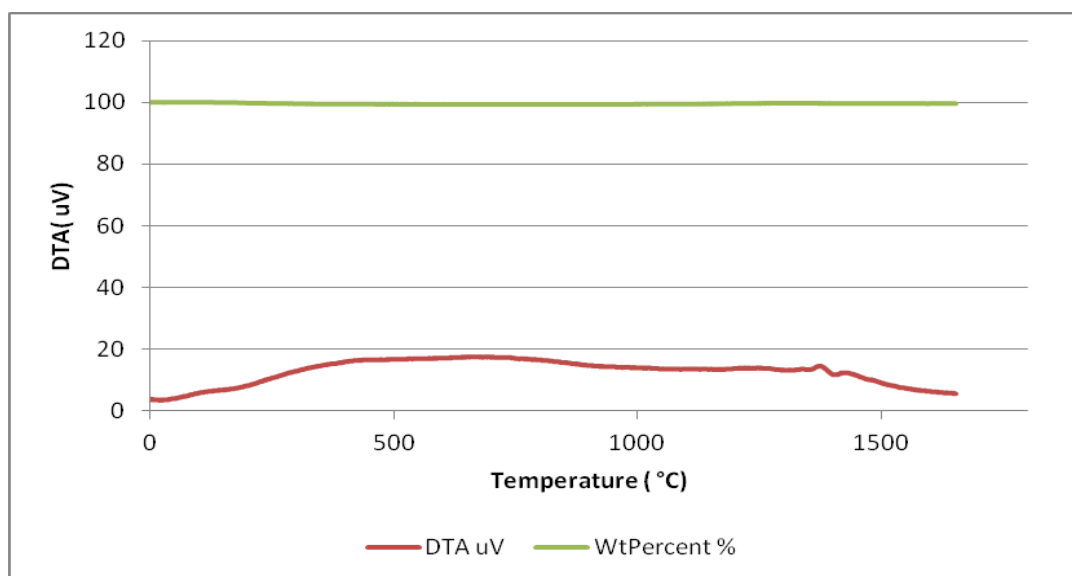
Figure 16 DTA/TGA of nHAp powder as supplied
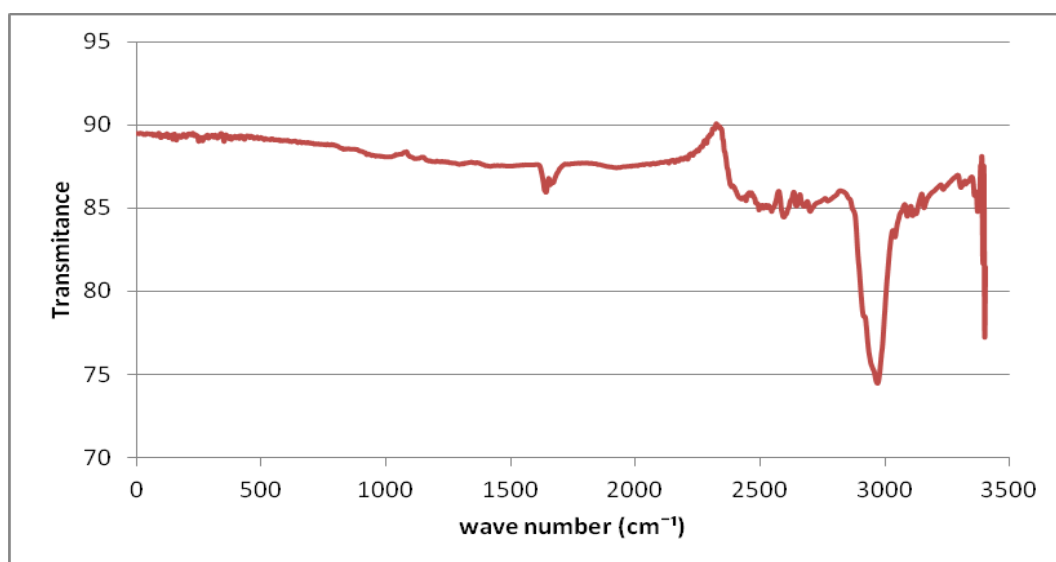
Figure 17 FT-IR spectrum of nHAp raw powder

Table 9 Infrared bands assigned for the supplied hydroxyapatite, nano powder [169]

Infrared frequency (cm^{-1})	Assignment
461	PO^4 bend υ4
622	OH structural
1040	PO^4 bend υ3
3455	OH structural

Silk fibroin

Silk protein was supplied in powder form having been extracted via hydrolyzation of the silkworm yarn. Silk fibroin is a white crystallized soluble powder, prone to be absorbed by the human body, due to its abundance of aminoacids (glycin, alanine, alpha-amino-beta-hydroxyrpropionic acid, beta-parahydroxy-phenylpropionic acid (up to 80%)) [171].
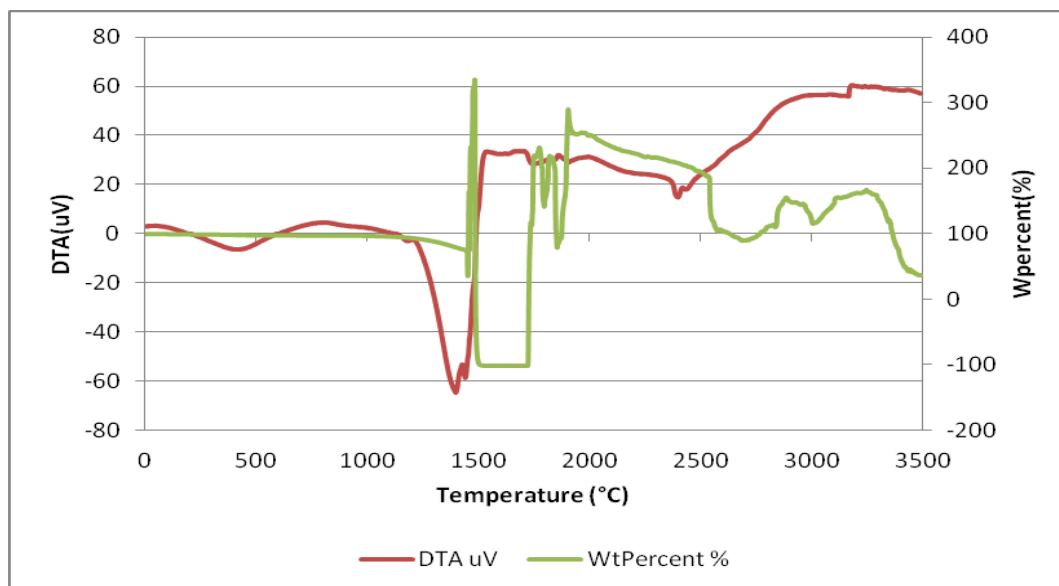
Figure 18 DTA/TGA curve for silk fibroin (SF) powder

The general appearance of the TGA/DTA thermograms of the dried silk fibroin particles depends strongly on relative humidity. Silk fibroin is highly hygroscopic and particles rapidly absorb approximately 6% water (20±C, 65% R.H.) [172]. The thermogram revealed several thermal transitions, such as a glass temperature transition at 174±°C and a sharp fusion peak at 1498±°C (Figure 18). These transition temperatures are slightly lower than the literature values [172]. The weight percent curve revealed several weight variations during the thermal process and these can be attributed to the water content of the powder.

Further chemical analysis was performed on silk fibroin powder using FT-IR (Figure 19). Silk fibroin characteristic bands (Table 10) are amide A and amide I, amide II, and amide III [173]. Amide A was is found at 3294 cm^{-1} and it represents the –N-H stretching vibration. Amide I can be found between 1500-1600cm^{-1}, amide II at 1380-1400 cm^{-1} and amide III at 1375 -1390 cm^{-1}. The three amides are attributed to the carbonyl)-C-O- stretching mode, combination peak of the main N-H in plane bending,

89

C-H stretching vibration, coupled peak of the main C-N stretching and the –N-H in plane bending vibration.
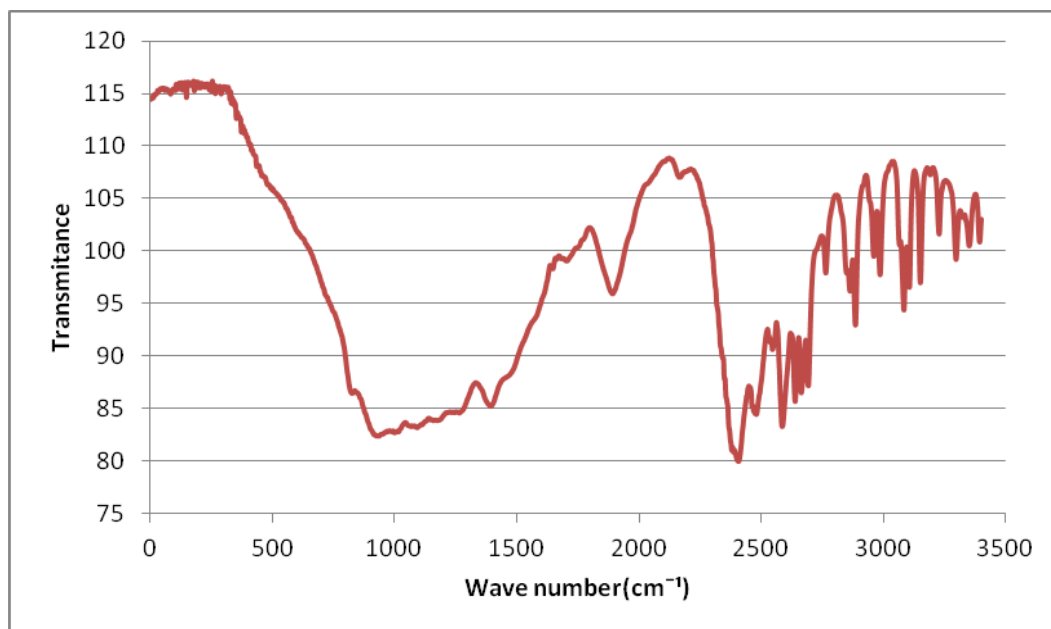
Figure 19 FT-IR spectrum for silk fibroin powder

Table 10 Infrared bands assigned for the supplied silk fibroin powder

Infrared frequency (cm^{-1})	Assignment
1375-1390 cm^{-1}	amide III
1380-1400 cm^{-1}	amide II
1500-1600 cm^{-1}	amide I
3294 cm^{-1}	Amide A (N-H stretching vibration)

4.3 Screening tests and characterisation of electrospun samples

Screening Process (Trial and Error)

In order to identify the range of compositions and sets of process parameters that could provide a series of uniform, smooth fibrous membranes and be used in a more detailed investigation using Design of Experiments.

1. SEM/EDX – morphology and confirm existence of chemical elements
2. FT-IR – confirm interaction/ lack of interaction of elements
3. Contact angle measurements
4. Preliminary biological testing (cell adhesion and proliferation)

Figure 20 Schematic of Step 2 of the research plan

Following the powders characterization phase, screening tests were conducted in order to find an optimum set of electrospinning parameters for the preliminary polymeric and composite solutions. Table 4 presented the forms of polymeric and composite solutions that were used during this research work and the naming convention used. Even though the PHB98-PHV2 polymer has previously been electrospun, the combination of PHB98-PHV2 and nHAp has not been directly electrospun [174, 175]. In earlier studies, polymeric fibres were immersed in solutions

containing Ca^{2+} to form an apatite layer on the surface of the fibres and improve their properties, or else other technique were used to incorporate the ceramic phase in the polymeric fibres [176].

The stages of the screening tests were as follows:

➢ Preparation of the polymeric solution

➢ Electrospinning of the polymeric solution

➢ Preparation of the composite solution

➢ Electrospinning of the composite solution

➢ Preliminary characterization tests
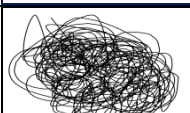
4.3.1 Preparation and electrospinning of the polymeric solution

The first step taken was to find the optimum concentration of polymer to be electrospun, in order to obtain continuous deposition of fibres. Figure 21 shows the chart of the pure polymeric solution testing. For the visual inspection of the deposited fibre, a grading scale was used, evidenced in Table 11. The set of parameters to start with were 15cm distance tip-collector (D), 5ml/h feed rate (FR), 19 gauge needle and polymer concentration of 1%, 4%, 7%, 10%, and 15%. The electrospun fibres were collected on an aluminium foil collector. A previous study achieved electrospun fibre deposition with a concentration of 1% polymer [177]. This concentration was used as a starting point and formulated higher concentrations of solution to work with.

Effect of varying polymeric concentration

Initially the solution concentrations were varied, then the voltage and thirdly the distance. For higher nanofibre production efficiency at this stage, positive and negative voltages were used at the same time (positively charge the needle and negatively charge the collector).

Table 11 Marking scale for the visual inspection of the collected fibres

Mark	Observations	Sample appearance
1	No electrospinning present	
2	Electrospitting (polymeric spots)	
3	Electrospraying and scarce electrospinning present	
4	Electrospinning present, random fibre deposition, solidification at the tip (every 1 min)	
5	Electrospinning present, slower solidification at the tip, smooth and uniform fibre deposition	
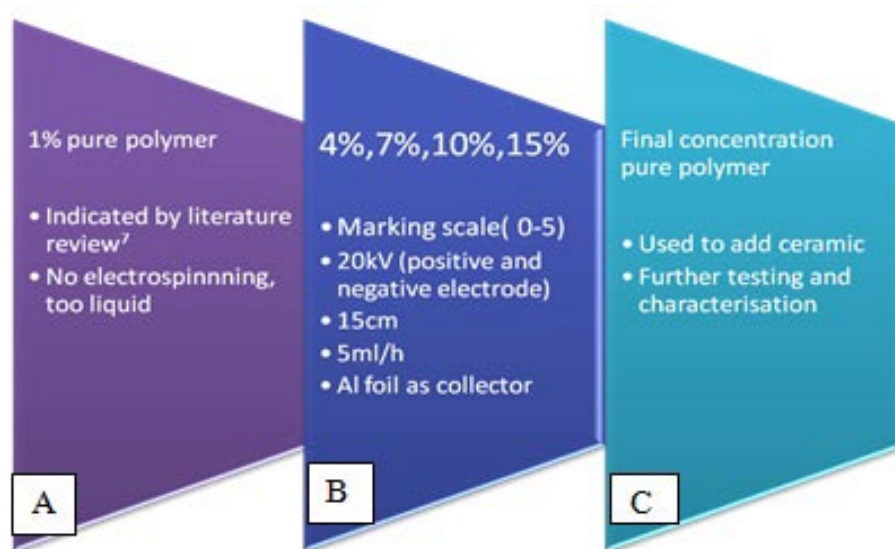
Figure 21 Pure polymeric solution screening tests chart

As indicated in Figure 21 several concentrations of PHB98-PHV2 solutions (1%, 4%, 7%, 10%, and 15% polymer in chloroform) have been tested in electrospinning and marked accordingly to the scale in Table 11. The same set of electrospinning parameters was utilised for all tests (Figure 21 (B)) and after visual inspection of the samples collected, further testing was conducted with 10% and 15% concentrations (Figure 21 (C)).

Effect of varying voltage

Further, testing the two solution (10% and 15%), the voltage was varied in four points (10kV, 15kV, 20kV and 25kV) and the collected samples were again visually inspected, using the same marking scale (Table 11). As observed before, for the various

voltage values solidification of the polymeric solution at the tip of the needle during electrospinning was visible (e.g., 10% PHB/PHV). Table 12 highlights the observations made while electrospinning the various polymeric solutions.

Table 12 Marking scale for the visual inspection of the collected fibres

kV / % PHB/PHV	10	15	20	25
10	0	0	1 Solidification at the tip	1 Solidification at the tip
15	0	0 Poor fibres formation and slow deposition	1 Aligned fibre deposition Smooth and continuous fibres deposition	0 Flame at the tip of the needle

The fibre morphologies were investigated using the SEM. Figure 22 shows that using 20 kV and 25 kV, the solvent did not fully evaporate and the deposited fibres were discontinuous and irregular shaped. As the voltage increased the fibres appeared thicker, more flat and with varying shapes. The fibres collected at 15kV were thin, smooth, and continuous, with a much smaller diameter, as compared to the fibres obtained using higher voltages. Further to the SEM morphology, 15kV and 15%PHB-PHV were the chosen voltage and solution concentration for future testing as using this voltage uniform deposition and small diameter of the fibres were achieved.
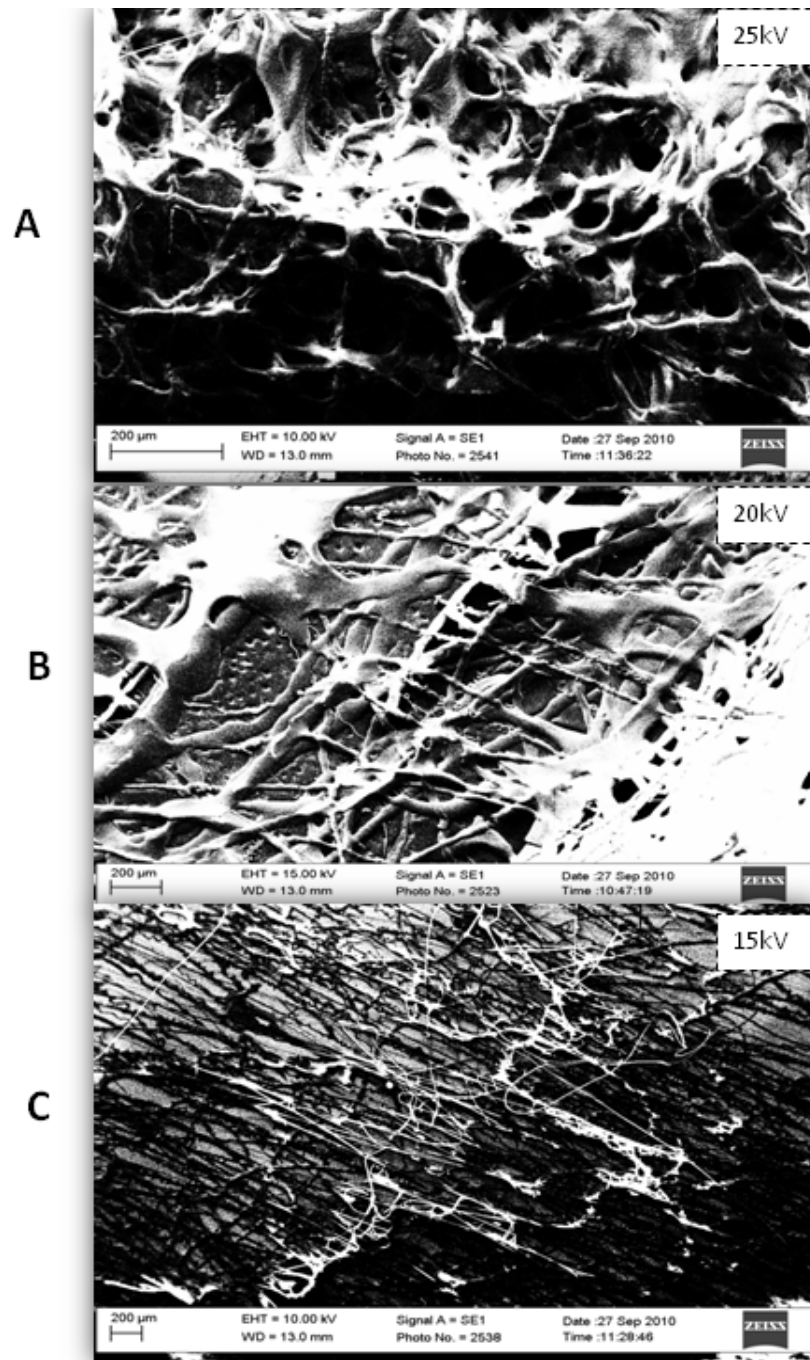
**Figure 22 SEM images of the P15 fibres deposited at (a) 25kV, (b)   20kV and (c)
15Kv**

Effect of varying collection distance (D)

The next step was to vary the collection distance (5 cm, 10 cm, 15 cm), in order to improve the deposition time and fibres morphology. An example of distance variation collection plate is shown in Figure 23. Poor deposition and fibre distribution was obtained at 5 cm, while at 10 cm the fibres were collected on the same spot, and not on the whole collector as expected. When using $D = 15$ cm the fibres collection time was shorter. Combining all the above tests, $D = 15$ cm was chosen to be used for the next phases of the research.
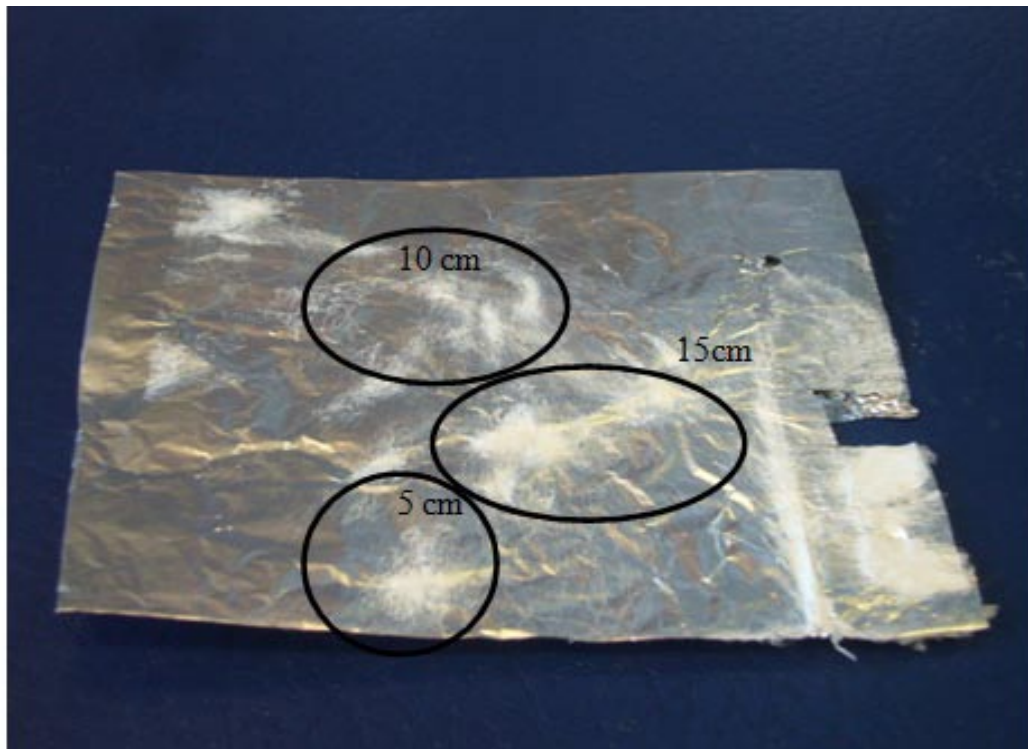
Figure 23   Photograph of aluminium foil collector with P15 fibres deposited at 5cm,   10cm and 15cm needle-collector distance

Effect of varying the feed rate (FR)

The feed rate was varied from 2-5 ml/h and as expected, the SEM images showed a slight increase in fibre diameter with increasing feed rate (Figure 24). It should be noted that the diameter values are not the smallest possible; they represent values that were found to produce consistent and useful fibrous membranes. It was observed that for low feed rate (2ml/h, 3ml/h) the fibres were discontinuous and more fragile when prepared for chemical/ morphological examination. It was evidenced that all the fibres exhibited microporosity on their surface (Figure 25).
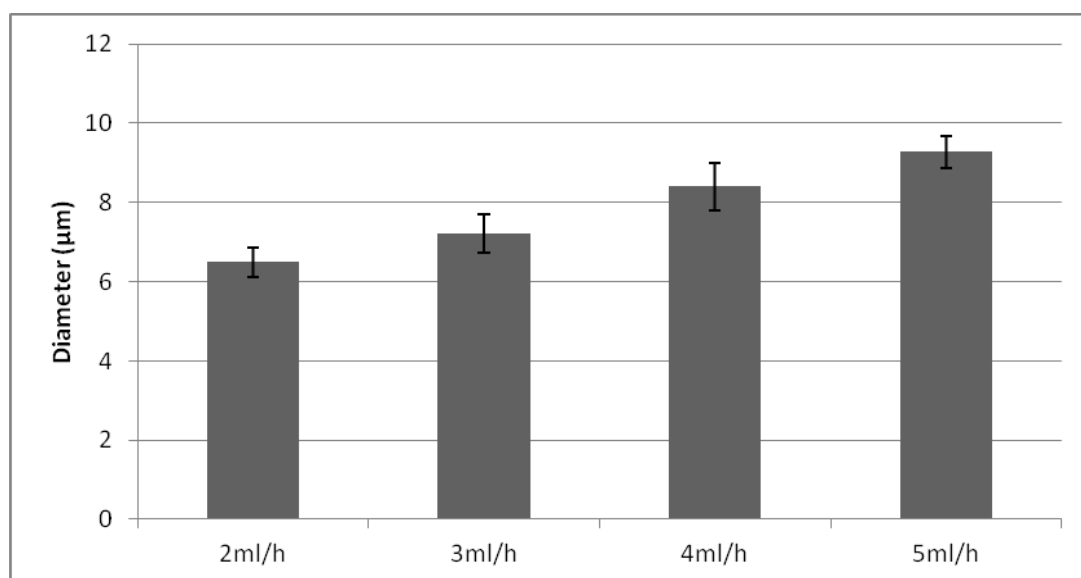
Figure 24   Fibre diameter measurement for feed rate variation from 2ml/h to 5ml/h (n =20)
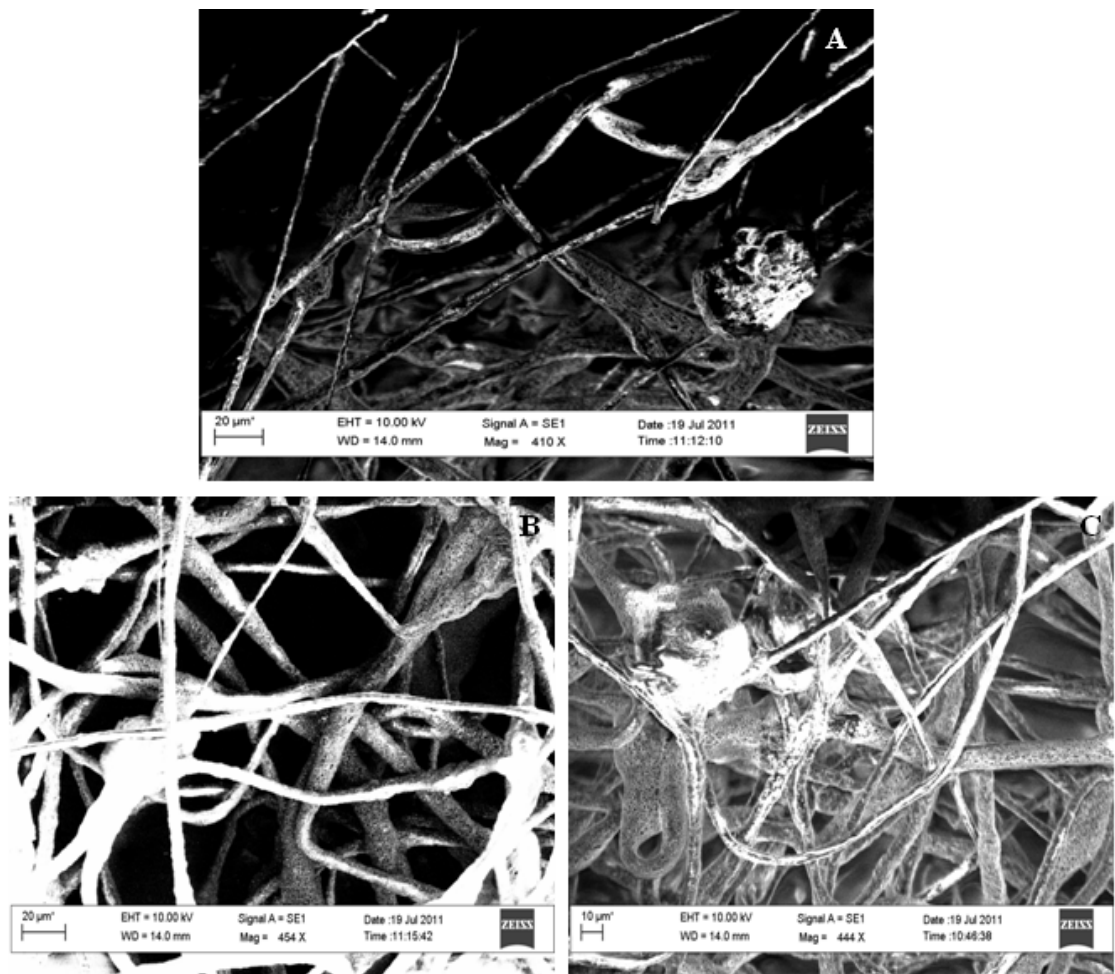
Figure 25 Electrospun polymeric fibres (P15H0S0) obtained when   using (A) 2ml/h feed rate, (B-C) 4ml/h feed rate Both SEM images show microporosity of the fibres surface

Another step of the research was the improvement of the deposition rate and the integrity (continuity) of the electrospun fibres. Further it was observed that the fibrous samples collected on the aluminium foil collector were very difficult to remove and physical damage was incurred when doing so. In order to overcome these drawbacks, different collector materials were tested (aluminium plate 2.5 mm, glass slide, copper

plate 2.5mm) at D = 15cm, FR = 5ml/h, deposition time of 10 minutes. Examples of

different collectors are shown in Figure 26.
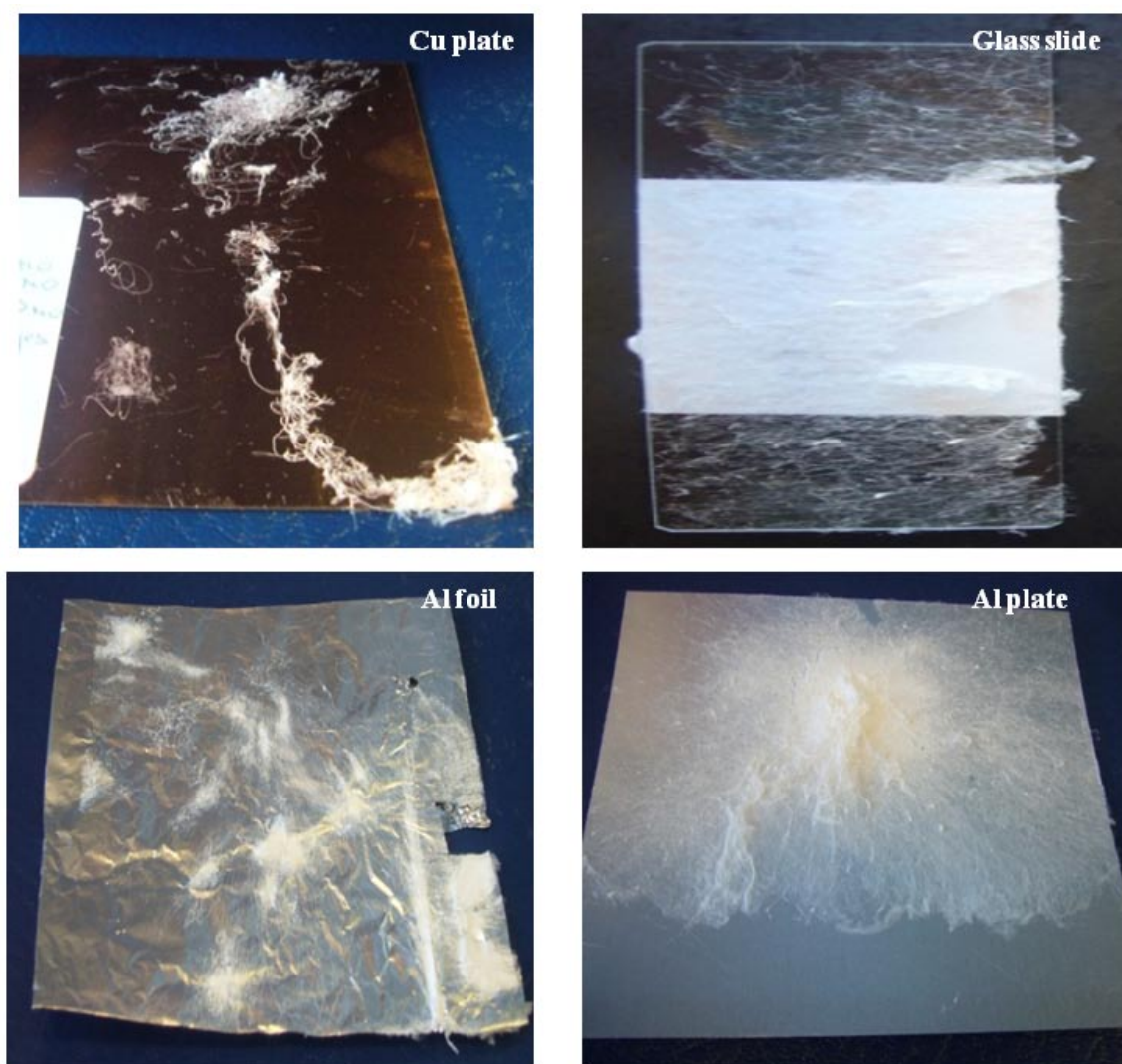
Figure 26 Various collectors for the electrospun 15%PHB98-PHV2 fibres collection

As showed by the images, over the period of 10 minutes, the best deposition rate

was on the Al plate collector. The Cu plate and the Al foil collected fewer fibres during

the same time period, while on the glass slide the deposition was uniform, but poor. For

characterisation purposes such as mechanical, chemical and biological testing, samples

would need to be removed from the collector without damaging the structure. The glass slide and Al foil samples were difficult to remove without physically altering the samples (tearing), while the samples collected on Cu plate, and the sample collected on the Al plate respectively would peel off easily. Further thickness measurements (Figure 27) indicated that for the same deposition time the samples collected on the Al plate were thicker. In conclusion, the Al plate was chosen as the collector type for future testing. The morphology of the fibres collected on the Al plate was investigated using SEM (Figure 28). The fibres were smooth, continuous and no bead defect formation was detected.

On foot of the results so far, it was concluded that in order to obtain smooth and continuous fibre deposition, with no bead defect formation on the individual fibres, a solution of 15% PHBV in chloroform should be used. Furthermore the electrospinning conditions should be as follows: Al plate collector (2.5 mm), collection distance of 15cm, feed rate of 5ml/h and a deposition time of 10-20 minutes, until full coverage of the collector would be achieved.
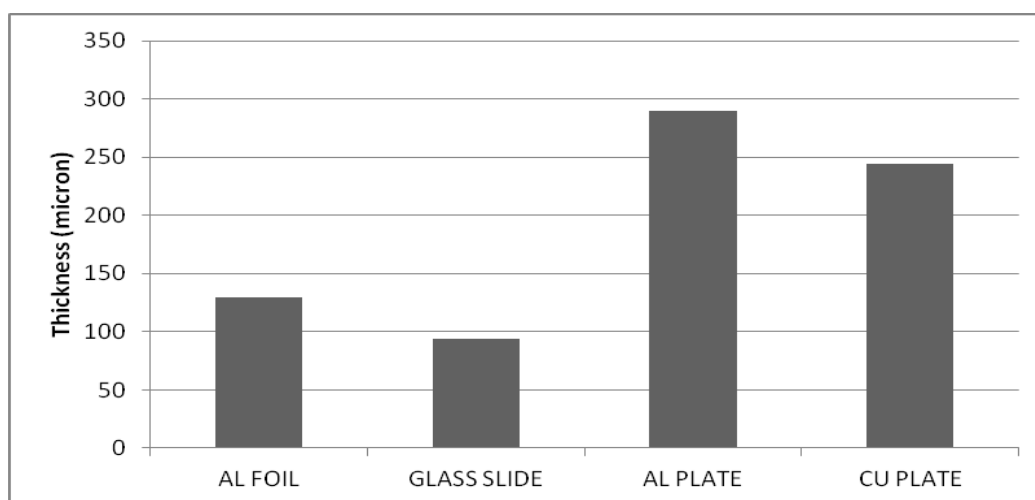
Figure 27 Thickness measurement for samples collected on various collector types

(n =5)

20 µm*	EHT = 11.12 kV	Mag = 503 X	Date :11 Nov 2010	ZEISS
	WD = 11.5 mm	Signal A = SE1	Time :10:14:57	
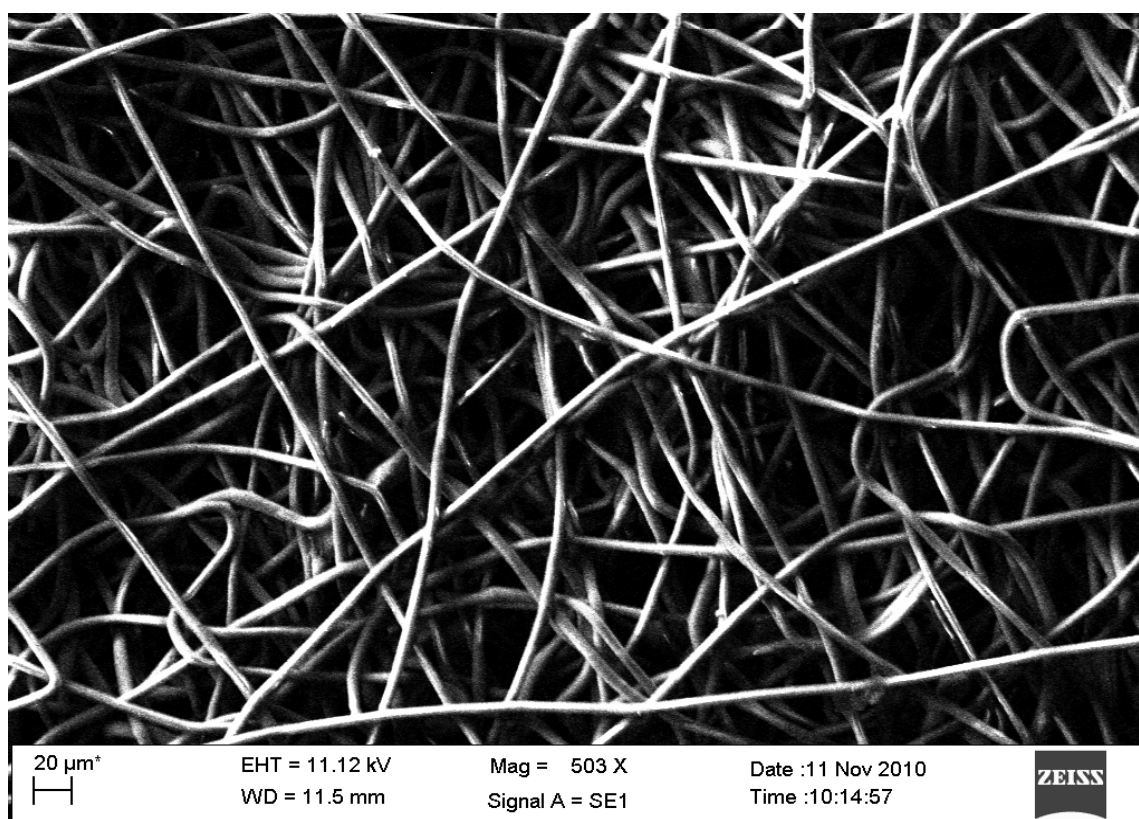
Figure 28 P15 fibres, collected on Al plate (FD= 5ml/h, D= 15cm, 15kV +/-)

4.3.2 Preparation and electrospinning of composite solution

The role of the scaffold is to allow target cells to attach, multiply and exhibit specific functions. Further, the cells will recreate the new tissue *in vivo* while the template (scaffold) degrades at an appropriate rate, ideally without toxic degradation products being released. The overall goal of this research work is to mimic the extracellular matrix of the bone, combining both morphological aspects and mechanical features of the fibrous structures with the biocompatibility and biodegradability of the materials to be used. While single polymeric scaffolds have been developed using both biodegradable and non-degradable polymers [178] a more biomimetic approach would be the use of composite materials. Bone itself is a perfect example of composite material designed by nature, where minerals are embedded as reinforcing elements while the collagen serves as matrix. A composite material contains two or more distinct constituent materials or phases, on a scale larger than the atomic. The properties of composite material are significantly altered in comparison with those of homogeneous materials [179].

PHB/PHV is a highly crystalline, brittle and relatively hydrophobic material while being a natural and biodegradable polymer [180]. In order to use the benefits of its biocompatibility andnon-toxic degradation products, such as D-β-hydroxybutyrate (HB, a normal component of the blood and tissue), it was mixed with hydroxyapatite nanosized particles [181]. Hydroxyapatite, a major component of mineralised tissue, such as bone and teeth has been used several times mainly as coatings, due to its

osteoinductivity. At the same time its brittleness and poor mechanical stability limited its use on its own for the regeneration of non-load-bearing bone defects [182].

Hydroxyapatite is used to modify the mechanical properties of polymeric implants for certain medical applications. While the nano sized particles of hydroxyapatite have an increased surface area, charge and have the ability to modify the absorption of chemical species(properties that can be used to promote cell activity and increase mineralization rate), the incorporation of nano sized hydroxyapatite particles into the polymeric matrix can also improve the mechanical properties and support calcium and phosphate delivery after implantation [183, 184]. Composites of PHB/PHV and HA with partial biodegradability and high mechanical strength and osteoconductivity were reported to be suitable for fracture fixation [185].

Several difficulties were encountered when adding the nano hydroxyapatite. The ceramic, due to its nano size tends to form agglomerates before its addition to the solution as well as when in solution. In order to avoid the formation of such agglomerates an ultrasonic bath was used. The ceramic phase was sonicated in the solvent, prior to addition of the polymeric phase. As a starting point, 1% nHAp and 2% nHAp were added to P15 solutions as the lowest reference starting points. Immediately after the addition of the ceramic phase, solution conductivity and the dynamic of the electrospinning process changed.Electrospinning of this composite solution proved to be difficult despite the various attempts to identify optimum sets of parameters. Figure 29 shows SEM images of electrospun samples of P15H2 collected over a period of 30 minutes. The as-electrospun composite fibres varied in size and shape, evidencing microporous structure on the surface of the fibre. Further bead formation was shown and this was attributed to the agglomeration of nano hydroxyapatite particles, due to

insufficient dispersion in the solution. As shown on the cross section of the composite construct image in Figure 29 (B) several layers can be identified. The red arrow indicates deposition of independent fibres, while the yellow arrow indicated a bundle of attached fibres, with no distinct shape. The sample as a whole was not a fibrous and porous structure, but bundles of fibres and sprayed polymeric fragments.
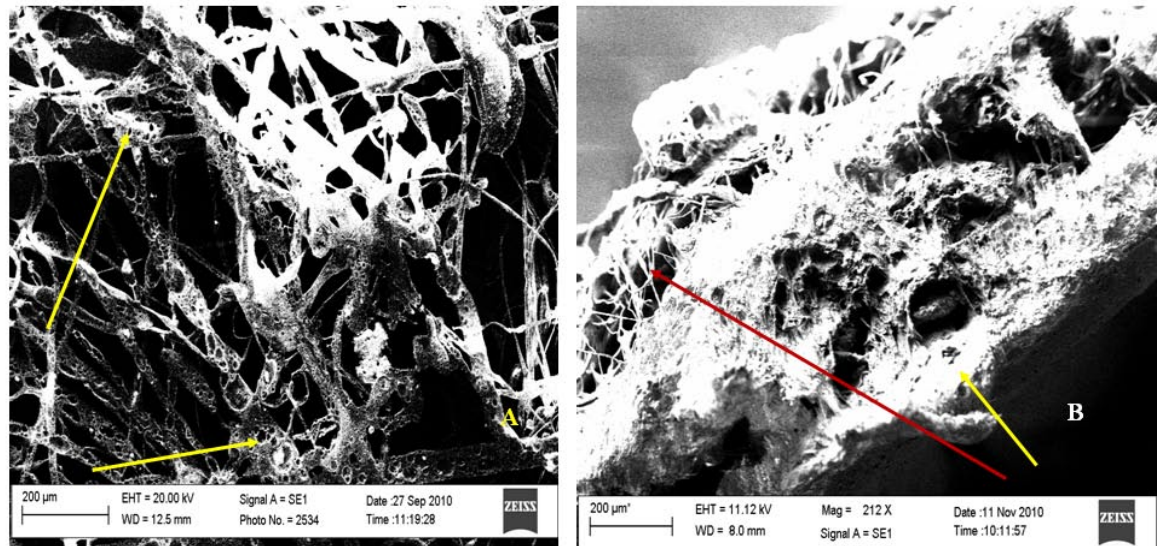
Figure 29 SEM images of P15H2 electrospun samples (A) and (B). The red arrow indicates deposition of independent fibres, while the yellow arrow indicated a bundle of attached fibres, with no distinct shape. The sample as a whole was not a fibrous and porous structure, but bundles of fibres and sprayed polymeric fragments.

In order to improve the morphology of the fibres and overcome the change in the conductivity of the composite solution, a new phase was added to the solution. Silk fibroin (SF) essence is a natural protein, rich in aminoacids, such as alanine, glycine, sericine and tyrosine grouped in sequences (Gly-Ala-Ser, Gly-Pro-Gly). When appropriately purified, silk fibroin is non-toxic, non-immunogenic and has been demonstrated to support cell and tissue growth [186, 187]. It is known that SF is

characterized by repetitive hydrophobic and hydrophilic peptide sequences. The repetitive sequence in hydrophobic residues dominates the β-sheet structure, forming crystalline regions in SF fibres and films. The formation of these β-sheets results in insolubility in water [188]. Due to its several distinctive biological properties such as good biocompatibility, biodegradability, low inflammation reaction, no blood clotting effects and good mechanical properties, silk fibroin protein has been extensively studied as one of the most promising materials for biomedical applications [189-191].

Silk fibroin essence was added to the solution to balance the effects of the nano hydroxyapatite and equal amount of silk fibroin and ceramic were added to the polymeric solution, respectively 2% SF. Electrospun samples of the tri-phasic composite are shown in Figure 30. Silk fibroin addition changed the dynamic of the solution which led to continuous electrospinning, and no beads formation. Silk fibroin, as already mentioned contains sequences of aminoacids, 3% of which are acidic aminoacids such as aspartate and glutamate. This acidic aminoacids provide active surface sites for hydroxyapatite deposition and nucleation, due to their carboxyl groups (-COOH). For this reason silk fibroin can also be used for apatite nucleation in the case of bone tissue engineering applications [192, 193].

Figure 30 Photograph of Eelectrospun tri-phasic composite solution (P15H2S2) at FD=2ml/h, D= 10cm, V=10kV

After successfully electrospinning the composite solution as already shown, the samples were morphologically, chemically, and physically analysed in order to determine if they are suitable as bone tissue candidates. The following tests were used: SEM/EDX, FT-IR, DTA/TGA, contact angle measurement, fibre diameter, degradation, weight and pH measurements, porosity measurement and preliminary qualitative biological assessment

SEM/EDX analysis

Tri-phasic composite fibres resemble the electrospun P15H0S0 fibres morphology, as shown in Figure 31 (A, B). They are randomly aligned, smooth and continuous, with

no beads formation. On a macroscopic scale, the electrospun polymeric sample of P15 exhibited a less rough surface compared with the tri-phasic membranes P15H2S2 which revealed macropores and higher irregularities on the surface. The SEM analysis showed that the fibres are randomly aligned which is the result of continuous deposition (no breaking was observed for individual fibres). Further single fibres presented a smooth surface and no bead formation. EDX verified the presence of Ca^{2+} and phosphate elements, confirming that hydroxyapatite is present both in the fibre structure as well as on its surface. The mono-phasic fibres measured 10-15µm in diameter, while the tri-phasic fibres are 13-17 µm in diameter (n = 20). The fibre diameter is slightly increased for the tri-phasic composites and this could be attributed to the presence of nano-hydroxyapatite particles agglomerations within the polymeric fibres. As mentioned before it should be noted that the diameter values are not the smallest possible; they represent values that were found to produce consistent and useful fibrous membranes. Fibre diameter was measured using Image J image processor (see appendix A for protocol).
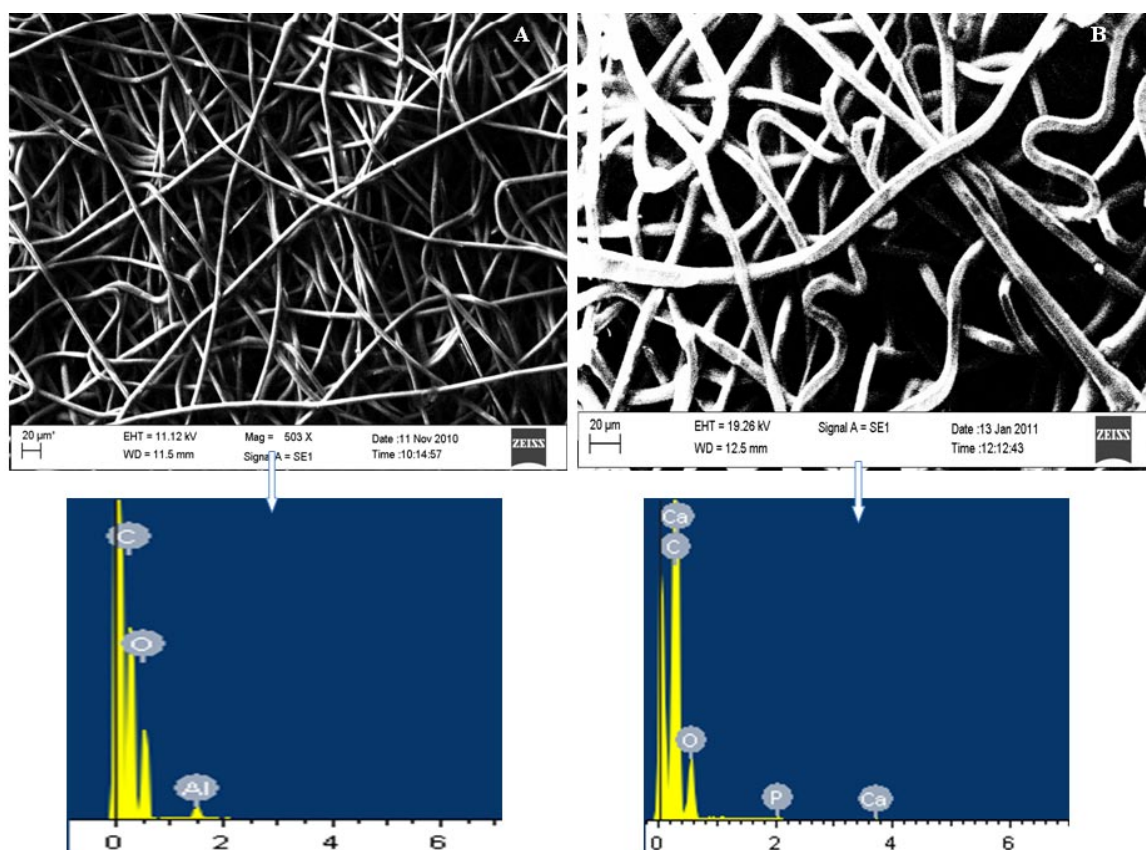
Figure 31 SEM fibre morphology and EDX analysis (A) P15 (B) P15H2S2

Thermal behaviour analysis

Compared to the thermal curve of the PHB/PHV, the one for the composite showed a recrystallization peak at ~382 º C which is attributed to the PHB/PHV itself. As seen in Figure 32 the thermal behaviour of the composite resembles that of the polyhydroxyalkanoate, because more than 80% of the composite was pure polymer.
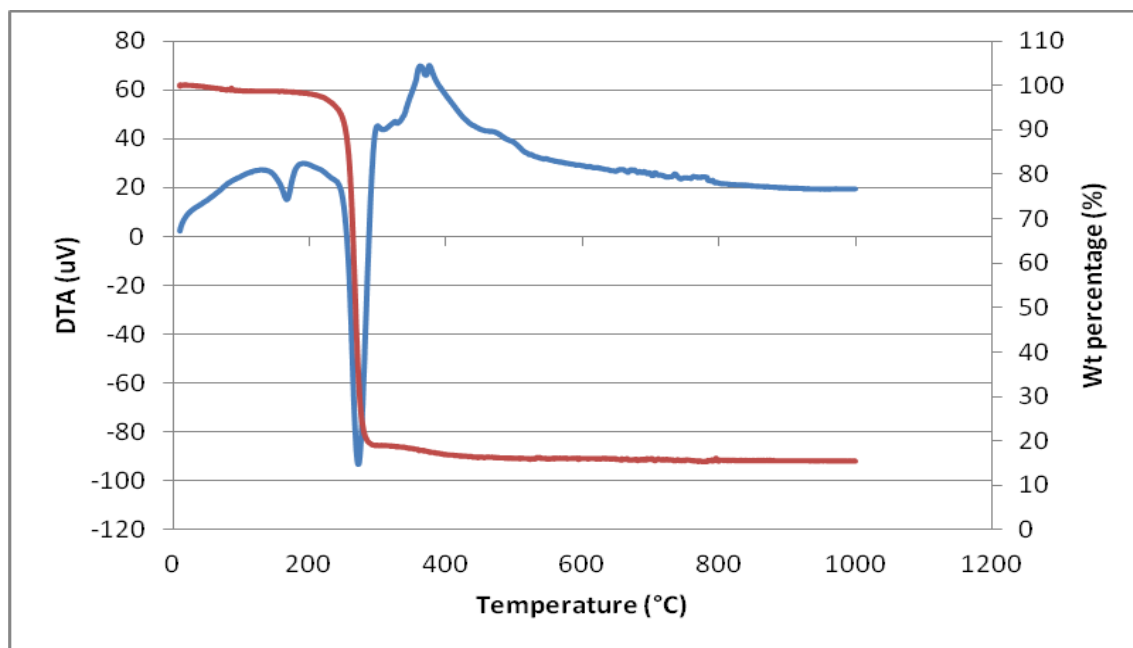
Figure 32 DTA/TGA analysis of the P15H2S2 composite

FT-IR spectra analysis

The spectra of the composite and of the P15 revealed several common peaks, since the matrix is the same. These absorption peaks were the symmetric stretching vibration of C–CH$_2$ at 2845 cm^{-1}, the carbonyl peak at 1647 cm^{-1}, the methyl peak at 1385 cm^{-1} and the stretching vibration of C–O at 1210 cm^{-1}.The FT-IR analysis of the composite revealed the presence of the three amides, characteristic for the silk fibroin and also the PO$_4^3$ vibration bands v$_3$ and v$_4$ of the hydroxyapatite. As can be observed the positions of the amides shifted and the vibration intensity apparently decreased with the addition of hydroxyapatite. The Ca^{2+} presence forced the –C-O and –N-H groups from the silk fibroin molecule to be absorbed by the hydroxyapatite solution. The PO$_4^3$ vibration bands were found at 1030 cm^{-1} and 987 cm$^-$

[1], with decreased vibration intensity. No additional peaks, than those corresponding to the PHB/PHV, and nHAp were found, which indicates that there was no chemical bonding between the ceramic particles and the polymeric matrix. Figure 33 presents the FT-IR spectra of the electrospun composite fibres and Table 13 presents the infrared frequency assignments
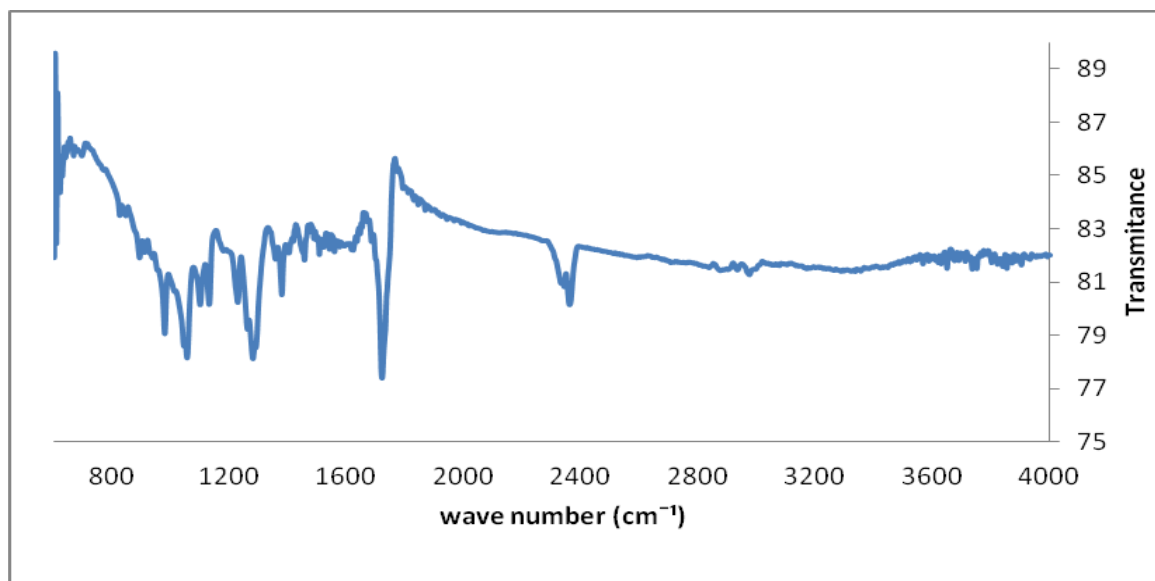
Figure 33 FT-IR analysis of P15H2S2 composite

Table 13 Infrared bands assigned for the P15H2S2 composite

Infrared frequency (cm^{-1})	Assignment
2845 cm^{-1}	Symmetric stretching vibration C-CH$_2$
1647 cm^{-1}	stretching vibration of the C=O bond
1385 cm^{-1}	C–H rock, methyl
1210 cm^{-1}	C-O stretching vibration
1375-1390 cm^{-1}	amide III
1380-1400 cm^{-1}	amide II
1500-1600 cm^{-1}	amide I
3294 cm^{-1}	Amide A (N-H stretching vibration)
987 cm^{1}, 1030 cm^{-1}	PO$_4$$^{3-}$ v 3 and v4 vibrations

Contact angle and porosity measurements

The wettability of the P15 electrospun fibres, and P15H2S2 electrospun nanocomposites fibres were determined by water contact measurement and the results are summarized in Table 14.

Table 14 Water contact angles of P15 and P15H2S2 electrospun composites

Composite	P15	P15H2S2
Contact angle (deg)	78.75±3.14	84.47±0.49

It can be seen from the table that the electrospun P15 is a relatively hydrophobic structure. Further, when adding silk fibroin to the P15H2S2, the average contact angle is higher than those of the polymeric solution fibres because the surface roughness of the pure polymeric fibres is lower than that of the composite structures. The water droplet could not easily slip on the rough surface of the hydrophobic fibrous nanocomposite membranes, and was almost supported on the semi-solid surface, resulting in a higher water contact angle. At the same time, the increase in roughness, demonstrated by the water contact angle value offers a higher surface area for cells to attach to.

Porosity measurements employed the helium pycnometer (Micrometirics, AccuPcyc 1330, USA) and were calculated from replicate measurements of volume and density, using the following formula where ρ_b is the bulk density and ρ_g is the grain density [194].

$$\varphi = (1- \rho_b/\rho_g) \times 100 \qquad \text{(Eqn. 3)}$$

In addition, the observed decrease in wettability of the composite samples could be the results of a decrease in porosity associated with the change in composition, as described in Table 15.

It was observed that porosity significantly decreased with increasing ceramic and proteic phase concentration, from 75% for P15 to 72%-70% for P15H2S2 while trabecular bone exhibits a porosity ranging anywhere from 50% to 90% [195]. This decrease of porosity could be attributed to the slight change in fibre diameter due to the presence of nano hydroxyapatite particles within the fibres [196]. Further, since the control of fibre morphology and alignment was not a goal of this preliminary stage of research, the random deposition could have been another factor for the change in porosity.

Table 15 Porosity of as-electrospun composite membranes (n= 5, p<0.05)

Composite	P15	P15H2S2
Porosity (%)	74.78±0.76	72.52±0.66

Conductivity and pH changes measurements

As seen from the Figure 34 (A-B), the degradation tests were carried out for a period of one month. Samples of P15 and P15H2S2 were cut into 1x1 cm pieces, weighed and immersed in deionised water at 37°C, in a water bath. After 4 weeks samples were taken out, dried and weighed, and the weight loss recorded. After one

month the composite lost no more than 2% of its initial weight while the P15 lost less than 1%.
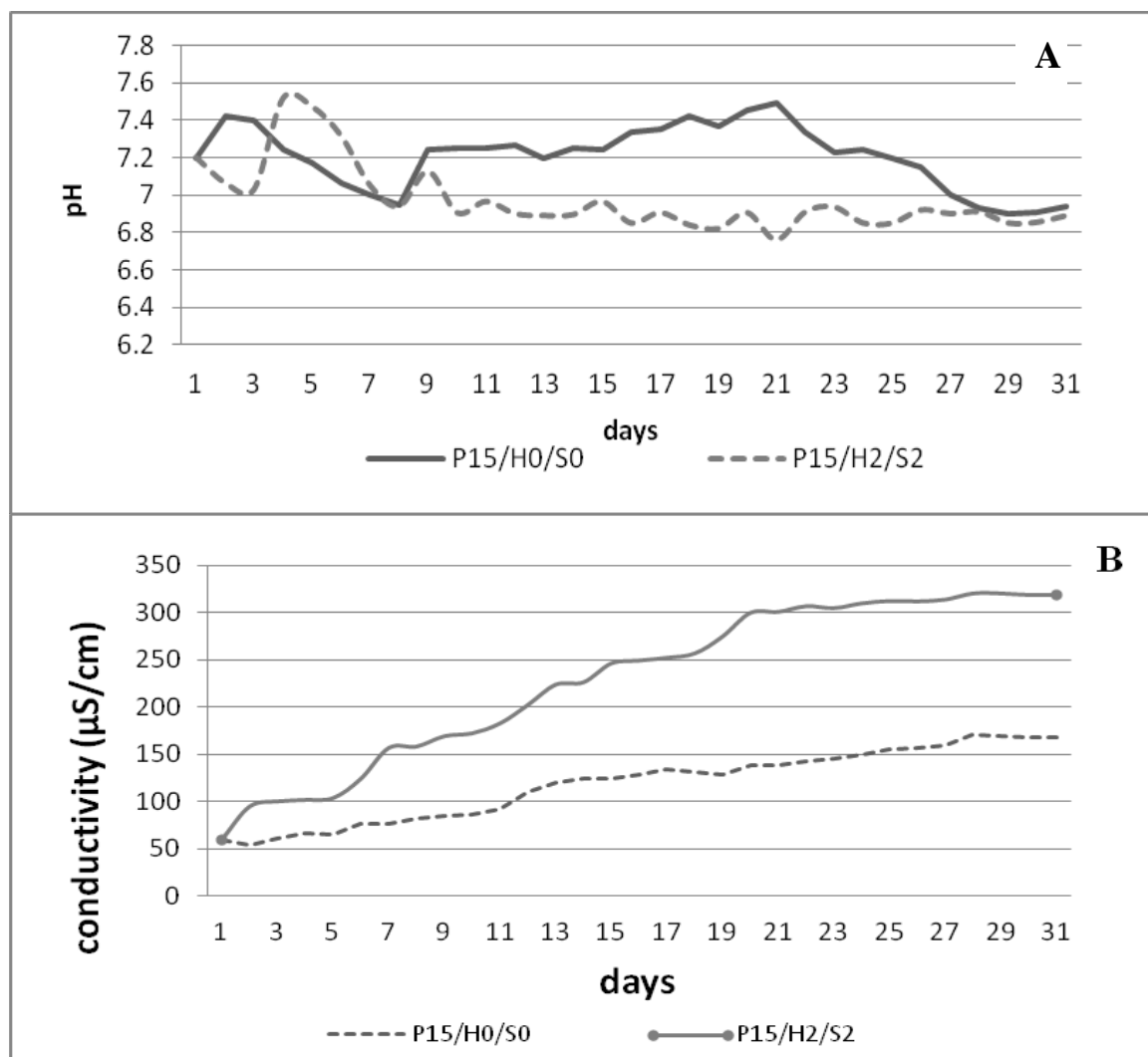
Figure 34 Degradation over one month period and pH measurements P15 and PH2S2 composites

pH was measurement every day, at the same hour for 31 days. SEM images were taken of the left samples, for comparison reason. Figure 35 shows the morphology of the 4 weeks degraded fibrous nanocomposite sample.

As the ceramic and silk fibroin were added to the polymeric solution in small amounts, no general significant difference was recorded in terms of pH changes. In the first 7 days, small variations were recorded and they are attributed to the presence of the composite phase.
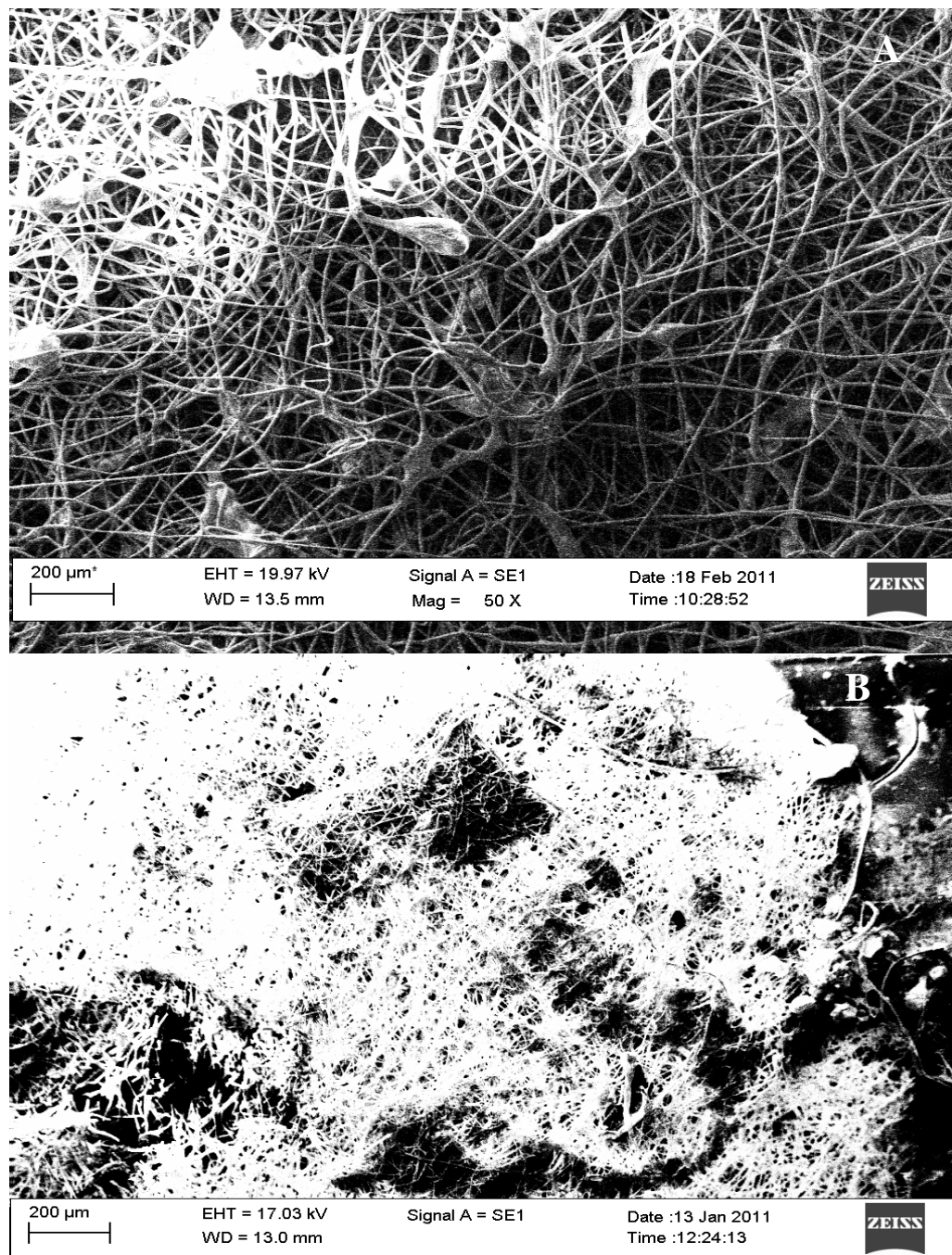
Figure 35 SEM morphology of P15H2S2 sample (A) prior and (B) after 1 month degradation test (magnification 50X)

Qualitative preliminary biological evaluation of the fibrous constructs

This qualitative study was done in collaboration with Dr. Joanna Podporska Carroll and Dr. Rosalleen Devery from School of Biotechnology DCU.

As a prerequisite for cell growth *in vitro*, a surface must support cell adhesion and spreading, thus proving to be non toxic to cells [197]. A preliminary qualitative biological study performed on the scaffolds showed that attachment and growth of human osteoblasts HOB cells was supported and that these cells maintained their morphology. The control for this experiment was the polymeric matrix (P15) which has been shown in the past that to support osteoblasts attachment and growth [198, 199]. Microscopy-based observations (SEM, fluorescent microscope) showed that the same trend was observed for modified (P15H2S2) and unmodified (P15) material. After 1 and 3 days of the experiment, cells were found to be attached to the fibres, demonstrating similar morphology with a flattened appearance and elongated shape on the surface of fibres (Figures 36 and 37). Additionaly LIVE/DEAD staining showed no cytotoxic effect of the tested materials on HOB. SEM images show that cells were able to penetrate cavities between fibres and no significant difference in their behaviour was observed between the test sample and control, despite difference in the materials composition and morphology . Figure 37(A), shows that After 1 day of culturing there are single dead cells visible in the control material (red colour). This can be associated with the process of cells seeding rather than with the material related cytotoxicity as after 3 days of experiment (Figure 37 B, D) no extra dead cells were observed on all tested materials. It can be seen that after 1 day, elongated and single round cells

116

werevisible while after 3 days all cells were elongated and well distributed within the
scaffolds structure.
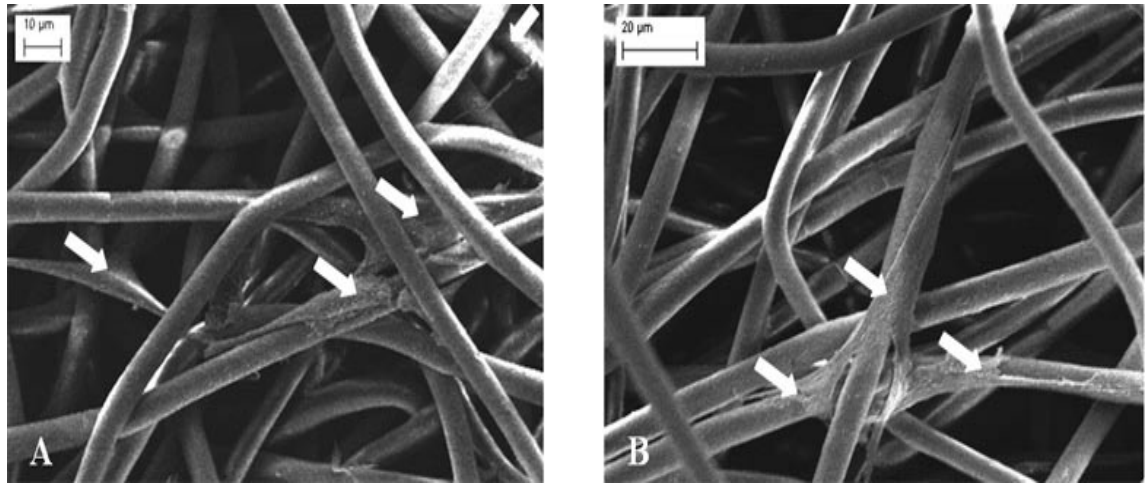
**Figure 36 SEM micrographs of HOB cells on the obtained scaffolds. A – P15H2S2
(3 days) B- control P15 (3 days).**
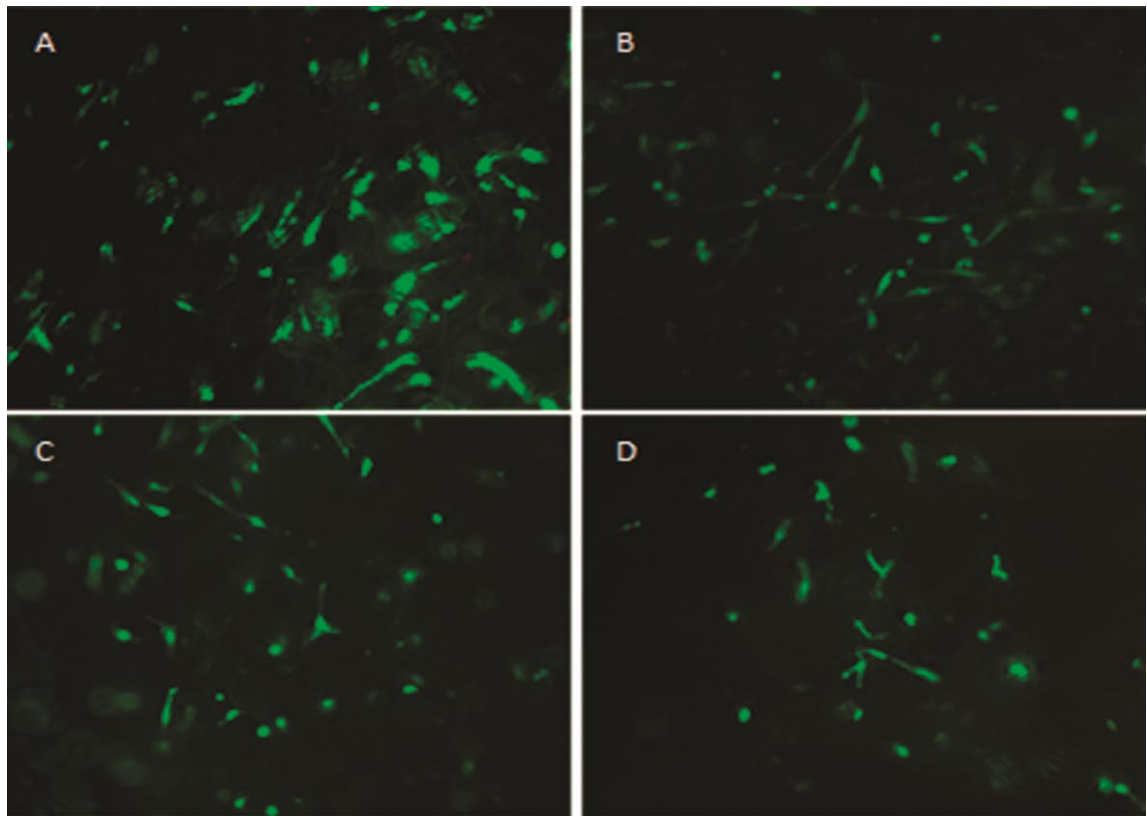
**Figure 37 Microscopic micrographs of Live/Dead staining after 1 day (A,C) and 3
days (B,D): A – control P15 (1 day), B- control P15 (3 days), C –
P15H2S2 (1 day), D –P15H2S2 (3 days). Live cells are stained green
and dead/damaged cells are stained red (original magnification 10x)**

Discussion

In line with the listed objectives (Section 1.4) the results presented above showed that nano-hydroxyapatite can be simultaneously electrospun within the polymeric matrix of PHB/PHV. Furthermore random and continuous deposition of smooth fibres was obtained for the screened composite formulation (P15H2S2). The collected two dimensional fibrous membranes were easy to peel off from the collector and handled for further analysis. The fibre diameter values were slightly smaller when compared to the pure polymeric fibres ones and this was attributed to the addition of nHAp and silk fibroin. EDX analysis confirmed the elements' presence within and on the fibres. The DTA curve also evidenced a ~ 12 % weight residue assumed to be the ceramic phase. This confirmed that the nHAp particles were incorporated within the composite fibres. In addition, the observed decrease in wettability of the composite samples could be the result of a change in porosity associated with the SF and nHAp additives. Significant porosity difference was found between the polymeric P15 samples and the composite sample, with values of ~75% for P0 and 72% for P15H2S2 ($p<0.05$), while the trabecular bone exhibits a porosity ranging anywhere from 50% to 90%. This change in porosity could be attributed to the slight change in fibre diameter due to the presence of nano hydroxyapatite particles within the fibres. Further, since fibre alignment control was not a goal of this preliminary stage of research, the random deposition could have been another factor for the change in porosity. In order to test the structures degradability and its suitability for bone regeneration applications degradation test were carried. The pH and conductivity measurement tests over 4 weeks degradation gave evidence that the fibrous structures have retained their porous structures with the fibres slightly swollen (SEM analysis). The conductivity results evidence a continuous release of ions from the samples, with a constant degradation rate for the composite

formulation, while the random fibres deposition and nHAp, respectively SF particles arrangement within the fibres may have influenced the rate of degradation.

4.4 Optimisation Experimental Design

DESIGN OF EXPERIMENTS (DOE) - RSM, ANOVA

Additional research step used in order to identify the effects of various constituents concentrationand electrospinning parameters levels on sample morphology and structure. Characterization methods include:

- SEM/EDX
- Contact angle
- Fibre diameter

Optimal Range of Composites and Set of Parameters
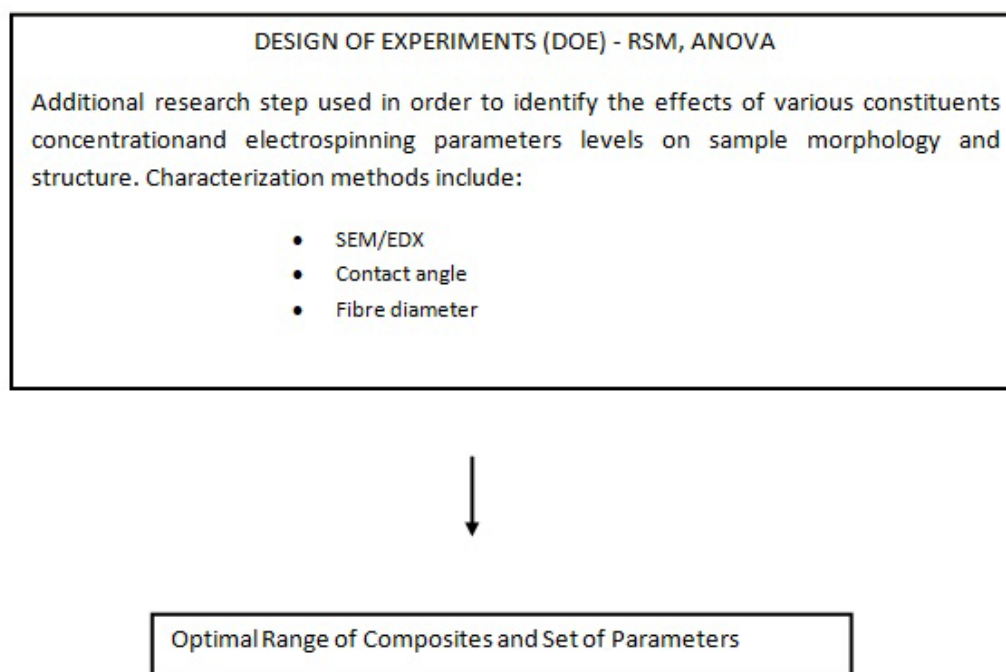
Figure 38 Schematic of Step 3 of the research plan

The next step in the research work involved the systematic investigation of a wider range of composition concentrations and electrospinning parameter values. This study offered a wider perspective on the effects these parameters have on the final structures and morphologies of the electrospun nanocomposite fibres and also offered information on the maximum ceramic, and silk fibroin concentrations respectively that can be electrospun simultaneously within the polymeric matrix. Along with this, fibre

smoothness was one of the main features investigated. Fibre smoothness refers to the absence of bead formation and uniformity of fibre morphology. To assess the interaction and the effects, statistical experimental design methodologies were used. This design of experiments approach is an efficient way to determine the effect of several parameters on a system's behaviour while reducing the necessary number of experiments. 2n factorial designs are also beneficial for the determination of interaction between several parameters changed between two levels. Box-Behnken design is ideal for observation and derivation of higher level models around a centralised experimental design. One factorial experimental design schemeand a Box Behnken design were developed using DesignExpert 8.0 software (StatEase, USA) for this purpose. Variables dealt with were:

- Ceramic phase concentration (%nHAp)

- Proteic phase concentration (%SF)

Three levels of each factor were taken for the experiments and all possible combinations of the three levels were checked for determination of the effects on sample morphology, particularly bead formation. In order to obtain a solution with viscosity characteristics that allow electrospinning a balance had to be kept between the concentrations of the two co-phases. A maximum of 6.5 g (poymer + ceramic + silk fibroin) could be added per 100ml chloroform and Table 16 shows the series designed and the investigated factors.

Table 16 Factors investigated for the observation of the different series (Series 30-35 % of nHap and Series 5 F – variation of 5 factors)

Series 30-35 General factorial	Factor code	Low level (-1)	Centre point (0)	High level (+1)
%nHAp	A	30	32.5	35
%SF	B	10	15	20
Series 5F Box-Behnken	Factor code	Low level (-1)	Centre point (0)	High level (+1)
%nHAp	A	10	22.5	25
%SF	B	10	25	30
Feed rate (FD)	C	3	4	5
Needle tip-collector distance (D)	D	10	15	20
Voltage (V)	E	7	10	13

Selections of the samples produced during this step of the research are shown in Figure 40. It has been observed that for higher nHAp and silk fibroin concentrations, it was difficult to initiate electrospinning with the composite solution, which can be attributed to the change in viscosity and poor dispersion of the nano particles within the polymeric matrix. Further increase in macroporosity was visually observed with increased silk fibroin concentration. The electrospun samples displayed continuous deposition of fibres and increased bead structure formation with increased ceramic and silk fibroin concentration. Samples with high amounts of silk fibroin exhibited a weakened matrix and a more elastic texture as opposed to those containing lower silk fibroin concentration. Additionally there were combinations of parameter levels (Figure 39) when fibres deposition was discontinuous or low, or where bulks of solution (Figure

39 –P15H15S15 sample) were collected instead of fibrous structures. Due to shape inconsistency such sample morphology was not considered suitable for further research work as they could not be used for future testing.

Figure 39   Photographs and SEM images s of electrospun samples of varied composition
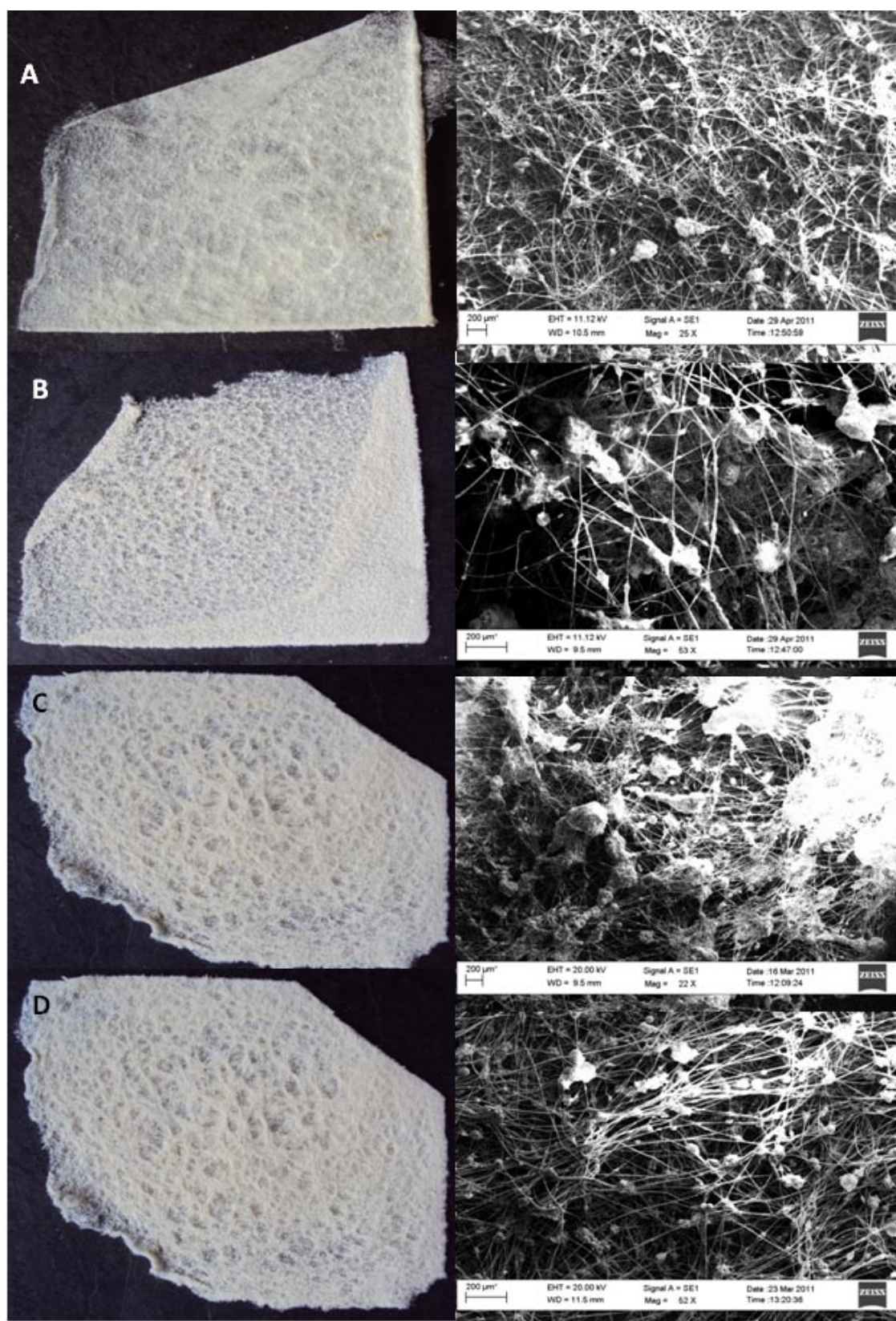
Figure 40 Selection of electrospun fibrous membranes and the corresponding SEM image

The full factorial design was run in order to investigate all the possible combination of the co-phases within the polymeric matrix for high concentration levels, with a limit of 6.5g of dry powder in 100 ml chloroform. Fibre diameter was the investigated response and Figure 41 presents the analysis. These results suggest an increase in fibre diameter with an increase in ceramic and silk fibroin concentration, as expected.
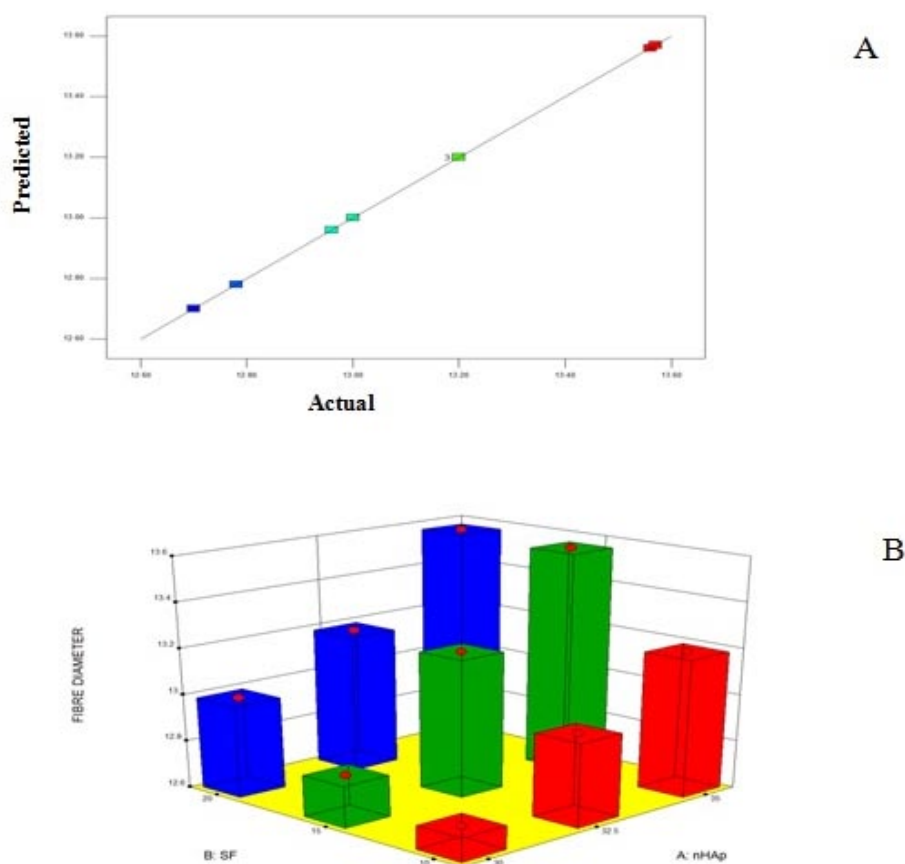
Figure 41 Analysis of Design of Experiment results for 30%-35%nHAp and 10%-20%SF: (a) predicted versus actual response for average fibre diameter, (b) 3D surface analysis for fibre diameter response

Furthermore they show a direct correlation between the concentration of nHAp and SF within the polymeric matrix and the fibre diameter for the range of 30%-35%nHAp and 10%-20% SF, with an increase in diameter for increased co-phases concentrations.

In addition, the Box Benhken design yielded a non significant model when investigating the effect of solution parameters (%nHAp, %SF) and electrospinning parameters (FD, V, D) (Figure 42- Box Benhken for 3 factors). The model included too many interactions between the factors and for future work a reduction in factors should be considered. The results obtained during this phase of the research are presented as supplementary results. Due to the samples' morphological appearance (e.g. bead defect formation) they have not been usedfurther in the research work .
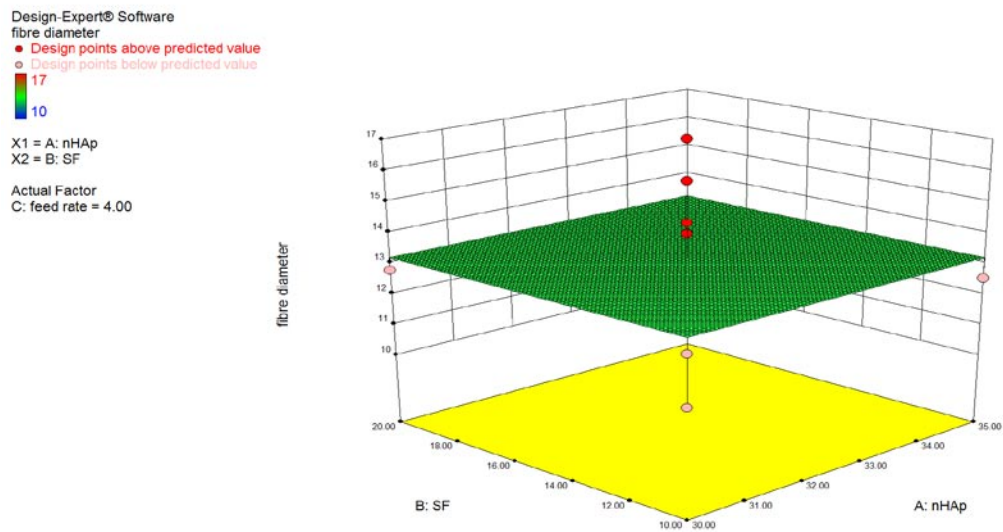
Figure 42   Analysis of Design of Experiment results. Response surface for fibre diameter with respect to %nHAP and %SF at constant value of distance (D) and voltage (V), and a feed rate (FD) of 4ml/h

Characterisation of high nHAp and SF concentration specimens arising from DOE

In order to assess the effect high contents of nHAp and SF have on the morphology, chemical interaction and *in vitro* biological behaviour of the scaffolds additional analysis of a selection of two as-electrospun samples (included FT-IR, SEM/EDX and biological evaluation of the constructs cytotoxicity). The SEM/EDX analysis revealed that the bead structures contained predominantly Ca^{2+} and PO^{4-} which are attributed to presence of nano hydroxyapatite particles (Figure 43). Figure 44 (a, b) shows the FT-IR spectrums for selected as-electrospun composite samples: two with varying ceramic concentration (P15H30S10 and P15H32.5S10), two with varying silk fibroin concentration (P15H32.5S10 and P15H32.5S15). The characteristics groups of all PHB/PHV, silk fibroin and hydroxyapatite were evidenced in the studied composites, thus confirming the presence of all the constituents.
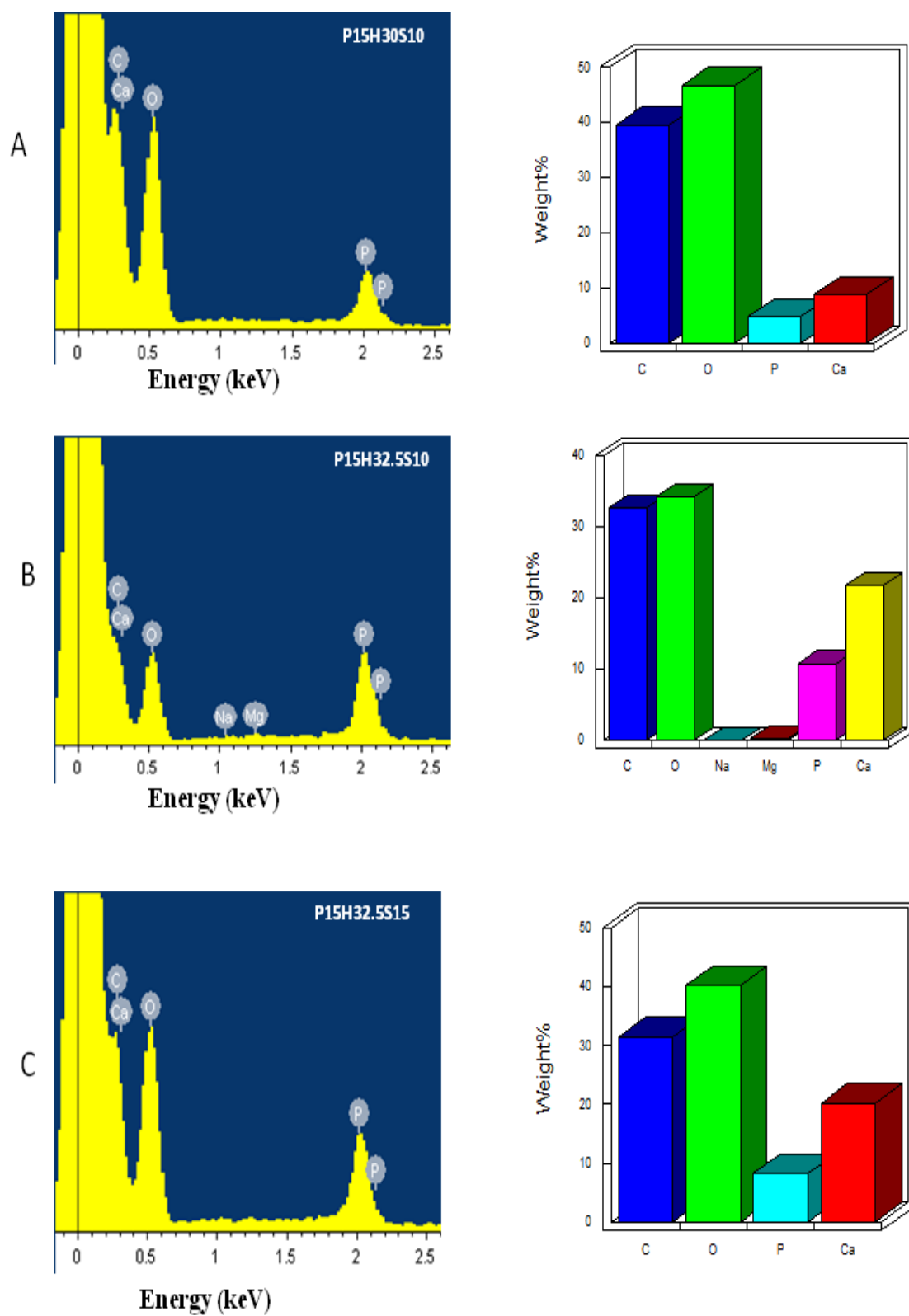
Figure 43 EDX analysis of (a) P15H30S10, (b) P15H32.5S10 and (c) P15H32.5S15
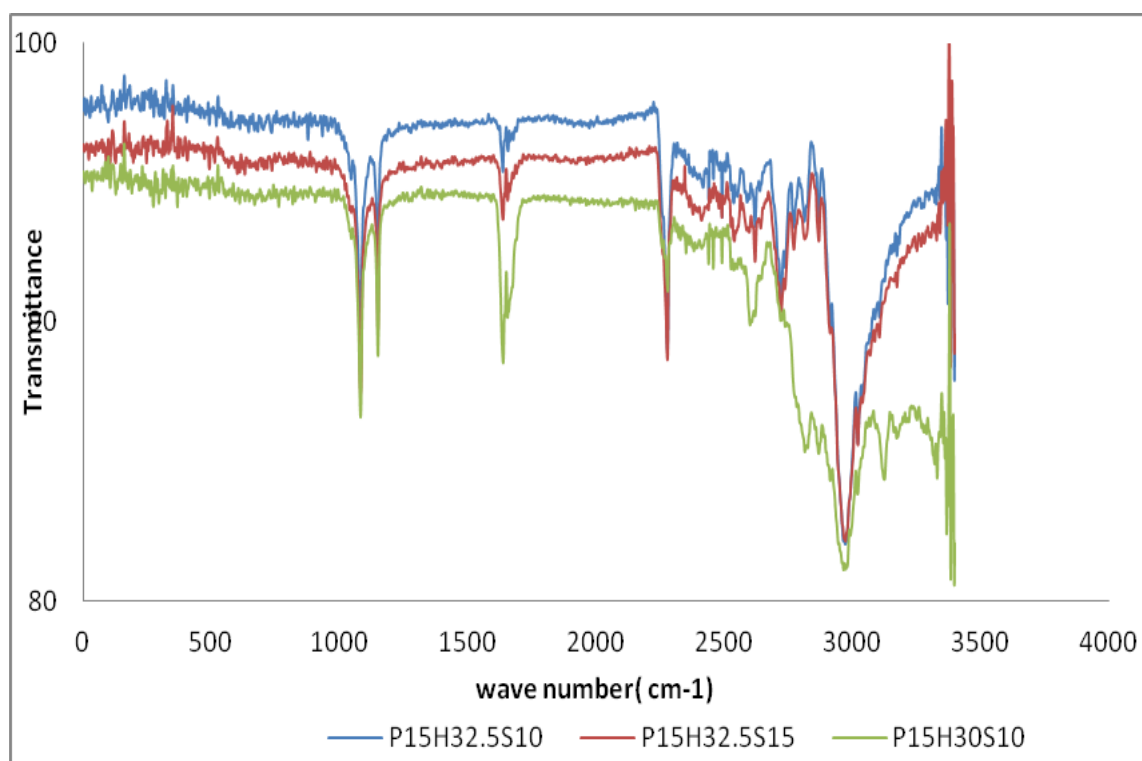
Figure 44   FT-IR spectrum for P15H30S10, P15H32.5S10 and P15H32.5S15 composite samples.

Qualitative biological toxicity evaluation

Qualitative biological evaluation of the produced samples toxicity was performed on a selection of as-electrospun samples (P15H17.5S10 and P15H25S10). Results show that attachment and growth of HOB cells is supported and cell maintain their morphology. Under SEM the cells were hard to detect due to the presence of bead structures. The control for this observation were the cells cultured on the polymeric matrix (P15) which has been shown in the past that to support osteoblasts attachement and growth [198, 199]. After 1 and 3 days of the experiments, cells were attached to the fibres, demonstrating similar morphology with a flattened appearance and elongated

shape on the surface of fibres (Figures 45). Additionaly LIVE/DEAD staining showed no cytotoxic effect of the tested materials on HOB. Cells were able to penetrate cavities between fibres and no significant difference in their behaviour was observed between the test sample and control, despite difference in the materials composition and morphology. It can be seen that after 1 day, elongated and single round cells are visible while after 3 days all cells are elongated and well distributed within the scaffolds structure. Further quantitative evaluation is needed to determine cell activity on the composite electrospun samples.
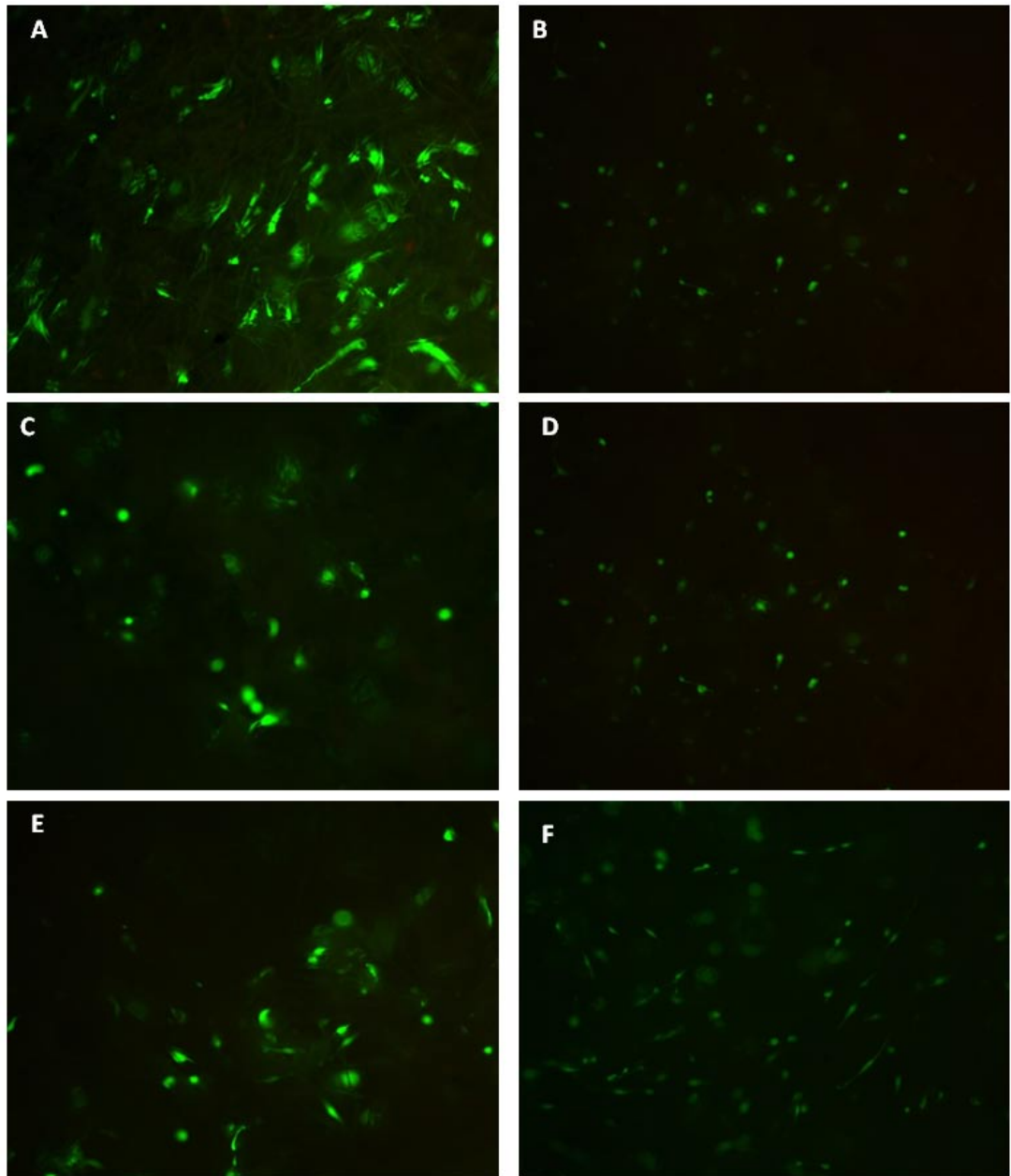
Figure 45 Microscopic micrographs of Live/Dead staining after 1 day (A,C,D) and 3 days (B,D,E): A – control P15 (1 day), B- control P15 (3 days), C – P15H17.5S10 (1 day), D - P15H17.5S10 (3 days), E - P15H25S10 (1 day), F - P15H25S10 (3 days). Live cells are stained green and dead/damaged cells are stained red (original magnification 10x).

Discussion

As mentioned above the samples obtained during this step of the research work were not used for future work or more indepth analysis. The DOE approach was taken in order to investigate the influence of various combinations of electrospinning parameters, different composite formulations and their influence on the samples and individual fibre morphology and diameter. In line with the aims and objectives listed in Chapter 1 it was observed that for higher percentages of nHAp and SF (% nHAp > 5, % SF>5) bead defect formation occurs and electrospinning can be hard to initiate. At visual inspection samples with increased SF content evidenced higher macroporosity, rugosity and elasticity. Some of the samples were too delicate to be handled and were not considered suitable for prospective load bearing applications, but could be suitable for soft tissue engineering. The chemical and biological analysis evidenced the samples composition (PHBV, nHAp and SF), with nHAp found to be present within the composite matrix and on the fibres surface, while the SEM revealed a fibrous structure, with random deposited fibres exhibiting non-uniform fibre diameter and bead defect formation. Furthermore the 3 days biological assessment of the selected samples (various composite formulations) showed that the osteoblasts attached and spread on the fibrous mats, with cells exhibiting filopodia elongations after 3 days in cultures. These results proved that the samples are biocompatible and can sustain cell attachement and proliferation, while further and more in depth test are needed to prove phenotype preservation and bone marker expression. Despite the wide range of parameters tested using DOE, the results proved that in order to obtain no bead defect formation with

smooth fibrous surface, smaller percentage of the composite phases should be used for the given set of parameters.

4.5 *In vitro* bioactivity test using Simulated Body Fluid (SBF)
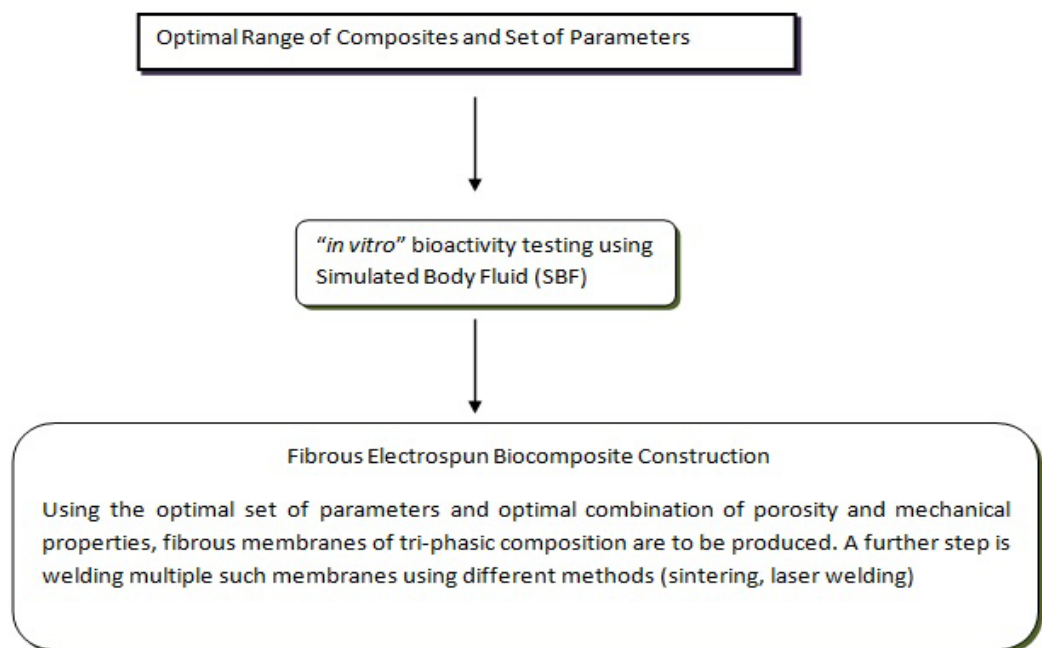
Figure 46 Schematic of in vitro bioactivity test and fibrous electrospun biocomposite construction research plan

Further to the Design of Experiment analysis (Step 3) and preliminary Trial and Error analysis (Step 2) it was observed that solutions containing more than 5% ceramic (nHAp), respectively 5% proteic (SF) phases within the polymeric (P15) matrix will lead to the formation of bead structures when used in combination with the following

set of electrospinning parameters (FR = 5ml/h, D = 15cm, V= 10 kV). In order to obtain a smooth and continuous fibrous structure, with no bead structures and uninterrupted fibre deposition, it was decided to further investigate solutions with a content of 2% nHAp- 2%SF, and 5%nHAp- 5%SF respectively within the polymeric matrix (P15).

The results for samples produced using this set of constituent concentrations were presented in Section 4.2 and included sample morphology and chemical analysis, fibre diameter and porosity measurements, wettability characterization and preliminary biological assessment (cell adhesion and cytotoxicity).

Following the concept of incorporating bioactive ceramic particles within the polymeric matrix in order to improve mechanical properties and bioactivity synthetic nHAp was used, which is similar to the main mineral phase of the bone, and has been widely used as a bone substitute material due to its biocompatibility and bone-bonding ability [200]. Further it is commonly believed that when bioactive materials are implanted in the body, they spontaneously bond to bone via an apatite layer deposited on their surface without forming the fibrous tissue around them [201]. However, the *in vivo* results are normally difficult to obtain and to interpret due the complexity of cellular responses. *In vitro* methods to assess the bioactivity of biomaterials include the use of Simulated Body Fluid (SBF), which specifically evaluates the substrate ability of apatite formation, protein adsorption or osteoblast cell culture studies.

In order to characterise the apatite formation ability of the electrospun samples the standard acellular *in-vitro* procedure as described by Oyane *et al.* [202] was used. For this purpose P15H2S2 nanocomposite fibrous pieces (1cm x1cm) were immersed in 100ml of acellular SBF (pH 7.30 at 37ºC, prepared in-house) in plastic flasks. The plastic flasks were placed in a water bath at 37ºC. The SBF solution was refreshed twice a week. The samples were removed from SBF solution after 7, 14, 21 and 28 days.

After removal from SBF, the samples were gently rinsed with deionised water and left to dry at room temperature for 24 h. Apatite formation was assessed using SEM/EDX and HATR-FT-IR analysis.

Figure 47 shows the SEM images of electrospun P15H2S2 fibrous membranes, after 7 days and 28 days in 1x SBF, while Figure 48 shows the apatite crystals formed on the surface of the fibres, at higher magnification. After 7 days no visible apatite crystals were formed. Instead after 28 days in SBF, a precipitated apatite layer was visibly covering the composite fibres. EDX analysis proved that the white layer formed on the surface of the fibres consists of Ca^{2+} and PO_4^{3-}, as shown in Figure 47 d and Figure 48. Elements, such as Mg^{2+}, Cl^- and Na^+ were present on the surface of the fibres, elements that are present in SBF composition too (see Table 17). This *in vitro* test shows that the composite is bioactive, and can initiate bone formation.

Table 17 Ion concentrations of simulated body fluid and human blood plasma

Ion	Concentration (mmol/dm^3)	
	Simulated body fluid (SBF)	Human blood plasma [202]
Na^+	142.0	142.0
K^+	5.0	5.0
Mg^{2+}	1.5	1.5
Ca^{2+}	2.5	2.5
Cl^-	147.8	103.0
HCO_3^-	4.2	27.0
HPO_4^{2-}	1.0	1.0
SO_4^{2-}	0.5	0.5
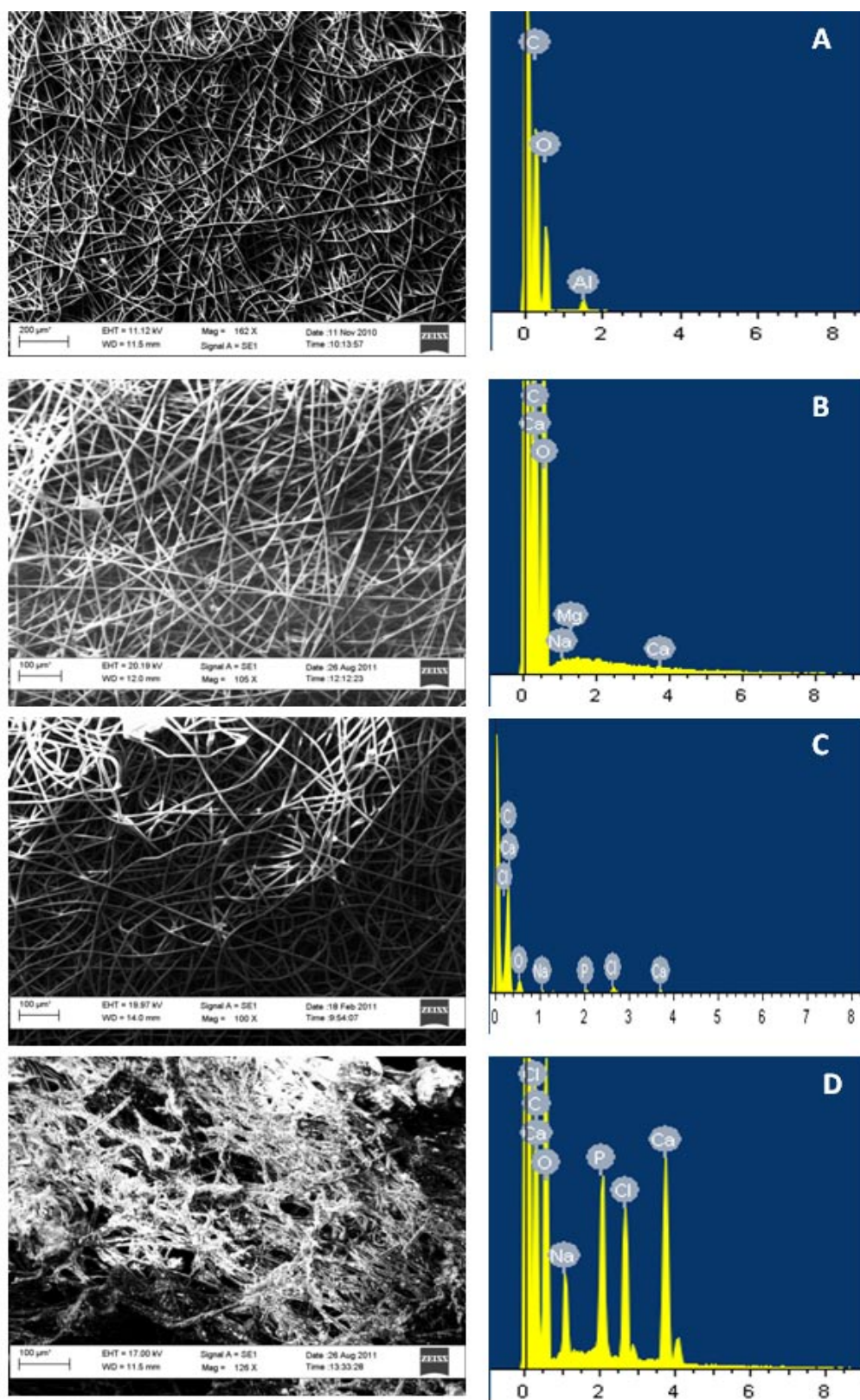
Figure 47 SEM/EDX images of P15 (A), P15H2S2 (C) prior to immersion in SBF and P15 (B), P15H2S2(D) after 28 days in 1x SBF (37 ºC, pH = 7.30).

The FT-IR spectra of the P15H2S2 composite scaffolds (Figure 49) displayed the expected vibrational bands for the PHB/PHV polymer (a $C=O$ stretch at 1720 cm^{-1}, various aliphatic C–H vibrational modes in the regions 1227–1478 and 979–826 cm^{-1} and C–O vibrational modes at 1183, 1133 and 1057 cm^{-1}) [203], as well as a significant vibrational band at 563 cm^{-1} (characteristic of HAp). After 28 days in SBF, spherical particles, ranging from 1 to 5 μm in size, were observed to be deposited within the composite scaffold (Figure 47 (D), Figure 48). The particles observed display similar morphology and size to those previously reported on the surfaces of scaffolds after immersion in SBF and are characteristic of HA deposited in SBF [204, 205].

The apatite phase was also identified on the Raman spectra (Figure 10) with a characteristic peak at 960 cm^{-1}, due to the $v1$ PO_4^{3}mode and a strong band at 1035 cm^{-1} and 1076 cm^{-1} corresponding to the symmetric stretching vibration (PO_4^{3-} $v3$). In addition, three other PO_4^{3-} modes are present in the region of 450-400 cm^{-1} (PO_4^{3-} $v2$) and 610-579 cm^{-1} (PO_4^{3-} $v4$) [52,53]. Table 18 summarizes the Raman peak positions and their assignments. Furthermore the presence of carbonate group on the spectra was confirmed from the molar Ca/P ratios which had values corresponding to non-stoichiometric biological apatite. This *in vitro* test shows that the composite is bioactive, and has the potential to initiate bone formation.

Table 18 Peak assignment of Raman spectra for P2 after immersion in SBF

Wave number (cm^{-1})	Assignment
430, 446	PO_4^{3-} mode $v2$
578, 594, 610	PO_4^{3-} mode $v4$
960	PO_4^{3-} mode $v1$
1035, 1076	PO_4^{3-} mode $v3$
720	CO_3^{2-} mode $v4$
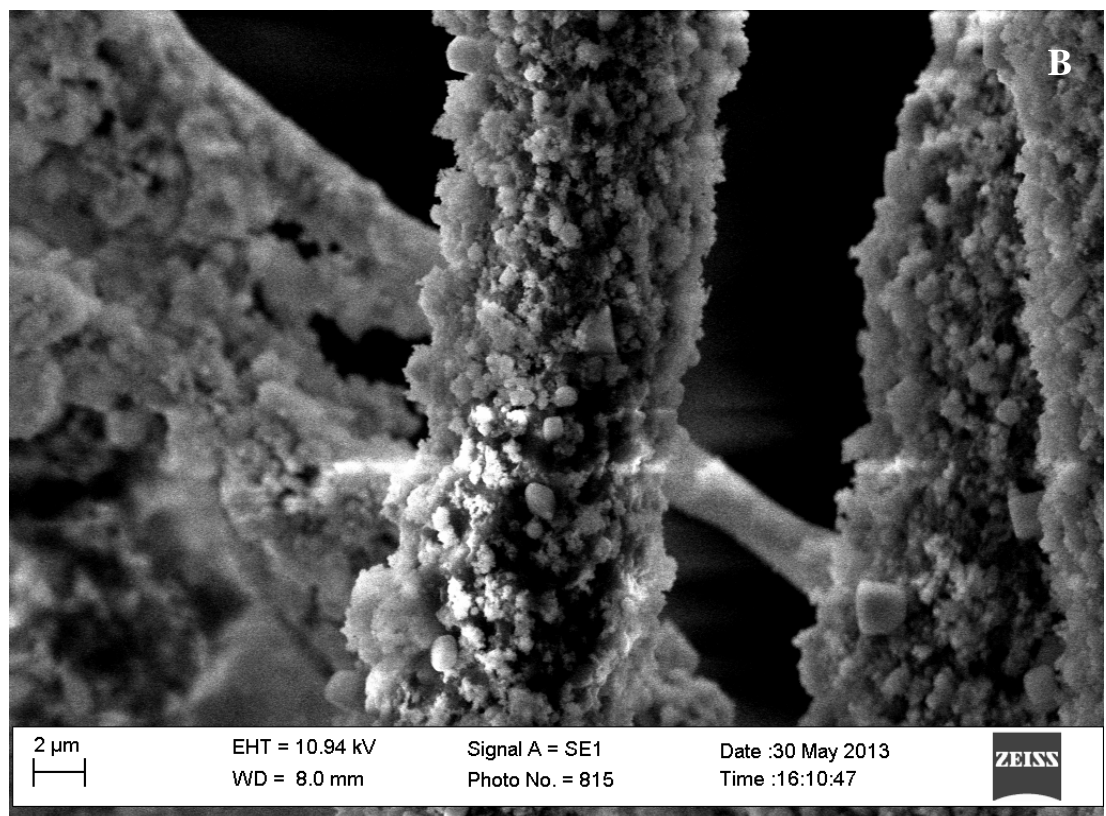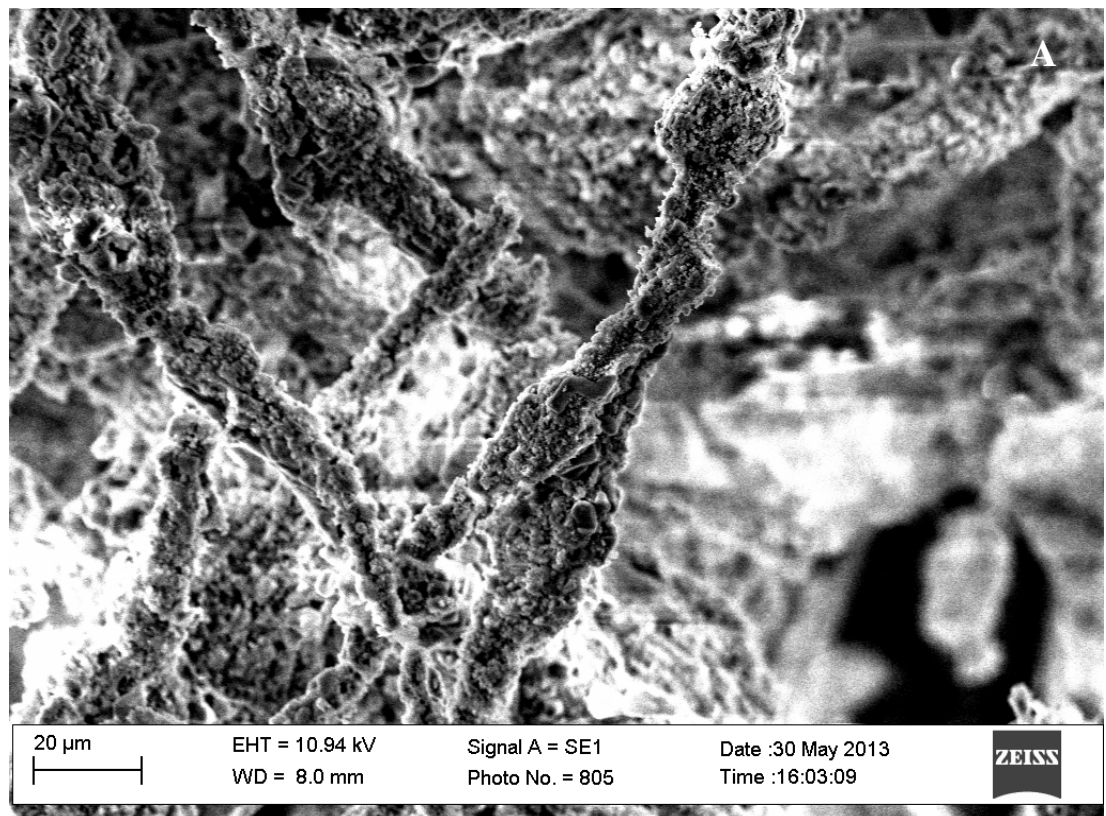
Figure 48 SEM of P15H2S2 after 28 days in SBF (a) 800x (b) 1000x
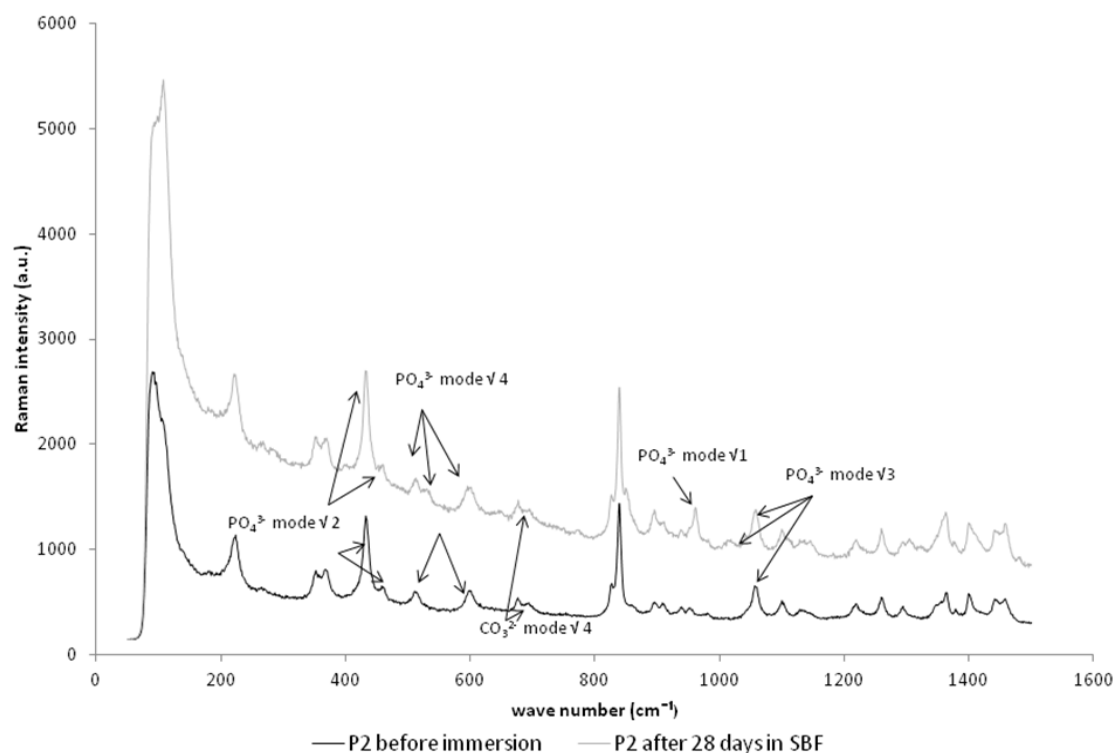
Figure 49 Raman spectra of P15H2S2 composite prior and after 28 days in SBF

4.6 Three dimensional scaffold assessment
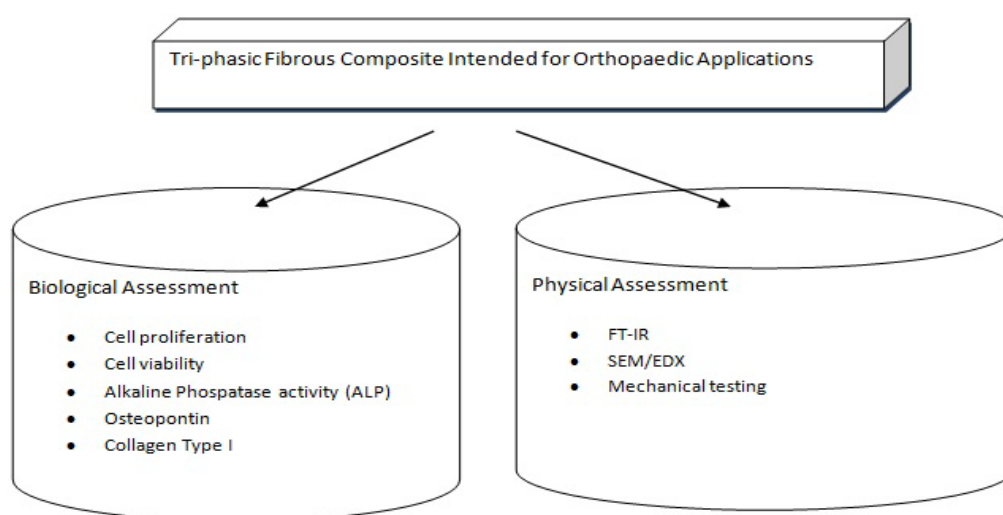
Figure 50 Schematic of Step 5 of the research plan

4.6.1. Scaffolds manufacturing

Results have shown that the composite fibrous structures have the ability to initiate and support bone-like apatite formation on their surface (Figure 48). Furthermore, the two dimensional structures support cell attachment on their surface and cell infiltration within the porous structure (Figure 45).

A goal of using engineered tissue in biomedical research is to bridge the gap between traditional two-dimensional (2D) cell culture and the *in vivo* settings with an approach that places cultured cells in an environment that more closely represents the complex 3D structure of native tissue. In particular, 3D models have the potential to provide powerful information regarding the expression of genes that interact with the extracellular matrix and predict *in vivo* integration of the tissue engineered construct [206].

Depending on the location of implantation, a scaffold can vary in shape and thickness, from membrane-like scaffolds to thick 3D blocks. With this structure cells can then adhere to the scaffold, proliferate and initiate bone formation (*in vitro* and *in vivo*). At the same time electrospinning has been limited by an inability to produce large three-dimensional scaffolds, as it typically produces a flat sheet of material that is approximately 200–500 μm in thickness [207]. As the construct increases in size, greater amounts of polymer are needed to attain a similar size increase because the density of the construct increases. In addition, as deposition of polymer increases, the polymer begins to shield the electrode from the newly deposited polymer, which can negatively impact fibre deposition [207-209]. Improving electrospinning's capability to

produce unique three-dimensional architectures is a vital step for the process to become a valuable tissue-engineering scaffold-fabrication technique because it will allow production of scaffolds for large tissues, including bone and muscle [210].

Various techniques for generating 3D porous structures (hydrospinning, stacking, laser welding, sintering) were attempted and the viable ones were further tested according to research plan in Figure 50.

Previous research has shown that 3D electrospun structures have been created using the hydrospinning method [211]. Using roughly the same set-up, 3D porous constructs have been produced in our laboratory. The fibres were collected on the surface of the liquid (deionised water), where a thin layer was rapidly formed, and was kept afloat. This thin layer was picked from the surface of the liquid on a glass at certain time intervals, eventually creating a hydrospun scaffold composed of many fibrous layers. Despite their 3D structure, the scaffolds were very delicate when manipulated and were time consuming to produce. Each layer was spun for 20 minutes and each 3D construct was composed of 5-10 hydrospun layers.

Another method employed to produce prototype 3D structures used laser welding. The laser welding trials were performed by Blueacre Technology. The laser used to weld the sample was a Synrad CO^2 laser operating at 10.6μm wavelength. Laser power was modulated to 4W at 5kHz, laser spot size was approximately 300 um at the $1/(e^2)$ point, laser was scanned across samples using galvanometer moving at 200mm/s, with 3 passes being made in total. SEM images of the welded samples are shown in Figure 51. As can be observed, the polymeric fibres were melted by the laser beam, and thus the fibrous structure was destroyed. For future work several recommendations could be made: a) an inert atmosphere, b) higher densities at the

140

points where welded as the material tends to collapse when heated, c) a method of holding the layers firmly together without crushing the scaffold.
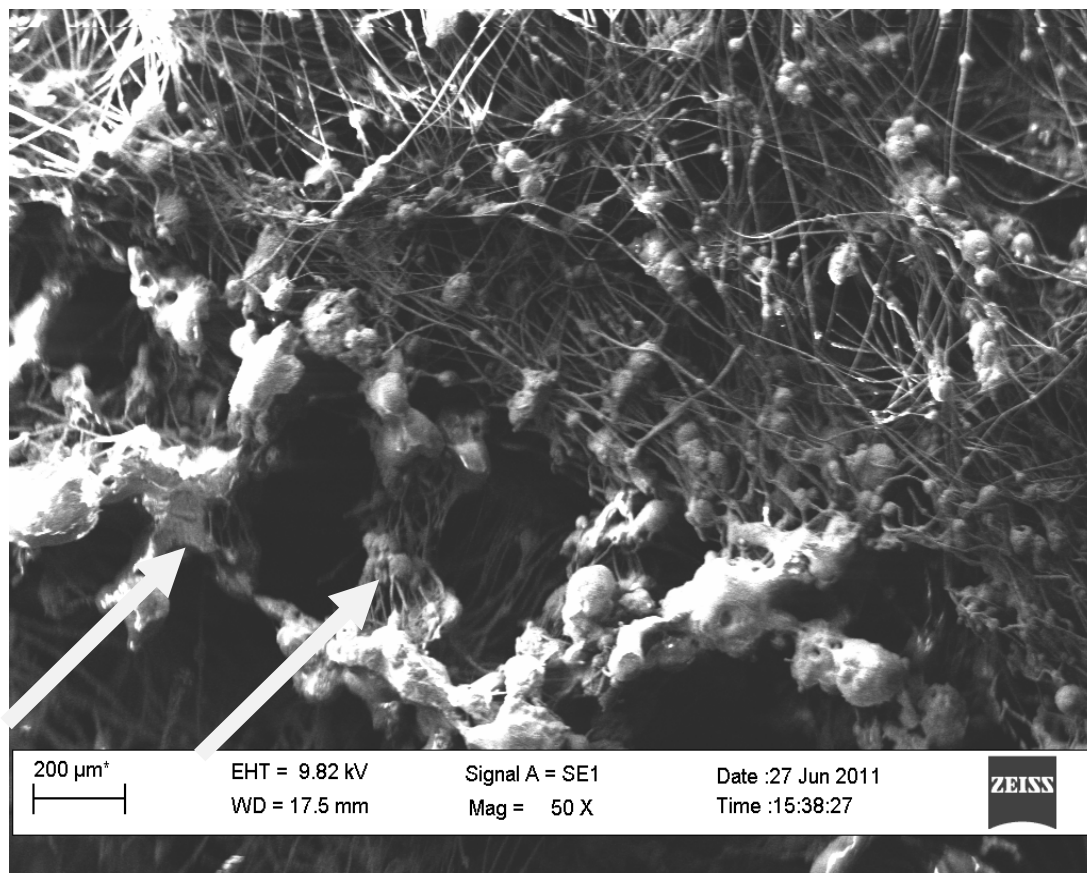
Figure 51 Laser welding of two as-electrospun composite membranes. Arrows indicate the melted polymer when laser treated.

Another attempt of building 3D constructs was made by using sintering to weld 2-5 composite sheets (T = 60ºc, t = 5min, 10min, 20min). For samples sintered for 5 minutes no welding was observed, while for samples heated for 10 min, 20 min a brownish layer attributable to silk fibroin degradation was observed. Figure 52 shows sintered fibrous composite constructs. As can be observed, the fibrous morphology had been replaced by a beaded rough surface. It was assumed that the polymer melted and then re-arranged itself within the matrix. The round edges on the surface appear to be the nano- hydroxyapatite particles, which form clusters together with melted polymer.
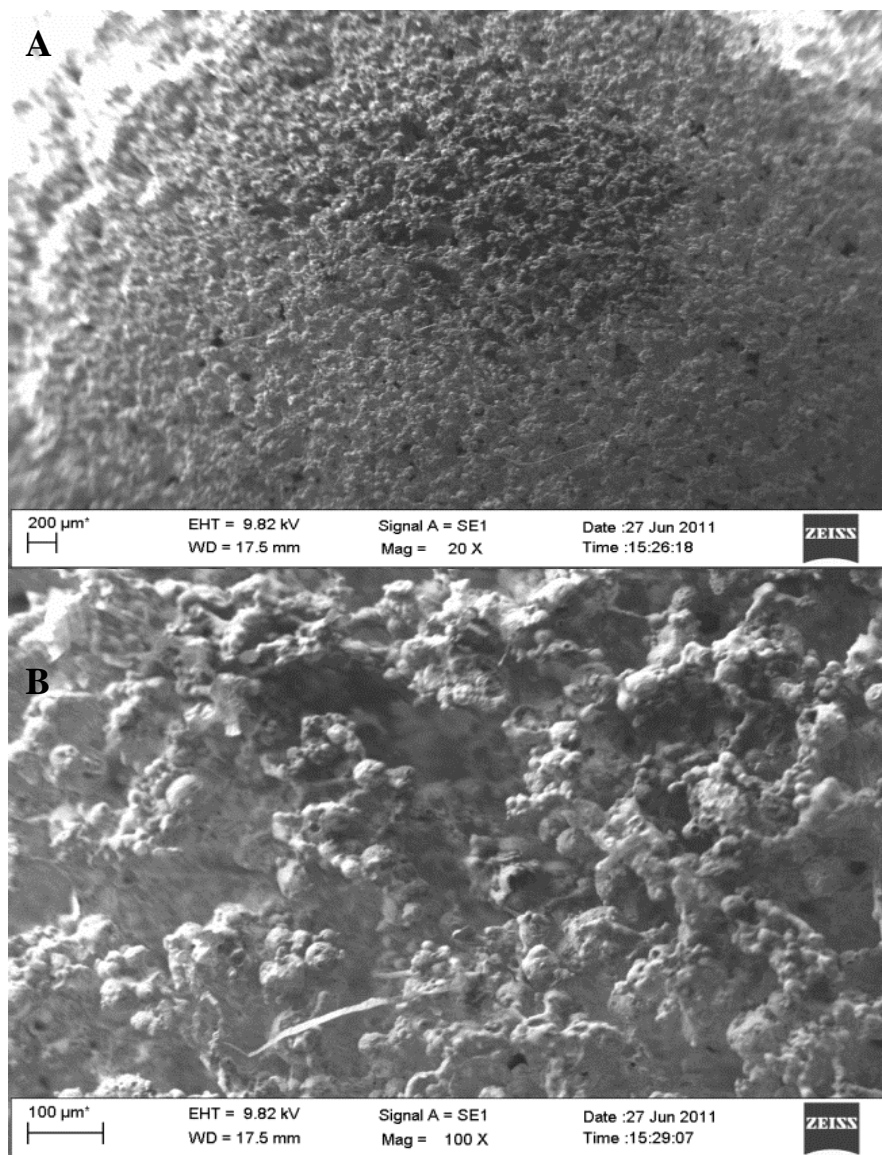
Figure 52 SEM images of two sintered electrospun composite membranes in an attempt to buuild a three dimensional construct. (a) 20x (b) 100x

Another further attempt was made to build thicker 3D structures by folding, or rolling one single membrane. Wright *et al.*[210] have successfully built thicker 3D constructs by rolling and heat-sintering the composite electrospun samples, but no work on folded electrospun membranes has been reported to our knowledge. Figure 53 presents the folded 3D constructs. It could be observed that after manipulating the membrane the fibrous network was maintained and thickness increased.

Based on the posibility of creating a thick 3D structure that would retain its porous fibrous structure as shown in Figure 53, from the above mentioned techniques the chosen one was the flat membrane rolling/ folding. While the other two were time consuming/ laborious techniques, the folding one was easy to use, economic from a time point of view and could be used to create samples of various shapes and sizes. Furthermore if proven that the created scaffolds support bone formation using specific in vitro tests, this technique can be improved and extended to be used for other tissue engineering applications.
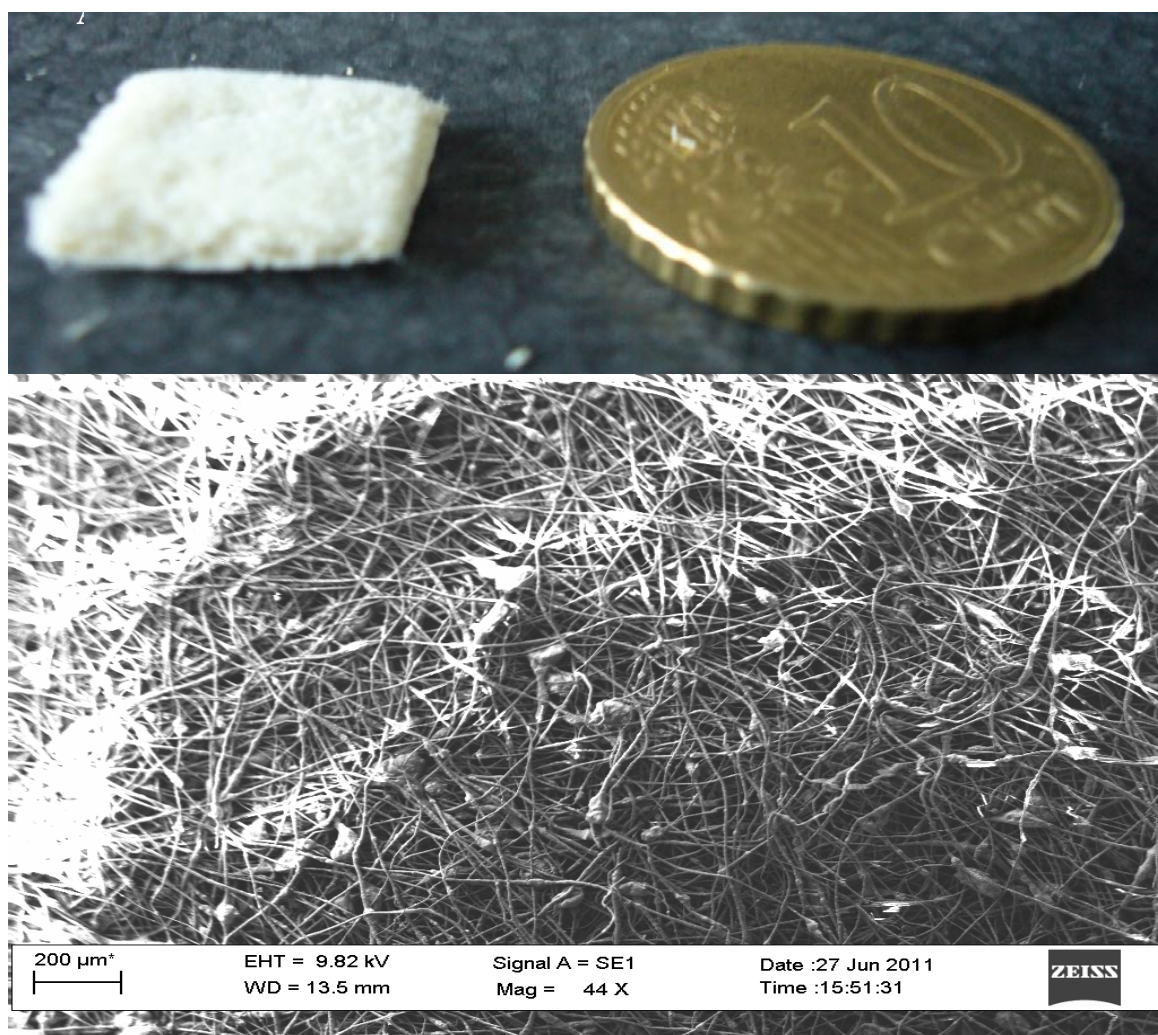
Figure 53 (a) Folded 3D construct from one single electrospun composite (P15H2S2) membrane (b) SEM image of the same 3D sample

The SEM analysis of all of the electrospun samples produced during the entire research programme has shown an increase in bead structure formation associated with an increase in silk fibroin content. The 5% silk fibroin, 5%nHAp composition has been shown to be the lower limit for bead formation within the matrix. Since our work aims to produce non- beaded fibrous structures, it was decided to include the P15H5S5 composite samples together with the P15 control and the P15H2S2 samples in the further programme of biological and physical assessment (P15 as control, P15H2S2 and P15H5S5 as test cases).

The further physical assessments of the selected three-dimensional constructs consisted of tensile and compressive strength evaluation. The initial biological evaluation included qualitative and quantitative bone-specific gene expression, such as osteopontin, collagen type I and bone phosphatase alkaline.

4.6.2 Uni-axial tensile and compressive test of the 3D composite fibrous constructs. FT-IR and EDX chemical analysis

Tensile tests were applied to the PHB/PHV electrospun matrix (P15), as well as to composite fibres with 2 wt% each and 5 wt% each of nHAp and silk fibroin in PHB/PHV (P15H2S2, P15H5S5 respectively).

The tensile strength (Figure 54) and Young's modulus (Figure 55) of the composite fibres decreased with increased content of nHAp and SF phase. This can be attributed to the lack of sufficient interfacial interaction between the nHAp and SF

phases respectively and the polymeric matrix. The presence of polar groups on the hydroxyapatite particles and the abundant moderate polar groups in the chemical makeup of PHB/PHV lead to an expectation of some interfacial interaction between the two; although from the FTIR analysis, no chemical or hydrogen bond interactions between the moderately polar groups of the two components were observed [212]. According to the results, the P15H2S2 composite samples revealed increased ultimate tensile strength and Young modulus when compared to the pure polymeric sample (control) (p<0.05). The P15H5S5 composite exhibited significantly lower values for UTS when compared to the control samples, while the tensile strength did not change too much. It could be assumed that the addition of the nHAp and silk phases had a significant effect on the tensile properties of the P15H2S2, while increasing the concentration of these co-phases above 2% wt leads to no improvement of the mechanical properties of the composite samples.

The compressive mechanical properties were measured as well for the PHB/PHV electrospun matrix and forthe composite fibres with 2 wt% and 5 wt% of nHAp, respectively silk fibroin in PHB/PHV. The secant modulus is shown in Figure 59. The secant modulus is useful in describing the behaviour of materials that have been stressed beyond the elastic region. It was shown that with increasing ceramic concentration, the secant modulus decreased from 3.32 MPa for P15 to 0.48 MPa for the P15H5S5 composite. Even so, the compressive mechanical properties of the composites are comparable to some load-bearing tissues. Kurkijarvi*et al* [213] measured elastic and dynamic moduli of full-thickness, cartilage-bone cylinders of human (nonarthritic) knees to range from 0.15 to 2.14 MPa and 0.8–15.58 MPa.

Therefore, electrospun materials such as the one presented do have possibilities in terms

of tissue engineering of large load-bearing tissues.
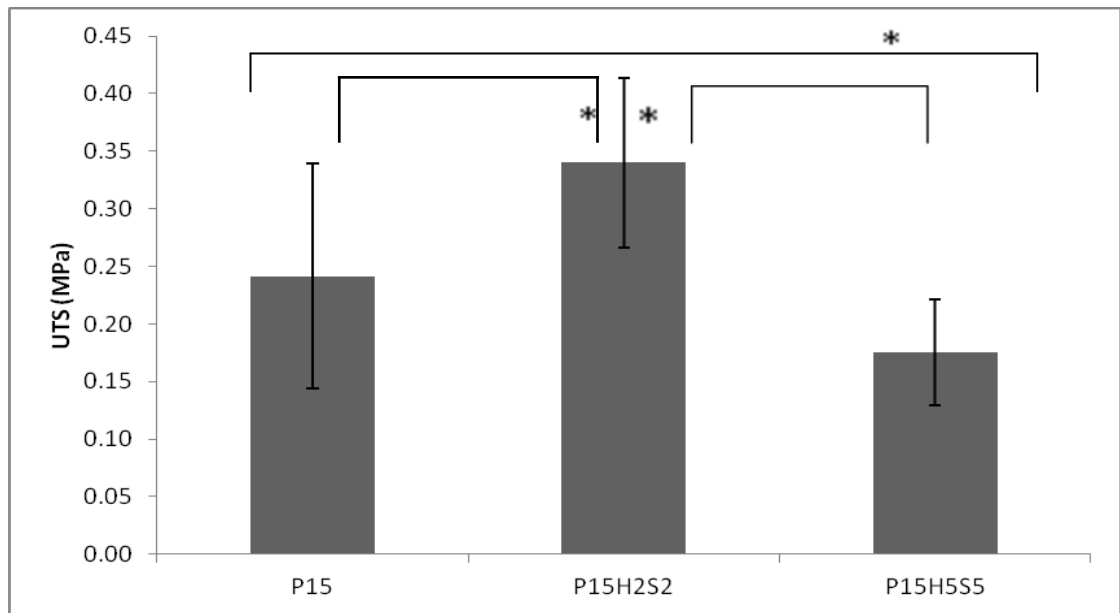
Figure 54 Ultimate tensile strength for P15, P15H2S2 and P15H5S5 electrospun composites (p<0.05, n=6)
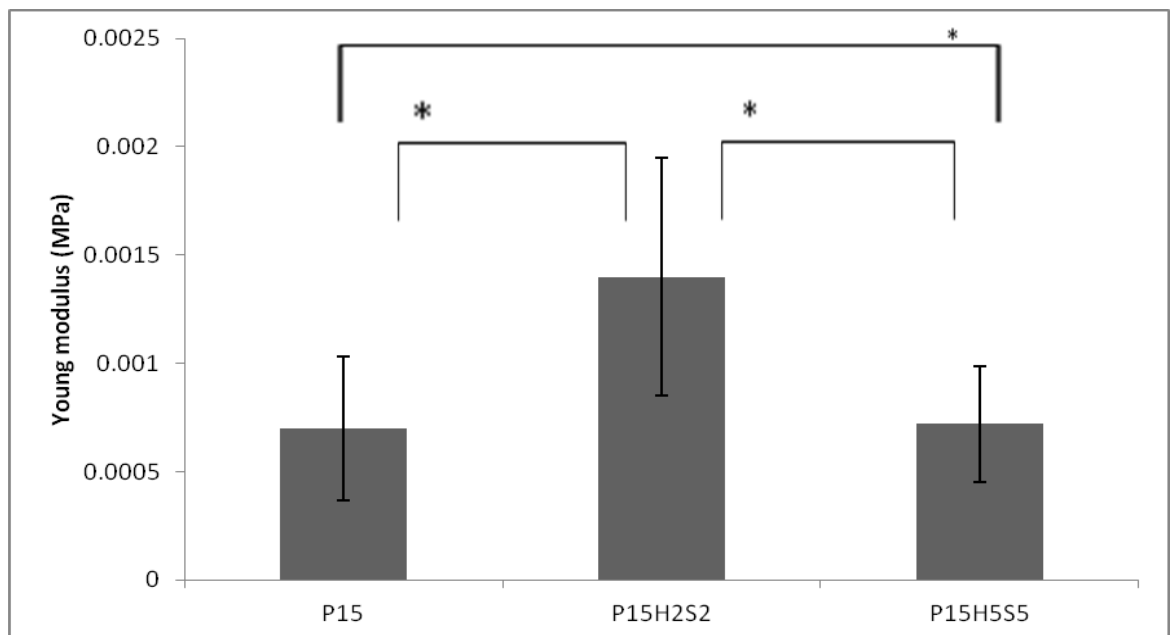
Figure 55 Young modulus in tension for P15, P15H2S2 and P5H5S5 electrospun composites (p<0.05, n=6)
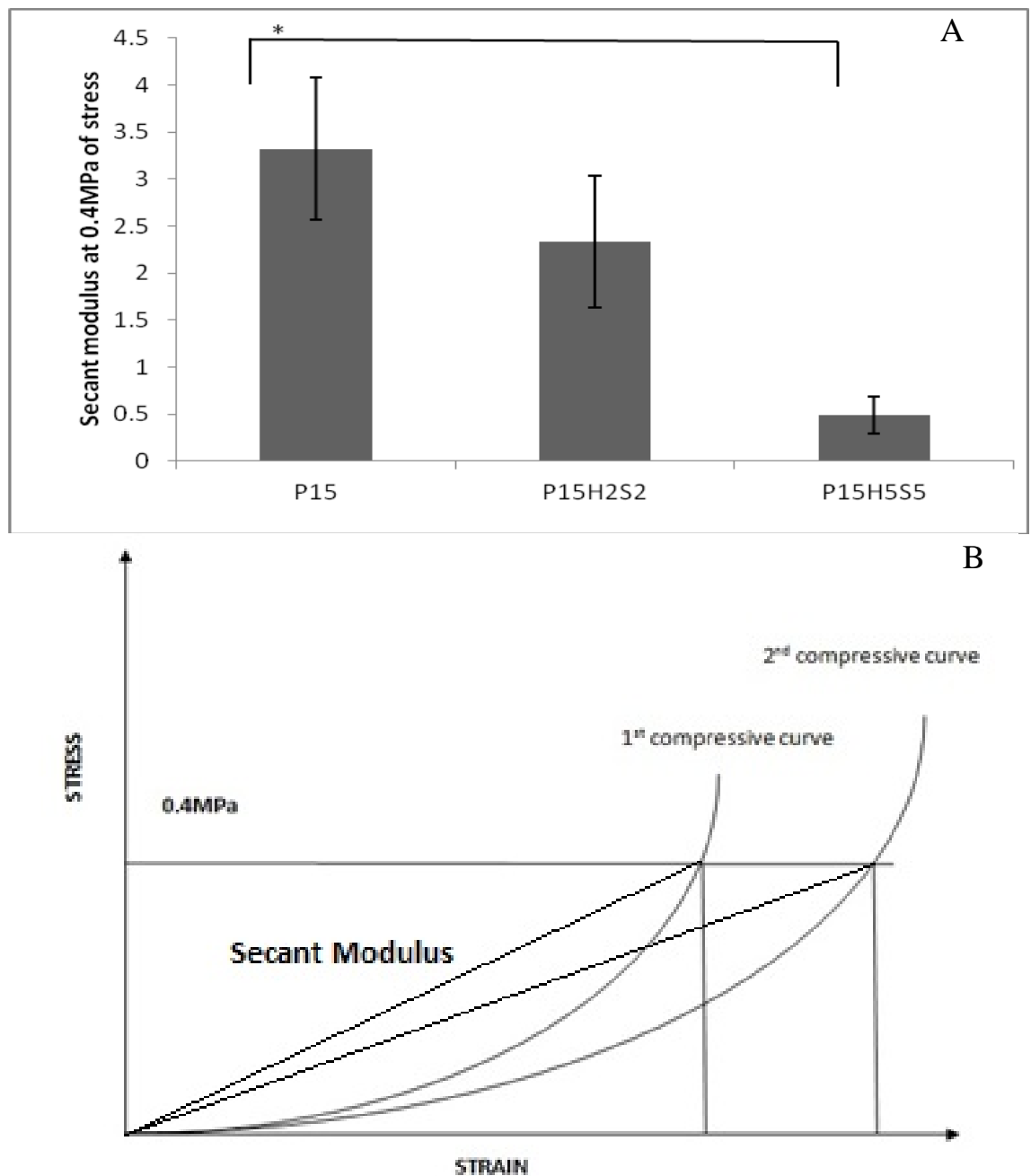
Figure 56 **(a) Compressive secant modulus of P15, P15H2S2 and P15H5S5 electrospun composite samples (b) secant modulus representative (p<0.05, n=6)**

It can be hypothesised, based on previous research that the inclusion of silk fibroin could reduce the solubility of composite samples in the cell culture medium and improve the mechanical properties by changing the configuration of the protein, from

random coil conformation to β –sheet and insolubility in water by immersion in methanol [214, 215]. In order to induce a change in the configuration of the protein as mentioned above samples P15H2S2 and P15H5S5 were immersed in pure methanol for 10 min and once taken from the liquid left to dry at room temperature for 24 h. Figure 57 shows the Young modulus in tension for methanol treated samples (M) and non-methanol treated samples (NAM). The results show a significant increase in tensile strength for the composite sample of P15H2S2 and P15H5S5 after methanol treatment suggesting that this led to conformation changes of silk fibroin from amorphous to β-sheet. FT-IR spectra of the composite before methanol treatment support these results (Figure 58).
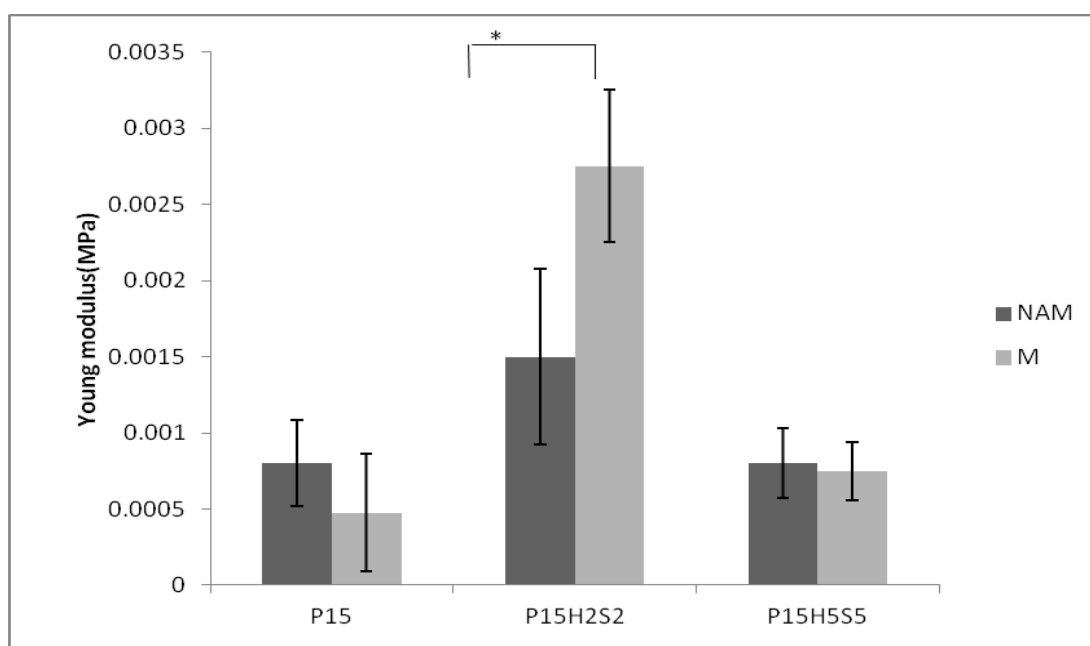
Figure 57 Young modulus in tension for composite sample before (NAM) and after treatment (M) with methanol (n = 6, p <0.05)
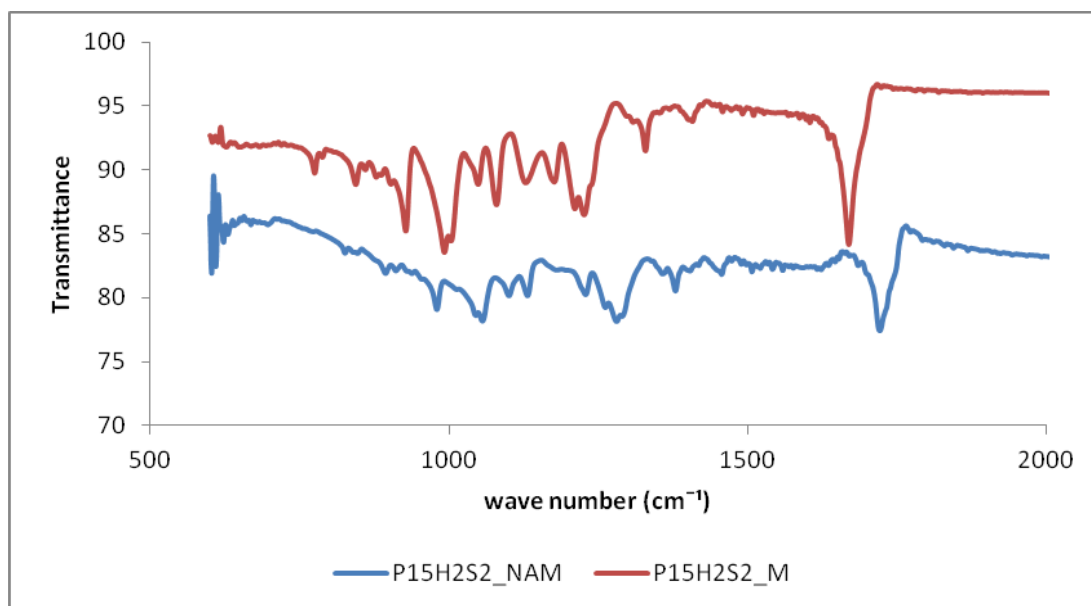
Figure 58 FT-IR spectra of P15H2S2 composite before and after immersion in pure methanol for 10min at room temperature

The non-methanol treated P15H2S2 spectrum reveals the silk fibroin characteristic amide as follows: amide A at 3294 cm^{-1}, amide I between 1500-1600 cm^{-1}, amide II at 1380-1400 cm^{-1} and amide III at 1375 -1390 cm^{-1} while the methanol treated spectrum reveals an increase in transmittance and shifted peaks for amide II and III suggesting β-sheet conformation change was induced for the samples treated with methanol..

Compressive tests of methanol treated samples (M) evidence a significant increase in the secant modulus for P15H2S2 only versus P15 samples (Figure 59) and this could be attributed to the silk content of the composite samples. It could be suggested that the difference between secant modulus values for P15H2S2 and P15H5S5 could be the result of the random distribution of the ceramic and proteic phases within the polymeric matrix, as reinforced by the element mapping EDX analysis (Figure 60).
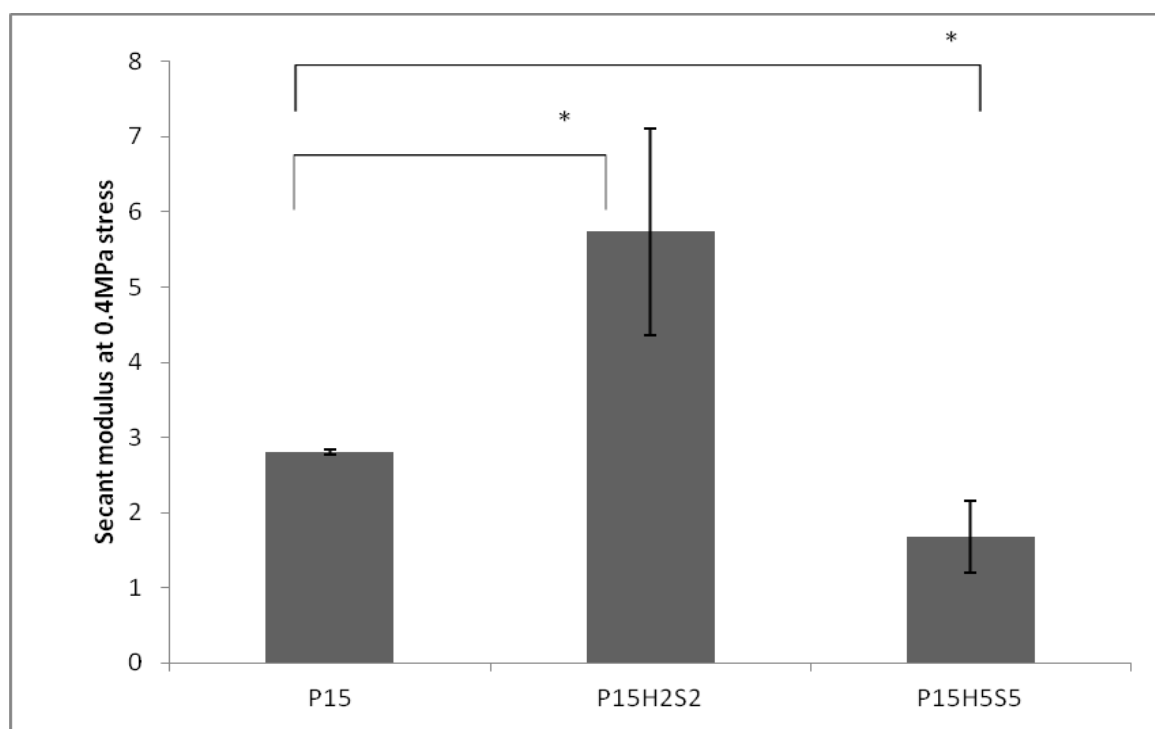
Figure 59 **Compressive secant modulus of methanol treated P15, P15H2S2 and P15H5S5 electrospun samples (n = 6, p <0.05)**
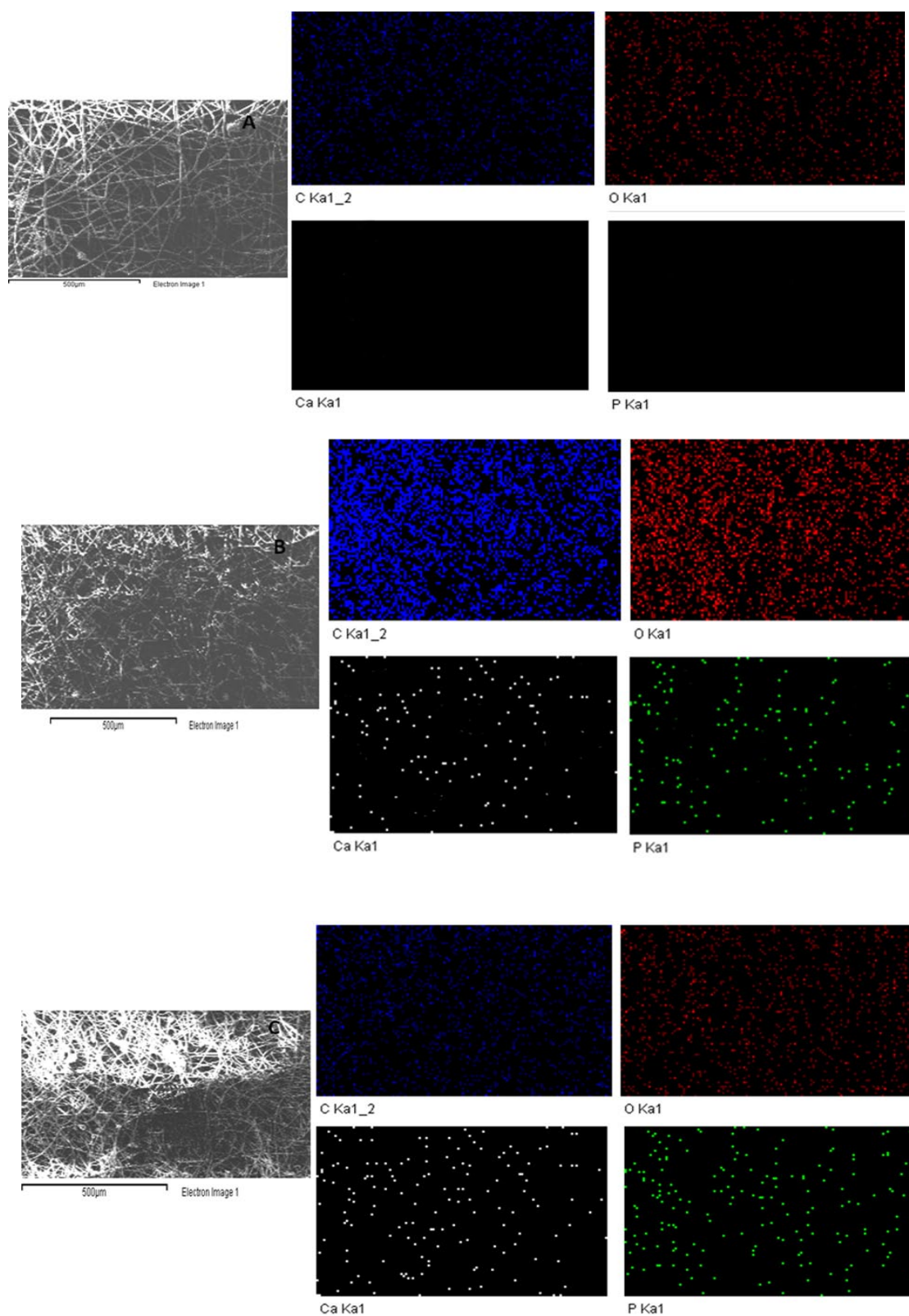
Figure 60 EDX element mapping analysis of (A) P15H0S0, (B) P15H2S2 and (C) P15H5S5

In order to prepare the electrospun samples for *in vitro* biological assessment the methanol treated constructs needed to be sterilised prior to cell seeding. The chosen method of sterilisation was autoclaving at 121°C for 20 min, which is a standard for this technique. In order to assess if samples chemical conformation and mechanical properties have changed after autoclaving, FT-IR and mechanical analysis were used to characterise the sterilised samples (MA). Figure 61 shows the FT-IR spectrum of samples after autoclaving (MA). It can be observed that the main signal was given by methanol which indicated that a high amount of alcohol was present on the samples. This residue was so strong that might have been masking the sample bands in the spectra. Methanol spectrum has been included in Figure 61 for comparison reasons. At this stage a washing step using distilled water was included in order to remove traces of methanol. In this direction methanol treated samples were washed 3 times, 10 minutes each with distilled water and left to dry for 24 hours in the fume hood, followed by the autoclaving step the next day [216]. Figure 62 shows the FT-IR spectra of the washed and autoclaved samples. The results showed that the traces of methanol have been removed and that autoclaving did not affect the chemical conformation of the samples.
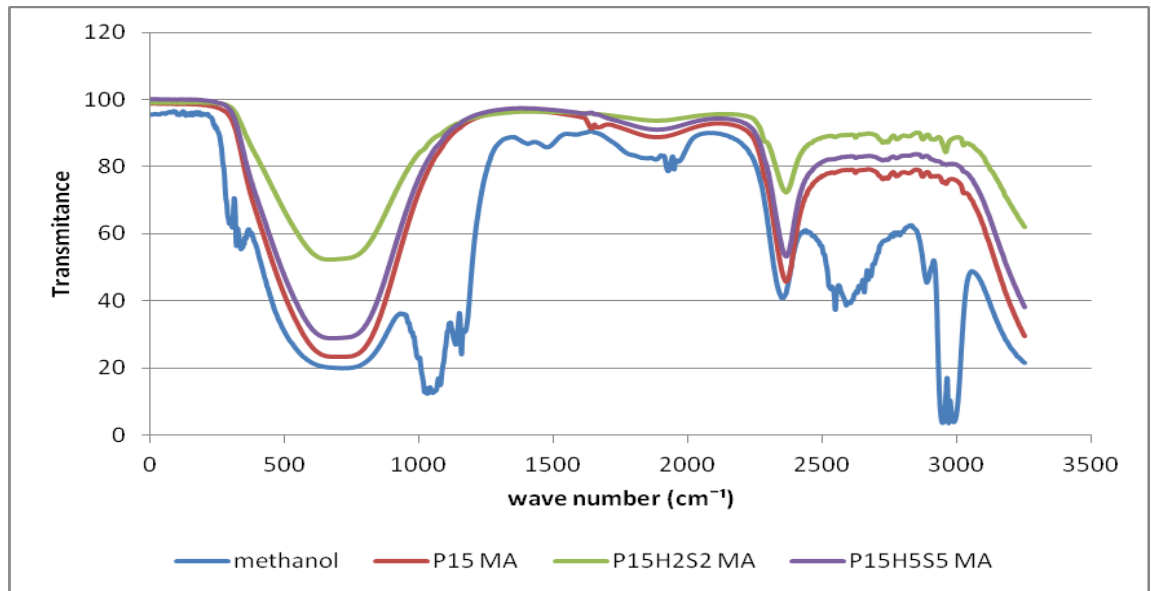
Figure 61 FT-IR spectra of methanol treated -autoclaved samples and methanol samples as control
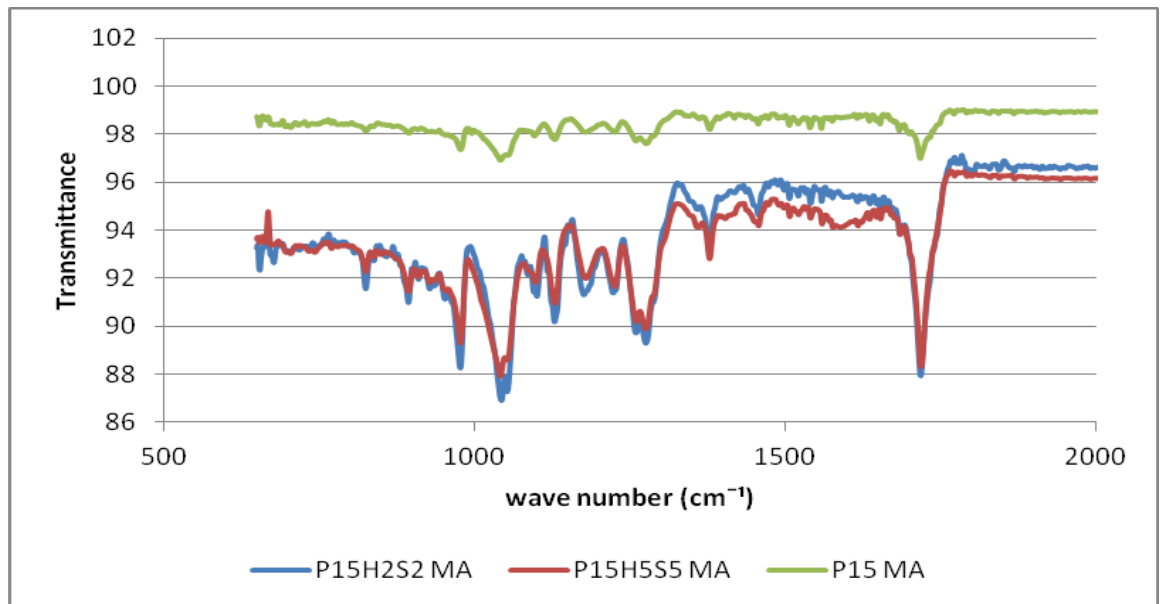
Figure 62 FT-IR spectra of methanol treated-autoclaved samples after methanol the washing step

Figure 63 shows the Young modulus results for the non-methanol treated (NAM), methanol treated (M) and autoclaved samples (MA) and Figure 64 the results for secant modulus for the same group of samples. It has been evidenced that Young modulus of

153

P15H2S2 – M samples decreased significantly after sterilisation in the autoclave. Further the Young modulus of P15H2S2 - MA samples were the same as those of the NAM ones, while P15- MA samples showed a significant increase in their Young modulus after sterilisation compared to the non – methanol treated (NAM) and methanol treated (M) ones.

Compressive tests results showed that autoclaving causes a decrease in the secant modulus of all the samples as opposed to the secant modulus of the methanol – treated ones. Furthermore the secant modulus of the P15H2S2 and P15H5S5- MA samples are higher than those of the NAM ones, suggesting that both the methanol immersion and autoclaving treatements improved the secant modulus of the composite samples. As opposed to the composite samples, P15 constructs exhibited a decrease in the secant modulus when compared to the NAM P15 samples, results that suggest that both treatement led to conformational changes of the polymeric material that can not withstand the same amount of compressive force as the non treated and sterilised composite fibres.
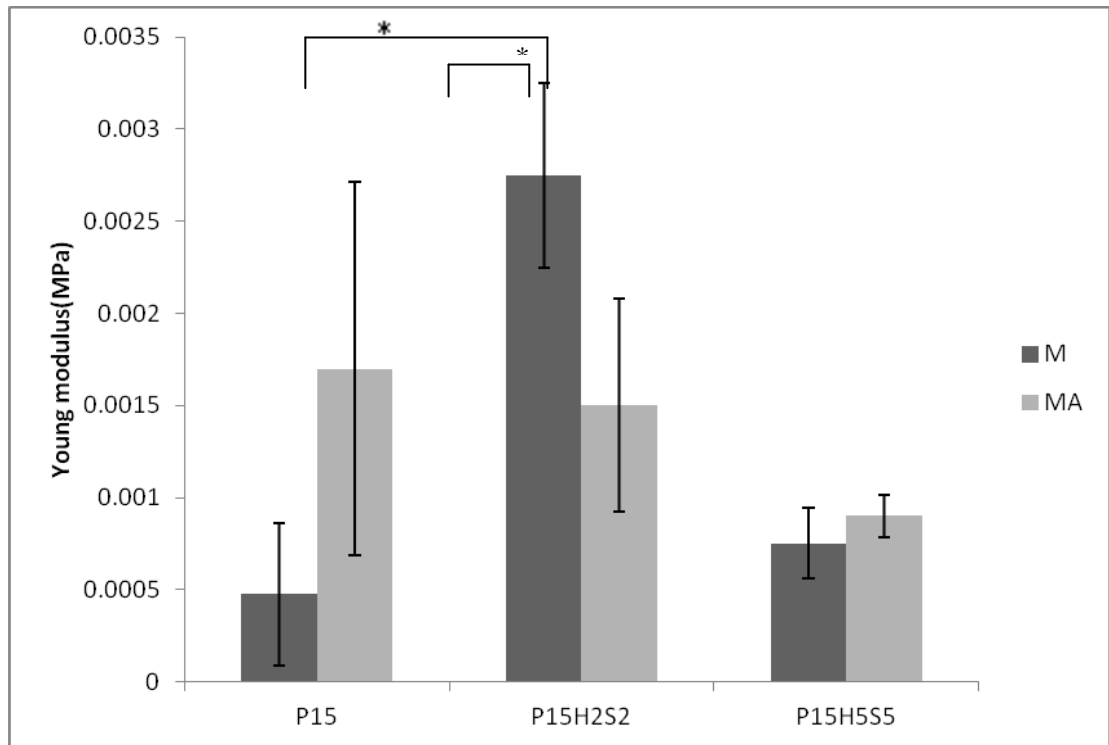
Figure 63 Young modulus of P15, P15H2S2 and P15H5S5 methanol treated and methanol treated -autoclaved samples (n = 6, p <0.05)
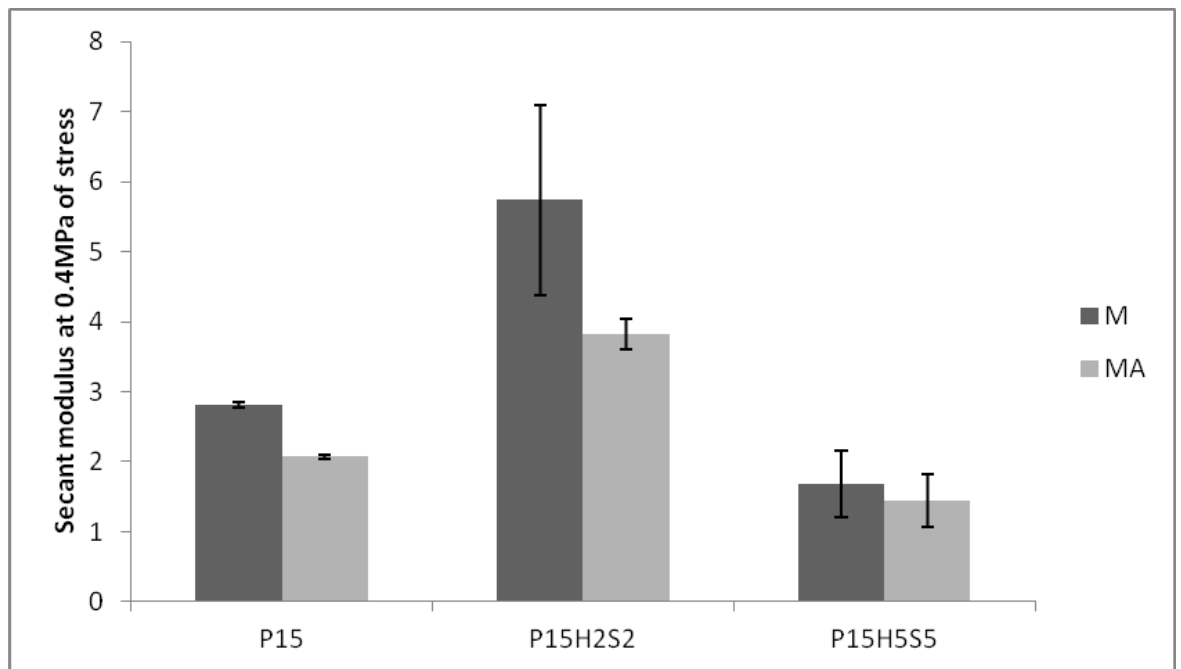
Figure 64 Compressive secant modulus of P15, P5H2S2 and P15H5S5 methanol treated (M) and methanol treated-autoclaved (MA) samples (n = 6, p <0.05)

4.6.3 Biological evaluation of the electrospun three-dimensional scaffolds

Tissue engineering ultimate goal is to applythe fundamentals and innovations of biology, medicine and engineering to develop andmanipulate viable, three dimensional physiologic substitutes that are capable of rebuilding, sustaining, or recovering thefunction of tissues and organs. The composition and architecture of a tissue engineered scaffoldresult in cell environment interactions thatdetermine the structure's fate. The main goal is to enable the body (cellular components) to heal itself by introducing a tissue engineered scaffold that the body recognizes as "self", and in turn, uses to regenerate "neo-native" functional tissues [217].

Repair of bone tissue by autogenous osteoblast transplantation is one of the most definitive treatments for bone defects.The success of this new type of treatment for bone defects partly relies on a scaffold of these cells. The appropriate carrier should fulfil the following conditions while mimicking the natural bone matrix: to be biocompatible and degradable *in vivo* so that it can be absorbed and metabolized; to offer the scaffolds for osteoblasts; and to maintain or enhance the phenotype of osteoblasts [218, 219]. Natural bone is a biocomposite compose ofinorganic (mainly hydroxyapatite crystals) andorganic (mainly Type I collagen matrix) materials. To mimic the matrix, electrospinning is known as a promising technique due to its facile method for producing ultrafine and continuous sub-micron fibres and/or nanofibres.

Recent studies have shown that nanofibrous structures developed by electrospinning technology provide attractive extracellular matrix conditions for the anchorage, migration, and differentiation of tissue cells, bone cells in particular. While

osteoblast-like cell lines and bone marrow stromal cells were shown to favor the nanofibre/microfibre scaffold for their proliferation and production of alkaline phosphatise, the materials used in the development of electrospun nanofibres are considered to have properties that are specifically suitable for the calcified hard tissues [219].

Ito *et.al* [220] used biodegradable and abiocompatible poly (3-hydroxybutyrate-co-3-hydroxyvalerate) (PHB/PHV) copolymer from a microbial polyester and electrospun it to a nanofibrous web and composited with hydroxyapatite (HAp) by soaking in simulated body fluid (SBF). In this work, nanofibrous film was compared with a cast film. The surface of the nanofibrous film showed enhanced cell adhesion over that of the flat film, although cell adhesion was not significantly affected by the combination with HA. Kim and coworkers [221] electrospun silk fibroin (SF) and applied it as a device in bone and periodontal regenerative therapy because of its favorable biological properties. This study was done to evaluate the biocompatibility of the SF nanofibre membrane. Cell proliferation, morphology, and differentiation were investigated to examine the biocompatibility of the electrospun SF membrane. Results showed that the cell numbers and osteocalcin level were significantly increased in accordance with culture period.Cells (human bone marrow stromalcells (BMSCs)) had a star-like shape and broad cytoplasmic extensions on the membrane. In *in vivo* tests, a complete bony union across the defects was observed after 8 weeks and complete bone formation with defect healing at 12 weeks. Based on these results it was suggested that SF membranes should be useful as a tool for guided boneregeneration.

Yoshimoto and coworkers [222] fabricated microporous, non-woven poly-caprolactone (PCL) scaffolds. For biological study, mesenchymal stem cells (MSCs)

derived fromthe bone marrow of neonatal rats were cultured, expanded and seeded on electrospun PCL scaffolds. Scanning electron microscopy (SEM), histological and immunohistochemical examinations were performed. Scaffold penetration of cells and abundant extracellular matrix were observed in the cell-polymer constructs after 1week. SEM results demonstrated that the surfaces of the cell-polymer constructs were covered with cell multilayers at 4 weeks. In addition, mineralization and type I collagen were observed at 4 weeks.

Further Ngiam *et al* [223] prepared poly-L-lactic acid (PLLA) and PLLA/collagen (50% PLLA+50% collagen; PLLA/Col) nanofibres using electrospinning. They mineralized these nanofibres using a modified alternating soaking method. To assess the biological properties of the nanofibrous composites, human bone–derived osteoblasts (HOB) were cultured on the materials for up to 1 week. Results showed that, the bonelike nanohydroxyapatite (nHAp) was successfully deposited on the PLLA and PLLA/Col nanofibres. They observed that the formation of nHAp on PLLA/Col nanofibres was faster and significantly more uniform than on pure PLLA nanofibres. Based on these observations, the authors demonstrated that nHAp deposition on nanofibres is a promising strategy for early cell capture [217].

The cell adhesion behaviour and the proliferation rates on the functionally graded scaffolds are important and determine the quality and suitability of the scaffold for the targeted application. The present biological study evaluated the *in vitro* biocompatibility of the electrospun novel composite scaffolds. In the past, the mouse pre-osteoblast cells from bone-calvaria (MC3T3-E1) have been extensively used to investigate the change in morphology, bone matrix formation, mineralization, and expression of bone related proteins [224]. Generally, the initial cell attachment and a rapid cell division period are

followed by a transitional period of formation of type I collagen-rich extracellular matrix (ECM) as evidenced in Figure 65. In the final stage achieved after the elapse of approximately 2 weeks upon cell seeding, the expression of bone related proteins and mineral deposition further promote the osteoblastic differentiation [224]. The cells progress through three general phases: (*i*) proliferation, (*ii*) extracellular matrix deposition and maturation, and (*iii*) mineralization. High-level expression of genes thought to contribute to the differentiated state of osteoblasts occurs at discrete time points during the differentiation process. Alkaline phosphatase (ALP), a1-collagen (COL I), and osteonectin (OSN) are expressed at high levels near the end of the proliferative period and during the period of extracellular matrix deposition and maturation. Genes expressed at or near the time of mineralization include osteopontin (OSPN) and osteocalcin (OSC) [225].
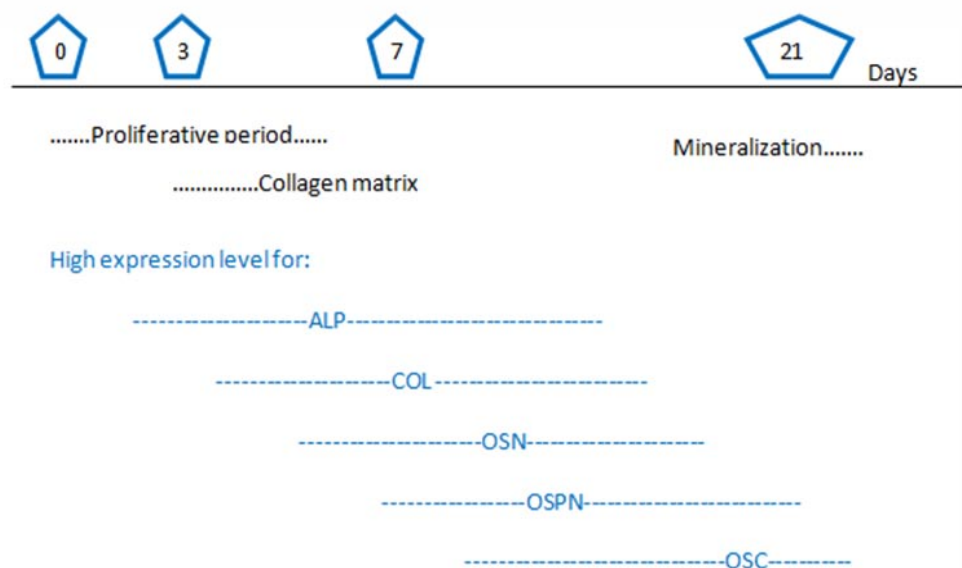
Figure 65 Temporal expression pattern of markers typical of osteoblast development in MC3T3-E1 cells.

Cell attachment and proliferation –DAPI staining

Cultivation of MC3T3-E1 on electrospun fibrous scaffolds proved successful and osteogenic differentiation was observed. The MC3T3-E1cells were able to attach and propagate on and in the fibrous structure (Figure 66a). Counting of DAPI stained cell nuclei indicates a statistically significant increase in cell number for all types of electrospun composite constructs (P15, P15H2S2, P15H5S5) from an average of 45.33±3.51 cells per visual field (P15), 73.66±5.85 cells per visual field (P15H2S2), 68.33±6.11 cells per visual field (P15H5S5) on day 1 to 183±11.53 cells per visual field (P15), 200.66±11.93 cells per visual field (P15H2S2), 84±3.60 cells per visual field (P15H5S5) on day 5. The cell number decreased on day 3 and this can be attributed to cell proliferation in the depth of the scaffold as confirmed by the DAPI staining/ confocal microscopy image of the fibrous structure at day 1 and 3 after seeding. On day 1 cell nuclei could be visible in bigger number on the surface of the fibres while on day 3 nuclei were visible in the depth of the fibrous scaffold too (Figure 66). Further the number of cells stayed more constant after day 5 and even decreases (Figure 68; day 7 (190.66±13.57, p <0.05) and 28 (182.33± 9.29, p <0.05), indicating that the cells are differentiating (terminally differentiated/mature cells do not divide) rather than propagating at later time points in co-culture. The immunocytochemistry results indicated that the MC3T3-E1 cultured on/in the fibre structure have stained positive for the bone markers osteopontin and Collagen type I and expressed increased bone marker expression starting with day 3 for osteopontin and with day 7 for Collagen type I according to Figure 65 [225].
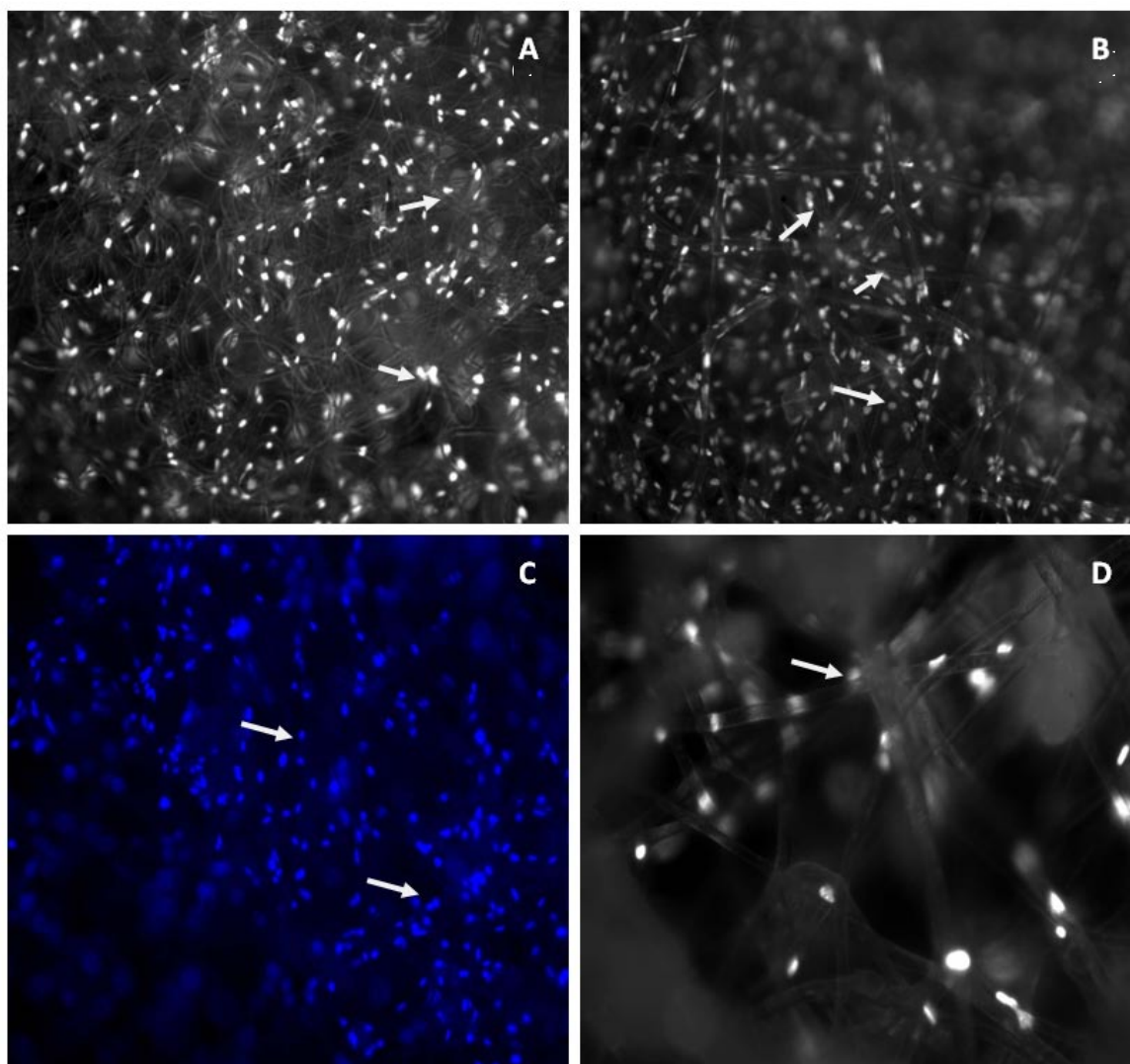
Figure 66 DAPI staining/ confocal microscope image of P15H2S2 at (a) day 1 (b-d) day 3 after seeding with arrows showing cells (a) attached on the outer fibrous layer of the scaffold and (b-d) cells infiltrated within the fibrous structure. (a-c) 10X magnification (d) 20X magnification
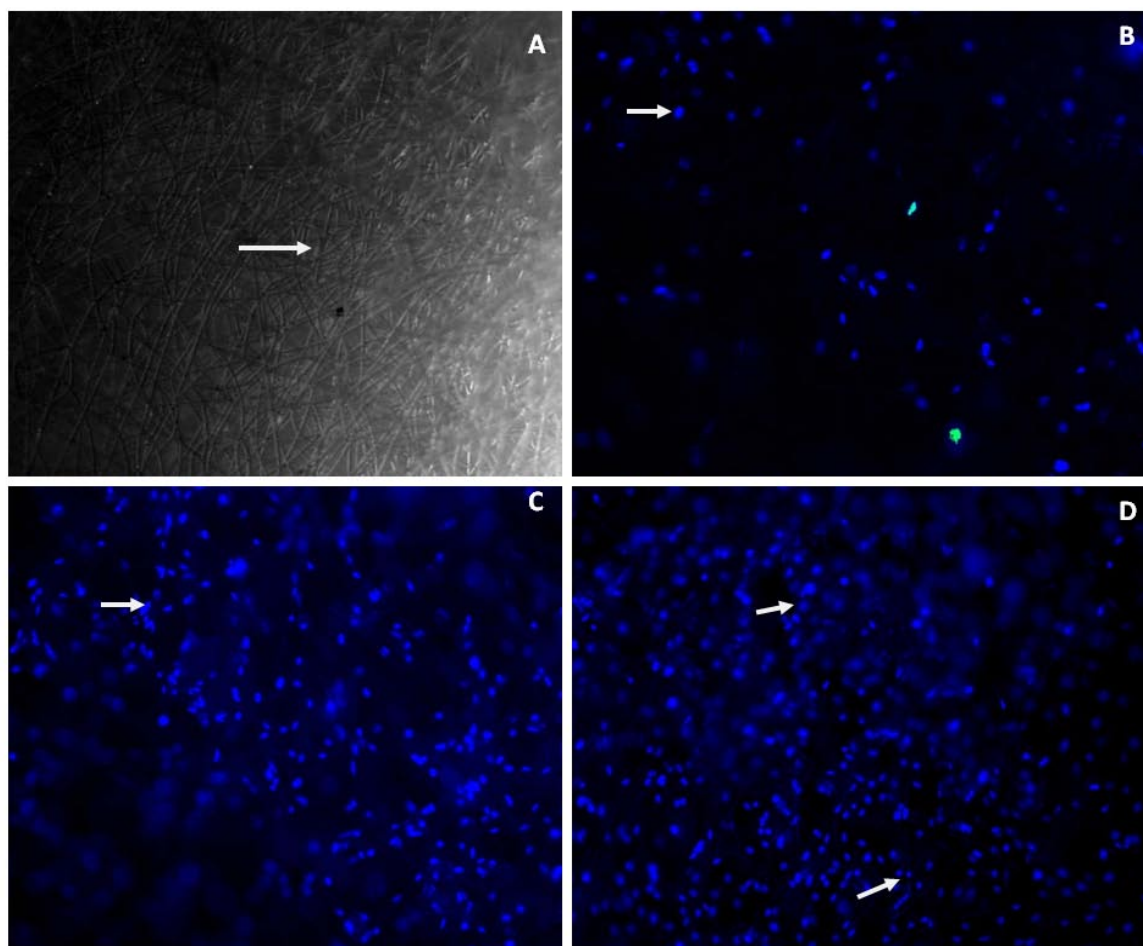
Figure 67 Representative microscopy images of electrospun P15H2S2 construct (A) before seeding the empty fibrous structure is evidenced; (B) after 1 day in culture the fibrous matrix (C) at 3 days in culture ;(D) after 14 days in culture (DAPI-blue nuclei, all images are taken at 10X magnification). White arrows evidence (a) empty fibre (b-d) DAPI stained nuclei
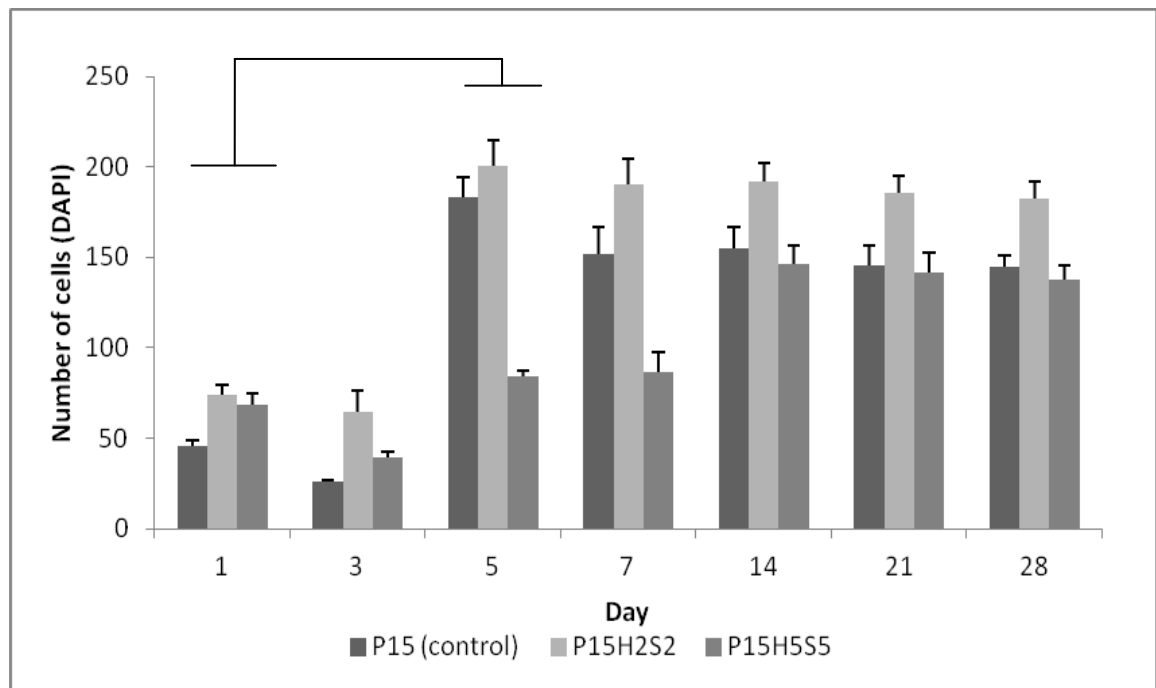
Figure 68 Total cell number per visual field (10x magnification) (n = 5, p< 0.05)

The cell number increased dramatically from day 1 to day 5 of co-culture, and after that the cell number stabilizes or slightly decreases indicating the generation of a more mature cell population that does not proliferate (divide). The total number of cells/visual field ($10\times$ magnification) is presented here. The cell number in three separately cultured fibrous constructs pieces was counted per time point and at least 5 fields of view were counted per fibrous construct. The cell number is presented as the mean $\pm$ SD.

Cell morphology –SEM

Figures 69-74 present SEM micrographs showing the morphology and proliferation of MC3T3-E1 on composite (P15H2S2, P15H5S5) and polymeric (P15) fibrous

membranes after 1, 3, 7, 14, 21 and 28 days of culture. It can be seen that cells have attached to and proliferated on the surface of membranes for the duration of the 28 days. Few osteoblast cells adhered to the composite and polymeric scaffolds after 1 day of incubation for P15, P15H2S2 and P15H5S5 membranes (Figure 69) and some cell spreading was observed after 3 days of incubation (Figure 70) as the membranes were partially covered with MC3T3-E1 cells. Further after 3 days in culture P15H2S2 and P15H5S5 membranes evidenced good cellular interaction and integration as shown in Figure 70. On day 7 there was a pronounced difference between the composite P15H2S2, P15H5S5 membranes (test) and the polymeric P15 membrane (control) (Figure 71 a). More cells had attached to the test materials, the cells had spread well and the pseudopodia were stretched on the test membranes as opposed to the cells on the polymeric control membrane, while higher magnification discloses the cells penetrating the pores (Figure 71 b). Furthermore, on both test scaffolds the cells had started to form sheets, indicating good attachment. On the control scaffold, cells were fewer and more widely separated. On day 14, 90% of the surface area of the P15H2S2 membrane was covered with a thick layer of MC3T3-E1 cells (Figure 72). The membranes cultured with cells evidenced a confluent and full coverage of the surface at 14 days (Figure 72) for the P15H2S2 composite and at day 21 for the P15H5S5 composite (Figure 73), while the P15 membrane evidenced partial coverage on day 28 (Figure 74). Furthermore ECM had formed on both test scaffoldsby day 21. Results indicate a slower rate of proliferation on P15 polymeric membrane as compared to the P15H2S2 and P15H5S5 composite membranes. This may suggest an influence of the fibres composition on the cells proliferation rate, in particular for the P15H2S2 composite as indicated by the cell number results (Figure 68).

164
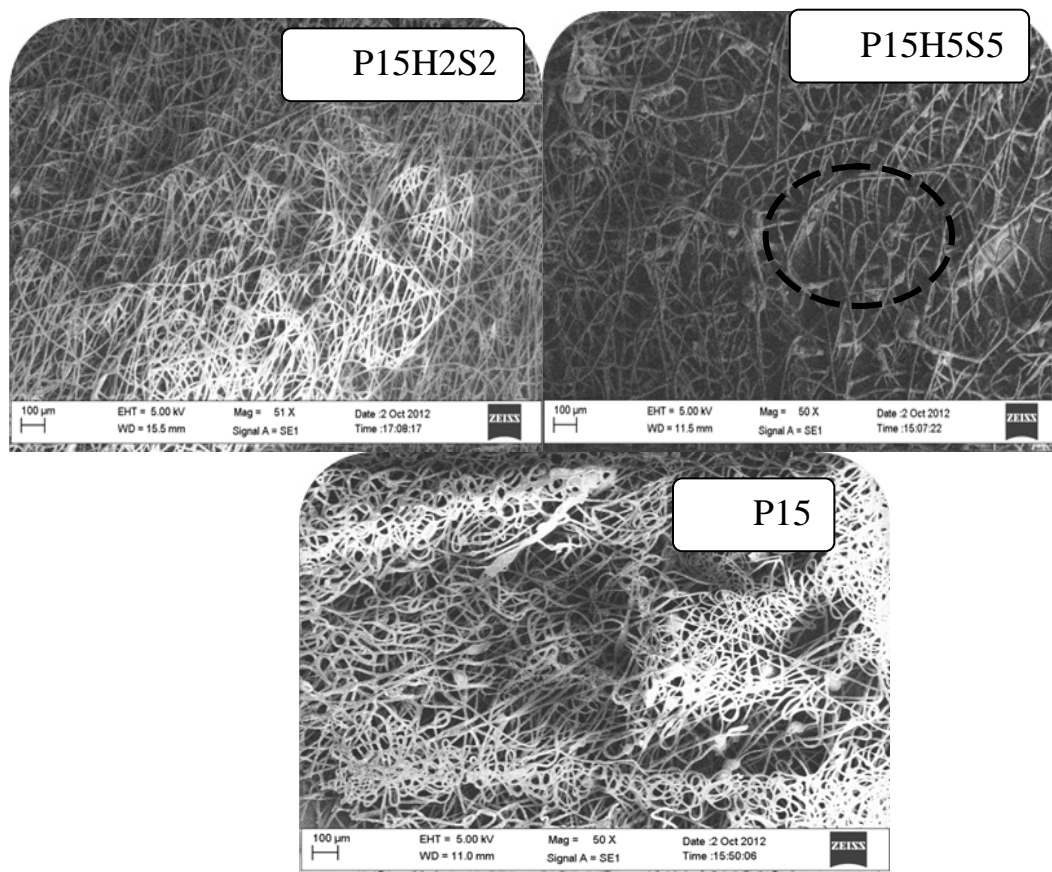
Figure 69 SEM micrographs of MC3T3-E1 cells grown on composite and polymeric fibrous membranes after 1 day in culture. Cell seeding density was 5 x 10^4 cells/ml.

Figure 70 SEM micrographs of MC3T3-E1 cells grown on composite and polymeric fibrous membranes after 3 days in culture. Cell seeding density was 5×10^4 cells/ml. Arrows and dashed line show cells attached and spreaded on the surface of the fibrous construct.
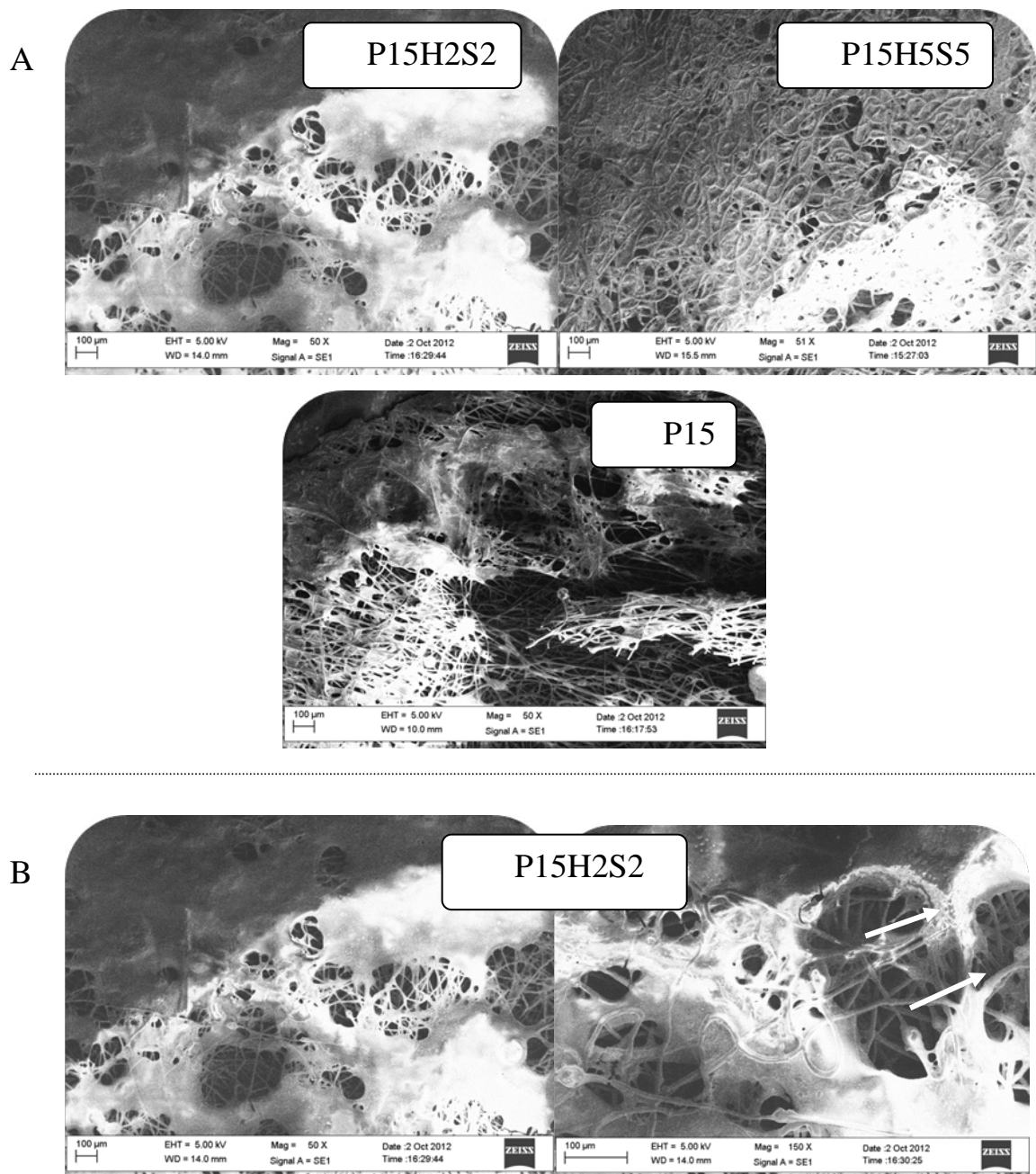
Figure 71 (A) SEM micrographs of MC3T3-E1 cells grown on composite and polymeric fibrous membranes after 7 days in culture; (B) MC3T3-E1 cells grown on P15H2S2 composite after 7 days and penetratingthe pores (yellow arrows) . Cell seeding density was 5 x 10^4 cells/ml.
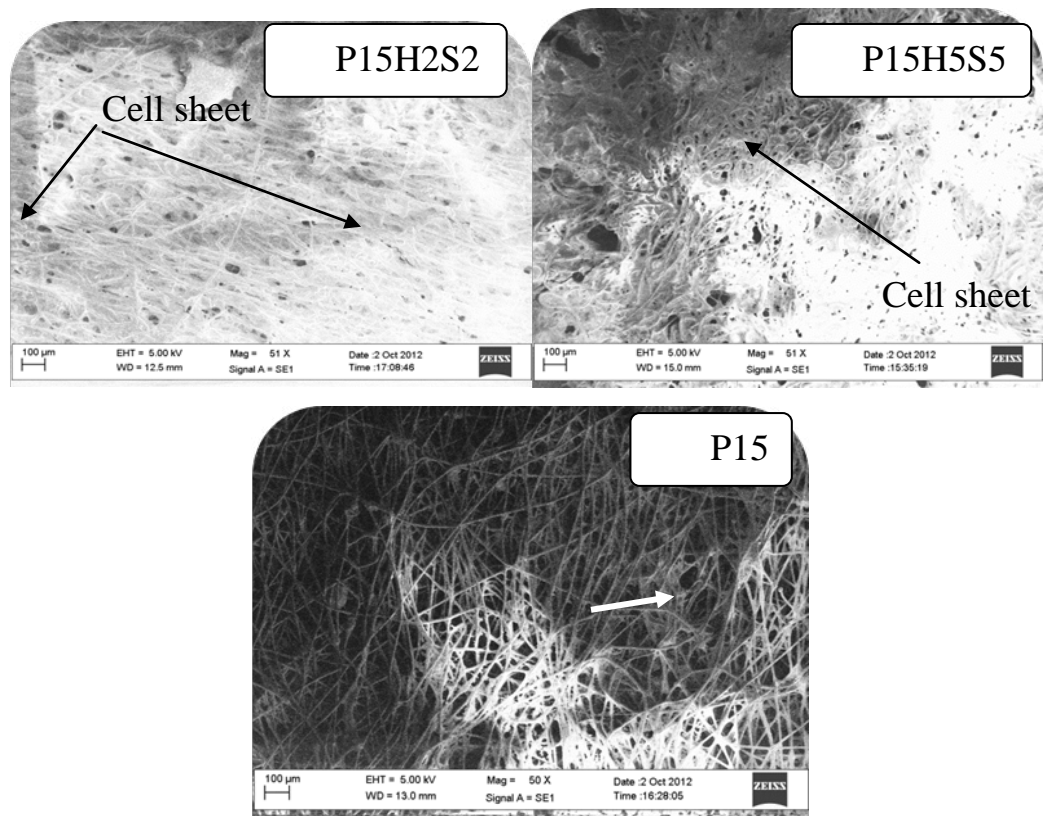
Figure 72 **SEM micrographs of MC3T3-E1 cells grown on composite and polymeric fibrous membranes after 14 days in culture. Cell seeding density was 5 x 10^4 cells/ml. Arrows evidence the spreaded cells that on P15 and P15H2S2 constructs have formed a covering sheet.**
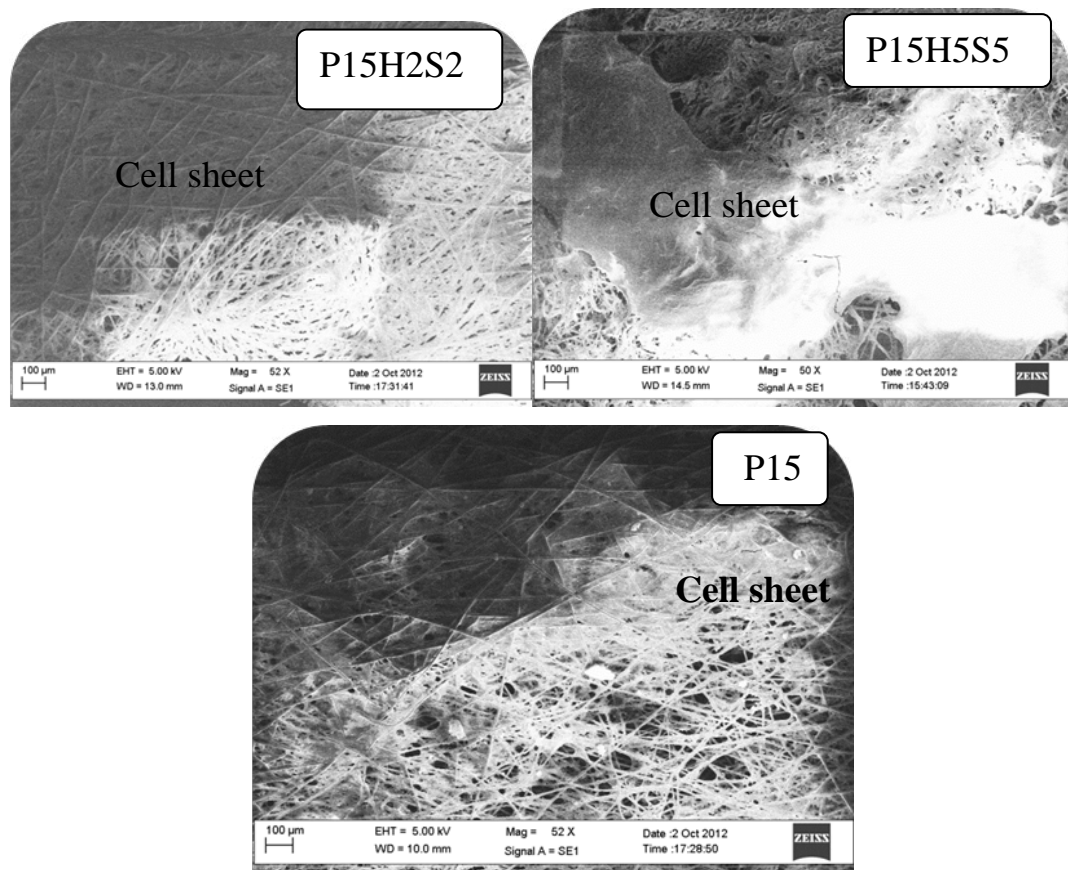
Figure 73 SEM micrographs of MC3T3-E1 cells grown on composite and polymeric fibrous membranes after 21 days in culture.Cell seeding density was 5 x 10^4 cells/ml.

Figure 74 SEM micrographs of MC3T3-E1 cells grown on composite and polymeric fibrous membranes after 28 days in culture.. Cell seeding density was 5 x 10^4 cells/ml

Osteopontin and Collagen type I expression

Osteopontin (OSPN), known as bone sialoprotein I, is a highly phosphorylated sialoprotein that is a prominent component of the mineralized extracellular matrices of bones and teeth. Regulation of the osteopontin gene is incompletely understood. Different cell types may differ in their regulatory mechanisms of the OSPN gene. OSPN expression in bone predominantly occurs by osteoblasts and osteocyctes (bone-forming cells) as well as osteoclasts (bone-resorbing cells) [226]. Osteopontin has been implicated as an important factor in bone remodelling such as playing a role in anchoring osteoclasts to the mineral matrix of bones.

Collagen type I alpha (COL I) is a human gene that encodes the major component of type I collagen, the fibrillar collagen found in most connective tissues. The COL I gene produces a component of type I collagen, called the pro-alpha1(I) chain. Collagen is a protein that strengthens and supports many tissues in the body, including cartilage, bone, tendon and it is expressed during the initial period of proliferation and extracellular-matrix biosynthesis [227].

In order to prove bone formation by osteoblasts the production of osteopontin and collagen type I, which are two of the bone markers for osteoblasts, were evaluated [228-230]. OSPN and COL I expression was visualized by targeting the specific protein antigen in the cell via specific epitopes (red colour – OSPN, green colour – COL I). As presented in Figure 75 the results showed that the osteopontin production increased in accordance with time up to day 28 for the MC3T3-E1 cells cultured on the P15H2S2 membranes. The same trend was evidenced for the cells cultured on the P15H5S5 membranes, as opposed to the ones cultured on the P15 membranes where the OSPN expression increased gradually up to day 7 and decreased

in the following period up to day 28. OSPN levels were low at day 1, day 3, day 14, day 21 and day 28 for P15 membrane, at day 1, day 3, and day 7 for P15H2S2 and P15H5S5 membranes, which followed typical development for osteoblasts cultures [231]. In addition, there was a significant difference in OSPN production between P15 and P15H2S2, P15H5S5 membranes at day 21 and day 28 ($p < 0.05$). Furthermore as evidenced in Figure 77 COL I expression was low at day 1, day 3 and day 7 for all types of membranes followed by an increase in expression up to day 28 for P15H2S2 and P15H5S5 fibrous membranes. Figure 76 and Figure 78 present the control staining of non seeded composite fibrous scaffold in order to exclude primary, secondary antibody and DAPI staining binding on the fibres. Further representative merged and split images of OPN and DAPI, respectively COL I and DAPI are presented.
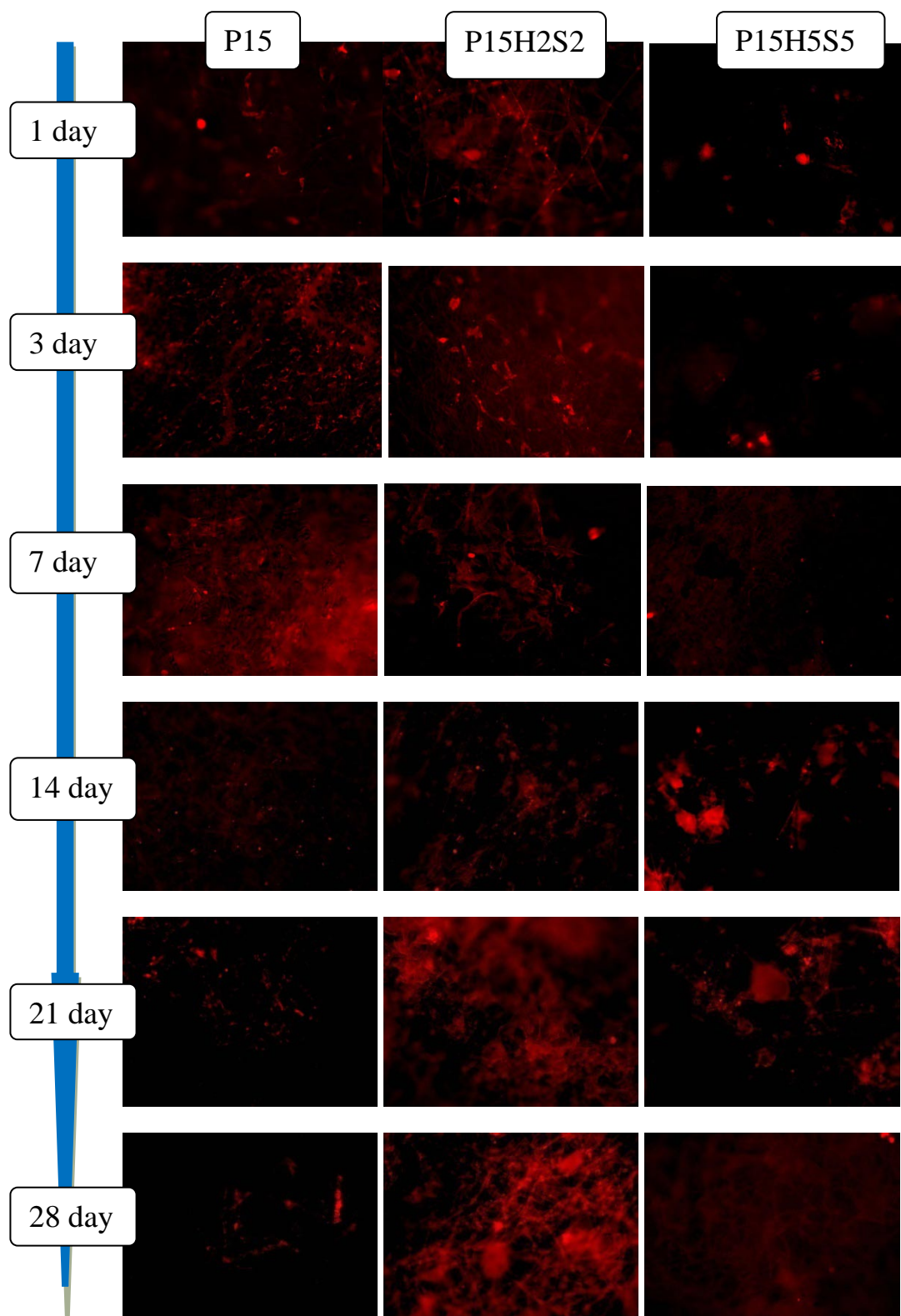
Figure 75 Osteopontin expression on P15_control, P15H2S2 and P15H5S5 fibrous polymeric and composite membranes after 1, 3, 7, 14, 21 and 28 days in culture. Cell seeding density was 5 x 104 cells/ml. Magnification 4X

A

P15   P15H2S2   P15H5S5

B

DAPI   OPN   Merged
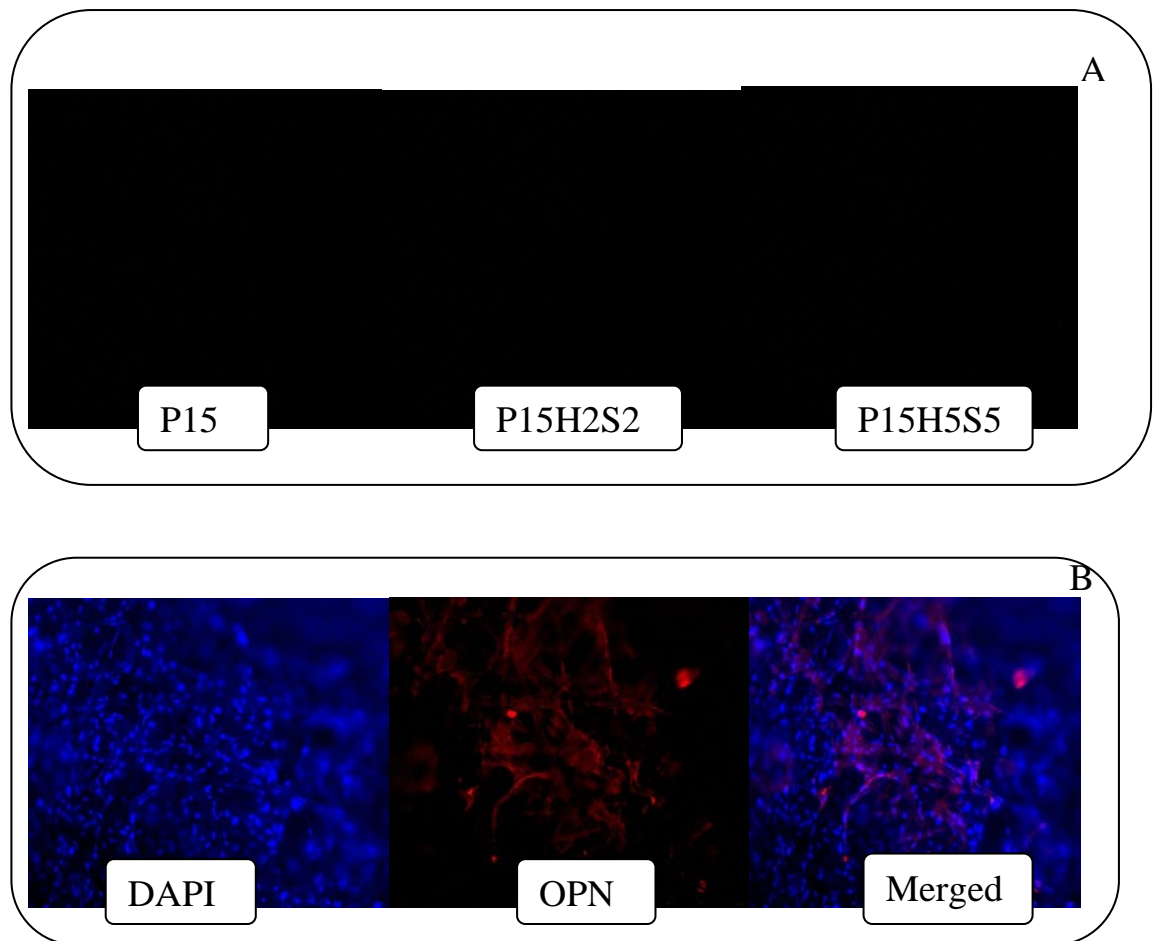
Figure 76 **(a) control staining of fibrous scaffolds (P15, P15H2S2, P15H5S5) without cells that shows no primary and secondary antibody or DAPI staining of the composite fibres; (b) representative merged and split images of OPN antibody and DAPI staining of P15H2 composite, day 7. Magnification 4X**
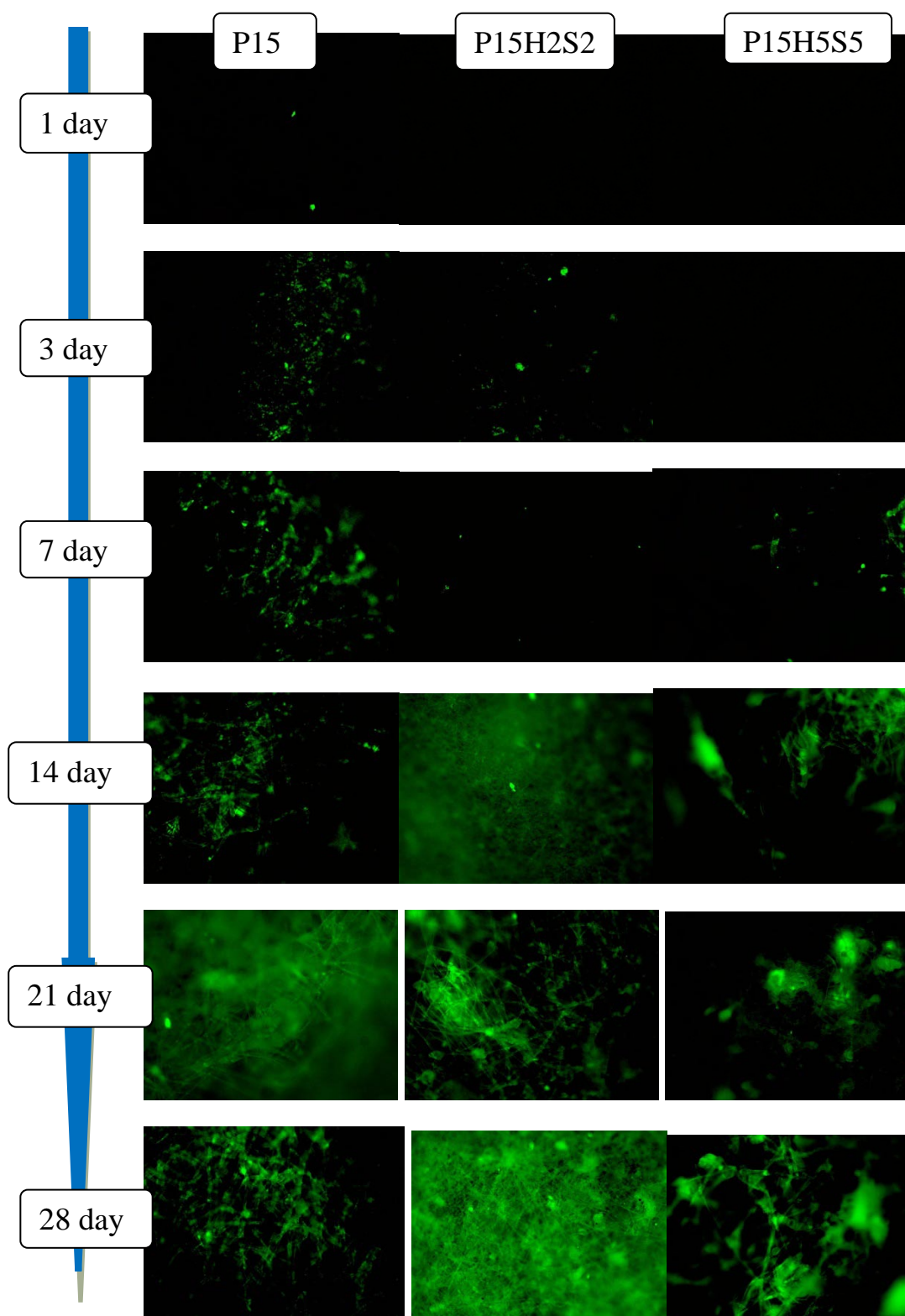
Figure 77 Collagen type I expression on P15_control, P15H2S2 and P15H5S5 fibrous polymeric and composite membranes after 1, 3, 7, 14, 21 and 28 days in culture. Cell seeding density was 5 x 104 cells/ml. Magnification 4X

A

P15   P15H2S2   P15H5S5

B

DAPI   COL I   Merged
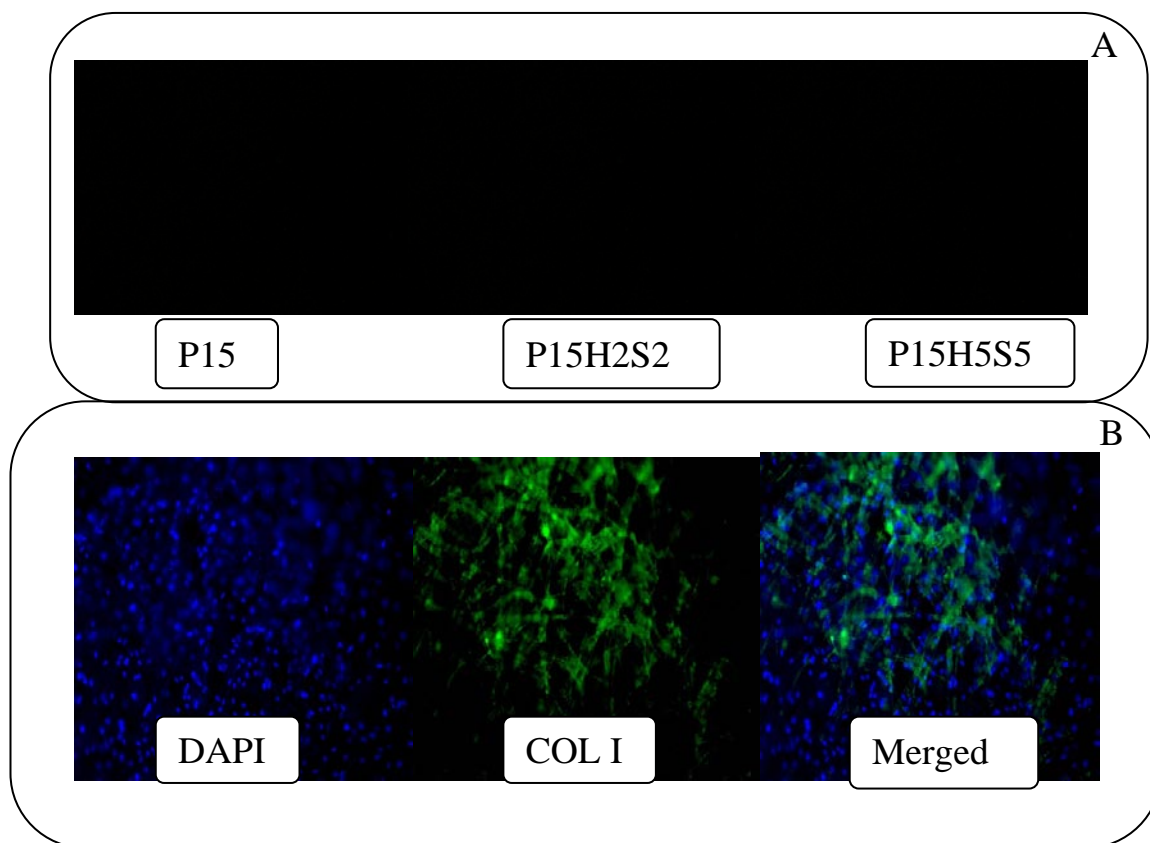
Figure 78   **(a) control staining of fibrous scaffolds (P15,P15H2S2,P15H5S5) without cells that shows no primary and secondary antibody or DAPI staining of the composite fibres; (b) representative merged and split images of COL I antibody and DAPI staining of PO composite, day 28. Magnification 4X**

Quantitative real time-PCR

To further evaluate osteogenic differentiation on scaffold surfaces quantitative real time RT-PCR measurements were performed. The expression of OSPN and COL I were determined using primers and probes specificfor each osteogenic marker gene and were normalised tothe housekeeping gene GAPDH. Gene expression levels were expressed as fold changes relative tothe expression of the control sample (cells seeded on TCPS). Figure 79 and Figure 80 present the results as (a) comparison between control, P15 and P15H5S5 and (b) P15H2S2 fibrous membranes. Statistical analysis disclosed that at day 14, 21, and 28 MC3T3-E1cells cultured on the P15 and P15H2S2 scaffolds expressed significantly higher mRNA levels for OSPN gene ($p < 0.05$) examined than cells cultured on the control and P15H5S5 scaffolds (Figure 79 a). OSPN expression by MC3T3-E1 grown on the P15 scaffold increased more than 50 fold on day 14 and more than 200 fold on 21 day. As shown in Figure 79 b MC3T3-E1 cells cultured on P15H2S2 composite membranes evidenced an increase in OSPN gene expression. Further higher mRNA levels for Col I gene ($p<0.05$) were evidenced for MC3T3-E1 cells cultured on P15 (Figure 80 a) and P15H2S2 scaffolds (Figure 80b) as compared to P15H5S5 levels for day 21 and day 28. Further COL I expression increased 120 fold on day 21 and 28 on P15 fibrous membrane and almost 35 fold on P15H2S2 composite membrane when compared to gene expression for cells cultured on TCPS plate. It has to be noted that the medium used for these studies was not supplemented with ascorbic acid, which was shown to initiate the formation of a collagenous extracellular matrix and synthesis of several osteoblast-related proteins [232, 233].
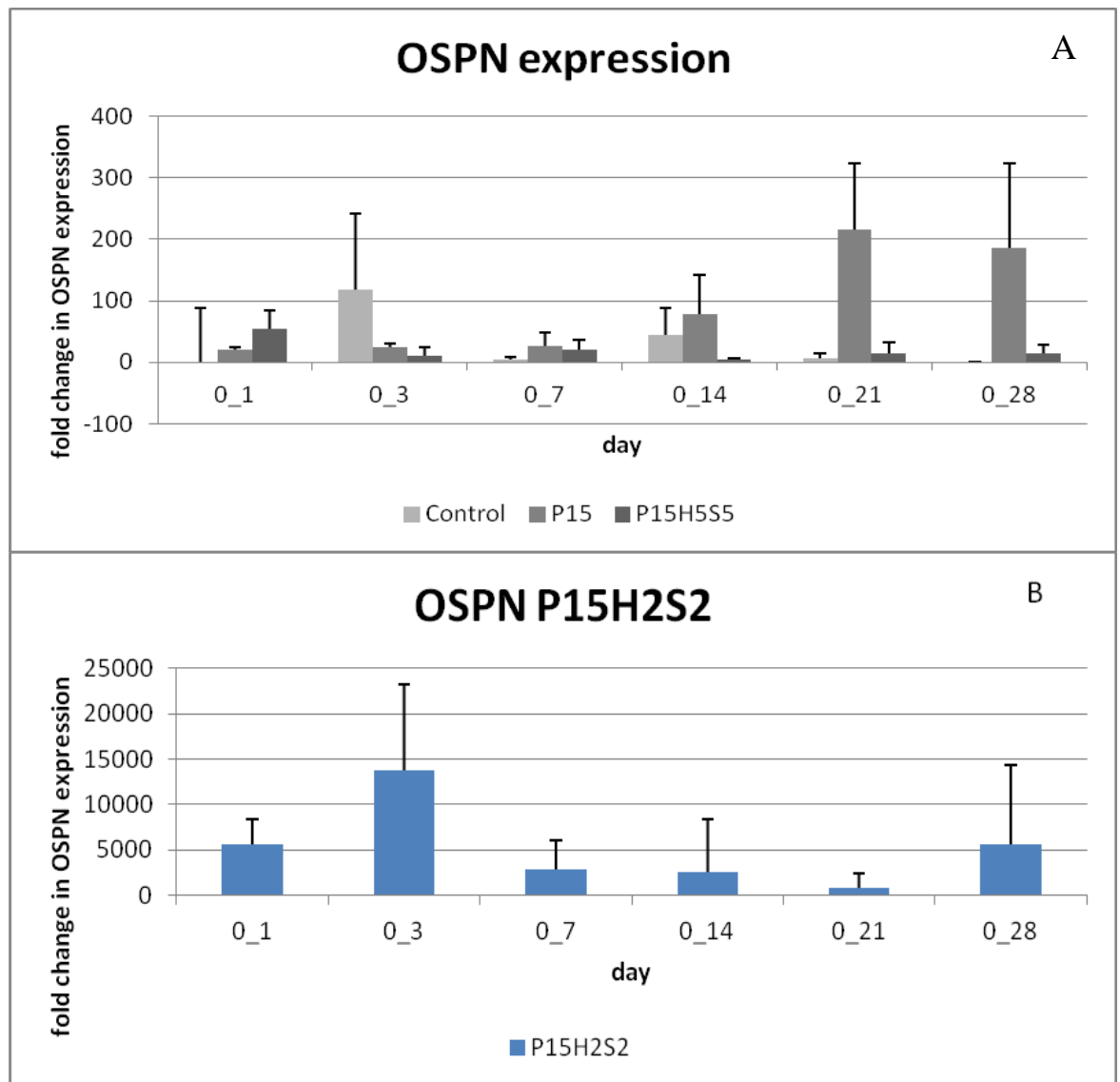
Figure 79 Messenger RNA expression levels of OSPN bone marker after 0, 1, 3, 7, 14, 21 and 28 days of culture MC3T3-E1 cells on : (a) TCPS, P15, P15H5S5 scaffolds, (b) P15H2S2 scaffold . Data have been normalized to the housekeeping gene GAPDH using TCPS as control sample. The results are shown as $2^{-\Delta\Delta CT}$. *p < 0.05 compared with the TCPS (control); 0 day accounts for prior to seeding cells on scaffolds/TCPS plate
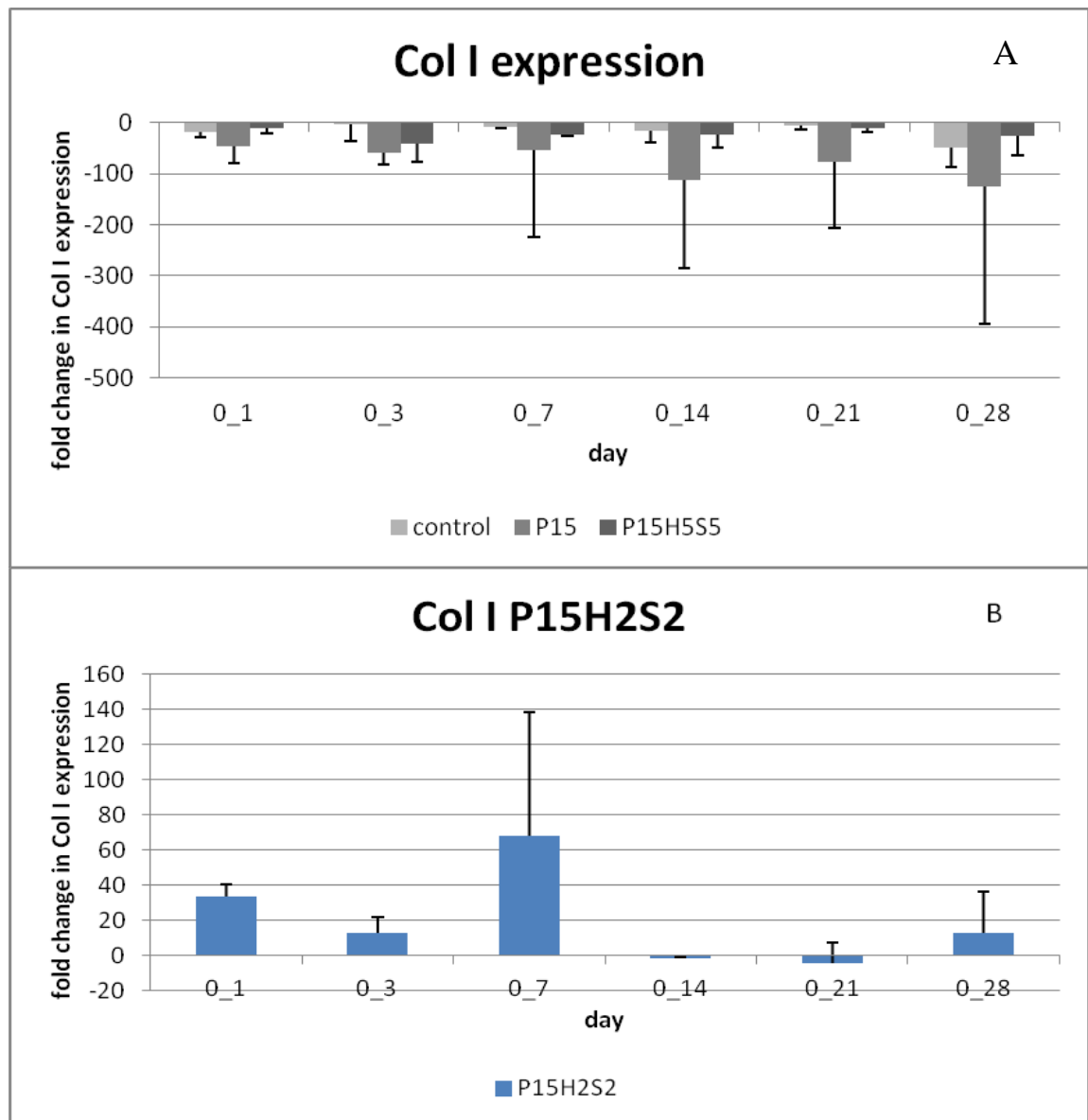
Figure 80 Messenger RNA expression levels of Col I bone marker after 0, 1, 3, 7, 14, 21 and 28 days of culture MC3T3-E1 cells on (a) TCPS, P15, P15H5S5 scaffolds, (b) P15H2S2 scaffold.Data have been normalizedto the housekeeping gene GAPDH using TCPS as control sample. The results are shown as $2^{-\Delta\Delta CT}$. *p < 0.05 compared with the TCPS (control); 0 day accounts for prior to seeding cells on scaffolds/TCPS plate

Bone alkaline phosphatise (BALP) activity (ELISA assay)

Differentiation on the various substrates was characterised using BALP as an early bone differentiation marker. Bone alkaline phosphatase, an ectoenzyme produced by osteoblasts, is believed to involve in the degradation of inorganic pyrophosphate providing a sufficient local concentration ofphosphate or inorganic pyrophosphate for mineralization toproceed. Among the various biological functions of osteoblasts, secretion of alkaline phosphatase (ALP) is an important indicator determining the activity of the cells on a scaffold [234]. Cells adhering to P15H2S2 scaffolds exhibit significantly higher activity of the enzyme than on the P15H5S5 and the control (P15) on days 21 and 28, while P15H5S5 scaffolds exhibit higher activity levels on days 1 3,5 and 14 (Figure 81). ALP kinetics show asignificant increase in specific activity of the enzyme on P15 and P15H5S5 porous scaffolds at each time point for days 1 and 3 followed by a decrease for days 5 and 7. In contrast, the pattern of ALP activity on P15H2S2 does not resemble the other two constructs, which consists of a slow increase over the first week (days 1, 3, 5, 7), with significantly increase for days 14, 21 and 28. We observed two peaks in activity at day 3 and day 14 for the P15H5S5 scaffolds, while P15H2S2 scaffolds exhibit one peak in activity at day 28.
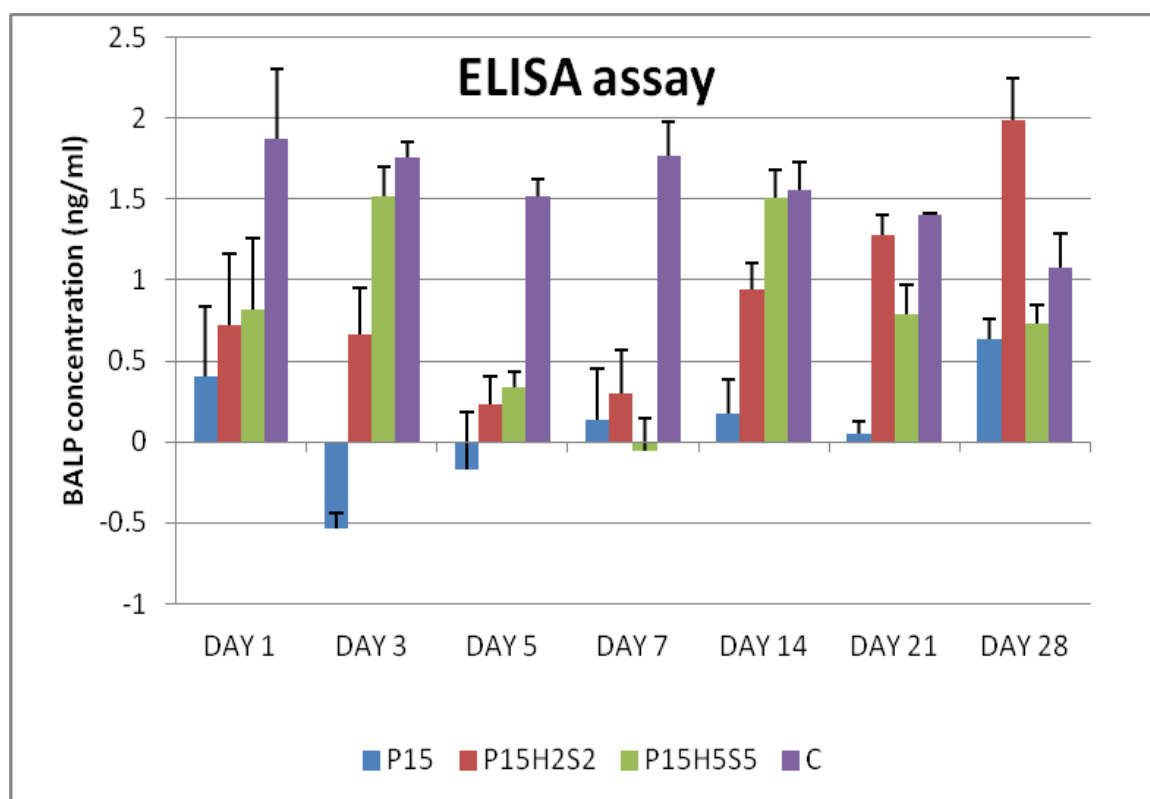
Figure 81 Alkaline phosphatase activity of electrospun composite scaffolds seeded with MC3T3-E1 over 28 days. Enzyme activity was measured from release from constructs into cell culture medium. Experimental groups were P15, P15H2S2 and P15H5S5 Data represent means±standard deviation for n=3.

Discussion

After successfully electrospinning a flat membrane exposing continuous and smooth fibres entagled in a porous structure resembling the ECM, thicker 3D scaffolds were manufactured by a simple and time effective method, that is folding/rolling of the flat membrane. The thick structures were further assessed from a physico-chemical and biological point of view, in order to determine their suitability as prospective bone tissue substitutes, in line with the listed aims and objectives. The results from this

section of Chapter 4 proved that thicker electrospun structures can be created and that these can support bone regeneration, by sustaining cell attachement and proliferation, while preserving cells phenotype for over a 28 days culture period. Furthermore the composite fibrous supports show good mechanical properties, supporting their applicability for load bearing applications. It has been evidenced that silk fibroin inclusion improves the ceramic electrospinning within the polymeric PHB/PHV matrix. Furthermore the proteic phase leads to improved mechanical properties under compression, after methanol treatement; this treatement induces changes in the chemical conformation of the silk fibroin as shown by previous research [Ref if possible]. Additionally the *in vitro* biological evaluation has proven that the thick structures are able to support osteoblasts attachement and proliferation over a period of 4 weeks. After an initial period of cell number increase, the osteoblasts are able to penetrate into the depth of the scaffolds (as shown by the ICC images), evidencing filopodia extensions. Cells have been shown to present their characteristic stellar and elongated shape, while increased levels of BALP, COL I and OSPN have been evidenced for the composite scaffolds (P15H2S2 predominantly).

4.6.4 Summary

Overall, this project was successful in defining novel composite solutions that can be electrospun into biocompatible, bioactive, biodegradable and non – toxic fibrous membranes. Further it has been proven that the chosen ceramic phase can be electrospun as part of the composite solution. Finally, the two dimensional membranes

were used for the construction of three-dimensional structures and these were fully characterised in order to prove their suitability for bone tissue regeneration applications. The relevance of these results is not only in the fact that the structures obtained were comparable to the natural extracellular matrix, mimicking its morphology, but also that their physico-chemical and biological properties allow their use as potential bone- cells supports. Table 19 highligths the various composite samples produced during this study and their properties ranked. Values from 1-3 were used to score the samples potential applicability as bone tissue scaffolds, with 1 - not suitable, 2 average/ further improvement needed, 3- good/ suitable. Based on the ranking it could be concluded that the P15H2S2 was found to be best suited for the chosen application, achieving a score of 32 out of potential 36, followed by the P15H5S5 composite with a total 28 and the control P15 construct with a total of 27.

Table 19 Tests results ranking

Sample	P15	P15H2S2	P15H5S5
Morphology	3	3	3
Porosity	3	3	3
Hydrophilicity	2	2	2
Bioactivity	2	3	3
UTS	2	2	1
Young's modulus	2	2	1
Compressive secant modulus	1	3	1
Cell attachement	3	3	3
Cell proliferation	3	3	3
OSPN	2	3	2
COL I	2	3	2
BALP	2	3	3
TOTAL	**27**	**32**	**28**

CHAPTER 5 CONCLUSIONS AND RECOMMENDATIONS

5.1 Conclusions

Large bone defects caused by injuries or pathological lesions are a major challenge for the reconstructive surgery. While bone can be regenerated by auto- and allograft, both alternatives present drawbacks such as donor site infection and morbidity, graft rejection or disease transmittance. A promising approach currently under investigation is tissue engineering (TE). For bone regeneration tissue engineering uses three-dimensional structures of large surface area and high porosity as constructs (scaffolds) on which cells with osteogenic properties are seeded and further implanted into the area of interest. However, several disadvantages have been observed with these structures, including weak structural integrity, non biodegradability and host immune reactivity. In our study, resorbable composite membranes were prepared as a fibrous mesh by electrospinning to overcome these disadvantages and improve applicability for guided bone regeneration. Electrospinning is a polymer fabrication technique with promising application in the fieldof tissue engineering. The process offers a relatively simple method of creating polymer scaffolds with micron fibre diameters in a highly porous network similar to the ECM of native tissue. The high surface per unit volume ratio achieved in electrospun constructsis ideal for encouraging cellular attachment, proliferation and migration [221].

The outcomes of this project have largely contributed to the field of composite electrospinning and fibrous scaffold manufacturing for bone tissue regeneration, in particular electrospinning nano hydroxyapatite powder simultaneously with the polymeric solution. In fact, the main challenges identified at the start of this project were successfully overcome.

The research work questioned if nHA_P can be electrospun simultaneously within a polymeric matrix. Furthermore it questioned if thick fibrous structures evidencing adequate mechanical and biological features as to support bone regeneration could be manufactured using such a composite solution.In other words the designed and fabricated three- dimensional fibrous composite scaffolds were intended to mimic the extracellular matrix of the bone in terms of chemistry and morphology, while supporting bone cell attachment, proliferation and bone cells phenotype expression.

The first phase of the study was to select an appropriate polymer to be studied as the basis of the composite solution. PHB/PHV is a copolymer of polyhydroxyalkanotes (PHA).This group of polymers are aliphatic polyesters produced by micro-organism under unbalanced growth conditions. The major advantages of using this natural copolymer is that it presents no toxic effects when implanted in the body, has a lower flexural modulus or level of crystallinity, which makes ittougher and more flexible than the other polymers of the PHA family. The crystallinity and mechanical properties of PHB/PHV can change with the variation of the percentage ratio of the respective monomers. Knowles and Hastings [235] reported that the copolymer PHB/PHV degrades slowly andtherefore can be suitable for implant device applications in bone replacement applications. When it is reinforced with bioactive ceramics particles such as HAp was found to have improved osteointegrative properties and interaction with tissue and this was due to the excellent physical-mechanical characteristics of these

composites, which are similar to those of bone tissue [236]. Luklinska and Schluckwerder [237] showed that, after one month of implantation, lamellar bone structure has well developed around the HAp/PHB/PHV implant surface. At three months, marrow cells were observed in the new bone structure. At six months, the bone layer was compact and continuous around the composite implants. PHB/PHV is very particular for the bone tissue engineering applications. It has been demonstrated that a potential component bone tissue adaptation response can be produced with no verification of an undesirable chronic inflammatory response after implantation for periods of up to 12 months [87]. Another unique property of PHB/PHV is its piezoelectricity, whichwas claimed to induce bone reformation in load-bearing sites [237]; this makes it a potential candidate for orthopaedic applications since electrical stimulation has been knownto promote bone healing [237].

In order to investigate the potential for in-house production of electrospun PHB/PHV/nHAp based scaffolds, the second phase of this thesis included the development and optimisation of a composite solution electrospinning protocol. The first task of protocol optimization was to screen different solution concentrations of PHB/PHV in CHO and assess the resultant effects on electrospun fibre morphologies. Further variations of electrospinning parameters were investigated and their effect on the fibres morphology and electrospinning process continuity. Results have indicated that PHB/PHV/nHAp electrospinning is difficult to initiate and continuous fibre deposition almost impossible to achieve. For this reason a third phase was added to the composite solution, that of silk fibroin (SF). Silk fibroin (SF), a protein extracted from the silk produced by culture silkworms and spiders, is composed of 17 amino acids thus being biocompatible and biodegradable. When appropriately purified, SF is non-toxic, non-immunogenic and has been demonstrated to support cell and tissue growth. At the

186

same time, silk is a thermally stable material, allowing processing over a wide range of temperatures (up to about 250°C), which makes it a good candidate for autoclave systems without loss of functional integrity [69]. The addition of the proteic phase lead to electrospinning initiation and continuous fibre deposition for composite solution of P15, P15H2S2 and P15H5S5 for settings of 15kV (P15) and 10kV (P15H2S2, P15H5S5), 15cm distance and 5ml/h feed rate. Once a protocol was set up and prototype fibrous composite membranes were produced a third phase of optimisation was employed, using the DoE approach to investigate broader ranges of variations of electrospinning parameters and composite solution concentrations.The additional DoE study phase indicated that electrospinning of higher concentration of ceramic and proteic phases lead to bead defects formation within the fibrous structure and increase in membrane fragility when handled. At the same time preliminary biological *in vitro* assessment using HBO showed that the produced fibrous samples sustained cell attachment and proliferation for up to 3 days in culture. Future investigation and optimisation of the samples physical properties with higher concentration nano hydroxyapatite and silk fibroin is necessary for potential use as bone tissue engineering constructs.

Analysing all the obtained results samples of P15, P15H2S2 and P15H5S5 in compositions were considered further. The fourth step of the research investigated if the electrospun samples are bioactive, thus sustaining apatite formation on their surface while immersed in simulated body fluid (SBF) over 28 days. Results have shown that the produced fibrous construct are bioactive, supporting apatite formation on their surface. As stated before it is commonly believed that when bioactive materials are implanted in the body, they spontaneously bond to bone via an apatite layer deposited on their surface without forming the fibrous tissue around them [201]. However, the *in*

vivo results are normally difficult to obtain and to interpret due the complexity of cellular responses. *In vitro* methods to assess the bioactivity of biomaterials include the use of Simulated Body Fluid (SBF), which specifically evaluates the substrate ability of apatite formation, protein adsorption or osteoblast cell culture studies.

The next step of this research was to produce thicker constructs, such as three dimensional scaffolds that can sustain cell culture and bone regeneration. Several techniques have been assessed in this direction, such as hydro-spinning, sintering, laser welding, and stacking/folding. As opposed to the other techniques which either destroyed the fibrous structure (laser welding, sintering) or were time consuming (hydrospinning), stacking/ folding technique allowed the production of three-dimensional constructs that retained their fibrous morphology and porosity. These three-dimensional scaffolds were assessed in terms of their physical and biological properties and the results were presented in the fifth and sixth step of the research study. It was evidenced that the ultimate tensile strength and Young's modulus of the composite fibres decreases with increased content of nHAp and SF phase. This can be attributed to the lack of sufficient interfacial interaction between the nHAp and SF phases respectively and the polymeric matrix. Further it could be assumed that the addition of the nHAp and silk phases had a significant effect on the tensile properties of the P15H2S2, while increasing the concentration of these co-phases above 2%wt led to no significant improvement of the mechanical properties of the composite samples. In terms of compressive strength the properties of the composites were comparable to some load-bearing tissues as shown by Kurkijarvi *et al* [213]. Furthermore, it was hypothesized that that the inclusion of silk fibroin could reduce the solubility of composite samples in the cell culture medium and improve the mechanical properties by changing the configuration of the protein, from random coil conformation to β –

sheet by immersion in methanol [214, 215]. Results showed a significant increase in tensile strength for the composite sample of P15H2S2 and P15H5S5 after methanol treatment suggesting that the methanol treatment led to conformation changes of silk fibroin as hypothesized.

Viable biodegradable thick PHB/PHV - based composite scaffolds were obtained (utilising various composite formulations); these composites are very promising candidates to act as bone scaffolds, either for *in vitro* or *in vivo* use (to support bone formation outside the body for an initial period of time or *in vivo*, post implantation).

The chemical functionality of PHB/PHV-based composites was retained following the electrospinning process, with polymer-characteristic peaks remaining visible throughout the spectra. Even though, the exact mechanism of interaction between surface properties and cells is not fully understood; it is broadly recognised that the chemistry and topography of scaffold surfaces determine to a large extent the biological performance of the implanted devices. This furthermore confirms that the rough, hydrophilic and chemically stable constructs obtained, are ideal candidates for bone tissue applications.The degradation by-products of the pure polymeric membrane and of the composite nHAp integrated (various concentrations) were not acidic in nature and did not generate a hostile implantation environment *in vitro* with regards to pH levels.

The conductivity measurements of PHB/PHV-based composites showed that composite samples had a much larger conductivity potential than pure polymeric ones. It was assumed that the conductivity of the fibrous membranes was enhanced by the addition of an nHAp and / or silk fibroin phases.

The degradation of the composite nHAp integrated constructs was minimal during the first month of the *in vitro* analysis, which guarantees the mechanical integrity of the scaffolds post-implantation, when the desired application is load-bearing orthopaedic implants, and could provide a system with a long-lasting integrity.

The preliminary biological assessment showed that the performance of composite constructs after 1 day and 3 days in culture was superior to the pure polymeric ones in terms of cell attachement and scaffold penetration, suggesting a faster osteointegration post-implantation. While the integration of inert implant/scaffolds in orthopaedic applications is a passive process that results in mechanical fixation only, which may lead to its loosening and anchorage failure, the bioactive polymer (PHB/PHV) will therefore increase the biointegration of the implant and the bone tissue.

The SBF immersion test results confirmed that the composite structures are bioactive, thus they can induce and support bone formation *in vivo.* Over a period of 4 weeks samples were exposed to a concentrated solution resembling the human body's plasma composition. The chemical conformation of the composite structures led to an apatite layer formation on their surface, with Ca/P ratio similar to the hydroxyapatite found in the body.

As a final step, scaffolds were evaluated for cellular attachment, proliferation and bone marker expression using a MC3T3-E1 cell line over a period of 28 days. All the scaffolds supported cellular attachment, as indicated by the cell count number and DAPI staining. Also, over the period of 28 days, values for every group of scaffolds increased indicating cellular proliferation.

Initially more cells attach to the composite scaffolds (P15H2S2 and P15H5S5) and after 14 days more extensive ECM formation and cell growth were seen. There were significant differences between P15H2S2 and P15H5S5 groups after the day 7 point.

Enhanced osteoblast proliferation and differentiation were demonstrated by increased mRNA expression of the BALP, COL I and OSPN genes by the cells cultured on the P15H2S2 composite fibrous construct as opposed to the P15 polymeric fibrous structure. Particular interest was paid to whether or not these fibrous scaffolds could support the osteoblastic phenotype expression of MC3T3-E1 and analyses of the expression levels of bone-related markers (OPN, COL I and BALP) were conducted in this direction.

Results showed that the cells adhering to P15H2S2 scaffolds exhibited significantly higher activity of BALP than on the P15H5S5 and the control (P15) on days 21 and 28. This can be attributed to the higher number of cells attached and proliferated on P15H2S2 as compared to P15 and P15H5S5 on the indicated time points. On the contrary, the BALP activity of the cells grown on P15 (control) was the lowest at any given time point, despite the relatively high number of cells attached on its surface.

MC3T3-E1 cultured on the surface of P15H2S2 composite exhibited the greatest amount of OPN gene for all given time points after cell culturing when compared to those cultured on the P15 and P15H5S5. This translated to the greatest extent of mineralization for the cells grown on the surface of P15H2S2, followed by that for the cells grown on P15H5S5 and P15, respectively.Compared to the control scaffolds (P15), the test materials supported osteoblast maturation, increasing the secretion of bone matrix, which aids in bone regeneration. The findings of this work

support the hypothesis that the proposed composite scaffolds enhance the osteoblast phenotype and suggest that P15H2S2 and P15H5S5 scaffolds are appropriate cell carriers for osseous tissue engineering when compared to the PHB/PHV polymer scaffolds (P15).

5.2 Future recommendations

Due to the novelty of the composite solution formulation and the technique implemented, the work presented in this thesis has significant potential to be developed as a scaffold for bone regeneration. In order to achieve this aim, future work needs to be carried out in terms of cell proliferation assessment (e.g. histology) in order to determine how far the cells travel in the depth of the scaffold and if they are viable when reaching the middle of the construct. A further step can be made with *in vitro* dynamic analysis of the seeded scaffolds, to investigate if they maintain their phenotype when placed in an environment more appropriate to the *in vivo* one, while investigating if the fibrous structures support neovascularisation would be another potential direction to follow. Extending application to other tissues regeneration, such as cartilage could also be viable.

REFERENCES

[1]   Transplant Gift, "The Gift of a Lifetime," 2004.

[2]   Sommerfeldt, D. W. and Rubin, C. T., "Biology of bone and how it orchestrates the form and function of the skeleton," Eur *Spine Journal,* vol. 10, pp. S86-S95, 2001.

[3]   Rodan, G. A., "Introduction to Bone Biology," *Bone,* pp. S3-S6, 1992.

[4]   Burg, K.J.L,. Porter, S. and Kellam, J. F. "Biomaterial developments for bone tissue engineering," *Biomaterials,* vol. 21, pp. 2347-2359, 2000.

[5]   Ma, P.X. and Elisseeff, J., *Scaffolding in Tissue Engineering,* Florida, USA: Taylor and Francis Group Ltd., 2005,

[6]   Huang, Y.-C. and Mooney, D. J., "Modifed alginates for tissue engineering," in *Scaffolding in Tissue Engineering* Ma, P.X., Elisseeff, j., Ed. Boca Raton, Florida: Taylor and Francis Group Ltd., 2005, pp. 301-334.

[7]   Nikkhah, M., Edalat, F., Manoucheri, S. and Khademhosseini, A., "Engineering microscale topographies to control the cell-substrate interface," *Biomaterials,* pp. 1-17, 2012.

[8]   Hynes, R. O., "The extrcellular matrix: not just pretty fibrils," *Science,* pp. 1216-1219, 2009.

[9]   Loca, D., Locs, J., Salma, K., Gulbis, J., Salma, I. and Berzina-Cimdina, L., "Porous Hydroxyapatite Bioceramic Scaffolds for Drug Delivery and Bone Regeneration," *OP Conf. Ser. : Mater. Sci. Eng.,* vol. 18, pp. 192019, 2011.

[10]   Seal, B. L., Otero, T. C. and Panitch, A., "Polymeric biomaterials for tissue and organ regeneration," *Mater. Sci. Eng. R,* pp. 147-230, 2001.

[11]   Ni, J. and Wang, M., "*In vitro* evaluation of hydroxyapatite reinforced polyhydroxybutyrate composite," *Mater Sci Eng C-Bio S,* pp. 101-109, 2002.

[12]   Doyle, C., Tanner, E.T. and Bonfield, W., "*In vitro* and *in vivo* evaluation of polyhydroxybutyrate and of polyhydroxybutyrate reinforced with hydroxyapatite," *Biomaterials,* pp. 841-847, 1991.

[13]   Galego, N., Rozsa, C., Sanchez, R., Fung, J., Vazquez, A. and Tomas, J.S., "Characterization and application of poly(b-hydroxyalkanoates) family as composite biomaterials," *Polym Test,* pp. 485-492, 2000.

[14] Teo, W.-E., He, W. and Ramakrishna, S., "Electrospun scaffold tailored for tissue-specific extracellular matrix," *Biotechnol. J.,* pp. 918-929, 2006.

[15] Best, S.M., Porter, A.E., Thian, E.S. and Huang, J., "Bioceramics: Past, present and for the future," *Journal of the European Ceramic Society,* vol. 28, pp. 1319–1327, 2008.

[16] Wan, H., Williams, R.L., Doherty, P.J and Williams, D.F., "A study of cell behaviour on the surfaces of multifilament materials," *J Mater Sci: Mater Med,* pp. 47-51, 1997.

[17] Sanders, J.E, Stiles, C.E. and Hayes, C.L., "Tissue response to single polymer polymer fibers of varying diameters: Evaluation of fibrous encapsulation and macrophage density," *J Biomed Mater Res,* pp. 231-237, 2000.

[18] Fujihara, K., Kotaki, M. and Ramakrishna, S., "Guided bone regeneration membrane made of polycaprolactone/calcium carbonate composite nano-fibers," *Biomaterials,* pp. 4139-4147, 2005.

[19] Kim, H.-W., Song, J.-H. and Kim, H.-E., "Nanofiber generation of gelatin–hydroxyapatite biomimetics for guided tissue regeneration, 2005; 1988–1994." *Adv Funct Mater,* pp. 1988-1994, 2005.

[20] Xu, X., Chen, X., Liu, A., Hong, Z. and Jing, X., "Electrospun poly(l-lactide)-grafted hydroxyapatite/poly(l-lactide) nanocomposite fibers," *European Polymer Journal,* pp. 3187-3196, 2007.

[21] Deng, X.L., Sui, G., Zhao, M.L., Chen, G.Q. andYang, X.P., "Poly(l-lactic acid)/hydroxyapatite hybrid nanofibrous scaffolds prepared by electrospinning ," *J Biomater Sci Polym Ed,* pp. 117-130, 2007.

[22] Sui, G., Yang, X., Mei, F., Hu, X., Chen, G., Deng, X. and Ryu, S., "Poly-l-lactic acid/hydroxyapatite hybrid membrane for bone tissue regeneration," *J Biomed Mater Res, Part A,* pp. 445-454, 2007.

[23] Venugopal, J., Vadgama, P., Kumar, T.S.S. and Ramakrishna, S., "Biocomposite nanofibres and osteoblasts for bone tissue," *Nanotechnology,* pp. 1-8, 2007.

[24] Catledge, S.A., Clem, W.C., Shrikishen, N., Chowdhury, S., Stanishevsky, A.V., Koopman, M. and Vohra, Y.K, "An electrospun triphasic nanofibrous scaffold for bone tissue engineering," *Biomed Mater,* pp. 142-150, 2007.

[25] Prabhakaran, M.P, Venugopal, J. and Ramakrishna, S., "Electrospun nanostructured scaffolds for bone tissue engineering," *Acta Biomaterialia,* pp. 2884-2893, 2009.

[26] Wang, L. C., "Preparation and physicochemical properties of a novel hydroxyapatite/chitosan–silk fibroin composite," *, Carbohydrate Polymers,* pp. 740-745, 2007.

194

[27] Franco, P.Q., João, C.F.C., Silva, J.C. and Borges, J.P., "Electrospun hydroxyapatite fibers from a simple sol–gel system," *Materials Letters,* pp. 233-236, 2012.

[28] Guan, D., Chen, Z., Huang, C. and Lin, Y., "Attachment, proliferation and differentiation of BMSCs on gas-jet/electrospun nHAp/PHB fibrous scaffolds," *Applied Surface Science,* pp. 324-327, 2008.

[29] Ito, Y., Hasuda, H., Kamitakahara, M., Ohtsuki, C., Tanihara, M., Kan, I-K. and Kwon, O-H., "A composite of hydroxyapatite with electrospun biodegradable nanofibers as a tissue engineering material," *Journal of Bioscience and Bioengineering,* vol. July, pp. 43-49, 2005.

[30] Cui, W., Li, X., Xie, C., Zhuang, H., Zhou, S. and Weng, J., "Hydroxyapatite nucleation and growth mechanism on electrospun fibers functionalized with different chemical groups and their combinations," *Biomaterials,* pp. 4620-4629, 2010.

[31] Remant Bahadur, K.C., Kim, K.C., Khil, M.S., Kim, H.Y. and Kim, I.S.,"Synthesis of hydroxyapatite crystals using titanium oxide electrospun nanofibers," *Materials Science and Engineering: C,* pp. 70-74, 2006.

[32] Nie, H., Soh, B.W., Fu, Y.C. and Wang, C.H., "Three-dimensional fibrous PLGA/HAp composite scaffold for BMP-2 delivery," *Biotechnol Bioeng,* vol. 99, pp. 223-234, 2008.

[33] Nie, H. and Wang, C.H., "Fabrication and characterization of PLGA/ HAp scaffolds for delivery of BMP-2 plasmid composite DNA," *J Control Release,* vol. 120, pp. 111-121, 2007.

[34] Jose, M.V., Thomas, V., Johnson, K.T., Dean, D.R. and Nyalro, E., "Aligned PLGA/HA nanofibrous nanocomposite scaffolds for bone tissue engineering," *Acta Biomaterialia,* vol. 5, pp. 305-315, 2009.

[35] Everts, V., Delaissé, J.M., Korper, W., Jansen, D.C., Tigchelaar-Gutter, W., Saftig, P. and Beertsen, W., "The bone lining cell: its role in cleaning Howship's lacunae and initiating bone formation," *J Bone Miner Res,* vol. 17, pp. 77-90, 2002.

[36] Hench, L.L. and Jones, J.E., *Biomaterials, Artificial Organs and Tissue Engineering,* Woodhead, Boca Raton; Cambridge: CRC Press, 2005,

[37] van Gaalen, S., Kruyt, M., Meijer, G., Mistry, A., Mikos, A., van den Beucken, J., Jansen, J., de Groot, K., Cancedda, R., Olivo, C., Yaszemski, M. and Dhert, W., "Tissue engineering of bone," in *Tissue Engineering* van Blitterswijk, C.,Thomsen, P., Lindahl, A., Hubbell,J., Williams, D.F., Cancedda, R., de Bruijn , J.D. and Sohier, J., Ed. Academic Press, 2008, pp. 559-610.

[38] Stevens, M.M., "Biomaterials for Bone Tissue Engineering," *Materials Today,* vol. 11, pp. 18-25, 2008.

[39] Benayahu, D., Gurevitzt, O.A. and Shamay, A., "Bone-related Matrix Proteins Expression *in vitro* and *in vivo* by marrow stromal cell line," *Tissue and Cell,* pp. 661-666, 1994.

[40] Pidaparti, R. M. V., Chandran, A., Takano, Y. and Turner, C. H., "Bone Mineral Lies Mainly Outside Collagen Fibrils: Predictions of a Composite Model For Osteonal Bone," *Journal of Biomechanics,* pp. 909-916, 1996.

[41] Rho, J. Y., Kuhn-Spearing, L. and Zioupos, P., "Mechanical Properties and the Hierarchical Structure of Bone," *Medical Engineering & Physics,* vol. 20, pp. 92-102, 1998.

[42] Orlovskii, V. P., Komlev, V. S. and Barinov, S. M., "Hydroxyapatite and Hydroxyapatite-Based Ceramics," *Inorganic Materials,* vol. 38, pp. 973-984, 2002.

[43] Clarke, B., "Normal Bone Anatomy and Physiology," *CJASN,* vol. 3, pp. S131-S139, 2008.

[44] Yaszemski, M. J., Payne, R. G., Hayes, W. C., Langer, R. and Mikos, A. G. "Evolution of Bone Transplantation: Molecular, Cellular and Tissue Strategies to Engineer Human Bone," *Biomaterials,* pp. 175-185, 1996.

[45] Caranoa, R.A.D. and Filvaroff, E.H., "Angiogenesis and Bone Repair", *Drug Doscovery Today,* vol. 8 (21), pp. 980–989, 2003

[46] Chan, B. P. and Leong, K. W., "Scaffolding in tissue engineering: general approaches and tissue-specific considerations," *Eur Spine J,* vol. 17 7(Suppl 4), pp. 467–479, 2008.

[47] Ratner, B.D. and Bryant , S.J.,"Biomaterials: where we have been and where we are going," *Annu Rev Biomed Eng.,* vol. 6, pp. 41-75, 2004.

[48] Kim, B.S., Baez, C.E. and Atala, A., "Biomaterials for tissue engineering," *World J Urol,* vol. 18, pp. 2-9, 2000.

[49] Hubbell, J.A., "Biomaterials in tissue engineering," *Biotechnology (N Y),* vol. 13, pp. 565-567, 1995.

[50] Gilbert, T.W., Sellaro, T.L. and Badylak, S.F., "Decellularization of tissues and organs," *Biomaterials.,* vol. 19, 27. 2006.

[51] Badylak, S.F., "Xenogeneic extracellular matrix as a scaffold for tissue reconstruction," *Transpl Immunol.,* vol. 12, pp. 367-377, 2004.

[52] Orive, G., Hernández, R.M., Rodríguez Gascón, A., Calafiore, R., Chang, T.M., de Vos, P., Hortelano, G., Hunkeler, D., Lacík, I. and Pedraz, J.L., "History, challenges and perspectives of cell microencapsulation.," *Trends Biotechnol. Feb;22(2):87-92,* vol. 2, 22. 2004.

[53] Orive, G., Hernández, R.M., Gascón, A.R., Calafiore, R., Chang, T.M., De Vos, P., Hortelano, G., Hunkeler, D., Lacík, I., Shapiro, A.M. and Pedraz, J.L., "Cell encapsulation: promise and progress," *Nat Med. ,* vol. 9, pp. 104-107, 2003.

[54] Chevalier, E., Chulia, D., Pouget, C. and Viana, M., "Fabrication of porous substrates: a review of processes using pore forming agents in the biomaterial field," *J Pharm Sci.,* vol. 97, pp. 1135-1154, 2008.

[55] Yang, S., Leong, K.F., Du, Z. and Chua, C.K., "The design of scaffolds for use in tissue engineering. Part II. Rapid prototyping techniques", *Tissue Eng.,* vol. 8, pp. 1-11, 2002.

[56] Lee, K.Y. and Yuk, S.H.,"Polymeric protein delivery systems," *Prog Polym Sci.,* pp. 669–697, 2007.

[57] Hans, M.L. and Lowman, A.M., "Biodegradable nanoparticles for drug delivery and targeting," *Current Opinion in Solid State and Materials Science,* pp. 319–327, 2002.

[58] Rezwan, K., Chen, Q.Z., Blaker, J.J. and Boccaccini, A.R., "Biodegradable and bioactive porous polymer/inorganic composite scaffolds for bone tissue engineering", *Biomaterials 27(18),* pp. 3413-3431, 2006.

[59] Cheung, H.-Y., Lau, K.-T., Lu, T.-P. and Hui, D. "A critical review on polymer-based bio-engineered materials for scaffold development," *Composites: Part B,* vol. 38, pp. 291-300, 2007.

[60] Jayakumar, R., Divya Rani, V.V., Shalumon, K.T., Sudheesh Kumar, P.T., Nair, S.V., Furuike, T. and Tamura, H., "Bioactive and osteoblast cell attachment studies of novel chitin membranes for tissue- engineering applications," *International Journal of Biological Macromolecules,* pp. 206-209, 2009.

[61] Madhumathi, K., Binulal, N.S., Nagahama, H., Tamura, H., Shalumon, K.T., Selvamurugan, N., Nair, S.V. and Jayakumar, R., "Preparation and characterization of novel ˇ-chitin–hydroxyapatite composite membranes for tissue engineering applications," *International Journal of Biological Macromolecules,* vol. 44, pp. 1-9, 2009.

[62] Madhumathi, K., Shalumon, K.T., Divya Rani, V.V., Tamura, H., Furuike, T., Selvamurugan, N., Nair , S.V. and Jayakumar, R., "Wet chemical synthesis of chitosan hydrogel–hydroxyapatite composite membranes for tissue engineering applications," *International Journal of Biological Macromolecules,* pp. 12-15, 2009.

[63] Miller, F.P., Vandome, A.F. and McBrewster., J., *Collagen,* Alphascript Publishing, 2010, pp. 68.

[64] Al-Munajjed, A.A., Plunkett, N.A., Gleeson, J.P., Weber, T., Jungreuthmayer, C., Levingstone, T., Hammer and J., O'Brien, F.J., "Development of a biomimetic collagenhydroxyapatite scaffold for bone tissue engineering," *Journal of Biomedical Material Research B :Applied Biomaterials,* pp. 584-591, 2009.

[65] Wolfe, P.S., Sell, S.A. and Bowlin, G.L.,"Natural and synthetic scaffolds," in *Tissue Engineering: From Lab to Clinic* Pallua, N. and Suschek, C.V., Ed. Springer, 2011,

[66] Di Martino, A., Sittinger, M. and Risbud, M. V., "Chitosan: A versatile biopolymer for orthopaedic tissue-engineering," *Biomaterials,* pp. 5983–5990, 2005.

[67] Venkatesan, J. and Se-Kwon, K. "Chitosan Composites for Bone Tissue Engineering—An overview," *Mar. Drugs,* pp. 2252-2266, 2010.

[68] Vepari, C. and. Kaplan, D.L., "Silk as a biomaterial," *Progress in Polymer Science,* pp. 991-1007, 2007.

[69] Zhang, X., Reagan, MR. and Kaplan. D.L., "Electrospun silk biomaterial scaffolds for regenerative medicine". *Adv. Drug Deliv. Rev. 61(12),* pp. 988-1006, 2009 .

[70] Li, C., Vepari, C., Jin, H.-J., Kim, J.H. and Kapla, D.L., "Electrospun silk-BMP-2 scaffolds for bone tissue engineering", *Biomaterials 27(16),* pp. 3115-3124, 2006.

[71] Wang, X., Kim, H.K., Xu, P., Matsumoto, A. and Kaplan, D.L, "Biomaterial coatings by stepwise deposition of silk fibroin," *Langmuir,* pp. 11335-11341, 2005.

[72] Minoura, N., Aiba, S., Gotoh, Y., Tsukada, M. and Imai, Y., "Attachment and growth of cultures fibroblast cells on silk protein matrices," *J. Biomed Mater Res,* pp. 1215-1221, 1995.

[73] Law, K.-L., Leung, Y-.K., Lawford, H., Chua, H., Lo, W.-H. and Yu, P.H., "Production of polyhydroxybutyrate by Bacillus species isolated from municipal activated sludge," *Applied Biochemistry and Biotechnology,* pp. 515-524, 2001.

[74] Chen, G. "Industrial Production of PHA," *Plastics from Bacteria,* pp. 121-132, 2010.

[75] Köse, G.T., Korkusuz, F., Korkusuz, P., Purali, N., Ozkul, A. and Hasirci, V., "Bone generation on PHB/PHV matrices: an *in vitro* study," *Biomaterials,* pp. 4999-5007, 2003.

[76] Knowles, J.C., Hastings, G.W., Ohta, H., Niwa, S. and Boeree, N., "Development of a degradable composite for orthopaedic use: *in vivo* biomechanical and histological evaluation of two bioactive degradable composites based on the polyhydroxybutyrate polymer," *Biomaterials,* pp. 491–496, 1992.

[77] Köse, G.T., Ber, S., Korkusuk, F. and Hasirci, V., "Poly(3-hydroxybutyric acid-co-3-hydroxyvaleric acid) based tissue engineering matrices," *J Mater Sci-Mater M,* pp. 121-126, 2003.

[78] Köse, G.T., Korkusuz, F., Korkusuz, P. and Hasirci, V."*In vivo* tissue engineering of bone using poly(3-hydroxybutyric acid-co-3-hydroxyvaleric acid) and collagen scaffolds," *Tissue Engineering,* pp. 1234–1250, 2004.

[79] Zheng, Y.D., Wang, Y.J., Chen, X.F., Ren, Y.B. and Wu, G.,"Chemical reaction of PHB/PHV/sol–gel bioglass foams for born tissue engineering in simulated body fluid," *Chem J Chin U,* pp. 1325–1328, 2003.

[80] Luklinska, Z. B. and Schluckwerder, H., "*In vivo* response to HA-polyhydroxybutyrate/polyhydroxyvalerate composite," *J Microsc-Oxford,* pp. 121-129, 2003.

[81] Chen, G. and Wu, Q. , " The application of polyhydroxyalkanoates as tissue engineering materials". *Biomaterials 26(33),* pp. 6565-6578, 2005.

[82] Matsumoto, K., Murata, T., Nagao, R., Nomura, C.T., Arai, S., Arai, Y., Takase, K., Nakashita, H., Taguchi, S. and Shimada, H., "Production of Short-Chain-Length/Medium-Chain-Length Polyhydroxyalkanoate (PHA) Copolymer in the Plastid of*Arabidopsis thaliana*Using an Engineered 3-Ketoacyl-acyl Carrier Protein Synthase II," *Biomacromolecules,* vol. 10, pp. 686-690, 2009.

[83] Zinn, M., Witholt, B. and Egli, T., "Occurrence, Synthesis and Medical Application of Bacterial Polyhydroxyalkanoate," *Advanced Drug Delivery Reviews,* pp. 5-21, 2001.

[84] Holmes, P. A.,"Applications of Phb - a Microbially Produced Biodegradable Thermoplastic," *Physics in Technology,* vol. 16, pp. 32-36, 1985.

[85] Otari, S. V. and Ghosh, J. S., "Production and Characterisation of the Polymer Polyhydroxy Butyrate-Co-Polyhydroxy Valerate by Bacillus Megaterium NCIM2475," *Current Research Journal of Biological Science,* vol. 1, pp. 23-26, 2009.

[86] Nair, L.S. and Laurencin, C.T., "Biodegradable Polymers as Biomaterials," *Progress in Polymer Science,* vol. 32, pp. 762-798, 2007.

[87] Sabir, M. I., Xu, X. and Li, L., "A Review on Biodegradable Polymeric Materials for Bone Tissue Engineering Applications," *Journal of Materials Science,* vol. 44, pp. 5713-5724, 2009.

[88] Iwata, T., Doi, Y. and Tanaka, T., "Enzymatic Degradation and Adsorption on Poly[(R)-3-Hydroxybutyrate] Single Crystals with Two Types of Extracellular PHB Depolymerases from Comamonas Acidovorans YM1609 and Alcaligenes Faecalis T1," *Macromolecules,* pp. 5290-5296, 1997.

[89] Lin, S., LeGeros, R.Z. and LeGeros, J.P.,"Adherent octacalciumphosphate coating on titanium alloy using modulated electrochemical deposition method," *Journal of Biomedical Materials Research Part A,* pp. 819-823, 2003.

[90] Schieker, M., Seitz, H., Drosse, I., Seitz, S. and Mutschler, W., "Biomaterials as scaffold for bone tissue engineering," *European Journal of Trauma,* pp. 114-124, 2006.

[91] Salgado, A.J., Coutinho, O. P. and Reis, R.L.,"Bone Tissue Engineering: State of the Art and Future Trends," *Macromol. Biosci.,* pp. 743-765, 2004.

[92] Liebschner, M. A. K. and Wettergreen, M. A., "Optimization of bone scaffold engineering for load bearing applications," in *Topics in Tissue Engineering ,* vol. 1, N. Ashammakhi and P. Ferretti, Ed. Oulu: 2003,

[93] Baksh, D., Davies, J. E. and Kim, S., "Three dimensional matrices of calcium polyphosphates support," *J Mater Sci: Mater Med,* pp. 743–748, 1998.

[94] Vacanti, C. A., Bonassar, L. J., Vacanti, M.P. and Shufflebarger, J., "Replacement of an Avulsed Phalanx with Tissue-Engineered Bone," *N Engl J Med,* pp. 1511-1514, 2001.

[95] Quarto, R., Mastrogiacomo, M. and Cancedda, R., "Repair of Large Bone Defects with the Use of Autologous Bone Marrow Stromal Cells," *N Engl J Med,* pp. 385-386, 2001.

[96] Petite, H., Viateau, V., Bensaïd, W., Meunier, A., de Pollak, C., Bourguignon, M., Oudina, K., Sedel, L. and Guillemin, G., "Tissue-engineered bone regeneration," *Nature Biotechnology,* pp. 959-963, 2000.

[97] Adams, C. S., Mansfield, K., Perlot, R. L. and Shapiro, I. M., "Matrix Regulation of Skeletal Cell Apoptosis: Role of Calcium and Phosphate Ions," *The Journal of Biological Chemistry,* pp. 20316-20322, 2001.

[98] Sá, M.J., Rezende, C.M., Silva Junior, V.A., Garcia, H.C., Griffon, D.J.and Silva,V.V., "*In vivo* behavior of zirconia hydroxyapatite (ZH) ceramic implants in dogs: a clinical, radiographic, and histological study," *J Biomater Appl.,* vol. 22, pp. 5-31, 2007.

[99] Burg Karen, J.L., Porter, S. and Kellam, J.F.,"Biomaterial Developments for Bone Tissue Engineering," *Biomaterials,* pp. 2347-2359, 2000.

[100] Tiedeman, J.J., Garvin, K. L., Kile, T. A. and Conolly, J. F. , "The Role Of A Composite, Demineralised Bone Matrix And Bone Marrow In The Treatment of Osseus Defects," *Orthopaedics,* pp. 1153-1158, 1995.

[101] Enneking, W. F., Eady, J. L. and Burchardt, H., "Autogenous Cortical Bone Grafts In The Reconstuction Of Segmental Skeletal Defects," *J Bone Jt Surg Am,* pp. 1039-1058, 1980.

[102] Sachlos, E. and Czernuszka, J. T., "Making Tissue Engineering Scaffolds Work. Review on the Application of Solid Freeform Fabrication Technology to the Production of Tissue Engineering Scaffolds," *Eur Cell Mater,* pp. 29-39, 2003.

[103] Swethaa,M., Sahithia, K., Moorthi, A., Srinivasan, N., Ramasamy, K. and Selvamurugan, N., "Biocomposites containing natural polymers and hydroxyapatite for bone tissue engineering," *International Journal of Biological Macromolecules,* pp. 1-4, 2010.

[104] Maeda, H., Kabanov, A., Kataoka, K. and Okano., T.,*Polymer Drugs in the Clinical Stage: Advantages and Prospects,* , vol. 519, Springer, 2003,

[105] Guo-Qiang Chen, Q. W.,"The Application of polyhydroxyalkanoates as tissue engineering materials," *Biomaterials,* pp. 6565–6578, 2005.

[106] Silvio, L.D., Dalby, M. and Bonfield, W. "*In vitro* response of osteoblasts to hydroxyapatite/reinforced polyethylene composites," *J Mater Sci Mater Med,* pp. 845–848, 1998.

[107] Wang, Y.W., Wu, Q. and Chen, G.Q, "Reduced mouse fibroblast cell growth by increased hydrophilicity of microbial polyhydroxyalkanoates via hyaluronan coating," *Biomaterials,* pp. 4621–4629, 2003.

[108] Hu, S.G., Jou, C.H. and Yang, M.C., "Biocompatibility and antibacterial activity of chitosan and collagen immobilized poly(3-hydroxybutyric acid-co-3-hydroxyvaleric acid)," *Carbohyd Polym,* pp. 173-179, 2004.

[109] Huang, Z.-M., Zhang, Y.-Z., Kotaki, M. and S. Ramakrishna, "A review on polymer nanofibers by electrospinning and their applications in nanocomposites," *Composites Science and Technology,* pp. 2223-2253, 2003.

[110] Bhardwaj, N., Kundu, S. C., "Electrospinning: a fascinating fiber forming technology," *Biotechnology Advances 28,* pp. 325–347, 2010.

[111] Tan, S-H., Inai, R., Kotaki, M. and Ramakrishna, S. "Systematic parameter study for ultra-fine fiber fabrication via electrospinning process," *Polymer,* pp. 6128-6134, 2005.

[112] Vince Beachley, X. W., "Effect of electrospinningparameters on the nanofiber diameter and length," *Materials Science and Engineering: C,* pp. 663–668, 2009.

[113] Merzak, A., Koochekpour, S. and Pilkington, G.J."Adhesion of Human Glioma Cell Lines to Fibronectin, Laminin, Vitronectin and Collagen I Is Modulated by Gangliosides *in vitro*," *Cell Adhesion and Communication,* pp. 27-43, 1995.

[114] Angelova, D. H. N., "Rationalizing the design of polymeric biomaterials," *Trends in Biotechnology,* pp. 409–421, 1999.

[115] O'Brien, F.J., Harley, B.A., Yannas, I.V. and Gibson, L.J., "The effect of poresize on cell adhesion in collagen-GAG scaffolds," *Biomaterials,* pp. 433–441, 2005.

[116] Boyan, B.D. and Hummert, T.W, "Role of Material Surfaces in Regulating Bone and Cartilage Cell Response," *Biomaterials,* vol. 17, pp. 137-146, 1996.

[117] Robinson, B., Hollinger, J.O., Szachowicz, E., and Brekke, J, "Calvarial Bone Repair with Porous dl-polylactide," *Otolaryng Head Neck,* vol. 112, pp. 707-713, 1995.

[118] Yannas, I.V., Lee, E., and Orgill, D.P, "Synthesis and Characterization of a Model Extracellular Matrix that Induces Partial Regeneration of Adult Mammalian Skin," *Proc Natl Acad Science,* vol. 86, pp. 933, 1989.

[119] Kim, S.S. and Utsunomiya, H., "Survival and Function of Hepatocytes on a Novel Three-dimensional Synthetic Biodegradable Polymer Scaffold with an Intrinsic Network of Channels," *Ann Surgery,* vol. 228, pp. 8-13, 1998.

[120] Nela Angelova, D. H., "Rationalizing the design of polymeric biomaterials," *Trends in Biotechnology,* pp. 409-421, 1999.

[121] Rubin, C.T. and Laynon, L. E., "Regulation of bone mass by mechanical strain magnitude," *Calcified Tissue International,* pp. 411-417, 1985.

[122] Carter, D. R., "Mechanical loading histories and cortical bone remodelling," *Calcified Tissue International,* pp. S19-S24, 1984.

[123] Hong,Y., Fan, H., Li, B., Guo,B., Liu, M. and Zhang, X. "Fabrication, biological effects, and medical applications of calcium phosphate nanoceramics," *Materials Science and Engineering: R: Reports,* pp. 225-242, 2010.

[124] Prabhakaran M.P, Venugopal J. and Ramakrishna S, "Electrospun nanostructured scaffolds for bone tissue engineering," *Acta Biomaterialia,* pp. 2884–2893, 2009.

[125] Wang, L. and Li, C., "Preparation and physicochemical properties of a novel hydroxyapatite/chitosan–silk fibroin composite," *Carbohydrate Polymers,* pp. 740-745, 2007.

[126] Franco, P.Q., João, C.F.C., Silva, J.C. and Borges, J.P., "Electrospun hydroxyapatite fibers from a simple sol–gel system," *Materials Letters,* pp. 233-236, 2012.

[127] Parsons, A.J., Ahmed, I., Han, N., Felfel, R., and Rudd, C.D., "Mimicking Bone Structure and Function with Structural Composite Materials," *Journal of Bionic Engineering,* pp. S1-S10, 2010.

[128] Li, W.J., Laurencin, C.T., Caterson, E.J., Tuan, R.S. and Ko, F.K., "Electrospun nanofibrous structure: a novel scaffold for tissue engineering," *J Biomed Mater Res.,* pp. 613-621, 2002.

[129] Chapekar, M. S., "Tissue Engineering: Challenges and Opportunities," *J Biomed Mater Res,* pp. 617-620, 2000.

[130] Romeo, V., Preparation and Characterization of Polymer Nanocomposites with New Techniques [Online]. http://www.unisa.it/uploads/1270/30._tesi_valentina_romeo.pdf [accessed: 2012,05/09]

[131] Baji, A., Wong, S.-C., Liu, T., Li, T. and Srivatsan, T. S, " Morphological and X-ray diffraction studies of crystalline hydroxyapatite-reinforced polycaprolactone". *J. Biomed. Mater. Res. B. Appl. Biomater. 81(2),* pp. 343-350 , 2007.

[132] Alsberg, E., Kong, H.J., Hirano, Y., Smith, M.K., Albeiruti, A. and Mooney, D.J., "Regulating bone formation via controlled scaffold degradation". *J. Dent. Res. 82(11),* pp. 903-908, 2003.

[133] Yua, S., Prakash Hariramb, K., Kumara, R., Cheanga, P. and Khiam Aik, K., "*In vitro* apatite formation and its growth kinetics on hydroxyapatite/polyetheretherketone biocomposites". *Biomaterials 26(15),* pp. 2343-2352, 2005.

[134] Qu, S., Fan, H., Chen, J., Feng, J., Fu, R., Wei, D. and Zhang, X.,"Effect of the crystallinity of calcium phosphate ceramics on osteoblast proliferation *in vitro*," *Journal of Materials Science Letters,* vol. 20, pp. 331-332, 2001.

[135] Woodruff, M. A. and Hutmacher, D. W., " The return of a forgotten polymer—Polycaprolactone in the 21st century", *Progress in Polymer Science 35(10),* pp. 1217-1256, 2010.

[136] Zhang, Y. and Tanner, K. E., "Effect of filler surface morphology on the impact behaviour of hydroxyapatite reinforced high density polyethylene composites" *J. Mater. Sci. Mater. Med. 19(2),* pp. 761-766, 2008.

[137] Soliman, S., Sant, S., Nichol, J.W., Khabiry, M., Traversa. E. and Khademhosseini, A., " Controlling the porosity of fibrous scaffolds by modulating the fiber diameter and packing density", *J. Biomed. Mater. Res. A. 96(3),* pp. 566-574, 2011.

[138] Sowmya, S., Sudheesh Kumar, P.T., Chennazhi, K.P., Nair, S.V., Tamura, H. and Jayakumar, R., "Biocompatible -chitin Hydrogel/Nanobioactive Glass Ceramic Nanocomposite Scaffolds for Periodontal Bone Regeneration," *Trends Biomater. Artif. Organs,* vol. 25, pp. 1-11, 2011.

[139] Xu, C. C. and Chan. R. W., "Pore architecture of a bovine acellular vocal fold scaffold", *Tissue Eng. Part A. 14(11),* pp. 1893-1903, 2008.

[140] Lam, C.X.F., Savalani, M.M., Teoh, S.-H. and Hutmacher, D.W., " Dynamics of *in vitro* polymer degradation of polycaprolactone-based scaffolds: Accelerated

versus simulated physiological conditions". *Biomed. Mater. 3(3),* pp. 034108-6041/3/3/034108. Epub 2008 Aug 8, 2008.

[141] Therin, M., Christel, P., Li, S., Garreau, H. and Vert, M., "*In vivo* degradation of massive poly(alpha-hydroxy acids): validation of *in vitro* findings," *Biomaterials,* vol. 13, pp. 594-600, 1992.

[142] Chen, Z., Mo, X. and Qing, F., " Electrospinning of collagen–chitosan complex", *Mater Lett 61(16),* pp. 3490-3494, 2007.

[143] Goldstein, P. J., "Electrospinning of ceramic and nanocomposite nanofibers," *UNIVERSITY OF FLORIDA,* 2004.

[144] NIST/SEMATECH. Engineering Statistics Handbook [Online]. http://www.itl.nist.gov/div898/handbook/ [accessed: 2012, 10/23]

[145] Kuhn, H. and Medlin, D., *Mechanical Testing and Evaluation,* , vol. 8, ASM International, 2000, pp. 998.

[146] Pierlot, C., Pawlowski, L., Bigan, M. and Chagnon, P., " Design of experiments in thermal spraying: A review", *Surface and Coatings Technology 202(18),* pp. 4483-4490, 2008.

[147] Box, G. E. P. and Behnken, D. W., "Some New Three Level Designs for the Study of Quantitative Variables," *Technometrics,* vol. 2, pp. 455-475, 1960.

[148] Hutmacher, D., Woodfield, T., Dalton, P. and Lewis, J,"Chapter 14 - scaffold design and fabrication," in *Tissue Enginnering,* ed. van Blitterswijk, C., Thomsen P., Lindahl,A., Hubbell, J., Williams, D.F, Cancedda, R., de Bruijn , J.D. and Sohier, J., Ed. Elsevier, 2008, pp. 403-454.

[149] Chaikof, E.L., Matthew, H., Kohn, J., Mikos, A.G., Prestwich, G.D. andYip, C.M. "Biomaterials and scaffolds in reparative medicine," *Ann NY Acad Sci,* vol. 961, pp. 96-105, 2002.

[150] Griffith, L.G., "Emerging design principles in biomaterials and scaffolds for tissue engineering," *Ann NY Acad Sci,* vol. 961, pp. 83-95, 2000.

[151] Levenberg, R. L. S. *Advances in Tissue Engineering Current Topics in Developmental Biology* ,vol. 61 ed.New York: Academic Press, New York, pp. 113-134.

[152] Antoniou, G., Mikos, A.G. and Temenoff, J.S., "Formation of highly porous biodegradable scaffolds for tissue engineering," *Electron J Biotechnol,* vol. 3, 2000.

[153] Pérez, R.A., Won, J.E., Knowles, J.C. and Kim, H.W., "Naturally and synthetic smart composite biomaterials for tissue regeneration", *Adv. Drug Deliv. Rev. i*n proof, corrected version, 2012

[154] Badylak, S., Gilbert, T., Myers-Irvin, J., "Chapter 5 - the extracellular matrix as a biologic scaffold for tissue engineering," in *Tissue Engineering* , 2008 ed.Clemens van Blitterswijk, Peter Thomsen, Anders Lindahl, Jeffrey Hubbell, David F. Williams, Ranieri Cancedda, Joost D. de Bruijn and Jérôme Sohier, Ed. Elsevier, 2008, pp. 212-143.

[155] Wang, M, "Bioactive ceramic-polymer composites for bone replacement." in *13th International Conference on Composite Materials (ICCM-13),* 2001.

[156] Chen, L. J. and Wang, M., "Production and evaluation of biodegradable composites based on PHB–PHV copolymer", *Biomaterials 23(13),* pp. 2631-2639, 2002.

[157] Basset, DC., *Developments in Crystalline Polymers,* ,2nd ed.London: Elsevier, 1987,

[158] Luzier, W.D., "Materials derived from biomass/biodegradable materials," *Proc Natl Acad Sci USA,* vol. 89, pp. 889-342, 1992.

[159] Gogolewski, S., Jovanovic, M., Perren, S.M., Dillon, J.G. and Hughes, M.K. "Tissue response and *in vivo* degradation of selected polyhydroxyacidspolylactides (PLA), poly(3-hydroxybutyrate) (PHB), and poly(3-hydroxybutyrate-co-3-hydroxyvalerate) (PHB/VA)," *J Biomed Mater Res,* vol. 27, pp. 1135-1148, 1993.

[160] Avella, M., Martuscelli, E. and Raimo, M., "Properties of blends and composites based on poly(3-hydroxybutyrate) (PHB) and poly(3-hydroxybutyrate-hydroxyvalerate) (PHB/PHV) copolymers," *J Mater Sci,* vol. 35, pp. 523-545, 2000.

[161] Chen, G, "Plastics completely synthesized by bacteria: Polyhydroxyalkanoates," in *Plastics from Bacteria: Natural Functions and Applications* G. Chen, Ed. Berlin: Springer, 2010, pp. 17-37.

[162] Reusch, R.N., "Low molecular weight complexed poly(3-hydroxybutyrate): a dynamic and versatile molecule *in vivo*," *Can J Microbiol, 41,* vol. Suppl. 1, pp. 50-54, 1995.

[163] Doyle, C., Tanner, E.T. and Bonfield, W., "*In vitro* and *in vivo* evaluation of polyhydroxybutyrate and of polyhydroxybutyrate reinforced with hydroxyapatite," *Biomaterials,* vol. 12, pp. 841-847, 1991.

[164] Lai, M.. Li, J.,Yang, J., Liu,J., Tong, X. and Cheng,H., "The morphology and thermal properties of multi-walled carbon nanotube and poly(hydroxybutyrate-co-hydroxyvalerate) composite," *Polymer International,* vol. 53, pp. 1479-1484, 2004.

[165] Fei, B. *et al.* , "Quantitative FTIR study of PHB/PHV/bisphenol A blends", *European Polymer Journal 39(10),* pp. 1939-1946, 2003.

[166] Knowles, J.C., "A review article: phosphate glasses for biomedical applications," *J Mater Chem,* vol. 13, pp. 2395-2401, 2003.

[167] Hench, L.L., "Bioceramics," *J Am Ceram Soc,* vol. 81, pp. 1705-1728, 1998.

[168] Hench, L.L., "Bioceramics: from concept to clinic," *J Am Ceram Soc,* vol. 74, pp. 1487-1510, 1991.

[169] Eslami, H., Solati-Hashjin, M. andTahriri, M.,"Synthesis and Characterization of Hydroxyapatite Nanocrystals via Chemical Precipitation Technique," *Iranian Journal of Pharmaceutical Sciences, SPring,* vol. 4, pp. 127-134, 2008.

[170] Komath, M. and Varma, H.K., "Development of a fully injectable calcium phosphate cement for orthopedic and dental applications " *Bull Mater Sci,* vol. 4, pp. 415-422, 2003.

[171] Huzhou Aotesi Biochemical. [Online]. http://www.silk-protein.com/silk-fibroin.html [accessed: 03/23]

[172] Kesenci, K., Motta, A., Fambri, L. and Migliaresi, C., "Poly(ε-caprolactone-co-D,Llactide)/ silk fibroin composite materials: Preparation and characterization," *Journal of Biomaterials Science, Polymer Edition,* vol. 12, pp. 337-351, 2001.

[173] Wang, J., Yu, F., Qu, L., Meng, X. and Wen, G."Study of synthesis of nano-hydroxyapatite using a silk fibroin template," *Biomedical Materials,* pp. 1-5, 2010.

[174] Sombatmankhong, K., Sanchavanakit, N., Pavasant,P., Supaphol, P.Bone scaffolds from electrospun fibre mats of poly(3-hydroxybutyrate), poly(3-hydroxybutyrate-co-3-hydroxyvalerate) and their blend, , *Polymer,* vol. 48, pp. 1419-1427, 2007.

[175] Gomes, M., Azevedo, H., Malafaya, P., Silva, S., Oliveira, J., Silva, G., Sousa, R., Mano, J. and Reis, R."Chapter 6 - natural polymers in tissue engineering applications," in *Tissue Engineering* ,First ed.Clemens A. Van Blitterswijk, Peter Thomsen, Ed. Elsevier, 2008, pp. 145-192.

[176] Wang, M., "Composite Scaffolds for Bone Tissue Engineering," *American Journal of Biochemistry and Biotechnology,* vol. 2, pp. 80-84, 2006.

[177] Ying, T. H., *et al.* Scaffolds from electrospun polyhydroxyalkanoate copolymers: Fabrication, characterization, bioabsorption and tissue response. *Biomaterials 29(10),* pp. 1307-1317, 2008

[178] Liu, X. and Ma, P.X. "Polymeric Scaffolds for Bone Tissue Engineering," *Annals of Biomedical Engineering, 2004, Volume 32, Number 3, Pages 477-486,* vol. 32, pp. 477-486, 2004.

[179] Lakes, R.S. "Composite biomaterials," in *Biomaterials* Joyce Y.Wong, Joseph D. Bronzino, Ed. Taylor and Francis Group, 2007, pp. 4-1.

[180] Sultana, N., "Production and characterization of tissue engineering scaffolds based on polyhydroxybutyrateco- hydroxyvalerate polymers," in *2012 International Conference on Biomedical Engineering (ICoBE),* 2012,

[181] Shan, C., Qiong, W., Yan, Z., Bing, Z., Guo-Qiang, C., "Effect of poly(hydroxybutyrate-co-hydroxyhexanoate) microparticles on growth of murine fibroblasts L929," *Polymer Degradation and Stability,* pp. 3191-3196, 2006.

[182] Wang, H. *et al.*, " Biocompatibility and osteogenesis of biomimetic nano-hydroxyapatite/polyamide composite scaffolds for bone tissue engineering". *Biomaterials 28(22),* pp. 3338-3348, 2007.

[183] Lao L., Wang Y., Zhu Y.,Zhang Y., Gao C., "Poly(lactide-co-glycolide)/hydroxyapatite nanofibrous scaffolds fabricated by electrospinning for bone tissue engineering," *J Mater Sci: Mater Med,* vol. 22, pp. 1873-1884, 2011.

[184] Venugopal J, Prabhakaran MP, Zhang Y, Low S, Choon AT, Ramakrishna S, "Biomimetic hydroxyapatite-containing composite nanofibrous substrates for bone tissue engineering," *Philisophical Transactions of the Royal Society A,* pp. 2065-2081, 2010.

[185] Galego, N, Rozsa, C, Sanchez, R, Fung, J, Vazquez, A. and Tomas, JS., "Characterization and application of poly(b-hydroxyalkanoates) family as composite biomaterials**,**" *Polym Test,* vol. 19, pp. 485-492, 2000.

[186] Altman, G.H., Diaz, F., Jakuba, C., Calabro, T., Horan, R.L., Chen, J., Lu, H. Richmond, J. andKaplan, D.L., "Silk-based biomaterials," *Biomaterials,* vol. 24, pp. 401-416, 2003.

[187] Meinel, L., Hofmann, S., Karageorgiou, V., Kirker-Head, C., McCool, J. Gronowicz, G., Zichner, L., Langer, R., Vunjak-Novakovic, G. and David L. Kaplan, "The inflammatory responses to silk films *in vitro* and *in vivo*," *Biomaterials,* vol. 26, pp. 147-155, 2005.

[188] Dyakonov, T., Yang, C.H., Bush, D., Gosangari, S., Majuru, S. and Fatmi, A, "Design and Characterization of a Silk-Fibroin-Based Drug Delivery Platform Using Naproxen as a Model Drug," *Journal of Drug Delivery,* 2012.

[189] Wang L., Nemoto R., Senna M., "Changes in microstructure and physico-chemical properties of hydroxyapatite–silk fibroin nanocomposite with varying silk fibroin content," *Journal of the European Ceramic Society,* pp. 2707-2715, 2004.

[190] Freddi, G., Monti, P., Nagura, M., Gotoh, Y., Tsukada, M., "Structure and molecular conformation of tussah silk fibroin films: effect of heat

treatment," *Journal of Polymer Science Part B: Polymer Physics,* pp. 841-847, 1997.

[191] Mikos, A. G. and Temenoff, J S, "Formation of Highly Porous Biodegradable Scaffolds for Tissue Engineering, Electronic Journal of Biotechnology," *Electronic Journal of Biotechnology,* pp. 114-119, 2000.

[192] Tanahashi, M. T., "Surface functional group dependence on apatite formation on self- assembled monolayers in a simulated body fluid," *Journal of Biomedical Materials Research,* pp. 305-315, 1997.

[193] Akari, T., Chikara, O., Toshiki, M., Hiromi, T., Masao, Y. and Masao, T. "Deposition of bone-like apatite on silk fiber in a solution that mimics extracellular fluid," *Journal of Biomedical Materials Research, Part A,* pp. 283-286, 2006.

[194] Coulson, I.M., Beech, M. and Nie, W., "Physical properties of Martian meteorites: Porosity and density measurements," *Meteoritics & Planetary Science,* pp. 1, 2007.

[195] Graham, J., Ries, M. and Pruitt, L., "Effect of bone porosity on the mechanical integrity of the bone-cement interface," *J Bone Joint Surg Am.,* vol. 85, pp. 1901-1908, 2003.

[196] Voger, E.A."Short-term cell-attachment rates: a surface-sensitive test of cell-substrate compatibility"; 1197-211," *J Biomed Mater Res,* pp. 1197-1211, 1987.

[197] Kumarasuriyar, A., *et al.* "Osteoblasts up-regulate the expression of extracellular proteases following attachment to poly(β-hydroxybutyrate-co-β-hydroxyvalerate). *Gene 428(1–2),* pp. 53-58, 2009.

[198] Köse, G. T., *et al.*, Bone generation on PHB/PHV matrices: An *in vitro* study. *Biomaterials 24(27),* pp. 4999-5007, 2003.

[199] Gshalaev, V.S, Demirchan, A.C., " *Hydroxyapatite: Synthesis, Properties and Applications".* Nova Science Publishers, 2012,

[200] Hench, L.L., *An Introduction to Bioceramics. Volume 1 of Advanced Series in CeramicsCeramics Advanced Series.* , vol. 1, London and Singapore: World Scientific Publisher, 1993, pp. 386.

[201] Oyane, A., Kim, H.-M., Furuya, T., Kokubo, T., Miyazaki, T., Nakamura, T., "Preparation and assessment of revised simulated body fluids," *Journal of Biomedical Materials Research Part A,* pp. 188-195, 2003.

[202] Bayari, S., Severcan, F., Gursel, I., Hasirci, V., Alaeddinoglu, G., "The FTIR studies of the poly(3-hydroxybutyrate) and poly(3-hydroxybutyrate-co-3-hydroxyvalerate)," *Biomed Health Res,* pp. 58-64, 1998.

[203] Zhang, R. and Ma, P.X.,"Biomimetic polymer/apatite composite scaffolds for mineralized tissue engineering," *Macromol Biosci,* pp. 100-111, 2004.

[204] Kawashita, M., Nakao, M., Minoda, M., Kim, H.M., Beppu, T.,. Miyamoto, T., "Apatite-forming ability of carboxyl group-containing polymer gels in a simulated body fluid," *Biomaterials,* pp. 2477-2484, 2003.

[205] Petersen, M.C., Lazar, J., Jacob, H.J., Wakatsuki, T., "Tissue engineering: a new frontier in physiological genomics," *Physiol Genomics,* pp. 28-32, 2007.

[206] Huang, Z. *et al.*, "A review on polymer nanofibers by electrospinning and their applications in nanocomposites", *Composites Sci. Technol. 63(15),* pp. 2223-2253, 2003.

[207] Lee, S.J., Yoo, J.J., Lim, G.J., Atala, A., Stitzel, J., *"In vitro* evaluation of electrospun nanofiber scaffolds for vascular graft application," *J Biomed Mater Res A. 2007 Dec 15;83(4):999-1008.,* vol. 83, pp. 999-1008, 2007.

[208] Smit, E., Bűttner, U., and Sanderson, R. D., "Continuous yarns from electrospun fibers" *Polymer 46(8),* pp. 2419-2423, 2005

[209] Wright, L D, Young, R T., Andric, T., Freeman, JW.,"Fabrication and mechanical characterization of 3D electrospun scaffolds for tissue engineering," *Biomed. Mater.,* pp. 055006 (9pp), 2010.

[210] Tzezana, R, Zussman, E, Levenberg, S., "A Layered Ultra-Porous Scaffold for Tissue Engineering, Created via a Hydrospinning Method," *Tissue Eng Part C Methods.,* vol. 14, pp. 281-288, 2008.

[211] Singh, S. *et al.*, "Renewable resource based biocomposites from natural fiber and polyhydroxybutyrate-co-valerate (PHB/PHV) bioplastic", *Composites Part A: Applied Science and Manufacturing 39(5),* pp. 875-886, 2008

[212] Kurkijarvi, J. E., Nissi, M.J., Kiviranta, I., Jurvelin, J. S,, Nieminen, M, T,, "Delayed gadolinium-enhanced MRI of cartilage (dGEMRIC) and T-2 characteristics of human knee articular cartilage: topographical variation and relationships to mechanical properties," *Magn. Reson. Med,* pp. 41-46, 2004.

[213] Meechaisue, C., Wutticharoenmongkol, P., Waraput, R., Huangjing, T., Ketbumrung, N., Pavasant, P., Supaphol, P., "Preparation of electrospun silk fibroin fiber mats as bone scaffolds: a preliminary study," *Biomed Mater.,* vol. 2, pp. 181-188, 2007.

[214] Hardy, J. G. and Scheibel, T. R., "Composite materials based on silk proteins", *Progress in Polymer Science 35(9),* pp. 1093-1115, 2010.

[215] Mobini, S., Solati-Hashjin, M., Peirovi, H., Samadikuchaksaraei, A., "Synthesis and characterization of fiber reinforced polymer scaffolds based on natural fibers

and polymer for bone tissue engineering application," *IRANIAN JOURNAL of BIOTECHNOLOGY,* vol. 10, pp. 184-190, 2012.

[216] Kanani, A.G., Bahrami, S.H., "Review on Electrospun Nanofibers Scaffold and Biomedical Applications," *Trends Biomater. Artif. Organs,* vol. 24, pp. 93-115, 2010.

[217] Yamanouchi, K., Satomura, K., Gotoh, Y., Kitaoka, E., Tobiume, S., Kume, K., Nagayama, M., "Bone Formation by Transplanted Human Osteoblasts Cultured Within Collagen Sponge with Dexamethasone *In vitro*," *J Bone Miner Res,* vol. 16, pp. 857-867, 2001.

[218] Shin, S.-H., Purevdorj, O., Castano, O., Planell, J.A. and Kim, H.-W., "A short review: Recent advances in electrospinning for bone tissue regeneration," *J Tissue Eng,* 2012.

[219] Ito, Y., Hasuda, H., Kamitakahara, M., Ohtsuki, C., Tanihara, M., Kang, I.K. and Kwon, O.H., "A Composite of Hydroxyapatite with Electrospun Biodegradable Nanofibers as a Tissue Engineering Material," *J Biosci Bioeng.,* vol. 100, pp. 43-49, 2005.

[220] Kim, K.H., Jeong, L., Park, H.N., Shin, S.Y., Park, W.H., Lee, S.C., Kim, T.I,, Park, Y.J., Seol, Y.J., Lee, Y.M., Ku, Y., Rhyu, I.C., Han, S.B. and Chung, C.P., "Biological efficacy of silk fibroin nanofiber membranes for guided bone regeneration," *J Biotechnol.,* vol. 21, pp. 327-339, 2005.

[221] Yoshimoto, H. *et al.*, "A biodegradable nanofiber scaffold by electrospinning and its potential for bone tissue engineering", *Biomaterials 24(12),* pp. 2077-2082, 2003.

[222] Ngiam, M., Liao, S., Patil, A.J., Cheng, Z., Yang, F., Gubler, M.J., Ramakrishna, S. and Chan, C.K., "Fabrication of Mineralized Polymeric Nanofibrous Composites for Bone Graft Materials," *Tissue Eng Part A.,* vol. 15, pp. 535-546, 2009.

[223] Erisken, C., Kalyon, D.M. and Wang, H., "Functionally graded electrospun polycaprolactone and b-tricalcium phosphate nanocomposites for tissue engineering applications," *Biomaterials,* vol. 29, pp. 4065-4073, 2008.

[224] Beck, Jr. G.R., Zerler, B. and Moran, E., "Phosphate is a specific signal for induction of osteopontin gene expression," *PNAS; Proc. Natl. Acad. Sci,* pp. 8352-8357, 2000.

[225] Wutticharoenmongkol, P., Pavasant, P. and Supaphol, P., "Osteoblastic Phenotype Expression of MC3T3-E1 Cultured on Electrospun Polycaprolactone Fiber Mats Filled with Hydroxyapatite Nanoparticles," *Biomacromolecules,* vol. 8, pp. 2602-2610, 2007.

[226] Aubin, J.E., "Bone stem cells," *J Cell Biochem Suppl.,* vol. 30-31, pp. 73-82, 1998.

[227] Idris, S.B, Arvidson, K., Plikk, P., Ibrahim, S., Finne-Wistrand, A., Albertsson, A.C., Bolstad, A.I. and Mustafa, K., "Polyester copolymer scaffolds enhance expression of bone markers in osteoblast-like cells," *J Biomed Mater Res A.,* vol. 94, pp. 631-639, 2010.

[228] Jaquiéry, C., Schaeren, S., Farhadi, J., Mainil-Varlet, P., Kunz, C., Zeilhofer, H.F., Heberer, M., Martin, I., "*In vitro* Osteogenic Differentiation and *In vivo* Bone-Forming Capacity of Human Isogenic Jaw Periosteal Cells and Bone Marrow Stromal Cells," *Ann Surg.,* vol. 242, pp. 859-867, 2005.

[229] Lin, Z., Solomon, K. L., Zhang, X., Pavlos, N. J., Abel, T., Willers, C., Dai, K., Xu, J., Zheng, Q. and Zheng, M., "*In vitro* Evaluation of Natural Marine Sponge Collagen as a Scaffold for Bone Tissue Engineering," *Int J Biol Sci.,* vol. 7, pp. 968-977, 2011.

[230] Stein, G.S., Lian, J.B., Montecino, M., van Wijnen, A.J., Stein, J.L., Javed, A. and Zaidi, K. "Involvement of nuclear architecture in regulating gene expression in bone cells," in *Principles of Bone Biology* L. G. R. P.B.Bilezikian G.A. Rodan, Ed. Orlando, Florida: Academic Press, 2002, pp. 169-188.

[231] Franceschi RT, Iyer BS, Cui Y., "Effects of ascorbic acid on collagen matrix formation and osteoblast differentiation in murine MC3T3-E1 cells." *J Bone Miner Res.,* vol. 9, pp. 843-854, 1994.

[232] Xiao, G., Cui, Y., Ducy, P., Karsenty, G. and Franceschi, R.T., "Ascorbic Acid-Dependent Activation of the Osteocalcin Promoter in MC3T3-E1 Preosteoblasts: Requirement for Collagen Matrix Synthesis and the Presence of an Intact OSE sequence," *Mol Endocrinol.,* vol. 11, pp. 1103-1113, 1997.

[233] Sombatmankhong, K., Sanchavanakit, N., Pavasant, P. and Supaphol, P., "Bone scaffolds from electrospun fiber mats of poly(3-hydroxybutyrate),poly(3-hydroxybutyrate-co-3-hydroxyvalerate) and their blend," *Polymer,* vol. 48, pp. 1419-1427, 2007.

[234] Knowles, J. C. and Hastings, G. W., "*In vitro* Degradation of a Polyhydroxybutyrate Polyhydroxyvalerate Copolymer," *Journal of Materials ScienceMaterials in Medicine,* vol. 3, pp. 352-358, 1992.

[235] Boeree, N. R., Dove, J. and Cooper, J. J., "Development of a Degradable Composite for Orthopedic use - Mechanical Evaluation of an Hydroxyapatite Polyhydroxybutyrate Composite-Material," *Biomaterials,* vol. 14, pp. 793-796, 1993.

[236] Nair, L. S. and Laurencin, C. T., "Biodegradable Polymers as Biomaterials," *Progress in Polymer Science,* vol. 32, pp. 762-798, 2007.

APPENDIX A

Table 20 Materials and chemicals use din the research work

Name	Product code	Source	Application
polyhydroxybutyrate (98%)/ polyhydroxyvalerate (2%) (PHB/PHV**)**		Good Fellow, UK	Main constituent of the fibrous structure
Silk fibroin (SF)		Huzhou Sunergy World Trade Co. Ltd, China	Composite formulation
nano-hydroxyapatite (nHAp) with particles of <200nm,	12167-74-7	Sigma – Aldrich, Ireland	Composite formulation
Chloroform (CHO)	67-66-3	Sigma Aldrich, Ireland	Solvent
Sodium chloride (NaCl)	S6014	Sigma Aldrich, Ireland	SBF formulation
Potassium chloride (KCl)	P3911	Sigma Aldrich, Ireland	SBF formulation
Name	Product code	Source	Application
Potassium phosphate dibasis trihydrate (K2HPO4*3H2O)	M2670	Sigma Aldrich, Ireland	SBF formulation
Hydrochloric acid- 1M (HCl)	HYAC-1041-22	Reagent, UK	SBF formulation
Calcium chloride (CaCl2)	120-95-1KG-R	Sigma Aldrich, Ireland	SBF formulation
Name	**Product code**	**Source**	**Application**
Sodium sulphate (Na2 SO4)	238597	Sigma Aldrich, Ireland	SBF formulation
Dulbecco's Phosphate buffer solution (PBS)	D8537	Sigma Aldrich, Ireland	Cell culture
Fetal Bovine Serum , Heat Inactivated (FBS)	16140-071	Bio-Sciences, Ireland	Cell culture
MEM-Alpha Medium	A1049001	Bio-Sciences, Ireland	Cell culture
Antibiotic/ Antimycotic	15240-062	Bio-Sciences, Ireland	Cell culture
Phalloidin-FITC	P5282	Sigma-Aldrich, Ireland	Immunocytochemistry technique (ICC)

AlexiFluor 546 labelled Anti Mouse IgG antibody		Invitrogen, Ca, USA	Immunocytochemistry technique (ICC)
Monoclonal Anti-Osteopontin	SAB4200018	Sigma-Aldrich, Ireland	Immunocytochemistry technique (ICC)
Collagen I antibody – FITC	Orb15142	Biorbyt, UK	Immunocytochemistry technique (ICC)
Alkaline phosphatise, Bone ELISA Kit	ABIN627592	Antibodies, Germany	ELISA assay
Mm_Spp1_1_SG QuantiTect Primer Assay (200)	QT00157724	Qiangen, Ireland	qRT-PCR
Mm_Col1a1_1_SG QuantiTect Primer Assay (200)	QT00162204	Qiangen, Ireland	qRT-PCR
Sterile pipettes, 24 well cell culture plates, 96 well ELISA reader plates,75 cm2cell culture flasks,		Applied Biosystems, USA	Cell culture

APPENDIX B

The following scientific instruments were used in the study:

- Gamma High Voltage Research power supply

- Infusion Syringe pump, (KDS KDS100, kd Scientific)

- Magnetic stirrer (Bibby, HB502, Sterilin UK)

- YDK 01 LP Density Measurement Kit (Sartorius AG, Germany)

- Zwick Z005 Test Machine (Zwick-Roell, Germany) equipped with a 20N load cell (tensile tests) and 5 kN load cell (compressive tests)

- DTA/TGA STA 1500 (PL Thermal Sciences Ltd, UK)

- EVO LS15 Scanning Electron Microscopy (Zeiss, Germany)

- Bx51 Olympus Microscopy (Olympus, Japan)

- Edwards Pirani 501 Scancoat sputtering coater (Edwards Laboratories, USA)

- Surftest-402 profilometer (Mitutoyo, Japan)

- FTA 200 angstrom sessile drop measuring machine equipped with a ArtCAM 130 MI BW monochrome camera (First Ten Ångstroms, USA)

- Hanna HI 9813 Handheld pH, EC and TCS Meter with Probe (Hanna Instruments, Inc.)

- Water bath (Clifton, Nickel Electro LTD, UK)

- Spectophotometer NanoDrop

- Rotor-Gene Cycler

APPENDIX C

Image J Protocol for fibre diameter measurement

(adapted from Tiffany Richelle Peña, PREPARATION AND CHARACTERIZATION OF ELECTROSPUNPOLY(D,L-LACTIDE-CO-GLYCOLIDE) SCAFFOLDS FOR VASCULARTISSUE ENGINEERING AND THE ADVANCEMENT OF AN *IN VITRO* BLOOD VESSEL MIMIC, Faculty of California Polytechnic State University, San Luis Obispo,June 2009)

This set of instructions allows one to count cells by drawing a straight line between the two transverse sides of one single fibre.

1. Open program ImageJ.
2. Select File > Open. Open a saved SEM image.
3. Select 'straight line' and draw a line along the SEM image's scale bar. Visually ensure the line is as close to the length of the scale bar as possible as this will affect the outcome of fibre diameter measurements.
4. On the tool bar, select Analyze > Set Scale.
5. Insert known image scale bar distance (ex. 20 μm). Set pixel aspect ratio to 1.0 and set appropriate unit length (ex. μm). Select OK. ImageJ is now calibrated to the image.
6. From Plugins>Analyze>Grid insert grid. Use the same numbers of grids for all the images to be used for measurement.
7. From the tool bar, select 'straight line'. Draw a line across the diameter of a single fibre to be measured. (Figure 82)
8. From the toolbar select Analyze > Measure. ImageJ will open a new window reporting Results. Fibre diameter is reported as Length in the Results window in proper units (ex. μm). (see Figure 82)
9. Leave the Measure window open and repeat Step 6 for all Fibre measurments for that image.

10. Repeat for all images. NOTE: Calibration is only necessary for the first image ONLY if all images being analyzed are at the SAME magnification. Re-calibration will be necessary for images taken at different magnifications.
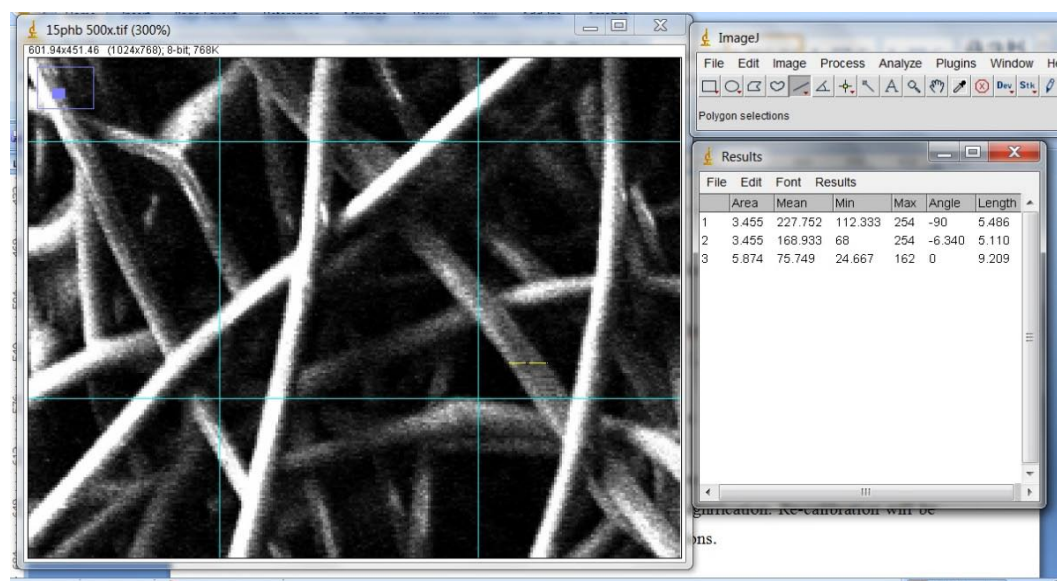

Figure 82   SEM image used for fibre diameter measurement using Image J protocol

APPENDIX D

Image J Protocol for Manual Cell Counting and Marking (plugin required)

(adapted from Integrated Light Microscopy Core, University of Chicago)

http://www.unige.ch/medecine/bioimaging/tricks/imagejtutorials/CellCounting.pdf

This set of instructions allows one to count cells by clicking in the cell image. Each click marks the cell with a colored square and adds the cell to a tally sheet.

1) First, the Cell Counter plugin must be installed. After plugin installation Image J must be re-started for the analysis folder containing the Cell Counter plugin to appear under the Plugins menu.

2) Open the image you want to count. Cell counter only works on single images, not stacks. One can use Image - Stacks - Stack to Images to convert a .tiff stack or .stk to single .tif files. It does not matter if the image is greyscale, single color or multiple colors. However, if the image is in greyscale and one wants the clicked squares to be in color, one must convert the image to an RGBcolor image with Image -Type - RGB color. Greyscale images are supported by the counter plugin, but the squares are white or black, so difficult to distinguish between types.

3) Select Plugins - Analysis – Cell Counter (or Plugins - Cell Counter). Two new windows will open a counter window with the image on top of a row of buttons, and a results window where cells will tally. Select Plugins- Analyze-Grid (lines) and click ok. A minimum of 5 visual fields will be used for cell counting (see Figure 83).

4) To begin counting, click one of the buttons at the bottom of the counter window. Then click directly on a cell/object one wishes to count. A white square will be left behind on the object, and a tally will start in the results window. If one clicks on an object by mistake, this can be undone by selecting Edit - Undo. One must undo right away, as no more than one object in a row can be undone. Use Results - Save as to save your counts as Excel formatted files.

5) If one does not see the marker squares in colour, one needs need to make the image an RGB image. To do this, close Cell Counter by closing the image window. Open the image again and use Image -Type - RGB color. It's okay if your image is still greyscale. Now when the image will open in Cell Counter and click for a marker, the markers will be in colour.

6) When the counting is finished, click the Results button. A total for each cell type plus a grand total of all clicks at the bottom of the Results window.
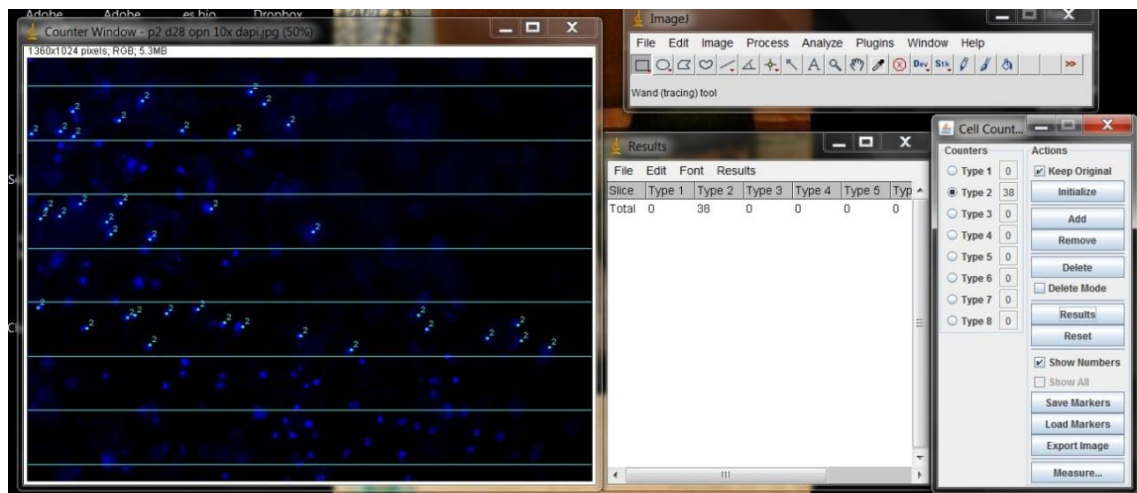

Figure 83 Example of DAPI image (10x) used for cell counting